EFFECT OF CLIMATE CHANGE ON A MONOLITHIC DESULPHURIZED TAILINGS COVER

Fiaz Ahmad

A Thesis Submitted to the Faculty of Graduate Studies

In Partial Fulfillment of the Requirements

For The Degree of

Master of Applied Science

Graduate Program in Civil Engineering

York University

Toronto, Ontario

October 2018

Abstract

Climate change is expected to impact the stability and functionality of several geotechnical infrastructures. Soil covers are one of the main classes of geotechnical infrastructure which would exhibit pronounced changes in its functional performance due to climate change. It is therefore imperative to study the effects of climate change on soil covers. The current study focuses on the effects of climate change on soil covers over tailings (tailings cover) at a site in Northern Ontario, Canada. Covers were analyzed using historical and future climate datasets using numerical modelling techniques. In addition to climate change, effects of changing hydraulic properties were also quantified. The results of this research show that fine grained covers performed better under adverse climate change conditions as compared to coarse grained covers. However, the performance of fine covers will deteriorate with time due to evolutionary changes in their hydraulic properties.

Keywords: climate change; geotechnical infrastructure; tailings cover; hydraulic properties.

Acknowledgements

I would first like to thank my thesis supervisors Dr. Rashid Bashir and Dr. Ryley Beddoe. The doors to Prof. Rashid and Prof. Beddoe offices were always open whenever I ran into a trouble spot or had a question about my research or writing. They consistently allowed this paper to be my own work, but steered me in the right the direction whenever they thought I needed it.

My special thanks to my Dr. Lal Samarasekera for his continuous support during the research and his valuable comments during the annual assessments meeting.

Last, but not the least, I dedicate this thesis to my beloved elder brother (late) who always supported and encouraged me through thick and thin of my life when he was alive. May his soul rest in peace and my prayers are always with him.

Finally, I must express my very profound gratitude to my parents and to my wife and my kids for providing me with unfailing support and continuous encouragement throughout my years of study and through the process of researching and writing this thesis. This accomplishment would not have been possible without them.

Ahmad

Table of Contents

List of Tables

List of Figures

List of Abbreviations

AE	Actual Evaporation
AR	Assessment Report
AEV	Air Entry Value/pressure
AMD	Acid Mine Drainage
ARD	Acid Rock Drainage
AGCM	Atmosphere General Circulation Models
BC	Baseline Climate
CC	Coarse desulphurized tailing over Coarse reactive tailings
CF	Coarse desulphurized tailing over Fine reactive tailings
CCDP	Climate Change Data Portal
DP	Deep Percolation
DLM	Detour Lake Mine
E	Evaporation
FF	Fine desulphurized tailing over Fine reactive tailings
FC	Fine desulphurized tailing over Coarse reactive tailings
FC-1	representative Future Climate 1
FC	Future Climate

GCM	General Circulation Model
GHG	Greenhouse Gases
GWT	Groundwater Table
HCF	Hydraulic Conductivity Function
INAP	International Network of Acid Prevention
IPCC	Intergovernmental Panel on Climate Change
LAMPS	Laboratory of Mathematics and Parallel Systems
MEND	Mine Environmental Neutral Drainage
NOAA	National Oceanic and Atmospheric Administration
O2	Oxygen
OCCP	Ontario Climate Change Portal
OF	Oxygen Flux
RH	Relative Humidity
RCP	Representative Concentration Pathways
PCF	Predicted Future Climate
Sat.	Saturated
S	Storage
SRES	Special Report on Emission Scenario

STDV	Standard Deviation
SWCC	Soil Water Characteristics Curve
T	Transpiration
Vol	Volume
VG	van Genuchten

List of Symbols

F	diffusive mass flux
De	effective diffusion coefficient
C	concentration of oxygen in soil
X	distance/depth in direction of diffusion
θ_a	volumetric air content.
S	water saturation or saturation
θ	volumetric water content
n	porosity of the soil
D_a	effective diffusion in the soil through air phase
D_w	effective diffusion in the soil through water phase
H	dimensionless form of Henry's equilibrium constant
D_a^0	air diffusion coefficient in open air
D_w^0	water diffusion in open water
T_a	tortuosity coefficient in air
T_w	tortuosity coefficient in water
n_{eq}	equivalent porosity of the media
n_a	air filled porosity of the media

n_w	water filled porosity of the media
D^*	apparent diffusion coefficient
K_r	effective reaction rate coefficient
k'	constant of reactivity of pyrite with oxygen
D_h	effective particle diameter
C_p	pyrite concentration
C_u	uniformity coefficient
D_{10}	grain diameter corresponding to 10 % passing
D_{60}	grain diameter corresponding to 60 % passing
L_d	length of daylight
N	number of days in the month
T_a	mean monthly air temperature
I	summation for 12 months of function $\left(\frac{T_a}{5}\right)^{1.514}$
a_t	complex function of variable I
T_{ef}	effective temperature
p	an empirical parameter, 0.72 was found statistically most feasible
$T_{max}.$	maximum daily air temperature
T_{min}	minimum daily air temperature

T_{avg}	average daily air temperature
Γ	slope of saturation vapor pressure versus temperature curve
Q_n	net radiation at the water surface
η	psychometric constant
E_a	a function of wind speed and vapor pressure deficit
W_w	wind speed
u_{v0}^{air}	vapor pressure in the air above the water or saturated surface
u_v^{air}	saturated vapor pressure at the mean air temperature
A	inverse of relative humidity at the soil surface
u_v^{soil}	vapor pressure in the soil at the ground surface temperature
u_{v0}^{soil}	saturated vapor pressure in the soil at the ground surface temperature
P	precipitation
PE	potential evaporation
NI	net infiltration
RO	runoff
PE_m	monthly potential evaporation
q	groundwater Darcy flux
k_s	saturated hydraulic conductivity

i	hydraulic gradient
h	hydraulic head
x	horizontal distance
$k(\Psi)$	hydraulic conductivity as a function of matric suction
$C(\Psi)$	specific moisture capacity
Ψ	matric suction
z	position
D	diffusivity
Θ	effective saturation
Ψ_a	air entry or bubbling pressure
λ	pore size distribution index
θ_s	saturated volumetric water content
θ_r	residual volumetric water content
α	curve fitting empirical parameter with inverse of air entry value
n	van Genuchten curve fitting empirical parameter
m	van Genuchten curve fitting empirical parameter
k	hydraulic conductivity
l	tortuosity parameters

T	temperature
T_x	absolute daily maximum temperature
T_n	absolute daily minimum temperature
I_m	Thornthwaite annual moisture index
θ_{sp}	post-construction saturated volumetric water content
k_{sp}	post-construction saturated hydraulic conductivity
α_p	post-construction van Genuchten α parameter
n_p	post-construction van Genuchten n parameter
ΔS	difference in net infiltration and deep percolation

Chapter One: Introduction

1.1 Introduction

Climate change is generally considered to be a global phenomenon, and the majority of the International scientific community agrees that it is happening (IPCC 2014). Soil covers are one of the main classes of geotechnical infrastructure which would exhibit pronounced effects due to climate change (Bashir et al., 2015). It is therefore essential to study and understand the future climate and its effects on the soil covers. Such a study will provide an opportunity to evaluate the long term performance of soil covers and select the appropriate remedial measures to deal with unexpected challenges likely to occur due to climate change.

Global annual precipitation is increasing during the last century with an increase of 0.03 mm/day per 100 years (Ren et al., 2013). However, the change in precipitation is different in different parts of the world. For example, Northern Europe, and the eastern part of North and South America and Northern and central Asia have increasing precipitation trends while it's on decline in Mediterranean, southern Africa and southern Asia (Pachauri and IPCC 2008). Similarly, the change in temperature, which has increased by 0.6 °C during last century, is also not uniform through continents (Houghton and IPCC 2001). The greatest increase in temperature is observed in the continental interior of Asia, north-western North America and south-eastern Brazil. The areas in the southern part of Greenland and some regions in North and South America have not seen significant temperature increases during the last century (IPCC 2007). Different countries in a

continent and even different regions in same country can expect different climate change trends.

Canada has experienced an increase in total annual precipitation by 16.5 % from 1950 to 2009. Of this increase, 12.5 % is in annual rainfall while about 4 % is in snowfall. An increasing annual snowfall trend is observed at recording stations in Northern Canada, while Southern parts have shown a decrease in annual snowfall (Mekis and Vincent, 2011). Similarly, during the same period, an overall increase in near surface air temperature is reported to be 1.3 °C in all over Canada which is more than twice the global average. Increasing temperature trend is observed in entire Canada (Barrow et al. 2004). These climate changes will impact most type of soil covers to varying degrees. Store and release covers and the covers that rely on permafrost for waste containments are expected to be most affected by climate change (Bashir et al., 2015). The changes in precipitation trends may impact the performance of store and release cover by generating increased percolation to the underlying waste by overwhelming its design storage capacity (Bashir et al., 2015). Similarly, the covers in the region(s) where precipitation trends are on decline may underperform due to less availability of water for maintaining a higher degree of saturation to control oxygen ingress to reactive tailings. Rising temperatures may result in failure of covers that rely on the permafrost for waste containments due to deteriorating permafrost conditions (Bashir et al., 2015). Increasing temperature can also compromise the cover performance by reduction in degree of saturation through evaporation.

Figure 1.1 is a trilinear plot of climate type, precipitation and evapotranspiration. It provides guidance for preliminary selection of soil covers for acid generating tailings

based on climatic conditions. Based on this figure, annual precipitation and evapotranspiration are important parameters for selecting a type of cover in a particular region. From this figure it can be observed that in Arid climatic conditions, store and release covers are generally suitable. Water covers or infiltration control covers are generally recommended for the humid climates depending upon the annual precipitation and evapotranspiration ratio. Permafrost thermal covers are recommended to be used in the high Arctic. This figure clearly shows that the climate is one of the most important parameters for cover selection and design.

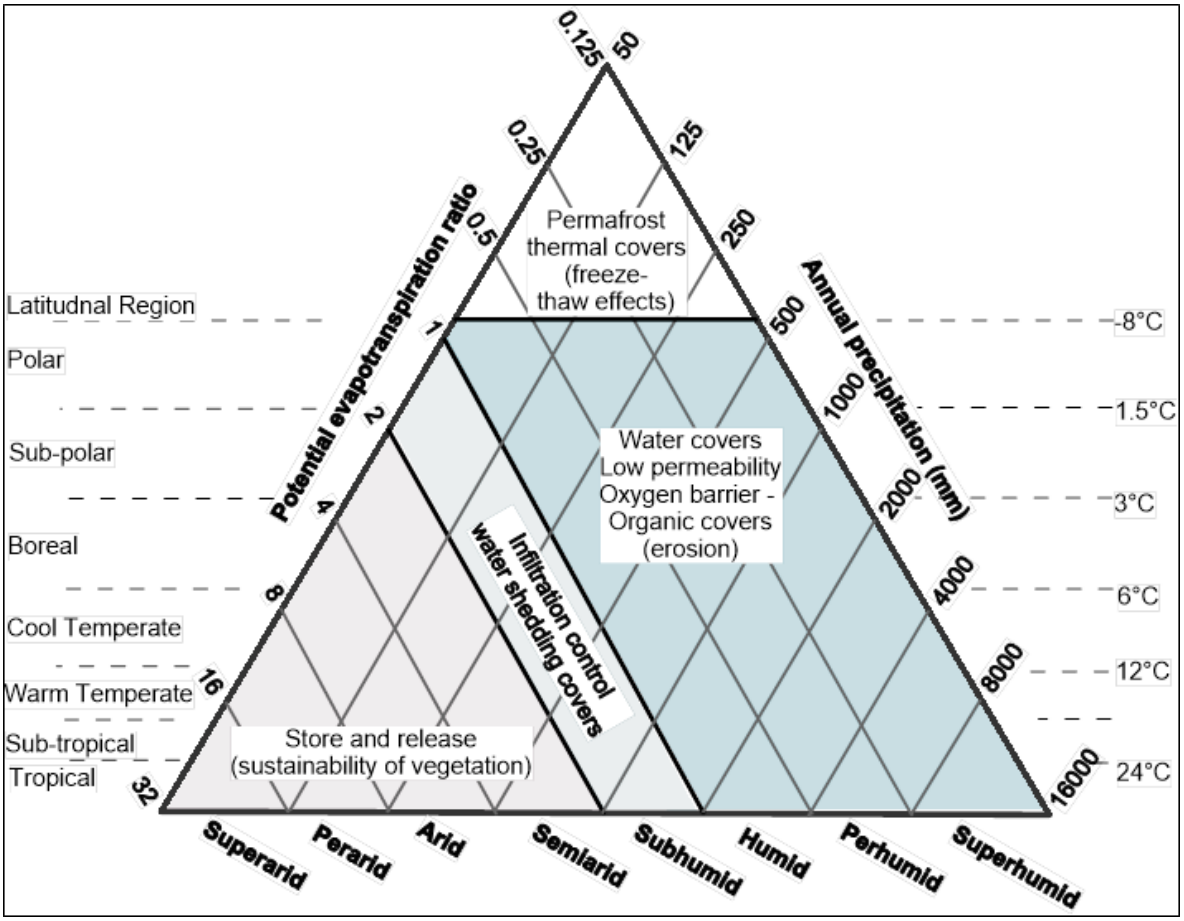

Figure 1.1. Schematic of cover type selection (modified from INAP 2009).

Soil covers also referred as dry covers are designed using engineered geologic materials to limit the production of acid mine drainage(AMD). These covers maintain high saturation to limit transport of atmospheric oxygen to acid generating tailings (Nicholson et al., 1989, Lindsay et al., 2015). The key external reactants involved in the production of AMD are oxygen (O2) and water. Limiting the exposure of these reactants will reduce the production of AMD. Limiting the supply of oxygen to the underlying tailings has been found to be a better practical option than limiting water ingress to tailings (Yanful et al., 2004, Pabst et al., 2014, 2017). Oxygen transport to the tailings can be limited by maintaining a higher degree of saturation in the cover. At low saturations, air-filled pores are generally connected and oxygen movement through pores is comparatively fast. However, once pores reach a certain degree of saturation, the remaining air voids are no longer connected and air-filled pores become disassociated. The rate of oxygen diffusion is four orders of magnitude lower in water than in air (Yanful 1993). Therefore, oxygen transport becomes extremely slow. The saturation level at which oxygen molecules are generally considered to be disassociated is ~85 % (Yanful 1993, Aachib et al., 2004). Therefore, tailing covers which can maintain a high degree of saturation are generally able to protect the underlying tailings from atmospheric oxygen (Yanful et al., 2004).

Tailing covers are generally spread over a large area and require substantial volume of fine materials for their construction. Therefore, there could be a significant costs associated with the acquisition and haulage of these materials. Use of processed tailings as the cover materials has evolved in last two decades to alleviate significant costs associated with the construction of soil covers (Bussie`re and Aubertin 1999, Akcil and Koldas 2006, Demers et al., 2008, Gosselin et al., 2011). The tailing covers constructed

with processed tailing materials are called desulphurized tailing covers as they are constructed with tailings that have been desulphurized. The key aspect of desulphurizing is to reduce the concentration of sulphide mineral to a certain level where it behaves as an inactive material (Nicholson et al., 1989, Pabst et al., 2014, 2017).

Figure 1.2 shows the schematic of the general effect of varying degree of saturation on the generation of AMD. It also shows that covers at certain saturation (≥ 85%) function comparable to that of water cover. Selection of a cover (dry or water) in a certain area depends on various considerations including the climate of the area.

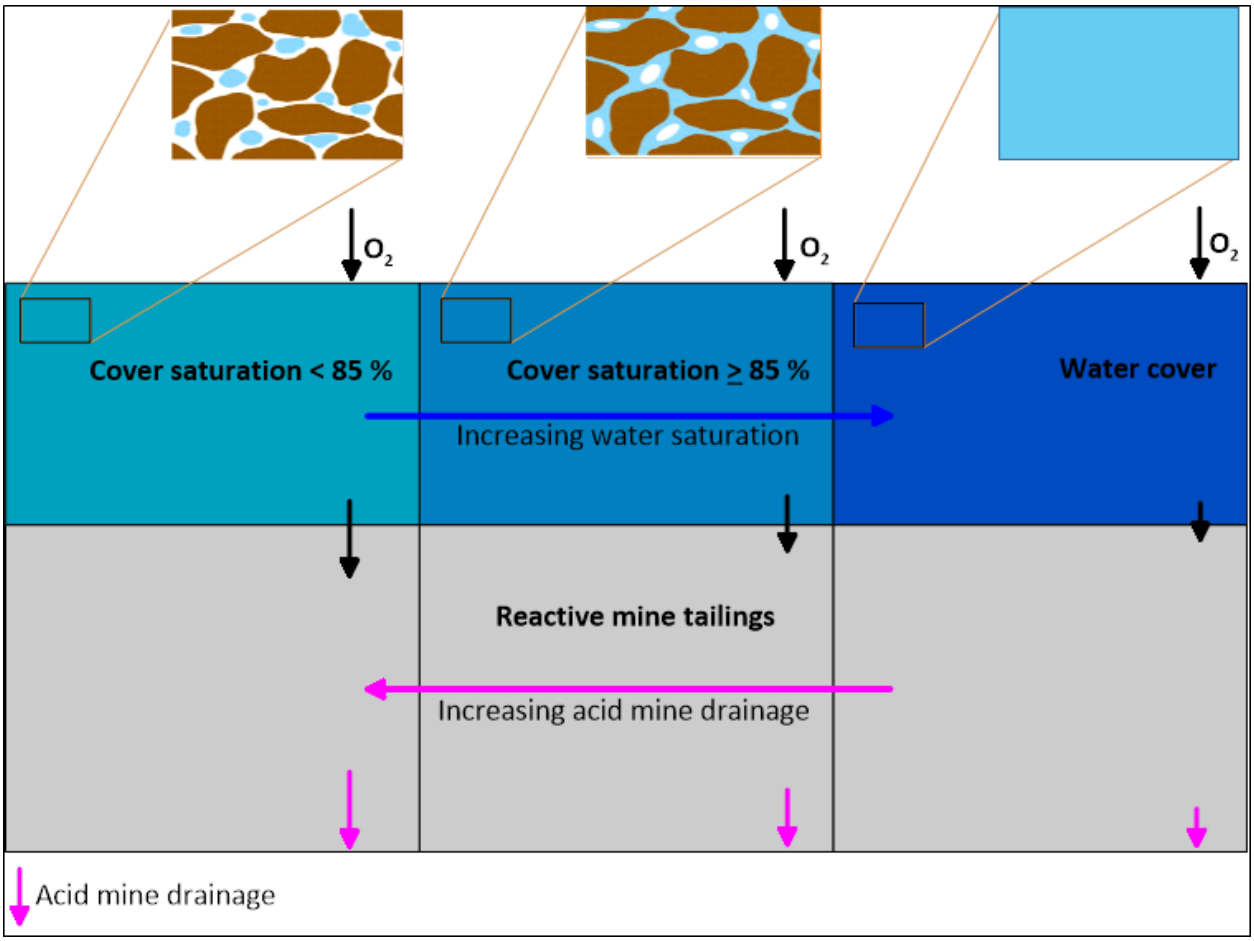

Figure 1.2. Effects of varying degree of saturation on acid mine drainage.

Oxygen ingress to the reactive tailings can be controlled by either maintaining a higher saturation in the cover or in the tailings themselves. A cover constructed with fine material will maintain higher saturation. Alternatively, the water table in the tailings can also be elevated by having a cover constructed with coarse material, which would act as evaporation barrier and would let most of the meteoric water infiltrate into the tailings.

1.2 Water Balance at Cover Surface

A part of the precipitation water will either infiltrate into the soil cover or will be evaporated back to the atmosphere. Additionally, in instances where the precipitation intensity is more than the infiltration capacity of the soil, some part of the precipitation water can either flow on the cover surface as surface runoff or can accumulate on the surface. The processes of infiltration, evaporation and surface runoff are dependent on the soil hydraulic properties and prevailing atmospheric conditions. In most instances the quantity of infiltration is controlled by the saturated hydraulic conductivity of the cover material. Similarly, the quantity of water that will be lost by evaporation is dependent on the evaporative demand, cover hydraulic properties and transient cover moisture conditions. Evaporative demand is solely the function of atmospheric conditions namely, temperature, relative humidity, wind speed and net radiation and is expressed in the form of potential evaporation. Potential evaporation refers to the maximum amount of water that can be evaporated if the cover surface remains saturated. The actual amount of water that will be evaporated is termed as actual evaporation and is dependent on the availability of water in the cover, which in turn is also dependent on the soil hydraulic properties. For example, coarse soils have low retention and high conduction. This results

in lower retention times for meteoric water in soil layers near the ground surface reducing the water availability for evaporation. On the contrary, finer soils have higher retention and lower conduction resulting in greater water availability for evaporation. Similarly, higher saturated hydraulic conductivity values for coarser soils result in less runoff than the finer soils which have lower saturated hydraulic conductivity values.

Net infiltration is the quantity of precipitation water that overcomes the evaporation and runoff and makes its way into the soil cover. It can be estimated by subtracting the actual evaporation and surface runoff values from precipitation. A part of the net infiltration can be stored in the cover, where some part of it can be extracted by the plants roots and released back in to the atmosphere through the process of transpiration. Additionally, net infiltration water can move further down in the soil cover and can make its way into the underlying tailings. This quantity of water is termed deep percolation. All the processes discussed in this section are schematically shown in Figure 1.3.

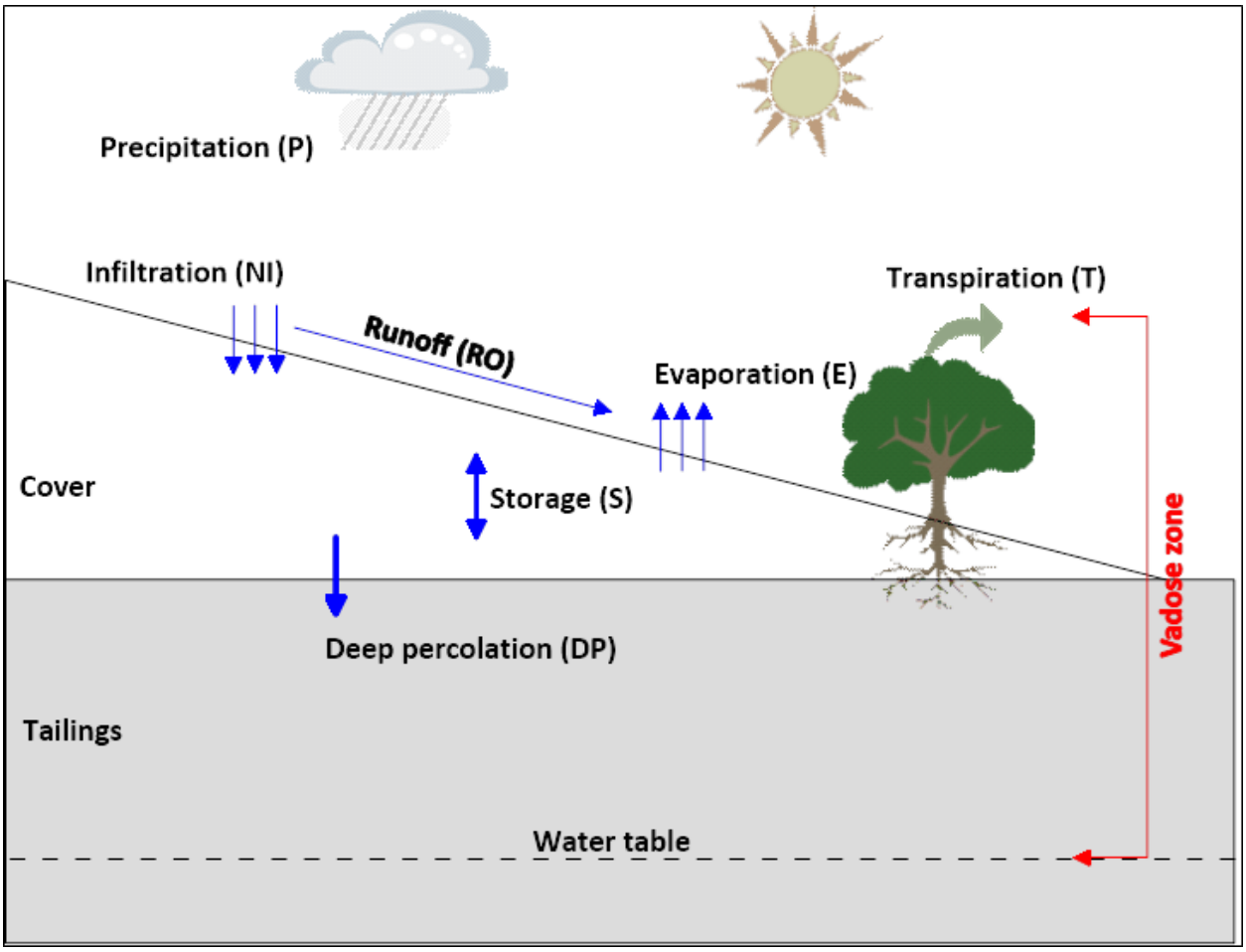

Figure 1.3. Hydrological cycle on soil cover.

1.3 Cover Behavior under Changing Climate

It is predicted that the climate will continue to warm during the 21st century across Canada (Barrow et al., 2004). The frequency of warmer summers (average temperature >+30 °C) is expected to increase all over Canada. However, this temperature increase will be greatest in Canada's high Arctic. Similarly, the predicted annual precipitation increase is greatest in the Arctic (40% to 50%) whereas the average annual precipitation is expected to increase by 10% all over Canada (Barrow et al., 2004). Higher temperatures will increase the evapotranspiration rates and may result in water deficits in some locations

(Barrow et al., 2004). Such weather conditions can have serious implications on the performance of tailing covers which control oxygen ingress by marinating higher saturations in cover materials. Decreased precipitation and/or increase in evaporation may lead to dry conditions (drought) which could potentially impact the tailing cover performance, which may experience difficulties in maintaining their required saturation level during dry spells (MEND 2011). Similarly, increases in precipitation intensities in excess of design values may result in more percolation in store and release covers (Bashir et al., 2015). This increased percolation could potentially increase leachate production

In addition to increasing the evaporation rates, higher temperatures can also increase the moisture holding capacity of the atmosphere. This increased moisture holding capacity has the ability to change the precipitation patterns (Trenberth 1999). In instances where the evaporation exceeds the precipitation, soil covers may tend to dry near the surface. If the drying cycle continues for a certain period of time desiccation cracks may appear on the surface of the (fine) soil cover due to substantial loss of moisture. The cracked surfaces will have an effect on the hydraulic conductivity of the soil cover (water will move faster in cracks as compare to soil matrix). Therefore, while studying the future climate change effects on soil cover, the evolution of hydraulic properties due to desiccation cracking also needs to be investigated.

1.4 Current Study

In this study a soil cover constructed over tailings management facility at Detour Lake mine is evaluated under changing climactic conditions. The cover is constructed with

desulphurized tailings and is meant to control oxygen ingress to reactive tailings. The cover is designed to control oxygen by maintaining high cover saturation and an elevated water table in the tailings. Detour Lake mine is a gold mining operation located approximately 290 km north east of Timmins close to the border between Ontario and Quebec. The site location of Detour Lake mine is shown in Figure 1.4. The mining operation at the site started in 1983 and produced about 14.3 million tonnes (Mt) of ore by 1999. During the same period, the milling operation at the site generated about 15 Mt of tailings which were contained in impoundment. The tailings had a considerable amount of Sulphur (1 to 2.5 %). Therefore, steps were taken to mitigate the effects of AMD to the surface and groundwater due to the presence of significant amounts of Sulphur in the tailings. The tailings impoundment was constructed at an area of about 300 hectare (ha). Most part of the tailings were deposited in water impoundment. The remaining portion, above the water level, near the dam was covered with a desulphurized tailings cover. The layout of desulphurized tailings cover at tailing management facility is shown Figure 1.5.

Historical variation in climate parameters (precipitation and temperature) during the last century are generally discussed in section 1.1 of this chapter along with their predicted future trends. Tailing covers generally aimed to have high saturation conditions to limit oxidation and saturation may be compromised due to climate change (especially during dry cycles). Similarly, dry and wet cycles in the future climate have the potential to introduce cracks on the surface of soil (fine) covers. It is therefore critical to study climate change and its effects on the soil cover.

Figure 1.4. Site location of Detour Lake Mine site (Map data @2018 Google).

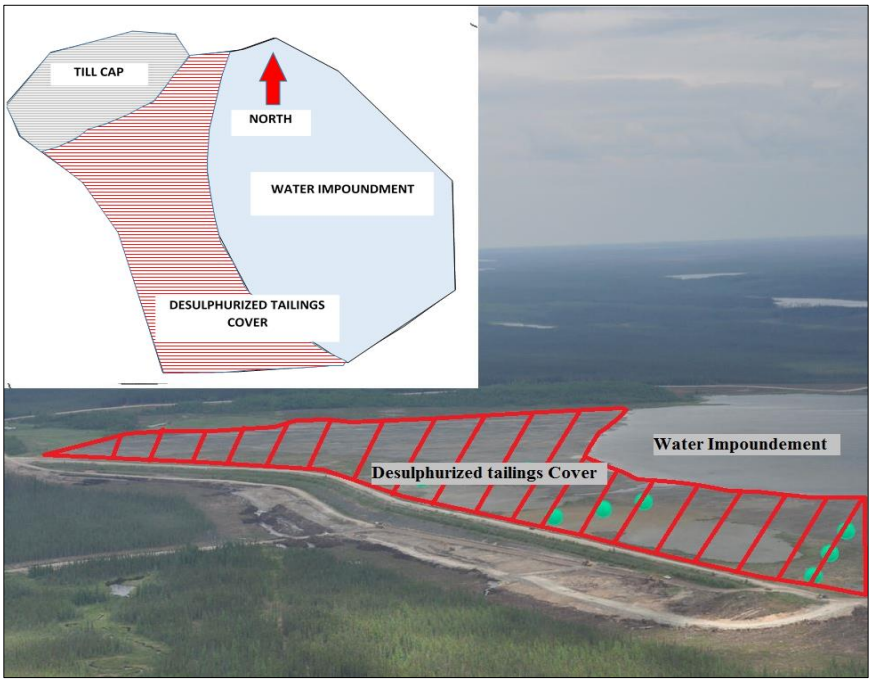

Figure 1.5. On-site desulphurized cover layout (modified from Cash, et. al. 2011).

The objective of this research was to assess the effects of changing climate on various configurations of tailing covers at Detour Lake mine. Major emphasis is on evaluation of hydrological behavior and performance assessment in terms of oxygen transport using numerical modelling techniques. To achieve the set objective, records for past and future climates were processed and soil atmosphere modelling was carried out using generalized soil profiles representing the site conditions. Modeling was carried out using the VADOSE/W an unsaturated flow and transport code capable of simulating the interaction between the soil cover and atmosphere. Historical climate data was taken from Environment Canada, while future climate data for various GCMs for different emission scenarios was sourced from Ontario Climate Data Portal (OCDP) housed at York University. Additionally, the effects of the changing climate on the hydraulic behavior of soil covers were also studied within the context of post-construction hydraulic properties for the cover materials. The soil profiles using the post-construction hydraulic properties were modelled using past and future climates. The modelling results were used to predict the effects of post-construction hydraulic properties and/or changing climate on the cover performance.

1.5 Thesis Outline

The thesis is organized into five chapters. Chapter 1 presents a general introduction on climate change and its effects on soil covers, the problem statement and objectives of this study. Chapter 2 provides a theoretical and/or technical background on acid mine drainage, oxygen transport in porous media, surface moisture flux, variable saturated flow in the porous media, climate change and processes involved in the evolution of soil

hydraulic properties. Chapter 3 presents a study on the effect of climate change on a monolithic desulphurized tailings cover. In this chapter, the tailing covers of various configuration of fine and coarse material are modelled for past and future climates and the cover performance is assessed based on its ability to control the oxygen ingress to reactive tailings. Chapter 4 provides the results with regards to the post-construction performance evaluation of monolithic desulphurized tailings covers. In this chapter, estimates of the post-constructional changes in hydraulic properties of the fine cover materials are made. The cover performance based on post-constructional changes are also presented in this chapter. In Chapter 5, general conclusions of this study are presented. Recommendations for future research are also part of this chapter.

Chapter Two: Background

2.1 Introduction

Mine reactive tailings enriched with sulphide content can be protected from the atmosphere through the use of dry covers (Demers et al., 2008). The term dry cover is coined to differentiate it from a water cover, where reactive tailings are flooded with water to control the ingress of oxygen to tailings. Dry covers can range from a single layer of earthen material to several layers of different material types, including but not limited to native soils, geo-synthetic materials, inactive tailings and/or waste rock, and organic materials. One of the primary purposes of these covers is to control the ingress of oxygen to the tailings. The oxygen from the atmosphere can travel through these covers and react with the wet tailings to produce acid mine drainage (AMD). The air-filled voids in the tailing covers generally favour the transport of oxygen (Yanful 1993). A certain degree of saturation can be maintained in the tailing covers to limit the transport of oxygen, as the movement of oxygen is significantly lower in water than in air (Barbour et al., 1993; Yanful 1993; Nicholson et al., 1989; MacKay 1997). The degree of saturation and thus the performance of the tailing covers is greatly controlled by the climatic conditions at their location and any change in the climate will effect on the performance of the cover. The degree of saturation may increase during periods of increased precipitation improving their performance in terms of reducing the oxygen ingress. The performance of covers may be compromised during drought conditions due to the scarcity of water (due to low precipitation and/or high evaporation). Therefore, it is important to understand the

phenomenon of oxygen transport in the covers and their behavior under various saturation conditions.

2.2 Acid Mine Drainage

Generation of acid mine drainage (AMD), characterized by low pH with considerable concentration of hazardous metals in sulphide enriched tailings, has historically been a challenge for the mining industry (Ouangrawa et al., 2009). This is a natural phenomenon and generally depends on the exposure of sulphide-bearing tailings to the atmosphere. The free and abundant supply of oxygen in the surrounding of tailings plays a major role in generation of AMD.

Water and oxygen (O2) are the two main external factors which control the oxidation of the sulphide mineral in the tailings; hence the production of AMD. The oxygen reacts with the sulphide in the presence of water and produces the acidic, sulphate rich drainage. In addition to acidic drainage, this reaction also produces metal contamination which depends upon the type of the parent rock (Akcil and Koldas, 2006).

Rock ores consist of various types of sulphide minerals like lead sulphide (galena), iron sulphide (pyrite) and zinc sulphide (sphalerite) (Akcil and Koldas, 2006). These are common sulphide minerals respectively for lead, iron and zinc ores. The most common type which is generally associated to this phenomenon is Iron sulphide (pyrite) (Akcil and Koldas, 2006). The generation of AMD by reaction of oxygen with pyrite is explained in the following section.

2.2.1 Chemical reaction of pyrite with oxygen and water

Oxidation of wet pyrite in absence of neutralization agent results in iron, sulphate, and hydrogen ions and the reaction can be shown as follows:

$$FeS_2 + \frac{7}{2}O_2 + H_2O \rightarrow Fe^{2+} + 2SO_4^{2-} + 2H^+ \quad (2.1)$$

where Fe^{2+}, SO_4^{2-}, and H^+ dissolve in water and the pH of the solution reduces. If the process continues and the supply of oxygen is uninterrupted the ferrous iron (Fe^{2+}) converts to ferric iron (Fe^{3+}) with following reaction:

$$Fe^{2+} + \frac{1}{4}O_2 + H^+ \rightarrow Fe^{3+} + \frac{1}{2}H_2O \quad (2.2)$$

The lowering of solution pH continues and at a certain pH (between 2.3 and 3.5), the ferric iron (Fe^{3+}) converts to ferric hydro oxide ($Fe(OH)_3$) which precipitates at the surface of the solution. This reaction can be shown chemically as follows:

$$Fe^{3+} + 3H_2O \rightarrow Fe(OH)_3 + 3H^+ \quad (2.3)$$

The residual $Fe^{3+}$from Eq. (2.2) which has yet to oxidize is utilized to oxidize the additional pyrite as per reaction shown in Eq. (2.4).

$$FeS_2 + 14Fe^{3+} + 8H_2O \rightarrow 15Fe^{2+} + 2SO_4^{2-} + 16H^+ \quad (2.4)$$

The Fe^{2+} produced from the reaction given in Eq. (2.4) precipitates again as $Fe(OH)_3$ with the same steps given in Eq. (2.1) to (2.3). The reactions (Eq. (2.1) to (2.3)) can be summarized in Eq. (2.5) as follows:

$$FeS_2 + \frac{15}{8}O_2 + \frac{13}{2}Fe^{3+} + \frac{17}{4}H_2O \rightarrow \frac{15}{2}Fe^{2+} + 2SO_4^{2+} + \frac{17}{2}H^+ \quad (2.5)$$

The reactions in the Equations. (2.1) to (2.5) are specifically for pyrite oxidation and the oxidizing agent is the atmospheric oxygen. For the case of other sulphide minerals, different reactions with different stoichiometries are expected (Akcil and Koldas, 2006).

2.3 Oxygen Transport in Porous Medium

In unsaturated soils the air in the soil exists either in continuous air phase or occluded air phase (Fredlund et al., 2012). In both phases, the oxygen transport occurs mainly through diffusion and/or advection. Advection flow in gas phase may occur due to barometric pressure gradient and wind (MacKay 1997). For the occluded air phase, advection flow occurs through the soil water. The trapped oxygen in the soil pores dissolves in the water and flows with the fluid at its pore velocity. The contribution of advection flow is negligible when dealing with the oxygen transport in tailings covers (Yanful 1993). However, diffusion dominates the oxygen transport in the mine tailings (MacKay 1997).

In diffusion the fluid transports from a point of high concentration to a point of low concentration. The gradient in the oxygen concentration can occur in the unsaturated soil due to plants respiration which is a well know phenomenon in the field of irrigation. In this process the plants roots create the imbalance in concentration of oxygen in soil and its

surroundings (Micheal 2010). Similarly, the oxidation of the sulphide mineral in the reactive tailings consumes most of the oxygen in the soil pores. As a result, the oxygen from the surrounding flows towards the tailings by diffusion.

The rate at which the transport of oxygen occurs due to diffusion generally depends on the medium in which it travels and the temperature of the system. Diffusion occurs at a molecular level and the change in temperature can affect the movement of molecules. With increasing temperature the rate of diffusion increases (Elberling 2005). The transport of the oxygen through the air phase is quite higher than through the occluded air phase due to a large difference in their diffusion rates (Fredlund et al., 2012).

Oxygen transport in the soil cover normally occurs through molecular diffusion (Yanful 1993; Aachib et al., 2004). When the saturation in the soil cover is less than 85 %, the movement of oxygen through the soil cover can occur freely in the gaseous phase. Once the saturation increases to more than 85 %, most of the air-filled voids are replaced with water and air becomes occluded. Under such conditions, the movement of oxygen has to take place through the water filled pores. This movement of oxygen in water-filled pores is limited by the maximum concentration of oxygen in water which is about 11 mg/L (at 11 °C). In comparison the equilibrium concentration of oxygen in the atmosphere is 280 mg/L, which is almost 25 times more than the concentration in water. Additionally, the rate of oxygen diffusion is four orders of magnitude lower in water than in air. Therefore, in order for the cover to effectively limit the oxygen movement, the saturation level of the cover should be kept at higher levels (between 85 % and 90 %) (Yanful 1993).

2.3.1 Desulphurized tailings material as oxygen barrier cover

Mining waste and its remedial measures to avoid environmental contamination have been an area of discussion specially amongst the mining environmentalists (Demers et al., 2008). Tailing facilities at the mine sites are one of the major sources of contamination. These are generally protected with a top cover in order to avoid any potential reaction of atmospheric gases. In order to construct these covers fine material is generally preferred due to its ability to maintain high saturation levels impeding the ingress of oxygen to reactive tailings. However, availability of fine materials to construct these covers at many sites is limited and sourcing of such material could be cost prohibitive.

In order to address the unavailability of fine materials to construct covers, the use of tailings themselves as a cover material has been found to be an alternate option. This generally requires additional processing of the tailings and extensive research in order to assess the effectiveness of such tailing materials for the cover construction has been carried out in the last couple of decades (e.g. Dobchuk 2002; Romano et al., 2003; Yanful et al., 2004; Demers et al., 2008; Mbonimpa et al., 2011; Dobchuk et al., 2013; Pabst et al., 2014;). Before reactive tailings can be used as cover materials they are processed to be converted to a material of low sulphide concentration and the resulting material is called desulphurized tailings. The concentration of sulphide in desulphurized tailings is lowered to a level at which the potential to react with oxygen and water are significantly minimized.

Bussie`re and Aubertin (1999) used desulphurized tailings and till material for their studies in order to evaluate the efficiency of covers with capillary barrier effects (CCBE). They

constructed six cells, including five with covers and one without a cover in 1995 and monitored them until 1999. All the covers were placed over reactive sulphidic tailings. The monitoring was carried out to record the volumetric water contents, matric suction, oxygen flux and chemical composition of the leachate. The experiment was conducted at a site near Val d'Or, Quebec. The sulphate and metal concentration results of fine desulphurized cover compared well with that for the till cover. It was concluded that the desulphurized tailings can be used as fine material in the CBCE for limiting the generation of AMD.

Demer et al. (2008) carried out a laboratory column study to assess the performance of a desulphurized tailing material to prevent AMD generation. In their study they considered different configurations of tailing column thicknesses with and without desulphurized tailing covers. Additionally, they also varied the water table to study the effects of elevated water table conditions. In addition to desulphurized tailing covers they also considered, water covers and covers constructed with coarse materials. They reported that placement of desulphurized tailing covers resulted in significant benefits in comparison to uncovered tailings. It was observed that the placement of mono layer desulphurized tailing cover resulted in no significant amount of metal in the effluent discharge at the bottom of the tailings and the pH generally remained close to neutral conditions. It was also observed that for elevated water table conditions the performance of mono layer desulphurized tailing was significantly better than the lower water table configuration. The oxygen flux at the interface between cover and reactive tailings was measured. It was noted that a certain amount of residual sulphur content in the desulphurized tailings covers initiated

the beneficial oxidation (without generating AMD) in the covers reducing the oxygen flux available to generate AMD.

Demers et al. (2009) carried out an experimental and modeling study in a follow up to their previous work (Demers et al., 2008). The study comprised of oxygen diffusion and consumption assessment by column testing and numerical modeling. The study employed low sulphide tailings covers in similar configurations to that of their previous study (Demers et al., 2008). It was concluded that the depth of the water table is a key parameter for the desulphurized tailing covers to work more efficiently. Additionally, they modelled the oxygen fluxes at different locations including the top, bottom and cover-tailing interface of the columns and observed that the oxygen fluxes were significantly lower at the interface of cover-tailings. It was noted that the thickness of the desulphurized cover had little effect on the oxygen diffusion through the covers.

2.3.2 Effect of saturation on oxygen diffusion

Two main components; soil solids and voids exist in soils (Fredlund et al., 2012). In unsaturated soils air and water fill the voids and control the hydro-mechanical behavior of soil (Estabragh et al., 2017). An increase in water saturation (amount of water) increases the water volume in a given soil sample. The water takes over some of the air filled spaces and hence the volume of air in the soil decreases. Conversely, the air takes over the voids if water is dispelled out from the soil. The water removal initiates generally from the soil macro-pores and then it continues in to the micro-pores as the saturation continues to reduce. If the process continues, more air fills the voids and water pathways become more tortuous. On the other hand, an increase in the degree of water saturation

makes the paths tortuous for the air phase, and if it increases to a certain degree of saturation the air in the soil becomes disassociated. The diffusion rate of oxygen in water is about 4 orders of magnitude lower than in air, therefore, the discontinuity in the air phase (which occurs at high saturation levels) impedes the oxygen transport in the unsaturated soils.

Different degrees of water saturation and their effects on the effective diffusion coefficient (D_e) for Heath Steele till was studied by Yanful (1993). Effective diffusion is a term which is generally used for the diffusion coefficient in the soil solute transport considering an effective distance (tortuous distance) between two points of variable concentration as opposed to the linear distance. In the experimental soil column, the concentration of the oxygen at the top of the column was maintained at a known value. The oxygen was allowed to diffuse through the soil and it accumulated at the base of the column. The experiment was run until steady state conditions were achieved. The experiment was carried out at different moisture content levels for the same soil. Based on the experiments, it was concluded that with an increase in the degree of saturation, the coefficient of diffusion decreased, with greatest decrease occurring at a saturation range of 85 % - 95 %. For a 10 % to 45 % saturation range no considerable effects on the diffusion coefficient were observed.

Higher degree of water saturation principle works in the oxygen barrier (tailings) covers to limit the supply of oxygen to the reactive tailings from surroundings. Humid climate generally favours these cover to maintain the high degree water saturation levels. Additionally, certain design parameters which can control the degree of saturation in a cover are water table and the hydraulic properties of the cover material.

2.3.3 Modelling of oxygen transport through soil cover

Molecular diffusion is the dominant process in the soil for oxygen transport (Troeh et al., 1982; Nicholson et al., 1988; Yanful 1993). This process is generally considered to be fickian in nature and can be represented with Fick's first law, which states that for steady state conditions the diffusive flux is directly proportional to the concentration gradient. Mathematically this can be expressed as follows:

$$F = -D_e(\frac{\partial C}{\partial x}) \quad (2.6)$$

where:

F = diffusive mass flux (kg/m^{2}s),

D_e = effective diffusion coefficient (m^2/s),

C = concentration (kg/m^3). In this study, it is concentration of oxygen in soil, and

x = distance in the direction of diffusion (m). For the case of soil covers oxygen generally travels from the atmosphere to the tailing through the soil cover, the distance is generally termed as depth.

The negative sign in Eq. (2.6) represents that the flux is flowing in the direction opposite to the increasing concentration. The determination of flux through Eq. (2.6) can be done analytically using relatively simple boundary conditions (Crank, 1975) or more recently through numerical calculations (Rowe and Booker, 1985; Bussie`re and Aubertin, 1999;

Aubertin et al., 2000). In all cases determination of effective diffusion coefficient is essential (Aubertin et al., 2000).

Effective diffusion is a function of volumetric air content (θ_a) in the soil because the diffusion in air is much higher than that in water (Aubertin et al., 2000). The volumetric air and water contents are functions of water saturation (S) commonly referred as just saturation. At 100 % saturation the volumetric air content (θ_a) is zero and at 0 % saturation the volumetric water content (θ) is zero. This can be mathematically represented as follows:

$$\theta_a = n(1 - S) \tag{2.7}$$

$$\theta = n - \theta_a = nS \tag{2.8}$$

where

n = porosity of the soil.

The effective diffusion coefficient is the weighted sum of effective diffusion coefficient in the air and in the water phase and can be expressed mathematically as follows:

$$D_e = D_a + HD_w \tag{2.9}$$

where:

D_a = effective diffusion in the soil through the air phase,

D_w = effective diffusion in the soil through the water phase, and

H = dimensionless form of Henry's equilibrium constant (0.028 at 25 °C). It is a ratio between the concentration of oxygen in aqueous and gas phases.

The effective diffusion coefficient for air and water can be expressed as follows (Aubertin et al., 2000):

$$D_a = \theta_a D_a^o T_a \quad (2.10)$$

$$D_w = \theta D_w^o T_w \quad (2.11)$$

where:

D_a^o = air diffusion coefficient in open air. Generally taken as 1.8 x10^{-5} m^2/s,

D_w^o = water diffusion coefficient in open water. Generally taken as 2.5 x 10^{-9} m^2/s,

T_a = tortuosity coefficient in air, and

T_w = tortuosity coefficient in water.

Collin (1987) and Collin and Rasmuson (1988) proposed the following relationships to estimate the values of tortuosity in air and water phases:

$$T_a = (\theta_a^{2X+1})/n^2 \quad (2.12)$$

$$T_w = (\theta^{2Y+1})/n^2 \quad (2.13)$$

where the typical values of X and Y for soils were proposed by Aubertin et al. (2000) which ranges from 0.6 to 0.75 with $X \cong Y$. Alternatively X and Y can be iteratively solved using the two equations below;

$$\theta_a^{2X} + (1 + \theta_a)^X = 1 \tag{2.14}$$

$$\theta^{2Y} + (1 + \theta)^Y = 1 \tag{2.15}$$

Substituting Eq. (2.7), Eq. (2.8), and Eq. (2.10) to Eq. (2.15) in Eq. (2.9), results as follows:

$$D_e = D_a(1 - S)^2[n(1 - S)]^{2X} + HD_w S^2(nS)^{2Y} \tag{2.16}$$

When solving for the effective diffusion using analytical or numerical methods it can be decomposed into equivalent porosity and apparent diffusion (Aubertin et al., 2000). In this case, the effective diffusion can be represented as follows:

$$D_e = n_{eq} D^* \tag{2.17}$$

where:

n_{eq} = equivalent porosity of the media, and

D^* = apparent diffusion coefficient.

Under completely dry or saturated conditions the equivalent porosity can be taken as "n". For any other saturation level between 0 and 100 % the two way paths (air and water) must be taken into account, and in this case Eq. (2.9) can be written as follows:

$$n_{eq} = n_a + Hn_w \tag{2.18}$$

Nicholson et al. (1988) noted that the consumption of oxygen also occurs during its transport through soil covers. The major factors which influence the rate of oxygen consumption are surface area, type of sulphide mineral, oxygen concentration, saturation and temperature. Using Eq. (2.6) and incorporating the consumption of oxygen in the cover, the one dimensional form of Fick's second law can be written as:

$$\frac{\partial}{\partial t}\left(\theta_{eq} C\right) = \frac{\partial}{\partial y}\left(D_e\right)\left(\frac{\partial C}{\partial y}\right) - K_r C \tag{2.19}$$

where:

K_r = effective reaction rate coefficient (1/s).

The effect of particle surface area on the effective reaction coefficient can be expressed by using equation proposed by Collin (1998) for pyrite oxidation.

$$K_r = \frac{k'6}{D_h}(1-n)C_p \tag{2.20}$$

where:

k' = constant of reactivity of pyrite with oxygen ((m^3O_2)/((m^2 pyrite).year)),

D_h = effective particle diameter (m), and

C_p = pyrite concentration (kg/kg dry tailings).

Collin (1998) approximated the value of k'as 15.8 x 10^{-3} (m^3O_2)/((m^2 pyrite).year) and Dobchuk (2002) and Dobchuk et al. (2013) also used this value in their calculation at Detour Mine tailings covers.

The value of D_h can be determined from the results of grain size distribution. Aubertin et al. (2000) proposed following equation to evaluate the value of D_h.

$$D_h = [1 + 1.17\, log(C_u)]D_{10} \tag{2.21}$$

where:

C_u = uniformity coefficient and ($= D_{60}/D_{10}$),

D_{10} = grain diameter corresponding to 10 % passing (m), and

D_{60} = grain diameter corresponding to 60 % passing (m).

2.4 Surface Moisture Flux

Hydraulic head and/or flux boundary conditions generally fulfill all the requirements to solve the problem related to moisture movement in classical soil mechanics. However, near the ground surface the moisture flux related to unsaturated soils requires a special type of boundary condition which interacts with atmospheric conditions at the ground surface. In this boundary condition the moisture flux at the ground surface moves upward during evaporation and during infiltration it enters in to the soil (Wilson et al., 1997).

Estimation of the magnitude and direction of the moisture flux at the ground surface is very important in predicting the water balance for engineered structures such as soil

covers. The water balance works on the principle of mass conservation in a closed system. A portion of water from precipitation which enters the soil surface will either come out of the system by evaporation or will percolate to the deeper layers resulting in an increase in moisture storage in the soil. If the intensity of a particular precipitation event exceeds the infiltration capacity of the soil surface runoff will be generated. The water balance at the ground surface can be mathematically expressed as follows:

$$NI = P - AE - RO \tag{2.22}$$

where:

NI = net infiltration (mm/day),

P = precipitation (mm/day),

AE = actual evaporation (mm/day), and

RO = surface runoff (mm/day).

Precipitation is the primary input parameter to the above mentioned equation and it is recorded at the weather stations on a sub-hourly, hourly or daily basis. It is generally recorded in the form of rain or snowfall.

The soil surface allows the water to infiltrate at a certain rate. This rate is controlled by the saturated hydraulic conductivity and the water storage capacity near the ground surface. If the rate of the precipitation remains lower than the saturated hydraulic conductivity of the soil surface, it will infiltrate. If the precipitation intensity is more than the saturated hydraulic conductivity of the soil surface, then the quantity in excess of

hydraulic conductivity will stay at the surface. This quantity will either result in accumulation of water at the ground surface or generation of surface runoff.

Actual evaporation (AE) quantifies the actual moisture movement from the soil surface to the atmosphere. It is generally less than the potential evaporation (PE). The potential evaporation is the amount of water that can evaporate if unlimited amount of water is available at the ground surface. Potential evaporation is the function of prevailing atmospheric conditions such as net radiation, wind speed, relative humidity and temperature. The net radiation form the sun and wind try to pull water away from the wet ground surface. In the process the ground surface starts to dry and the soil suction near the surface increases. This results in increase in the soil affinity to hold water. The struggle between climate and soil affinity to hold the water results in reduced evaporation (i.e. actual evaporation). In instances where the ground surface does not dry and remains wet with ample supply of water, the actual evaporation will become equal to the potential evaporation. In order to study the methods for predicting the actual evaporation, the principles related to the potential evaporation need to be understood (Fredlund et al., 2012).

2.4.1 Potential evaporation

Thornthwaite (1948) proposed an empirical equation to estimate the potential evaporation. The significance of his methodology is in its simplistic approach as it requires lower number of input parameters. The input parameters required to predict PE using Thornthwaite (1948) equation are mean monthly temperature and duration of daylight. Thornthwaite (1948) equation for the daily PE can be written as follows:

$$PE_d = 0.533\left(\frac{L_d}{12}\right)\left(\frac{N}{30}\right)\left(\frac{10T_a}{I}\right)^{a_t} \quad (2.23)$$

where:

PE_d = daily potential evaporation, mm/day,

L_d = number of daylight hours, h,

N = number of days in the month,

T_a = mean monthly air temperature, °C,

I = summation for 12 months of function $\left(\frac{T_a}{5}\right)^{1.514}$,and

a_t = complex function of variable I and can be written as follows:

$$a_t = (6.75 * 10^{-7})I^3 - (7.71 * 10^{-5})I^2 + (1.79 * 10^{-2})I + 0.492$$

Assuming a 30-day month and 12-h of daylight in each day of the month Eq. (2.23) for the monthly PE value can be written as follows:

$$PE_m = 16\left(\frac{10T_a}{I}\right)^{a_t} \quad (2.24)$$

where

PE_m = monthly potential evaporation, mm/month.

Thornthwaite (1948) method is widely used in different engineering disciplines to determine PE due to its simplicity and minimum input requirements. However, the method has some limitations in determining the peak PE values due to inherent time lag between

air temperature, peak surface temperature, and peak solar radiation (Wilson, 1990). Additionally this method may not be reliable over shorter time periods due to its use of mean monthly air temperature (Wilson, 1990).

Pereira and Pruitt (2004) described that Camargo et al. (1999) have reported that the monthly predictions of PE by Thornthwaite (1948) equation can be improved if the effective monthly temperature is used instead of the recommended average temperature. Camargo et al. (1999) determined the effective temperature empirically and found it to be a function of average temperature and the difference in daily extreme temperatures. The effective temperature can be expressed as follows:

$$T_{ef} = \frac{1}{2} p(3T_{max.} - T_{min.}) \quad (2.25)$$

where:

T_{ef} = effective temperature, °C,

p = an empirical parameter, 0.72 was found to be statistically most feasible,

$T_{max.}$ = maximum daily air temperature, °C, and

$T_{min.}$ = minimum daily air temperature, °C.

Penman (1948) proposed a method to predict the potential evaporation from water bodies or saturated ground surfaces. The method uses Dalton-typed formulation with the heat budget equation and requires routine climatic parameters such as relative humidity, air

temperature, wind speed, and net radiation. The Penman (1948) method can be expressed mathematically as following:

$$PE = \frac{\Gamma Q_n + \eta E_a}{\Gamma + \eta} \quad (2.26)$$

where:

PE = potential evaporation, mm/day,

Γ = slope of saturation vapor pressure versus temperature curve kPa/°C,

Q_n = net radiation at the water (or saturated ground) surface, mm/day,

η = psychometric constant, kPa/°C,

E_a = $2.625(1 + 0.146W_w)(u_{v0}^{air} + u_v^{air})$, mm/day,

W_w = wind speed, km/h,

u_{v0}^{air} = vapor pressure in the air above the water (or saturated ground) surface, kPa, and

u_v^{air} = saturated vapor pressure at the mean air temperature, kPa.

2.4.2 Actual evaporation

Actual evaporation and net infiltration are important parameters in order to quantify the water balance at the soil-atmosphere boundary. Wilson (1990) proposed an equation for determining the actual evaporation by extending the Penman (1948) approach for

predicting the PE from water (or saturated) surface. This equation is generally known as Penman-Wilson formulation (1990) and can be written as follows:

$$AE = \frac{\Gamma Q + \eta E_a}{\eta A + \Gamma} \tag{2.27}$$

Where:

AE = actual evaporation, mm/day,

A = inverse of relative humidity at soil surface.

The Penman-Wilson formulation accounts for net radiation, wind speed, and relative humidity of air and soil surfaces. The formulation reduces to the original form of Penman (1948) when the surface become saturated and the factor "A" in Eq. (2.27) becomes equal to unity.

In case the measurement of net radiation are not available, the AE can be determined using the known PE data as follows (VADOSE/W, 2014):

$$AE = PE\left[(u_v^{soil} - u_v^{air}) \,/(u_{v0}^{soil} - u_v^{air})\right] \tag{2.28}$$

where:

PE = potential evaporation, mm/day, and

u_v^{soil} = vapor pressure in the soil at the ground surface temperature, kPa,

u_v^{air} = vapor pressure in the air above the soil surface, kPa, and

u_{v0}^{soil} = saturated vapor pressure in the soil at the ground surface temperature, kPa.

2.4.3 Runoff

Runoff is the portion of precipitation which is unable to infiltrate into the soil. It stays at the surface and will flow down slope if it does not encounter any barrier or depression. Stone et al. (1996) states that the phenomenon of runoff can be well understood based on the infiltration capacity concept. In this concept Horton (1933) stated that the infiltration rate describes the maximum rate at which water can infiltrate the soil under the given conditions. At the beginning of a rainfall, the soil holds its maximum storage capacity for the duration of that event. With continuous precipitation, the soil storage increases while its potential to store water decreases. As the soil reaches its maximum storage and is unable to further store water, water starts accumulating at the soil surface. Initially, it starts filling the surface depressions and when the depressions are full., it starts moving on the surface in the direction of the sloped gradient. This surface overland flow is generally called as “Hortonian Overland Flow”. The runoff is reported as saturation-excess overland flow when the groundwater table intersects the ground surface (Dunne and Black, 1970).

2.4.4 Net infiltration

The net effect of precipitation, actual evaporation and runoff is called net infiltration at the ground surface. As defined by Horton (1933) infiltration is the process in which the soil soaks or absorbs water. The term is generally confused with “percolation”. But percolation is the process in which the water flows due to gravity under a zone of aeration (Horton,

1933). Net infiltration is the net available water at the boundary surface to flow into the soil.

2.5 Variably Saturated Flow in Porous Medium

Henry Darcy in 1856 presented his famous equation for the groundwater flow in saturated porous media. He described that the groundwater flow depends on the hydraulic gradient. The groundwater always flows in the direction from high hydraulic head to low hydraulic head. This is known as Darcy's law and can be mathematically represented as follows:

$$q = -k_s i \tag{2.29}$$

where:

q = groundwater Darcy flux, m/s,

k_s = saturated hydraulic conductivity, m/s,

i = hydraulic gradient ($i = \frac{dh}{dx}$),

h = hydraulic head, m, and

x = horizontal distance, m.

The negative sign in the equation shows that the direction of flow is from high hydraulic head to the low hydraulic head.

Buckingham (1907) studied the movement of soil moisture and found that the parameter "k" in Darcy's equation has a direct relation with matric suction in the soil. He described

that the hydraulic conductivity in the unsaturated porous media is a function of matric suction.

During his research on capillary conduction of liquids through porous mediums, Richards (1931) used Darcy-Buckingham principle to present his famous equation for flow in unsaturated porous media. The equation which is known as Richards' equation and can be expressed (in pressure head form) in one dimensional vertical form as following:

$$\frac{\partial}{\partial z}\left[k(\Psi)\left(\frac{\partial \Psi}{\partial z}+1\right)\right]=C(\Psi)\left(\frac{\partial \Psi}{\partial t}\right) \tag{2.30}$$

where:

$k(\Psi)$ = hydraulic conductivity as a function of matric suction, m/s,

$C(\Psi)$ = specific moisture capacity ($\frac{\partial \theta}{\partial \Psi}$),

Ψ = matric suction, kPa, and

z = position, m

Richards' equation is used to simulate unsaturated flow in many disciplines such as civil engineering, soil and environmental sciences (Mein and Larson, 1973; Freeze and Cherry, 1979).

The parameters "z" and "t" in Eq. (2.30) are independent variables. The matric suction "Ψ" is a dependent variable and closely related with volumetric water content through SWCC. The water content from of the Richards' equation can be expressed mathematically as follows:

$$\frac{\partial \theta}{\partial t} = \frac{\partial}{\partial z}\left[D(\theta)\left(\frac{\partial \theta}{\partial z}\right)\right] + \frac{\partial}{\partial \theta}k(\theta) \quad (2.31)$$

where:

D = Diffusivity, $(k(\frac{\partial \Psi}{\partial \theta})$

Use of volumetric water content instead of suction is sometimes advantageous due to its known general range (0 to 0.5) (Wilson, 1990). However, this equation has limited scope only works for homogenous systems. Additionally, water content form of Richards' equation becomes discontinuous when soil is fully saturated.

2.5.1 Soil water characteristics curve

Soil water characteristics curve (SWCC) provides a constitutive relationship between volumetric water content and matric suction. Soil water characteristics curves characterise different material types. The SWCCs of different materials are obtained by measuring the water content changes at a range of matric suction values during drying or wetting of the samples. However, for a particular material type, the SWCC is not unique and it shows a hysteretic behaviour between drying and wetting curves. Figure 2.1 shows a typical drying SWCC between volumetric water content and suction.

The key features of the SWCC are air entry value and residual water content. For the drying curve, the matric suction value at which the air starts entering the soil macro pores is called the air entry value or bubbling pressure (Ψ_a). In other words, it is the matric suction at which water starts draining out of the soil sample. The drainage of soil sample continues with increasing matric suction but at a certain high matric suction value the

water stops draining and beyond this point the volumetric water content remains relatively constant regardless of increasing matric suction pressure and this volumetric water content is called the residual volumetric water content (θ_r). The volumetric water content at 100 % saturation is called the saturated water content (θ_s) and it depends on the porosity of the soil.

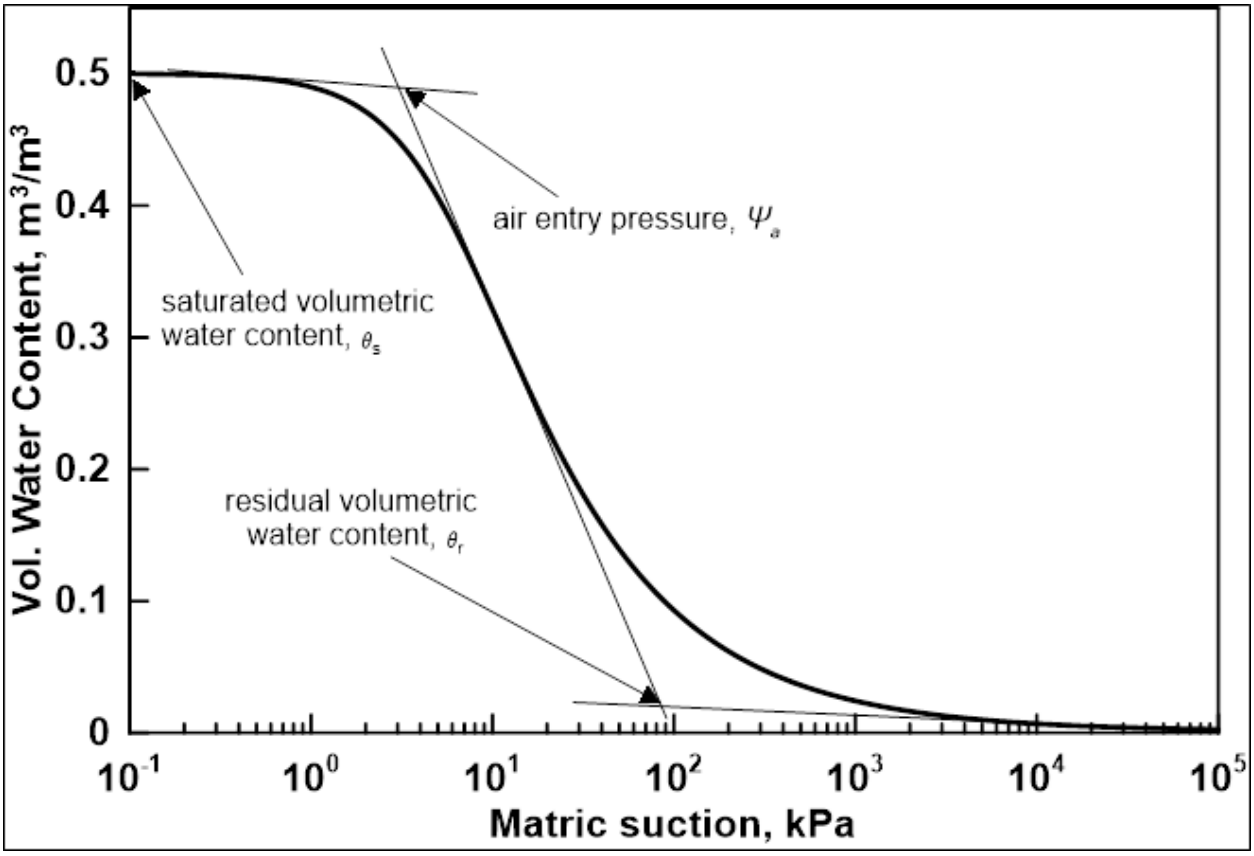

Figure 2.1. Soil water characteristics curve

Many constitutive relationships have been developed in order to numerically model the SWCC. The most widely used model was developed by van Genuchten (1980). However, the earlier developed model by Brooks and Corey (1964) has also been used by many researchers.

The soil water characteristic curve function given by Brooks and Corey (1964) can be mathematically expressed as follows:

$$\Theta = \left[\frac{\Psi_a}{\Psi}\right]^{\lambda}; \Theta = \frac{\theta - \theta_r}{\theta_s - \theta_r} \quad (2.32)$$

where:

Θ = effective saturation

Ψ_a = air entry or bubbling pressure, kPa,

Ψ = matric suction, kPa,

λ = pore size distribution index,

θ_s = saturated volumetric water content, and

θ_r = residual volumetric water content

The "λ" controls the shape of the SWCC. For smaller values of "λ" the curve shows a gradual decrease in the volumetric water content with increasing matric suction. The volumetric water content drops rapidly if the value of "λ" increases. Figure 2.2 shows two SWCCs with different "λ" prepared using Brooks and Corey (1964) model keeping all other parameters identical. In the figure, the curve "a" (has smaller "λ" value) shows gradual decrease in volumetric water content as compared to curve "b" (has larger "λ" value) which shows rapid drop in volumetric water content with increasing matric suction.

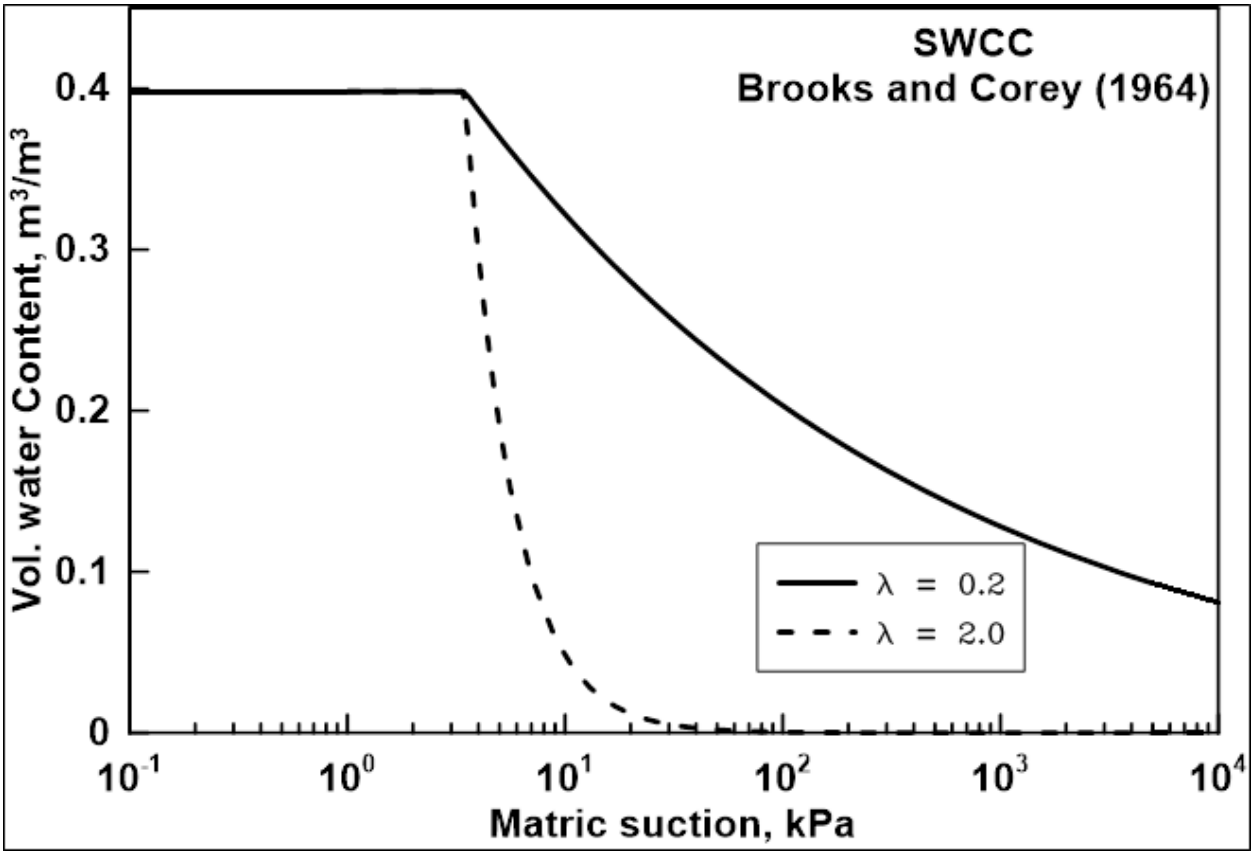

Figure 2.2. SWCC using Brooks and Corey (1964) model

van Genuchten (1980) proposed a closed-form equation to model SWCC. This model is shown in Eq. (2.33).

$$\Theta = \left[\frac{1}{1+(\alpha\Psi)^n}\right]^m \tag{2.33}$$

where:

α = curve fitting empirical parameter with inverse of air entry value, kPa^{-1},

Ψ = matric suction, kPa,

n = curve fitting empirical parameter, and

m = curve fitting empirical parameter.

The empirical parameter "n" controls the slope of the volumetric water content. The inverse of parameter "α" is generally related to the air entry value of the soil. Whereas the parameter "m" is generally constrained by the relation $m = 1 - 1/n$ (Bitterlich et al., 2004).

2.5.2 Soil hydraulic conductivity

Hydraulic conductivity of the soil is a measure of how easily the water can flow through the soil layer. It depends on various parameters such as the intrinsic permeability of the material, degree of saturation, density and viscosity. The hydraulic conductivity of the saturated media is a single value and known as the saturated hydraulic conductivity. However, the hydraulic conductivity of unsaturated soil is a function of matric suction and/or volumetric water content. It can be measured either through testing or estimated through a soil water characteristics curve.

Brooks and Corey (1966) proposed their equation for the prediction of the hydraulic conductivity function which can be written as follows:

$$k = k_s(\Theta)^{\frac{2}{\lambda}+l+2} \tag{2.34}$$

where:

k = hydraulic conductivity, m/s

k_s = saturated hydraulic conductivity, m/s,

l = tortuosity parameters, and

van genuchten (1980) proposed a closed-form equation for the hydraulic conductivity function using the Mualem (1976) capillary tube model . The equation is expressed as follows:

$$k = k_s \Theta^l \left[1 - \left(1 - \Theta^{\frac{1}{m}}\right)^m\right]^2 \; ; \Theta = \frac{\theta - \theta_r}{\theta_s - \theta_r} \; ; m = 1 - \frac{1}{n} \qquad (2.35)$$

where:

l = a constant generally taken as 0.5.

2.5.3 Hydraulic principles

Volumetric water content is a function of capillary or suction pressure and represents a state of saturation in unsaturated soil. At fully saturated conditions all pores are filled with water and the soil has a zero matric suction pressure. At this stage the volumetric water content is called the saturated volumetric water content. The suction pressure increases as the soil drains. The draining process in the soil starts with the macro pores in the soil.

2.5.3.1 Capillary principle

Figure 2.3 shows a volumetric water content relationship with pressure head. At zero pressure head, the soil saturation is 100 %. The grain size of the soil generally controls the shape of SWCC. Coarse grained soil exhibits generally more macro pores as compared to fine material. In Figure 2.3 sand material shows a sharper decline in water content for comparatively low air

entry pressure head. While the silt loam has a higher air entry value and shows a gradual decline in volumetric water content with increasing matric suction. Sand tends to drain more quickly with a small drop in pressure head as compare to the silt loam once they pass by their threshold pressure (air entry pressure) (Nicholson et al., 1989).

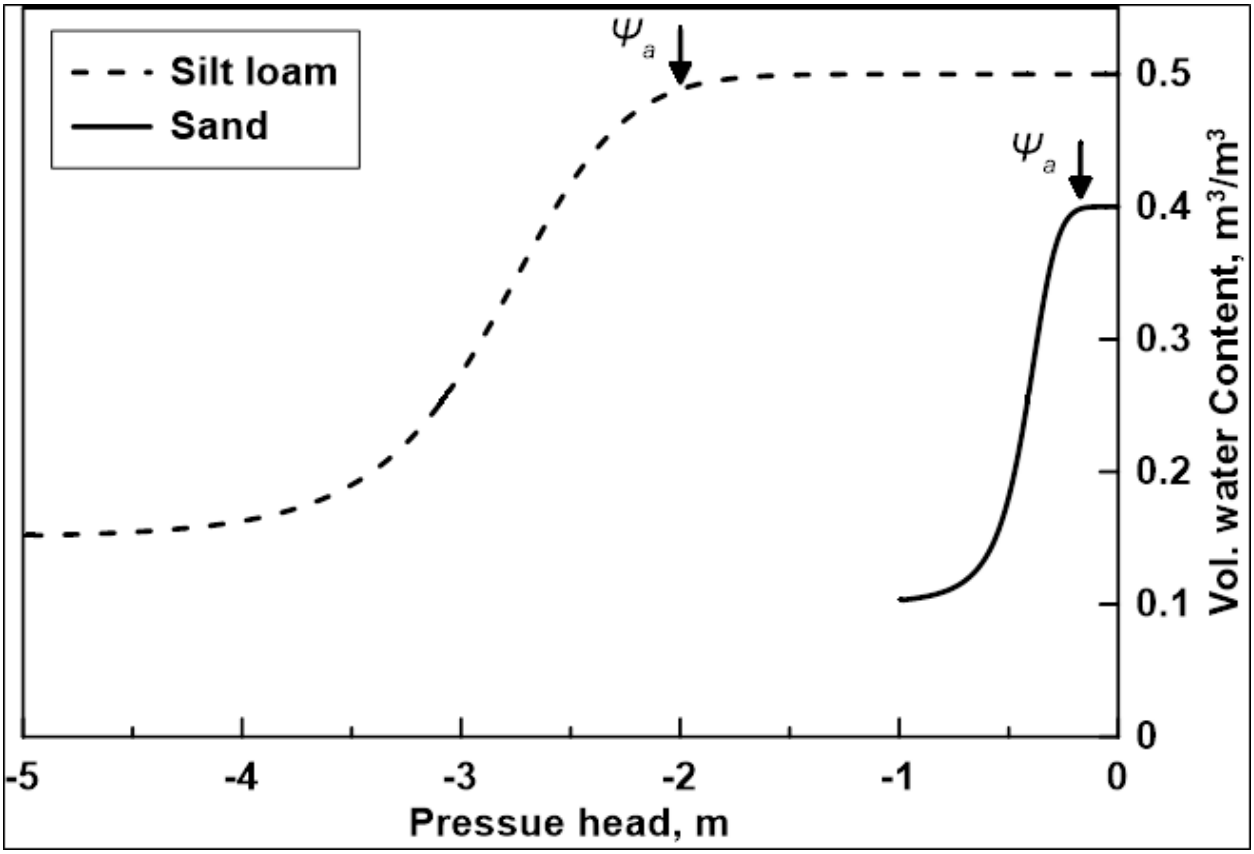

Figure 2.3. SWCC for sand and silt loam (modified from Gillham (1984)).

The soil having high air entry pressure head will generally show more capillary rise. Therefore, such soil can keep the conditions at or near to the saturation even a few meters above the water table. Figure 2.4 is the same figure as shown in Figure 2.3 but rotated by 90 degrees clockwise. Considering the ground surface at point B, the silt material will keep the soil saturated at or close to its saturation due to the capillary rise. However, sand will show its saturation close to its

residual water content conditions because the capillary rise is limited only for few centimeters. If the ground surface is considered at point C, which is also above the groundwater table will exhibit the high saturation conditions for both types of material. Based on this hydraulic principle, the high saturation condition can be achieved even above the groundwater table (Nicholson et al., 1989). If the fine material is used in the soil cover which will result in reduced oxygen transport to the tailings.

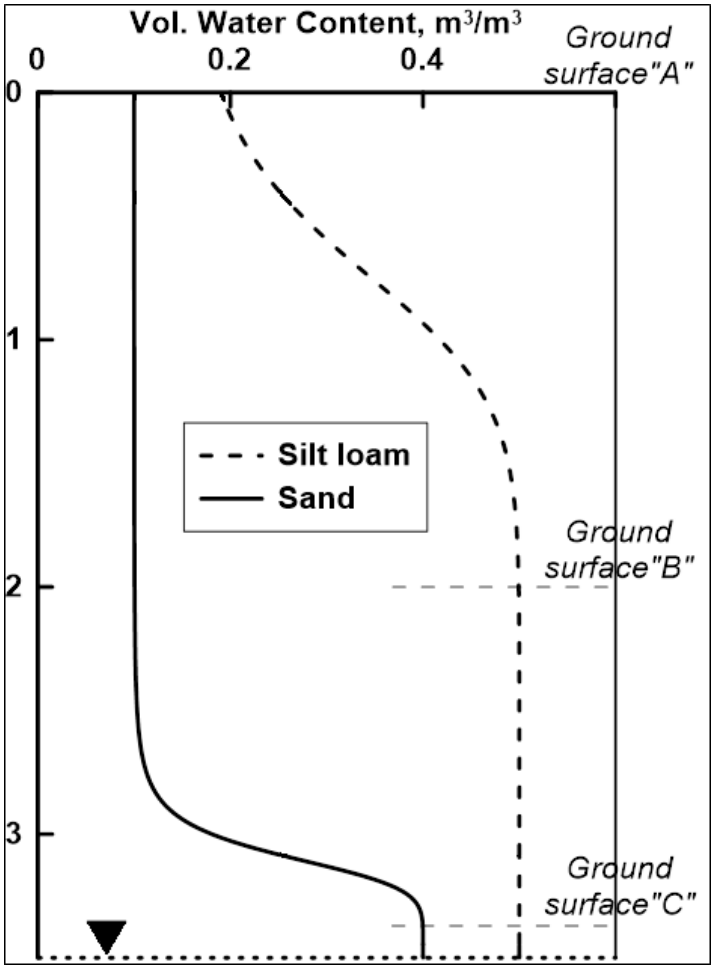

Figure 2.4. A hypothetical vertical section showing expected response of SWCC with depth for sand and silt loam units from Figure 2.3 (modified from Gillham (1984))

2.5.3.2 Capillary barrier effect

A capillary barrier considers a configuration of fine material overlaying a coarse material. It works under the principle that the fine and coarse layers have a high contrast in their hydraulic conductivity functions (Stormont and Anderson, 1999; Williams et al., 2011). The top fine layer in this configuration holds water until it is removed through evaporation, percolation or horizontal flow due to hydraulic gradient. The capillary barrier can be better explained with help of Figure 2.5. At dry conditions and low suction, the fine material has an indefinite hydraulic conductivity. As the soil gets more moisture the suction increases, and so does the hydraulic conductivity of fine material. The hydraulic conductivity during dry conditions is immeasurably small in the coarse material. The hydraulic conductivity of the coarse material shows insignificant increase with increase in moisture and suction until it overcomes the water entry value. With this principle, the fine layer achieves the increase in moisture without allowing the water to percolate to below coarse layer. However, breakthrough occurs when the suction value at the interface of fine and coarse layer drop below the water entry pressure of the coarse layer. At this stage the hydraulic conductivity of the coarse material increases drastically and the water flow starts percolating from fine to coarse layer (Dwyer 2003).

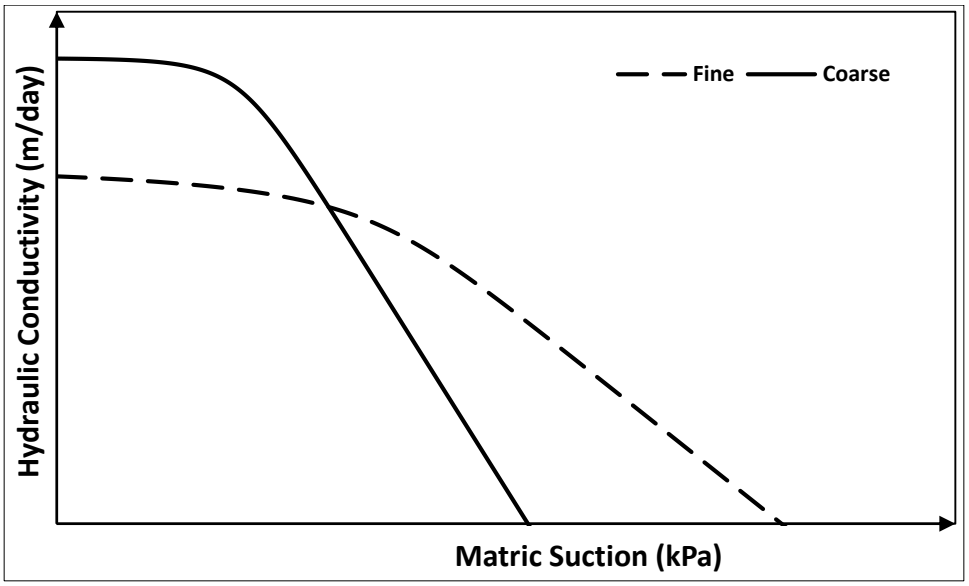

Figure 2.5. Hydraulic conductivity functions for coarse and fine material

2.6 Evolution of Soil Hydraulic Properties

Soil cover materials are generally selected based on the results of laboratory testing. However, post construction properties of the soil cover materials evolve under site specific geochemical, biological and physical process (Meiers et al., 2011). Such process may involve freezing and thawing, and wet and dry cycles, root growth and death, and burrowing of worm and insects. The freezing & thawing cycle and wetting and drying cycle bring volume changes to the soil. The root growth and death and burrowing worms creates voids in the soils (Benson et al., 2007).

The volume changes are more prominent in fine material. Soils with fine material experience desiccation cracks due to freeze/thaw and/or dry/wet cycles. These cracks influence the hydraulic properties of the soil. With development of cracks the hydraulic conductivity increases which will ease the flow of water in the cracks. The hydraulic

properties after evolution generally control the behavior of the water flow in the soil cover on long term basis (Benson et al., 2007).

Changes in the hydraulic behavior of soil covers due to desiccation cracking have been studied by various researchers (Benson et al., 1995; Yesiller et al., 2000; Nahlawi and Kodikara, 2006; Musso, 2013). Hydraulic conductivity increases with increase in extent and frequency of cracks in the soil. The extent of cracks shows no significant changes after two to three wet/dry cycles (Yesiller et al., 2000). Therefore, hydraulic conductivity of the material during first couple of wet/dry cycles would experience significant increase.

Benson et al. (2007) carried out an extensive study on water balance covers throughout the USA. In their study, they considered 10 sites in different states with variable climate conditions. They collected large diameter soil samples from each site to check their hydraulic properties in the lab and then compared them with the results collected at the time of construction. Large diameter samples were collected in a way to account for the changes in the soil due to all the process (freeze/thaw, root growth, burrowing). The comparison of the data at the time of construction and 2-4 years after construction showed that hydraulic conductivity increased by as much as 10^{-4} times from its original value. Coarse textured soil showed less variation in the hydraulic properties as compared to the fine material. The van Genuchten parameters "n" and "α" increased by as much as 1.3 times and 1000 times, respectively, from their original values.

Scanlan (2009) carried out extensive research to study the effects of root-induced changes in soil hydraulic properties. In his PhD dissertation, he mentioned that the plant roots can increase or decrease the hydraulic conductivity of the soil. He reported that

hydraulic conductivity was lower when the roots were young and growing. However, increases in the hydraulic conductivity were observed when the roots begin to decay. Decay of roots created voids in the soil and created small channels. He concluded that the changes in the pore geometry created by roots is the dominant process which control the hydraulic behavior of the soil.

Evolution of the hydraulic conductivity of covers on a saline-sodic overburden dump were studied by Meiers et al. (2011). The cover consisted of glacial soil and dumped shale material. They measured the hydraulic conductivity for the material at site after construction and compared it with its design values. The hydraulic conductivity of the underlying shale material was found to increase by one order of magnitude during a single cycle of freeze/thaw. They found that the dominant process for changes in the hydraulic properties were due to freeze/thaw cycles.

Climate is one of the major factors which influences directly or indirectly all the process (freeze/thaw, dry/wet, root growth, burrowing) occurring in the soil. Freeze/thaw and dry/wet cycles which influence the soil porosity are impacted due to extreme temperature variations. The amount of water availability (due to precipitation or soil water storage) have potential to effect the root growth and/or root decay. Migration of vegetation zone due to variation in in climate parameters can effect the burrowing animal (Karmakar et al., 2016). The process occurring in the soil as discussed are greatly controlled by the climatic conditions at their location and any change in the climate will effect on the its performance.

2.7 Climate Change

The era of late ‘80s to early ‘90s of the twentieth century is generally considered as the beginning period for the recent development in the field of climate change. In this very period the intergovernmental panel on climate change (IPCC) issued their first assessment report in 1990. This report can be considered as the real beginning for the current state of climate change knowledge (Pachauri and IPCC 2008). Since then the IPCC have issued five assessment reports and one supplementary report. The second assessment report was issued in 1995, third in 2001, fourth in 2007 and the fifth in 2013-2014. The report issued in 1992 was supplementary to the first scientific assessment report. Each assessment report composed of the three volumes prepared by separate working groups. It also includes the synthetic report and summary report for the policy makers.

Climate change is a global phenomenon. Global annual precipitation is increasing during the last century (Ren et al., 2013). However, the change in precipitation is different in different part of the world. For example, Northern Europe, and the eastern parts of North and South America have an increasing precipitation trend while it’s on decline in the Mediterranean, southern Africa and southern Asia (IPCC 2008). Similarly, the change in temperature, which overall increased by 0.6 °C during last the century, is also not uniform through continents (IPCC 2001). Proximate countries, even different regions within the same country can expect different climate change trends.

Canada has experienced an increase in the total annual precipitation by 16.5 % during 1950 to 2009 (Mekis and Vincent 2011). Of this, 12.5 % is from annual rainfall while about

the remaining 4 % is snowfall. Increasing annual snowfall is observed on recording stations in Northern Canada, while Southern parts have shown decrease in annual snowfall (Mekis and Vincent 2011). Similarly, during the same period, an overall increase in the near surface air temperature is reported to be 1.3 °C across Canada which is more than twice the global average (Barrow et al., 2004).

2.7.1 Prediction of future climate

The most highly developed tool which is used to predict the future climate is known as general circulation models (GCMs). These models depict the climate using a three dimensional grid over the globe using the mathematical models applying the laws of physics. The general horizontal resolution of these models is between 250 km to 600 km (IPCC 2001). To make the prediction viable and compare well to the expected climate, the GCMs are run first for a few decades. If the results compare well with the real climate of atmosphere and ocean, the model are repeated for increasing concentration of greenhouse generation scenarios. It is not necessary that concentration scenarios will represent the actual climate change, however, this provides different choices for the best estimate (IPCC 2001).

The recent circulation models used in Canada are fourth generation Atmosphere General Circulation Models (AGCM). These are upgraded models from the previous third generation models (Government of Canada, 2017).

As explained earlier that the prediction of climate is made for different greenhouse gases (GHG) emission scenarios. IPCC issued a Special Report on Emission Scenario (SRES)

in their third assessment report (AR3) published in 2000. Based on this report, the projections of climate change heavily depend on the human activity (future development) and predictions of future climate are made using an assumption of different levels of GHG generation by the year 2100. The report describes six families of emission scenarios namely; A1Fl, A1B, A1T, A2, B1, and B2. In this report A1 and A2 represent rapid economic growth and regionally oriented economic development respectively. B1 and B2 represent global and local environment sustainability respectively. These emission scenarios were also part of fourth assessment report (AR4).

The more recent assessment report (AR5) published in 2014 provides four different emission scenarios called representative concentration pathways (RCPs). The recommended RCPs are RCP 2.6, RCP 4.5, RCP 6.0, and RCP 8.5. The increasing number of RCP indicates more accumulation of radiative force; the RCP 2.6 represents the best case scenario with the lowest concentration of radiative forces by the end of 2100 whereas RCP 8.5 shows the worst case scenario where the concentration of radiative forces will be the highest at end of 2100. The RCP with number 4.5 and 6.0 are called intermediate emission scenarios (IPCC, 2013).

2.7.2 Climate change effects on soil cover

The basic function of the tailings covers is to limit the possible contamination due to generation of AMD to the surrounding surface and/or groundwater. These covers are generally designed for a longer period of times (sometimes a hundred to a thousand years). Climate is a key input for the preliminary design of these covers. The prediction of tailing covers to perform well on a long term basis depends mainly on its adaptability

to the future climate changes. The design considerations for the tailing covers to adapt the future climate variations, depend mainly on the prediction quality of the future climate. The design of the cover will be robust and effective if it is accounted for the climate change.

No detailed studies are available for the assessment of tailing covers in Canada for future prediction of climate change data. In 2011, the Mine and Environment Neutral Drainage (MEND) program entrusted Stratoes lnc. to study the risk of AMD for the Canadian Mining sector due to climate change. It was a high level risk assessment report and a broad range of regional impacts due to climate change were studied. In this report they focused on four climate conditions; 1) increase in average temperature, 2) change in mean annual precipitation, 3) increase in frequency and intensity of extreme weather events, and 4) permafrost degradation.

In Canada, the temperature is expected to increase by 2.5 to 3.5 °C in the area where most of the metal mimes are located. They concluded that there are on average 20 more days with rain as compared to the 1950s. It is expected that this high amount of precipitation and extreme daily precipitation will increase the rate of AMD percolation at mining sites. Moreover, an increase in annual temperature is also expected in Canada. Due to high rates of snow melting, flooding conditions are expected and a high intensity of surface runoff will occur in the snow covered area of Northern Canada. These high intensity runoffs may result in flooding conditions at the tailing impoundments and can impact the stability of the impoundment dams. Approximately half of permafrost covered

area of the Canada contains permafrost warmer than -2 °C. It is expected that it would disappear (thaw) with recent rate of climate warming.

It was also noted that simple covers, store and release covers, permafrost covers, and geo-synthetic covers are susceptible to the climate change up to certain degree. Amongst these covers, geo-synthetic covers are considered to be the least vulnerable to the effects due to climate changes.

Shurnik et al., (2012) assessed the performance of soil covers at Rio Tinto Mount Tom Price mine located approximately 1000 km north-northeast of Perth, Australia. In their study, they constructed two trial covers that were 4.0 m and 2.0 m thick with coarse and fine materials, respectively, over the waste rock. They monitored the climate at trial sites for approximately 8 years from 2003 to 2010 using a weather station. Additionally, they simulated the performance of soil covers for the measured historical climate, predicted 100-year historical and predicted 100-year future climate data. The predictions of future climate set were obtained from general circulation model (GCM) using OzClim website (CSIRO Australia, 2007). After careful evaluation of the performance of different GCMs provided on the website, CSIRO Mk3.5 was selected as it provided all the required input climate parameters for the modeling software. The emission scenario, A1FI which is characterised by “rapid economic growth, a global population that reached nine billion by 2050 and then gradually decline, the quick spread of new technologies, a convergent world, and an emphasis on fossil fuels”. It represents the worst-case emission scenario. The resultant future 100-year annual average rainfall showed 42 mm increase as compared to respective historical rainfall (362 mm). The numerical modelling results showed that the net percolation slightly increased for future climate as compared to the

100-year historical climate. However, the average net percolation rate in all cases remained below 5% of rainfall.

Chapter Three: Effect of Climate Change on a Monolithic Desulphurized Tailings Cover

3.1 Abstract

A soil cover system can be viewed as a thin interface placed between the atmosphere and the underlying waste. Climate is a primary design variable in soil cover design; therefore, climate change poses a number of challenges to design, operation and long-term performance of covers. In this research climate change effects on the hydraulic behavior of soil covers at Northern Ontario site were assessed. Covers were analyzed using historical and future climate datasets. Historical climate data was compiled from Environment Canada weather station near the site. The future climate datasets were generated for different Global Climate Models (GCM) for various representative concentration pathways (RCP). The covers at site were constructed with single layer of desulphurized tailings. Soil covers were aimed to reduce oxygen diffusion by limiting oxygen ingress through increasing saturation. Oxygen flux through soil covers for current and future climates were predicted using numerical modelling techniques. The results of this research indicate that the effect of climate change on soil cover depends on its moisture retention characteristics. Fine grained covers showed better performance under adverse climate change conditions as compared to the coarse grained covers. However, both types of covers showed cumulative increase in oxygen flux for future climates.

3.2 Introduction

Generation of acid mine drainage (AMD) from sulphide enriched tailings has been a significant environmental challenge within mining industries related to hard rock (Pabst et al. 2017). The sulphide mineral of heavy metals (e.g. iron, copper, gold etc.) in the rock has the potential to react with oxygen and water. This reaction not only results in the tailings exhibiting acidic behavior but also increases the concentration of metals. Leachate produced from acidic tailings can potentially contaminate the surrounding surface and/or groundwater. Therefore, intervention is needed to avoid adding such contaminants to the environment (Nicholson et al. 1989; Lindsay et al. 2015).

By limiting the supply of oxygen to the reactive tailings, one can control the production of AMD and thus reduce the risk. This risk can be further reduced if multiple strategies are used in an effective manner to limit the oxidation of the sulphide mineral. One way to limit the supply of oxygen, is to place a layer of water (water cover) either by flooding it or dumping the reactive tailing material under water (subaqueous deposition). The rate of oxygen diffusion in water is four order magnitudes lower than that in air and solubility of oxygen in water is quite low (11 mg/L at 20°C). Therefore, the water layer will act as a barrier and in the absence of convection; the rate of oxygen diffusion through water is too slow to be of any significance to sulphide mineral oxidation (MEND, 1997). However, use of water covers results in increased percolation rates and require that operators follow stringent environmental regulations for their design and construction (Yanful et al., 2004). Other limitation of water covers is its lack of physical stability over a long period of time

and in many instances the water cover discharge will require treatment to meet regulatory standards (MEND, 1997; Ethier el al., 2018).

The alternative to water cover is to create a disconnect between the tailings and surrounding oxygen by placing a soil cover over the reactive tailings. The soil cover, also referred as a dry cover, reduces the oxygen supply to the underlying tailings by providing a moisture barrier. Engineered soil covers with saturated fine gained material can be used effectively to limit the oxygen transport due to their potential to maintain high saturation. Other important purposes of dry covers can be to limit water percolation into the tailings and thereby reducing the amount of acid water formation and reclaiming the tailings management area for other uses by revegetating the cover surface.

The elevated water table control technique has also been used to reduce the generation of AMD over a long periods of time. (Dagenais et al., 2005 ; Dagenais et al., 2006 ; Demers et al., 2008 ; Pabst et al. 2014). This technique involves raising the water level in the tailings management facility so that tailings remain in the saturated or nearly saturated state with little ingress of oxygen. The three approaches to raise the elevation of water table and associated capillary fringe in the tailings are: constructing water flow barriers within the tailings, increasing the water retention properties of the tailings, and modifying the water balance of the tailings (MEND, 1996). The water balance of the tailings can be modified by increasing the water input to the tailings. Soil covers constructed of coarse grained materials with low retention and high conduction properties increase the infiltration of meteoric water and act as good evaporation barrier to maintain or elevate the water table (Dobchuk et al. 2013; Ethier et al. 2018).

The tailing facilities are generally spread over a large area ranging in tens of hectares to more than a few hundred hectares (Nicholson et al., 1989). Construction of a soil cover with considerable thickness (one meter to a few meters) over such large areas requires a substantial volume of material. Acquisition and hauling this soil to site could cost significantly. The concept of using processed tailing materials as the cover layer material could alleviate significant costs associated with soil cover construction. The tailings are normally processed through floatation. The key aspect for the processing of the sulphide tailings is to reduce the concentration of sulphide mineral to a certain level that they start behaving as inactive material (Nicholson et al., 1989; Pabst et al., 2014, 2017).

Oxygen transport in the soil cover normally occurs through molecular diffusion (Yanful, 1993, Aachib et al., 2004). When saturation in the soil cover is less than 85 %, the movement of oxygen through the soil cover can occur freely in gaseous phase. Once the saturation increases more than 85 %, most of the air filled voids are replaced with water and air becomes occluded. Under such conditions, the movement of oxygen takes place through water filled pores and oxygen transport becomes extremely slow due to lower rate of diffusion in water. Therefore, in order to expect the cover to effectively limit the oxygen movement, the saturation level of the cover should be kept at higher levels (between 85% to 95 %) (Yanful, 1993).

Cover objectives are site specific but generally include dust and erosion control, control of oxygen ingress, control of contaminant release by infiltration reduction, minimization of radon emission from radioactive tailings, and providing a growth medium for vegetation (Mylona et al., 2007). As most of these objectives are related to the water balance at cover surface therefore, climate is a primary design variable in any soil cover system. In

addition, soil covers must be designed for long-term or perpetual containment of the waste. Therefore, climate change poses a number of challenges to the design, operation and long-term performance of covers (Bashir et al., 2015). The loss of performance due to climate change might be in terms of increased ingress of water into the underlying waste or erosion of the cover to support vegetation due to increase in amount and intensity of the precipitation. Similarly, drought conditions compounded with increased temperatures could result in lower saturation in the cover resulting in increased oxygen ingress to reactive tailings or deterioration of hydro mechanical cover material properties affecting performance. The covers that are more prone to climate change effects are store-and-release covers or covers that rely on permafrost for their performance (Stratos Inc., 2011). Although climate change is a real threat to the design, maintenance, and long-term performance of soil coves, there is little evidence in the peer-reviewed literature of many studies in this regard. The cold regions cover system design technical guidance document published in MEND (2011) clearly states that cover designs should be based on evaluating the potential effect of climate changes and understanding the potential for change in cover material properties on a 100-year basis. However, the document does not provide any specifics and there is no evidence in peer-reviewed literature that any analysis or design of this type has ever been carried out.

In order to evaluate the long-term performance of soil covers and their sustainability it is important to examine their response under future climate conditions. In the past, much emphasis has been given to evaluate the cover performance using historical climate records. Such studies do not take into account the probable climate change effects and may not be reflective of long term cover performance. Recently, Shurnik et al. (2012)

evaluated the performance of soil covers for both historical and future climate for a site near Perth, Australia. However, the scope of the study was limited and details are scanty. No other studies that quantify the effect of climate change on soil covers can be found in the peer reviewed literature.

In this study, the soil cover at Detour Lake Mine in Northern Ontario (Canada) was selected for evaluation. The soil cover is monolithic and there is abundance of information available in literature for this cover. Soil-atmosphere modeling with oxygen transport is used to evaluate the performance of the cover for historical and future climates.

3.3 Theoretical Background

Oxygen generally transports through the soil covers to the underlying tailings by the processes of advection and diffusion. Additionally, dissolved oxygen can also be transported to the tailings through water infiltration. However, the main transport process responsible for the movement of oxygen through soil covers is diffusion (Nicholson et al. 1989).

The oxygen transport through reactive tailings can be modeled using modified Fick's second law which can be described as follows (Geo-Slope International Ltd. 2014);

$$\frac{\partial}{\partial t}\left(n_{eq}C\right) = \frac{\partial}{\partial y}\left(D_e \frac{\partial C}{\partial y}\right) - K_r C \qquad (3.1)$$

where C shows the concentration of oxygen in the pore air (kg/m^3), $n_{eq}$is the equivalent diffusion porosity defined as $\theta_a + H\theta$, θ_a is the air filled porosity or volumetric air content

(m^3/m^3), θ is the water filled porosity or volumetric water content (m^3/m^3), H is a dimensionless form of Henry's equilibrium constant, generally taken as 0.028 at 25 °C (°C), D_e is the effective diffusion coefficient (m^2/s), K_r is the effective reaction rate (1/s) and y is the elevation(m).

Collin and Rasmuson (1988) proposed a method to estimate the effective diffusion coefficient both in the air and water phases. Based on this method the effective diffusion can be estimated as follows:

$$D_e = D_a(1-S)^2[n(1-S)]^{2X} + HD_wS^2(nS)^{2Y} \quad (3.2)$$

where D_a is the diffusion coefficient of oxygen in air (m^2/s), S is a degree of saturation, n is the soil porosity, X and Y are empirical parameters, and D_w is the oxygen diffusion coefficient in water

Aubertin et al. (2000) proposed that the typical value for X and Y used in Eq. (3.2) are in the range of 0.6 – 0.75 with $X \cong Y$. The values for these two empirical parameters can also be estimated by the solving the following two equations iteratively;

$$[n(1-S)]^{2X} + [1-n(1-S)]^X = 1 \quad (3.3)$$

$$(nS)^{2Y} + (1-nS)^Y = 1 \quad (3.4)$$

The effect of degree of saturation on effective diffusion coefficient for oxygen is well studied (Runkles 1956, Yanful 1993, Aubertin et al. 2000, Romano et al. 2003, Mbonimpa et al. 2003, Demers et al. 2008, Dobchuk et al. 2013). INAP (2009) describes a

relationship between the degree of saturation and coefficient of oxygen diffusion and illustrated that the oxygen diffusion rapidly reduces by 3 to 4 order of magnitude as the saturation in the soil cover increases above 85 %. Therefore, estimates of degree of saturation are essential in order to calculate the oxygen flux passing through the porous media (soil cover). The change in saturation within the cover profile can be estimated based on the variably saturated flow equation proposed by Richards (1931), which can be described (in pressure head form) as follows;

$$\frac{\partial}{\partial z}\left[k(\Psi)\left(\frac{\partial \Psi}{\partial z}+1\right)\right]=C(\Psi)\left(\frac{\partial \Psi}{\partial t}\right) \quad (3.5)$$

where $k(\Psi)$ is the hydraulic conductivity as a function of matric suction (m/s), $C(\Psi)$ is the specific moisture capacity ($\frac{\partial \theta}{\partial \Psi}$), Ψ is the matric suction (kPa), and z is the position (m).

The solution of Eq. (3.5) requires knowledge of the initial distribution of the pressure head within the flow domain and appropriate boundary conditions. The boundary conditions can be specified in terms of specified pressure head, flux or gradient. The surface of the soil cover is exposed to the atmosphere. Therefore, the availability of the water flux at the ground surface which can enter or leave the cover surface needed to be estimated in order to predict the changes in the saturation of cover profile. This can be done by estimating the water balance at the ground surface using the following equation;

$$NI = P - AE - RO \quad (3.6)$$

where NI is net infiltration (mm/day), P is precipitation (mm/day), AE is actual evaporation (mm/day), and RO issurface runoff (mm/day).

Precipitation is a primary input parameter in above equation (Eq. 3.6) and historical records are generally available for most weather stations. Actual evaporation (AE) quantifies the actual moisture movement from soil surface to the atmosphere. It is generally less than the potential evaporation (PE). Potential evaporation is the amount of water that can evaporate if unlimited amount of water is available at the ground surface. Runoff is the portion of precipitation which is unable to infiltrate into the soil and it stays at the surface and will flow down slope if does not encounter any barrier or depression.

The AE can be estimated based on the estimates of PE and transient soil moisture conditions. In the case of saturated soil conditions, AE is equal to PE. As the soil dries out, the rate of evaporation starts decreasing from the potential value. This is due to the fact that as soil loses moisture, the suction near the surface increases resulting in increased soil affinity to hold on to water. Several methods were proposed by Wilson during the 1990s to estimate AE (Tran 2013).

One of these methods is the so-called “Limiting Function” as proposed by Wilson et al. (1997) as reported by Fredlund et al. (2012) is given as follows:

$$AE = PE\left(\frac{u_v^{soil} - u_v^{air}}{v_{vo}^{soil} - u_v^{air}}\right) \tag{3.7}$$

where u_v^{soil} is the partial vapour pressure in the soil at the ground surface, v_{vo}^{soil} is the saturated vapour pressure in the soil at the ground surface, and u_v^{air} is the vapour pressure in the air above the soil surface. The potential evaporation in the above-

mentioned equation can be a measured value or can be calculated using an appropriate method such as Penman (1948) or Thornthwaite (1948).

3.4 Cover Evaluation

3.4.1 Site conditions

Detour Lake Mine is a gold mine located about 290 km northeast of Timmins, Ontario. The mining operation at the site started in 1983 and stopped production in 1999. The mine tailings were deposited in a dam impoundment through end pipe discharge. The mine tailings at the site consisted of sulphide content ranging from 1 to 2.5 % which had potential to act as reactive tailings (Dobchuk et al., 2013). At the end of production, a major portion of tailings facility was designed to cover by placing water cover while remaining portion was covered with soil cover. The soil cover was designed to be constructed using on-site material after its desulphurization. The desulphurization process was carried out at pilot plant which was earlier used for floatation process at site. The initial design of the cover was to construct a capillary barrier which would keep the cover saturation at higher level (> 85%) to resist the ingress of oxygen. The placement of desulphurized cover was carried out using end pipe discharge at the surface of reactive tailings during 1998-1999. It was design to keep thickness of the cover greater than 1 m near the dam and 0.5 m at the pond (Dobchuk, 2002).

The climate at Detour Lake Mine can generally be classified as moist continental, mid-latitude. The annual precipitation is approximately 920 mm with the greatest precipitation contribution coming from rainfall (Dobchuk et al., 2013). The annual potential evaporation is approximately 800 mm. The site temperature fluctuates between 37 °C in summer and

-47 °C in winter. The relative humidity varies between 50% and 90% from May to October (Barbour et al., 1993, Dobchuk et al., 2003).

3.5 Historical and Future Climate

3.5.1 Historical climate data compilation and classification

Historical and future climate data is required to evaluate covers in a changing climate. Historical climate act as baseline against which future climatic changes can be quantified. The closest Environment Canada Weather Station to Detour Lake Mine site is 290 km away in Timmins, Ontario. Dobchuk et al (2013) reported that measurements of detailed climate data at the mine site for summer months of the years 2000 and 2001 were made. They also reported that climate data measured at the site for this period correlated well with the 1971-2000 Climate Normals for Timmins Victor Power Airport weather station. In absence of multi-year daily resolution climate data for the mine site, Victor Power Airport weather station was selected for climate data compilation. A climate dataset comprising of daily records for precipitation, maximum and minimum temperature and relative humidity, wind speed and net radiation was compiled for the period 1981-2010 as part of this research.

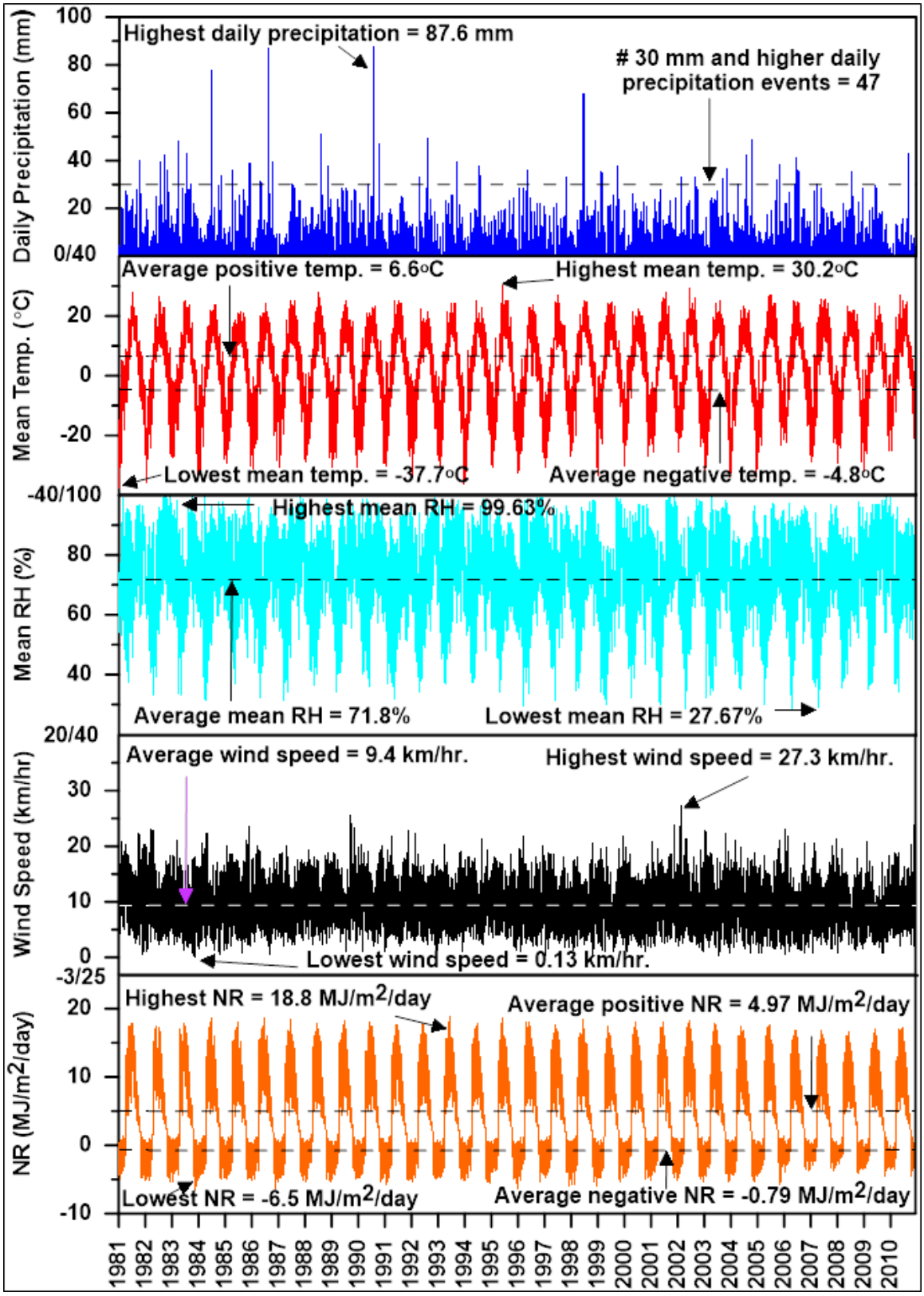

Figure 3.1. Base climate parameters at Timmins, Ontario.

Figure 3.1 shows the climate data for Timmins, ON for the period 1980-2010. Minimum, maximum and average yearly values for the data are also marked on this figure. The review of the data indicates that the average annual precipitation over the 30-years period is approximately 826 mm. Wettest year (annual precipitation approx. 1034 mm) conditions were observed in 1990, whereas the least annual precipitation (approximately. 510 mm) was recorded during the year 2010. The average annual temperature during the 30 period is 1.9 °C. Similarly, the mean annual minimum and maximum temperatures for the period 1981-2010 are -15.2 °C and 18.8 °C. The 30-year average mean relative humidity is 71.8 %. Based on the relative humidity data it is clear that mean relative humidity for inactive season is relatively higher than the active year. The 30-year average wind speed and net radiations are observed to be 9.4 km/h and 4.2 MJ/m^2/day respectively.

Climate classification can provide an estimate of water availability at the ground surface and is a useful tool in assessing the suitability of a particular type of cover considering the site's climate (Fredlund et al. 2012). The site climate classification can be done by using the Thornthwaite climate classification system (Thornthwaite 1931, 1948). Originally developed in 1931 by Charles Warren Thornthwaite the system was later modified by him in 1948. The system estimates the availability of water at the ground surface by taking into consideration the precipitation and potential evaporation at the site by estimating annual moisture index. The definition of annual moisture index was later modified as follows (Thornthwaite and Mather, 1955; Thornthwaite and Hare, 1955):

$$I_m = 100\left(\frac{P}{PE} - 1\right) \tag{3.8}$$

where I_m is the1955 Thornthwaite moisture index, P is the total annual precipitation and PE is the total annual potential evaporation. Potential evaporation in the above equation can be estimated using any appropriate method such as the Penman (1948) or Thornthwaite (1948) method. Penman (1948) is a radiation based method and requires measured values of temperature, relative humidity, wind speed and net radiation for estimation of potential evaporation. The Thornthwaite (1948) method on the other hand is the most simplified method and requires only temperature measurements for the estimation of PE (Tegos et al., 2015). As explained later in the climate change section, that reliable estimates of future climate variables apart from precipitation and temperate are difficult to obtain, therefore Thornthwaite (1948) method with a modification proposed by Pereira and Pruitt (2004) was used for the estimation of the PE in this research. According to Thornthwaite (1948), the daily PE can be estimated using mean monthly air temperature and length of daylight as follows:

$$PE_d = 0.5333\left(\frac{L}{12}\right)\left(\frac{N}{30}\right)\left(\frac{10T_a}{I}\right)^{a_t} \quad (3.9)$$

where PE_d is the daily PE (mm/day), T_a is the mean monthly air temperature (°C), I is a function of the mean monthly temperature i.e. $I = \left(\frac{T_a}{5}\right)^{1.514}$, and a_t is a function of I i.e.

$$a_t = (6.75 * 10^{-7})I^3 - (7.71 * 10^{-5})I^2 + (1.79 * 10^{-2})I + 0.492 \quad (3.10)$$

Pereira and Pruitt (2004) reported that Camargo et al. (1999) have suggested that the performance of Thornthwaite (1948) approach in monthly time scale can be improved

using effective temperature (T_{ef}) instead of the average temperature in Eq. (3.9). They expressed the effective temperature mathematically as follows:

$$T_{ef} = 0.345(3T_{max} - T_{min}) \tag{3.11}$$

where T_{max} and T_{min} are the daily maximum and minimum air temperatures, respectively.

Considering that reliable historical measurements of all the climate variables required to estimate PE using Penman (1948) method were available, a comparison between estimates from the Penman (1948) and Thornthwaite (1948) methods with the modification proposed by Pereira and Pruitt (2004) was made. The results were found to be comparable and are presented in Appendix-A. Figure 3.2 shows the climate classification for the city of Timmins for the period 1981-2010. This figure shows that on average the climate can be classified as humid, and that there is year to year variation in climate. The variation in climate reinforces that multi- year climate data sets need to be used for the design as yearly climatic conditions can vary from humid to dry subhumid.

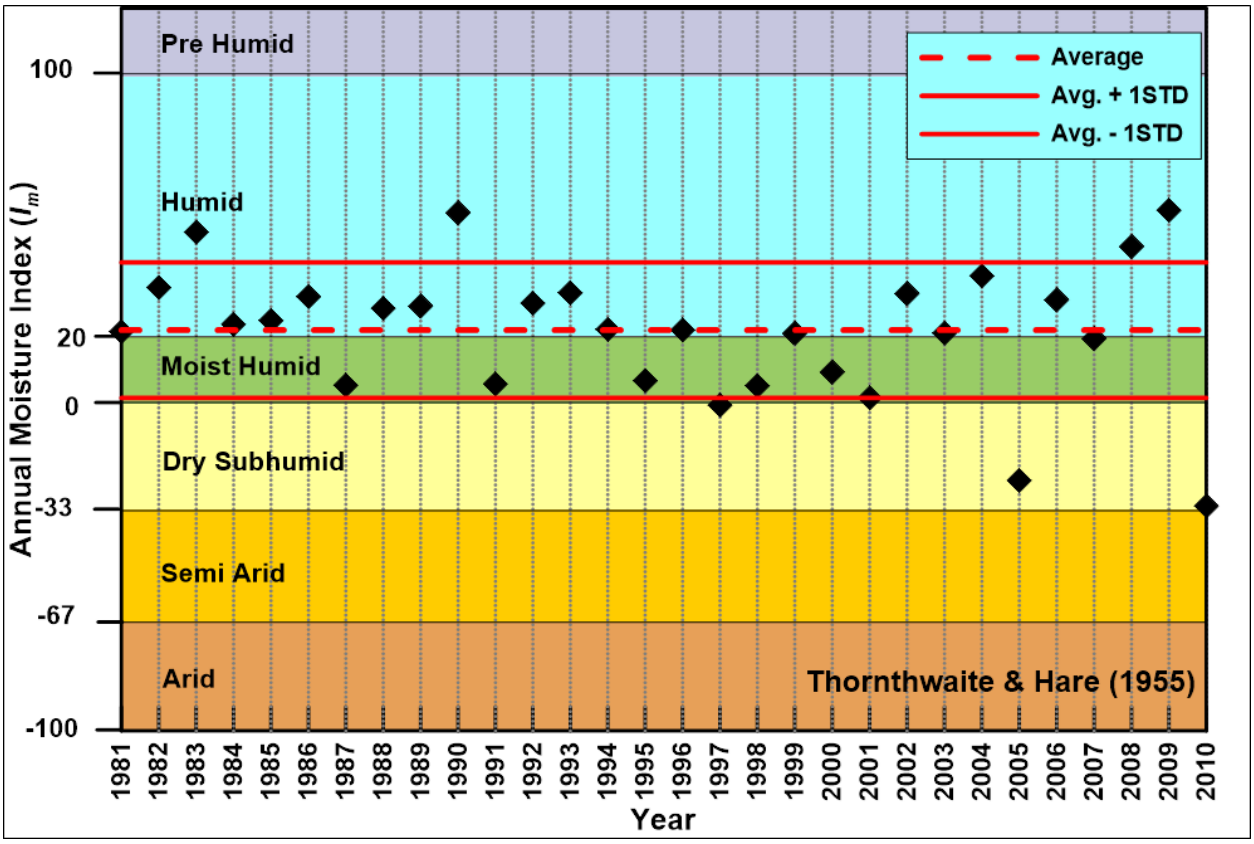

Figure 3.2. Annual Moisture Index for Timmins climate data for period 1981-2010.

3.5.2 Future climate data

Future climate data is generally generated by General Circulation Models (GCM) using different Representative Construction Pathways (RCP). The GCMs are climate models which are used for weather forecasting, understanding the climate and climate change predictions. These are computer based models which solve a set of complex equations related to the atmosphere and ocean using the applicable laws of physics to predict the earth's climate. Four different RCPs (RCP 2.6, RCP 4.5, RCP 6.0 and RCP 8.5) are suggested by IPCC (2014). Every RCP number expresses a different cumulative radiative forcing by the year 2100. The increasing number in RCP indicates more accumulation of radiative force; the RCP 2.6 represents best case scenario with the lowest concentration

of radiative forces by end of year 2100, whereas RCP 8.5 shows the worst case scenario where the concentration of radiative forces will be the highest at end of year 2100. Concentration of the greenhouse gases in the atmosphere is generally the basis for variation in the radiative forces.

The future climate data was sourced from Ontario Climate Data Portal (OCDP) housed at the laboratory of mathematical parallel systems (LAMPS) in the Department of Mathematics and Statistics at York University in Toronto, ON. The data portal provides future climate projections for precipitation, and maximum, minimum and average temperatures on 10×10 km grid resolution for the province of ON. The data is available for 33 different GCMs, and for all four RCPs (i.e., 2.6, 4.5, 6.0, and 8.5). The data covers the period from 1981-2100 (OCDP 2018), and can be downloaded from the OCDP webpage (http://lamps.math.yorku.ca/OntarioClimate/index.htm). In addition to the data with 10×10 km grid resolution, OCDP also provides data for different municipalities across Ontario. A bias-correction for the predicted climate with respect to the measured local climate data has also been applied to this data (Deng et al. 2017). Other sources of climate data for Ontario have been found to be of inferior performance in comparison to OCDP projections (Pk 2017).

The predicted future climate data for a number of different GCMs was assessed against the measured historical climate to check its performance in simulating historical climate. The predicted climate data between 1980 and 2010 was compared with the Environment Canada climate normals for the same period. The comparisons indicated that the general circulation models CCSM4, GFDL-ESM2M and HADGEM2-E5 for all RCPs performed satisfactory by predicting historical climate Normals quite well. It should be noted that the

comparison was made for both temperature and precipitation data details can be found in Appendix-B.

The future climates data was subdivided into thirty-year periods, and each period is designated as a climate ensemble. The 90 years (2011-2100) of future climate data from the three GCMs for four different RCPs formed 36 climate ensembles. Each ensemble refers to a particular GCM, RCP and a 30-year time period. Historical climate data (1980-2010) was designated as ensemble number one increasing the total number of ensembles to 37. A schematic of the climate ensembles with their corresponding GCM, RCP and time period is shown in Figure 3.3. It should be noted that ensemble # 1, comprising of historical climate is considered as base climate against which future climate datasets are evaluated.

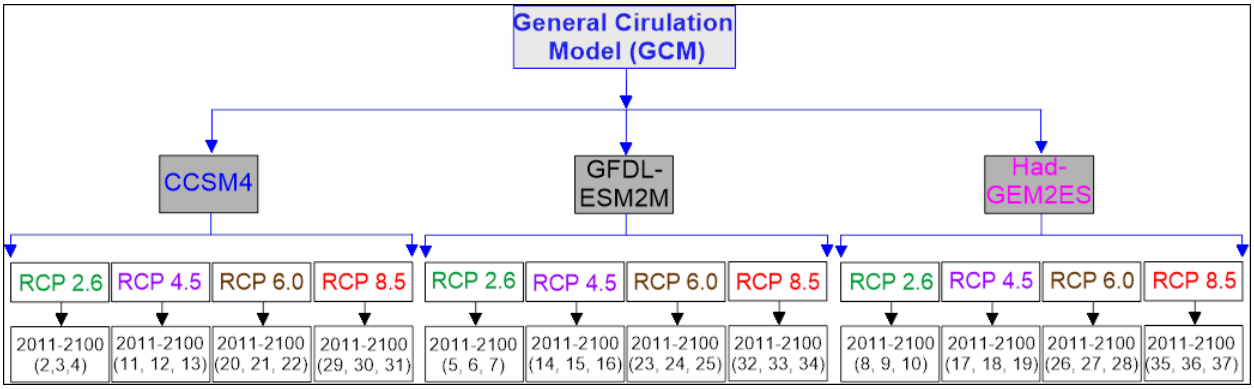

Figure 3.3. Climate ensembles corresponding to different GCMs and RCPs

The predicted data for 36 future climate ensembles was compared to the base climate. Figure 3.4 shows 30-year annual mean air temperature and cumulative precipitation for the base and future climate ensembles in the form of box and whisker plots. The lower and upper ends of the box show 1st and 3rd quartiles respectively, while the whiskers show

the two extreme values (maximum and minimum). The line in the middle of the box represents the median of the data. Review of the temperature data in Figure 3.4a shows that for all future climates ensembles the median temperature shows considerable increase over the median base value. The increasing trend in the temperature data is consistent for all GCMs and radiative forcing values. It can also be observed that in general the temperature is increasing with increasing RCPs and number of year. Consistent with the trend, the maximum temperature increase can be observed for scenarios predicted with RCP 8.5 with highest increase in temperature for the GCM Had GEM2-E5 (Climate ensemble #37).

Figure 3.4b shows 30 yearly cumulative precipitation values for all the climate ensembles. It can be observed that the median annual precipitation predicted for majority of future climate ensembles is more than the base climate. A maximum increase of approximately 17 % in in median value annual of precipitation is predicted for climate ensemble #28 (Had GEM2-ES with RCP 6.0). It can also be observed that only three out of 36 climate ensembles showed decrease in median values of precipitation, in comparison to the baseline value. The lowest median value of annual precipitation is predicted for climate ensemble #23 (GFDL-ESM2M with RCP 6.0). The extreme annual precipitation events increase for all climate ensembles irrespective of GCM, RCP or the time period. For all future climate data, the climate ensembles 35 and 32 showed extreme maximum and extreme minimum annual precipitation respectively.

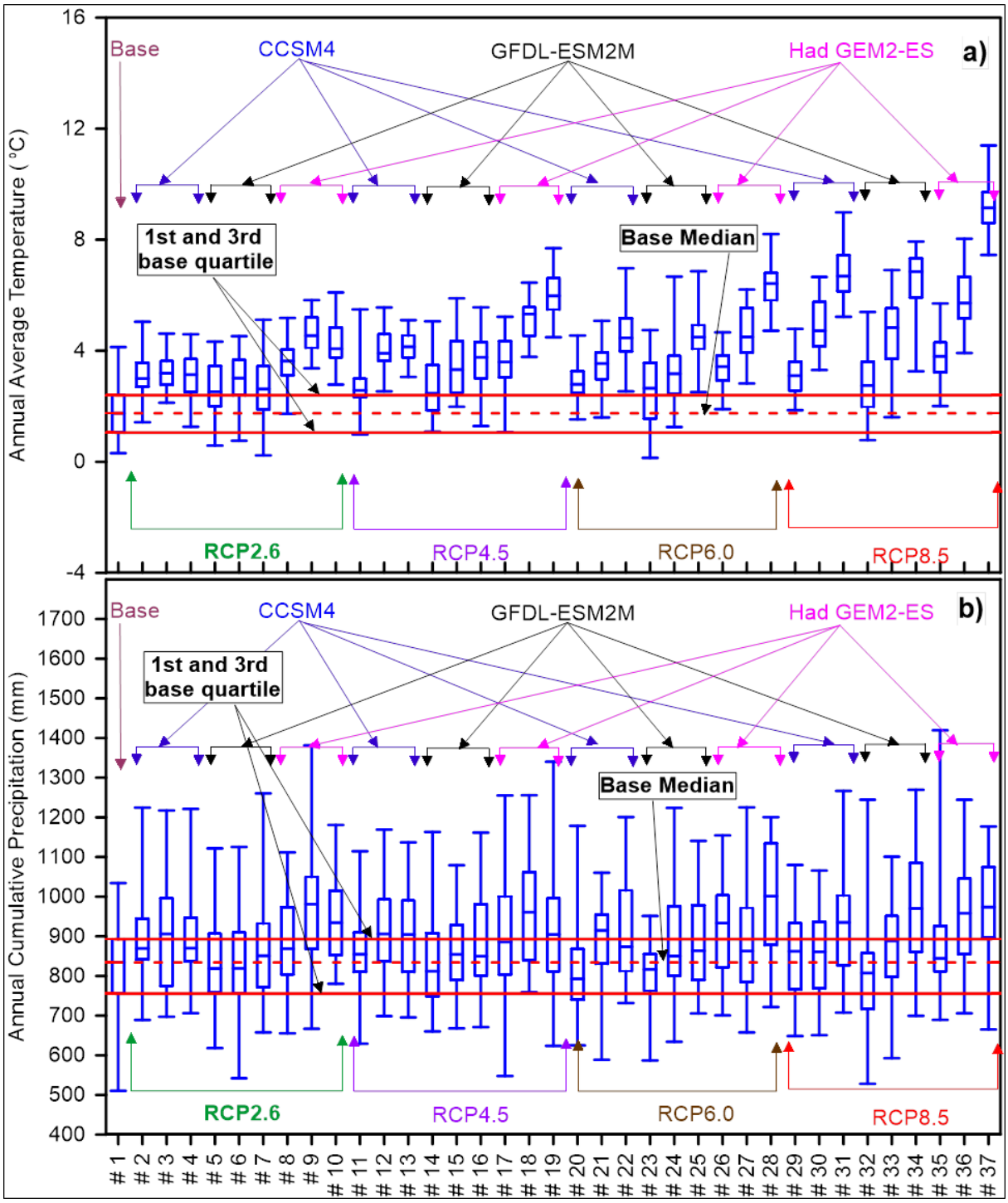

Figure 3.4. Box and whisker plot for a) annual mean temperature and b) annual precipitation for all climates.

3.5.3 Selection of future climate ensembles

For this study, the soil cover performance was assessed based on two representative future climate ensembles. The selection of these climates ensembles was based on the criteria of worst-case scenario. While selecting the representative climate ensembles it was assumed that the driest weather conditions will represent the worst cover performance, as it will result in decreased saturation resulting in increased oxygen ingress to the reactive tailings. Climate ensemble # 23 was selected as the first representative future climate (*FC-1*). This ensemble represents the lowest 30-year cumulative precipitation in all future climate ensembles as shown in Figure 3.4 above.

Lowest precipitation alone may not guarantee the driest conditions as the amount of meteoric water that enters the cover also depends on the available evaporative demand. As shown above (Figure 3.4a) a temperature increase is imminent for all future climate ensembles, it is therefore inevitable that there could be a proportional increase in the evaporative demand as well. In this instance, estimation of annual moisture index (I_m) and classification of climate for future climate ensembles is a useful exercise as it takes into consideration both the precipitation and the potential evaporation. Potential evaporation was estimated for all future climate ensembles using the modified Thornthwaite method described earlier. Estimated PE together with predicted P values were used to estimate I_m values for each individual year of every climate ensemble.

The selection of second representative future climate ensemble was based on the comparison of these I_m values. Figure 3.5 shows box and whisker plots of I_m for all climate ensembles. Each climate ensemble consists of 30 yearly values. It can be observed that climate ensemble #37 shows that the majority (more than 95 %) of the moisture indices

of this ensemble are less than the median value of the base climate ensemble. This observation indicates that the in most instances for this climate ensemble the water availability at the ground surface will be lower than the median water availability for the base climate. Therefore, this climate ensemble was selected to be second representative future worst case climate change scenario (*FC-2*).

The average annual precipitation for *FC-1* and *FC-2* are predicted to be 792 mm and 968 mm respectively. The average annual PE are predicted to be 712 mm and 950 mm respectively. It is also predicted that the mean annual temperature will increase by 0.6 °C and 7.3 °C respectively for *FC-1* and *FC-2*. As a whole, the climate is expected to act as 'moist humid' for these climate ensembles. (Figure 3.5).

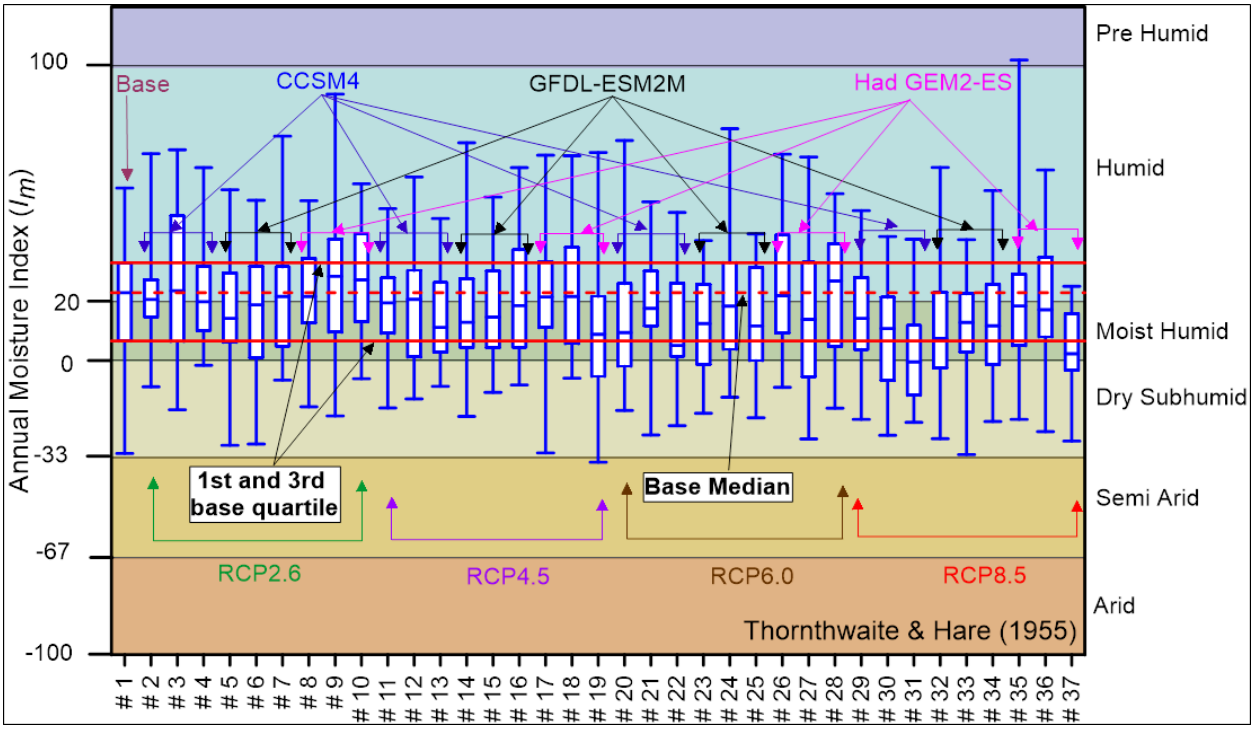

Figure 3.5. Box and whisker plot of annual moisture index for base and future climate ensembles.

3.6 Development of Soil Cover Models

3.6.1 Representative soil cover profiles

Field investigations carried out immediately after the cover placement revealed that interbedded layers of fine and coarse material exist in the engineered portion of the cover and underlying tailings (Dobchuk, 2002). This was attributed to the end-pipe discharge method of tailings and cover deposition where coarser tailings tend to get deposited near the pipe discharge and finer materials travels further away (Dobchuk et al., 2013). Representative cover and tailing profiles used in current study are shown in Figure 3.6. Dobchuk et al., (2013) used the same profiles in their numerical modeling study to investigate the controlling factors for the cover performance. These profiles are simplifications to represent complex field conditions with the intent to investigate the controlling factors of cover performance as opposed to specifically model the as-built cover (Dobchuk et al. 2013)

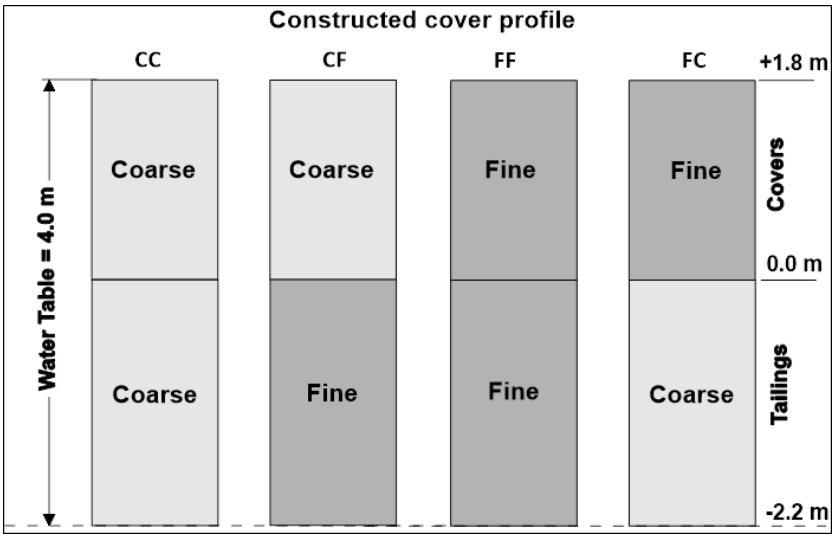

Figure 3.6. Representative profiles used for numerical modeling (Modified from Dobchuk et.al 2013).

The review of the cover profiles in Figure 3.6 indicates that for cover performance assessment a single cover thickness of 1.8 m can be assumed. The cover can either comprise of coarse or fine tailings to represent the heterogeneity observed in the cover materials during the field investigation. Similarly, covers comprising of a coarse or fine material can overlie coarse or fine acid generating tailings to represent the heterogeneity in tailings. Of the four resulting cover profiles, the profile FC represents the original cover design where the fine desulphurized tailings were to be deposited on coarse tailings to create a capillary break (Dobchuk, 2002, Dobchuk et al. 2013). According to Dobchuk et al. (2013), the CF profile most accurately represents the as-built desulphurized cover.

3.6.2 Material properties

Soil water characteristic curves (SWCC) relate the soil volumetric water content to matric suction. Frequently used form of relationship between matric suction and volumetric water content is given by van Genuchten (1980):

$$\Theta = \frac{\theta - \theta_r}{\theta_s - \theta_r} = \left[\frac{1}{1+(\alpha\Psi)^n}\right]^m \tag{3.12}$$

where Θ is effective saturation, θ is volumetric water content (m^3/m^3); θ_s and θ_r are saturated and residual volumetric water content respectively; Ψ is matric suction (kPa) and α, n and m are curve fitting parameters. $1/\alpha$ is generally related to the air entry value (kPa); n is measure of pore-size distribution and m can be related to n as $m = 1 - 1/n$. SWCCs generated based on Equation. (3.12) for fine and coarse materials are shown in Figure 3.7a. The air entry value of 6 kPa and 50 kPa were considered for coarse and fine

tailings material respectively and these are the same value which were used by Dobchuk et al., (2013). All other input parameters are also shown in Figure 3.7a.

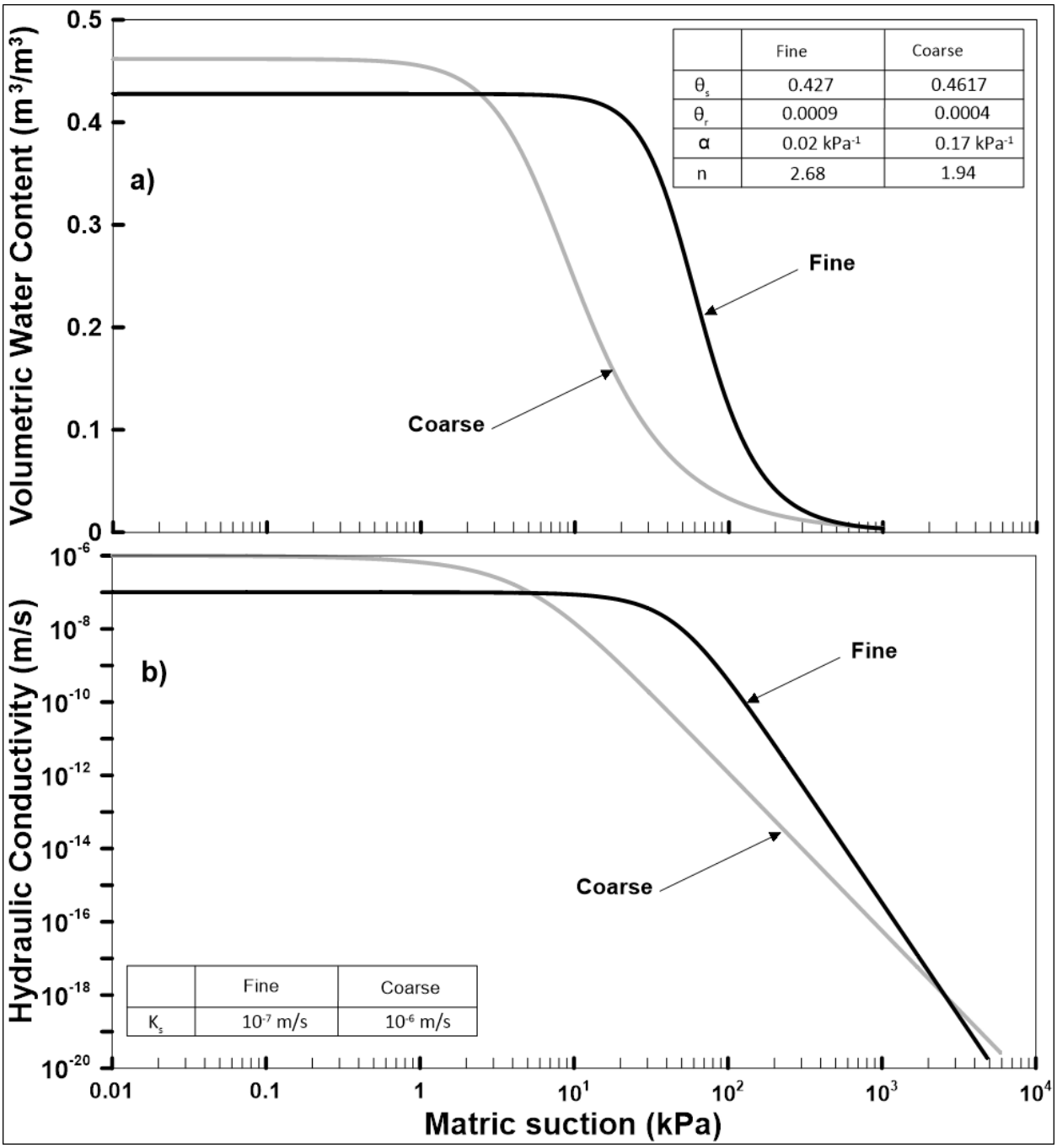

Figure 3.7. Soil hydraulic properties; a) soil water characteristics curves and b) soil hydraulic conductivity functions for coarse and fine tailings material.

van Genuchten (1980) proposed the following closed form equation to describe the hydraulic conductivity of soil as function of matric suction:

$$k = k_s \Theta^l \left[1 - \left(1 - \Theta^{\frac{1}{m}}\right)^m\right]^2 \quad (3.13)$$

where k is unsaturated hydraulic conductivity, k_s is saturated hydraulic conductivity of soil (m/s), l is constant and generally taken as 0.5, and m is an empirical parameter as explained above. The soil hydraulic conductivity function for the coarse and fine tailing materials are shown in Figure 3.7b using Eq. (3.13). The saturated hydraulic conductivity for the coarse and fine tailing material were taken as $1x10^{-6}$ m/s and $1x10^{-7}$ m/s respectively based on the measurement made by Dobchuk (2002).

3.6.3 Development of the numerical models

The numerical modeling was carried out using Vadose/W software, which is part of the Geostudio 2016 software package (Geo-Slope International Ltd. 2016). Vadose/W was primarily developed for the design of soil cover systems. It is a two-dimensional, simultaneous coupled heat transport and fluid flow finite element model with atmospheric coupling. The atmospheric coupling is achieved by estimating actual evaporation using the procedure developed by Wilson et al (1994, 1997). Vadose/W is also capable of simulating oxygen and radon transport through the soil covers. More details can be found in (Geo-Slope International Ltd. 2014 2014).

The modeling was carried out in one-dimensional domain. The model domains consisted of the cover and tailings profiles shown in Figure 3.8. The global element size in the

profiles was kept as 0.1 m. The cover layers were modeled with finer mesh as compared to the tailing layers. Additional elements were added in the geometry at the cover-tailings interface and near the ground surface. The purpose of these additional elements was to predict more precisely the flux changes at the interface and the near the ground surface layers.

Appropriate boundary conditions were applied to the soil cover models. For hydraulic boundary conditions, a zero pressure head boundary, corresponding to the depth of the existing groundwater table was applied at the bottom of the cover models. The top hydraulic boundary comprised of historical and future climate datasets. Climate datasets consists of daily values of temperature, relative humidity, wind speed, precipitation and PE. The daily values of temperature, relative humidity, wind speed and precipitation for the historical climate are generally gathered at weather station and based on these parameters, excluding precipitation potential evaporation is estimated using Penman (1948). The future predictions of daily values of temperature and precipitation are generally available through use of GCM. However, predictions of relative humidity using the temperature was estimated using Kimball et al. (1996) in current study. The predictions of relative humidity using this method were compared with other proposed methodologies and the results are shown in Appendix-C. The parameters in the climate dataset are assumed to show variation in a sinusoidal pattern over the 24-hours period except the daily precipitation. The daily precipitation is distributed uniformly over the 24-hours period. No surface vegetation was included in the model. The model was set in such a way that the surface run-off is generated without creating any additional hydraulic head on the column if the precipitation intensity exceeds the infiltration capacity of the

soil. For oxygen transport, oxygen concentration in the atmosphere is assumed to be 280 g/m^3 and is applied as the top boundary. A zero oxygen concentration boundary was assumed at the bottom of the domain. A generalized developed model is shown in Figure 3.8.

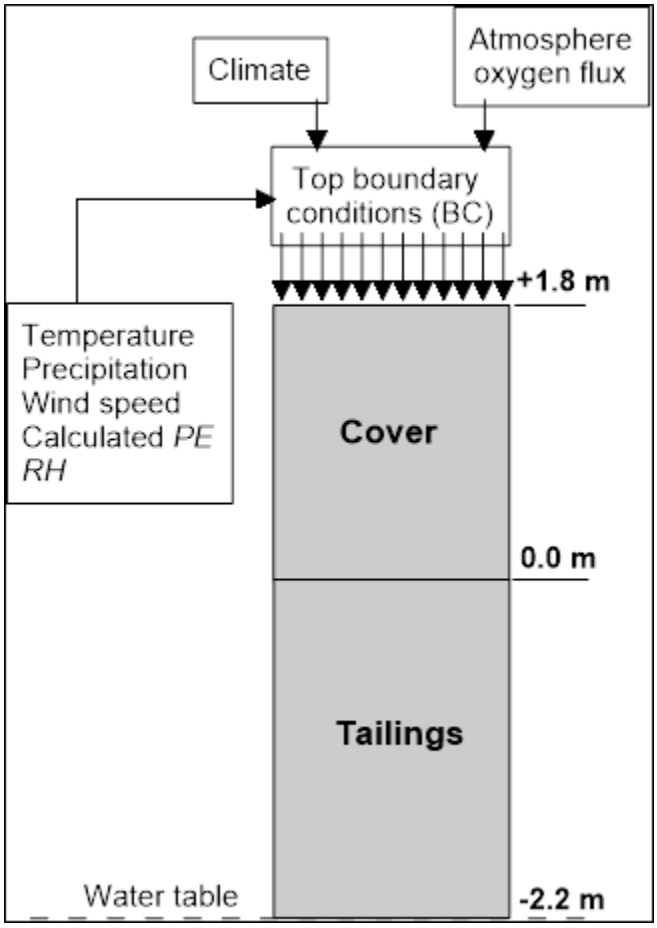

Figure 3.8. Generalized numerical model.

3.7 Modeling Results

3.7.1 Verification modeling

The ability of the VADOSE/W for predicting the water balance was investigated by Walter and Dubreuilh (2007). They compared the model outputs with the field measurements.

The results revealed that, in some instances, VADOSE/W predicted the water balance very close to the field measurements. However, in other instances, the model results did not correlate well to the field conditions. The reasons for the numerical code not being able to predict the field conditions could be due to uncertainty in the hydraulic properties, vegetation water use parameters, heterogeneous soil conditions, inaccurate representation of rainfall events, and/or unexpected generation of high surface runoff. Considering the uncertainty in the modeling results, it is generally suggested to verify / calibrate the model prior to its use for future modelling considerations.

Field measurements to verify/calibrate the model for the mine site are not available. Therefor an attempt was made to assess the suitability of the current modeling effort by reproducing the results of previous modeling studies carried out at Detour Lake Mine. Dobchuk (2002) predicted the water balance of the tailings covers at the site using the SoilCover numerical code. Although the modelling results were never quantitatively compared to the site condition, but were reported to provide a qualitative assessment of the tailings covers. The objective of the current study is to assess the climate change effects on tailings covers, therefore, verifying the model with Dobchuk (2002) modeling results will provide a consistent link to the previous research carried out at the site. To accomplish this, water balances for coarse and fine tailings covers are compared in Figure 3.9.

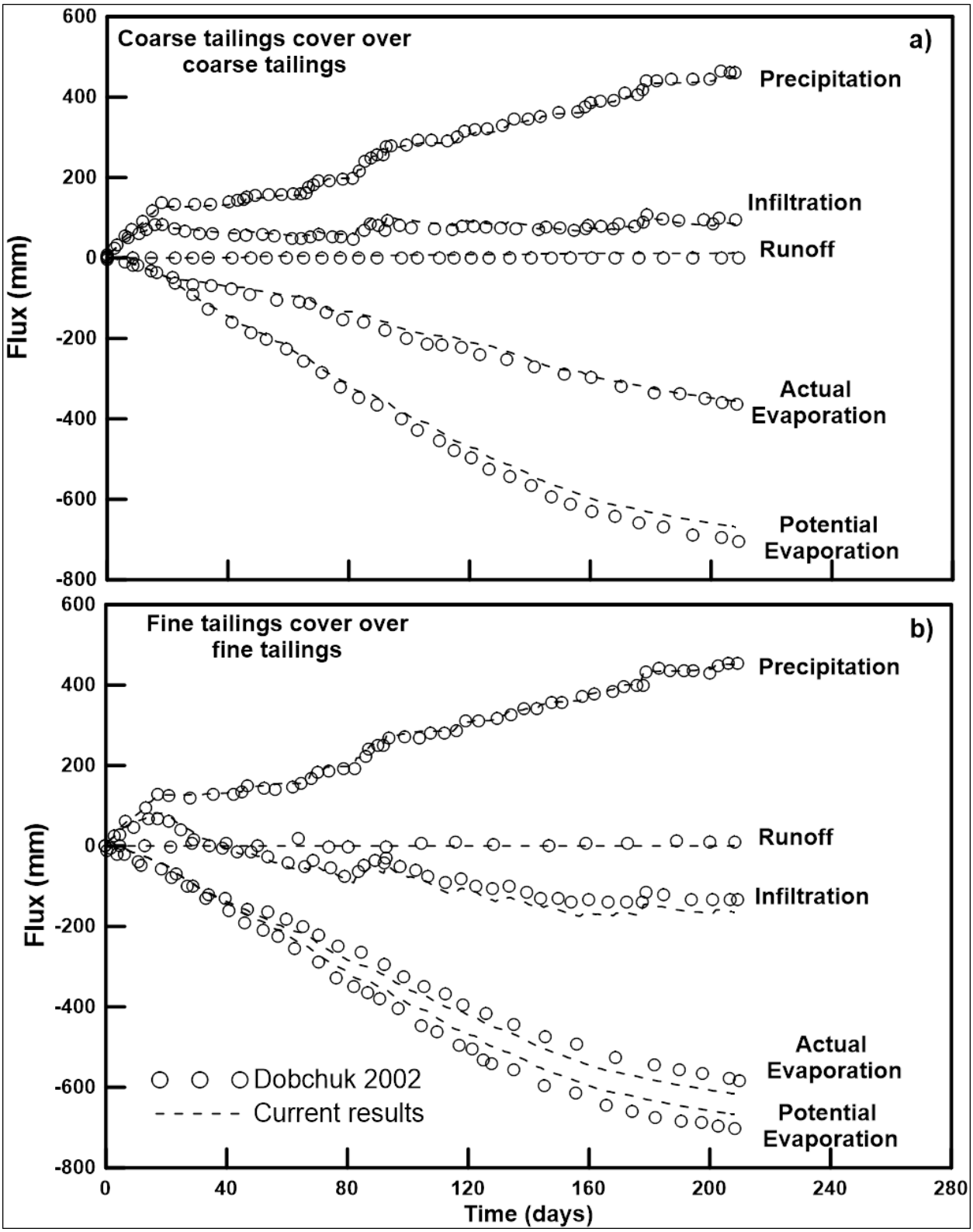

Figure 3.9. Water balance verification of a) a coarse and b) a fine tailing covers.

Figure 3.9a shows a comparison of the water balance for current and previous models for the homogenous coarse tailings cover (CC profile). The coarse tailings cover shows the annual net infiltration (NI) of about 2 % less in the current model to that of Dobchuk (2002). The current model predicts the annual surface runoff (RO) of 11 mm (2.3 %) whereas the previous results showed no surface runoff. The difference in annual actual evaporation (AE) between both models is insignificantly small (~0.01 %). About 5 % increase in potential evaporation (PE) is recorded in the current model as compared to the model by Dobchuk (2002).

The water balance comparison for the fine tailings cover are shown in Figure 3.9b. For the fine cover, both models show that the predicted annual AE is significantly more than the annual precipitation, therefore, the annual NI are negative indicating net water loss conditions at the ground surface. A difference of 6 % in NI and 7% in AE was observed between the current modeling results and those reported by Dobchuk (2002). The comparisons made in Figures 3.9a and b reveal that the water balance for the current models (coarse and fine tailings covers) are generally comparable to that of Dobchuk (2002) models. The minor variations in the results could be due to the use of different numerical code.

3.7.2 Predictive modeling

The performance of tailing covers to limit the production of AMD is generally assessed based on its ability to maintain a saturation of 85 % or higher. The *NI* and deep percolation (DP) are the key parameters which generally control the saturation in the tailings cover. Net infiltration is the quantity of meteoric water (precipitation) that enters the cover while

deep percolation is the quantity of water the moves across the tailings cover interface. The oxygen flux, that results in the generation of AMD, depends on the cover saturation. The results for water balance, oxygen flux and its relationship to time histories for the saturation and the oxygen concentration are discussed in the following section.

3.7.3 Water balance at the ground surface

The water balance at the ground surface quantifies the availability of water and evaporative demand together with quantities of water that enters or exits the ground surface. In this research the components of water balance which enter the ground surface are considered as positive while the components which exit the ground surface are considered negative. The exception is runoff which is also considered positive. The deep percolation which is the flux across the cover-tailings interface is considered positive if the flow is from tailings into the cover. Similarly, DP is expressed as a negative quantity if it flows is downwards from the cover to the tailings.

Figure 3.10 shows the water balance for the homogeneous coarse profile (CC) for dry and wet year climates for base (*BC*) and future climates (*FC-1* and *FC-2*). Dry and wet years were identified based on the lowest and higher I_m for the respective 30 years climate datasets. Annual cumulative precipitation (P) for dry years increases 19 % and 13 % for future climates *FC-1* and *FC-2* respectively in comparison to the base climate (Figure 3.10a). However, for the wet years the annual cumulative precipitation for *FC-1* is 21% lower than the baseline condition while for *FC-2* it is 9% greater than the baseline value (Figure 3.10b).

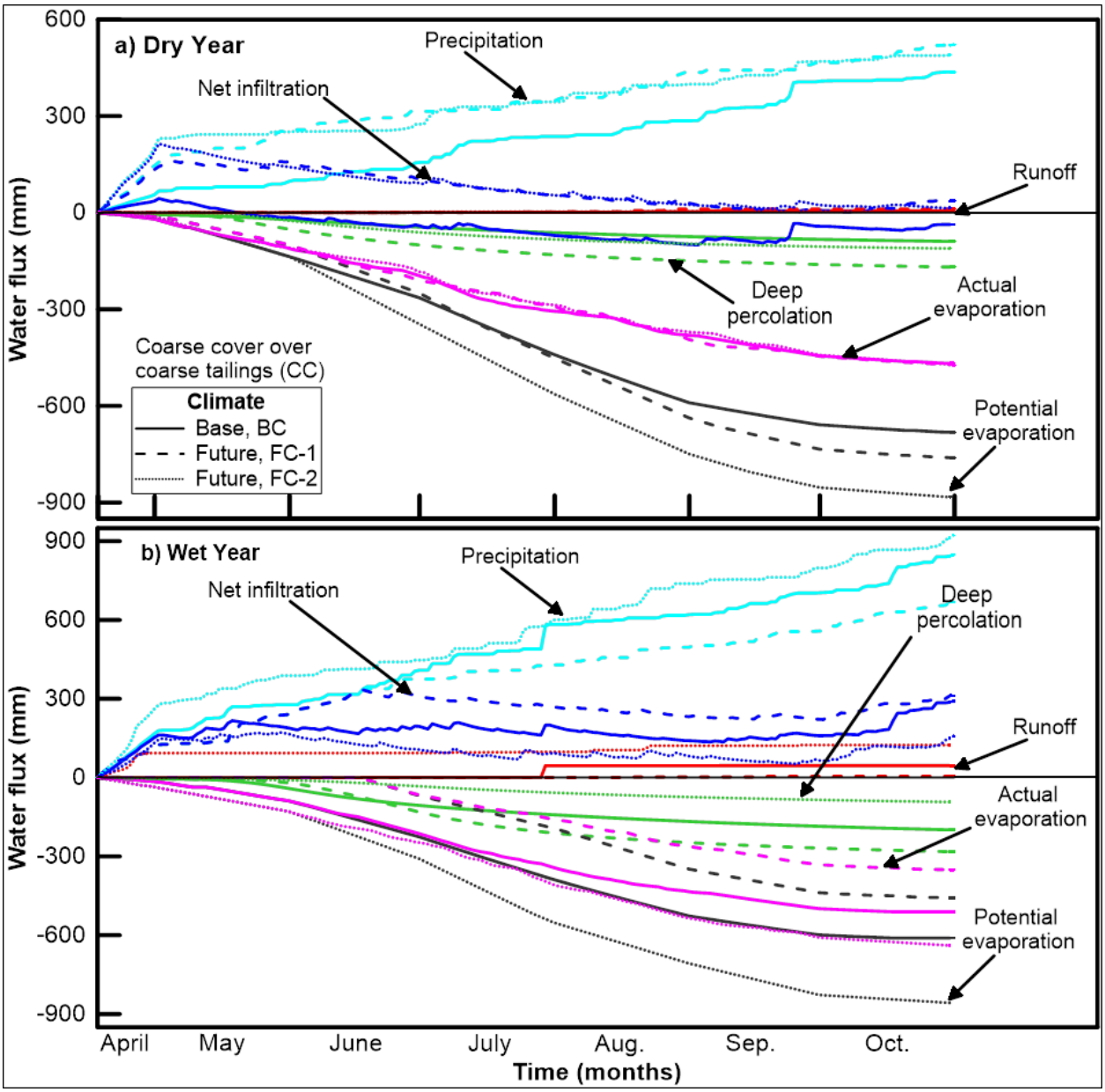

Figure 3.10. Water balance for homogeneous coarse profile, CC for a) dry year; b) wet year.

Runoff (RO) quantifies the water flowing at the ground surface and is also termed as surface runoff. The runoff generation is generally linked to the precipitation intensity, conduction and/or retention properties of the surface material. Higher precipitation intensity (than saturated hydraulic conductivity, k_s) and the soils with larger retention and

lower conduction have higher a probability to generate runoff. The homogeneous coarse profile (CC) for dry year experiences no runoff for base and future climates (Figure 3.10a). However, for wet year climates runoff quantities were observed. The maximum cumulative runoff was generated for *FC-2*, which is approximately 13 % (124mm) of the cumulative annual precipitation. Approximately 93 mm out of 124 mm runoff (which is three-fourth of the total runoff) was generated during the first few weeks of the active period. The runoff generated due to quick melting of winter accumulated snow at the start of active period is called spring runoff. It should also be noted that for *FC-2*, the precipitation received during first couple of weeks is also significantly high contributing to the generation of runoff (276 mm, 25% of the cumulative annual precipitation). The runoff of approximately 45 mm during wet year for base climate was also observed due to a single high intensity precipitation event (88 mm/day > k_s) at the end of month of July.

Potential evaporation (PE) is the total quantity of water that can be evaporated if the unlimited supply of water is available at the ground surface. The potential evaporation for dry years is lowest for *BC* followed by *FC-1* and *FC-2*. The increase in the potential evaporation relative to the base climate is 12 % and 30 % for *FC-1* and *FC-2* respectively (Figure 3.10a). However, for wet year the lowest PE can be observed for *FC-1* followed by *BC* and *FC-2*.

Actual evaporation is related to PE but also depends on the availability of water (due to precipitation) and potential moisture difference between earth surface and atmosphere. Although cumulative precipitation and PE of homogeneous coarse profile for dry years varies for base and future climates, the cumulative actual evaporation is almost similar (within 1 % difference). This is due to low retention and high conduction behavior of the

coarse material. Conversely, the actual evaporation varies considerably (up to 31 %) during wet year for base and future climates. The reason for larger variations in cumulative AE during wet year could be due to the variations in the amount of the precipitation. For example, if we look at the precipitation data in Figure 3.10b, the *FC-2* has more extreme events especially at the start. This implies that lot more availability of water in shorter period of time although the evaporative demand for that period is not too different among the three. The lowest cumulative actual evaporation was observed during *FC-1*, followed by *BC* and *FC-2* and this trend is in line with the precipitation trends of the wet year.

Net infiltration (NI) quantifies the amount of water entering or leaving the ground surface. It is calculated by subtracting the sum of AE and RO from the precipitation. The cumulative net infiltration during a dry year generally follows the precipitation trends for the homogeneous coarse profile (Figure 3.10a) with lowest during base climate, followed by *FC-2* and then *FC-1*. The homogeneous coarse cover profile shows positive net infiltration during dry and wet years of representative future climates. The profile (CC) also shows water gain conditions in wet year of *BC*. However, water deficit conditions were observed during dry year of *BC*. The lowest cumulative net infiltration of wet year was observed during climate *FC-2*, followed by *BC* and *FC-1* which inversely follows the precipitation trends of wet years of their respective climate ensemble. The reason for such trends (which inversely follows the precipitation) is due to actual evaporation values which are the highest during *FC-2*, followed by *BC* and *FC-1*.

The infiltrated water flow through gravity and enters in to the tailings is generally termed as deep percolation (DP). In addition to gravity, another competing process is a capillary

action in which water from the saturated portion of the tailings can rise and enter the cover. Since the homogenous coarse profile has low air entry value with little capillary rise, therefore, a major portion of infiltrating water during all climates flow through the cover and enters the tailings (Figure 3.10a and b).

The water balance for the homogeneous fine material profile of dry and wet years during base and future climates are shown in Figure 3.11. The cumulative precipitation and potential evaporation of dry and wet years for homogeneous fine profile during all the climates are identical to their respective climate ensemble of the coarse homogeneous profile as these (P and PE) are independent of the cover type. The cumulative runoff of the fine profile for the dry and wet year are considerably low (less than 5 %) for all the climate ensembles (*BC*, *FC-1* and *FC-2*). This is due to the lower saturated hydraulic conductivity of the fine cover material as compared to the coarse.

However, actual evaporations are significantly higher for homogenous fine profile as compared to the coarse for dry and wet years during all the climate ensembles. The relative higher cumulative AE for fine profile is due to its high retention and low drainage behavior. The variation in actual evaporation of dry year during for all climates is relatively small (within 5 % of *BC*). However, the difference in cumulative AE for wet year are high with the highest AE of 818 mm of *FC-2* (33 % more than *BC*), followed by *BC* (611 mm) and *FC-1* (443 mm). Again, the reasons for the variations in the AE could be the variations in the amount of precipitation in wet year for base and future climates.

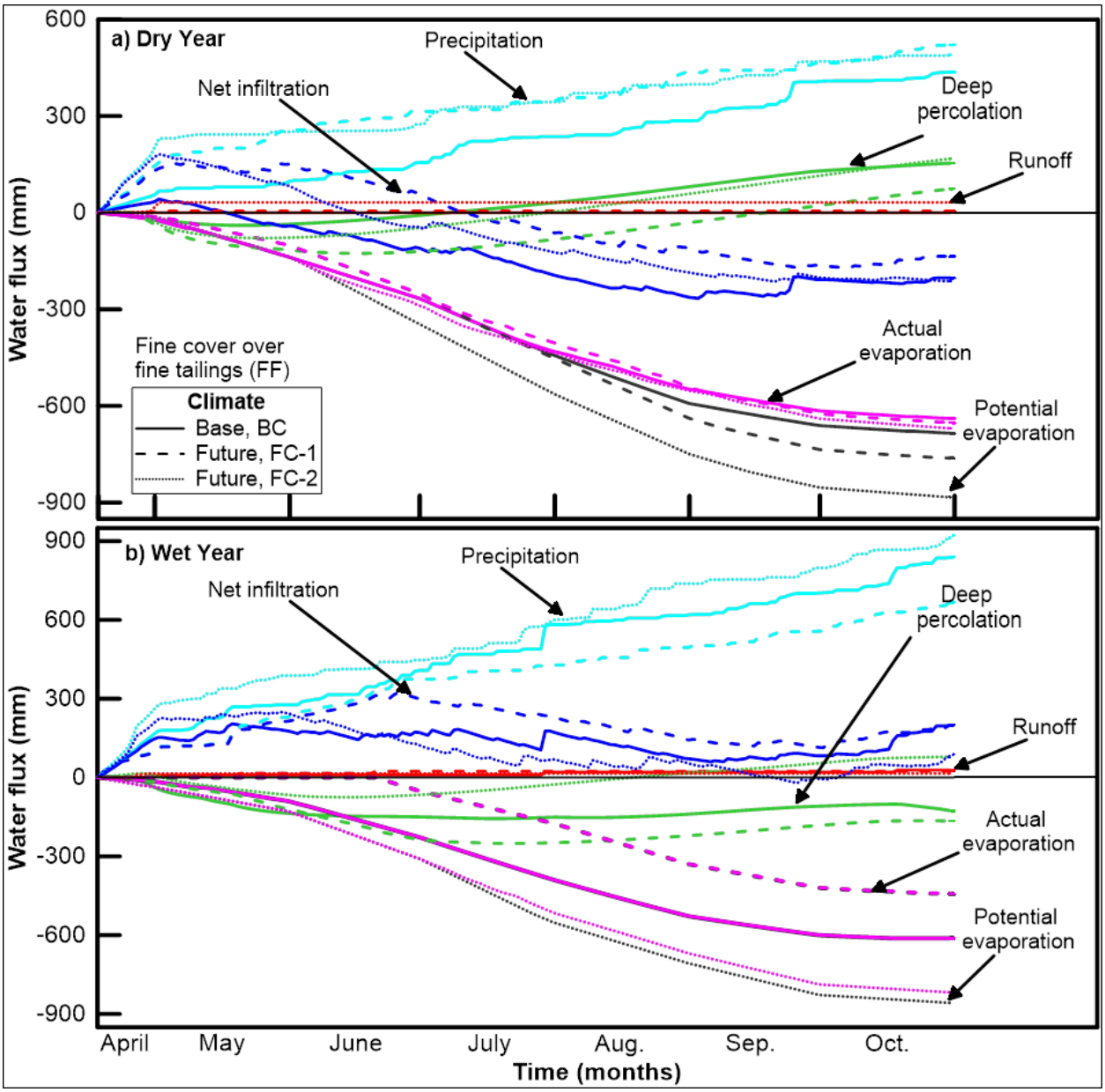

Figure 3.11. Water balance for homogeneous Fine profile, FF for a) dry year; b) wet year.

The net infiltration of the homogeneous fine profile for dry years showed water deficit condition of all the representative design climate ensembles. The water deficit conditions are due to increasing high actual evaporation and lower cumulative precipitation. Additionally, the higher air entry value (50 kPa) of the fine profile keeps the saturation at

a higher level above the groundwater table due to capillarity which results in generation of higher AE (Figure 3.11a). During wet years the net annual precipitation is more than the annual actual evaporation therefore, the wet years of base and future climate shows water gain conditions (Figure 3.11b).

For the case of a homogeneous fine profile, greater capillary rise due to higher air entry value of the fine tailings is expected. At the beginning of the active year, the flow of water in the cover is predominantly controlled by gravity drainage. As the time passes, water flows across the cover-tailings interface in upwards direction due to capillary rise. During dry year, due to higher AE and lower P, the water flows from the tailings to the cover due to capillary rise will result in net gain to the cover storage. Conversely, during wet year, the water flows across the interface from cover to the tailings for *BC* and *FC-1*. This is due to the higher amount of precipitation (P>(AE=PE)) during wet years. However, for wet year during *FC-2*, the cover experience net gain in its storage. It is due high AE (comparable to P) which create potential continuous water deficit conditions at ground surface which in turn are compensated by groundwater flow from the tailings to the cover due to capillarity.

The water balance results for coarse cover profile over fine tailings (CF) showed similar trends to that of profile CC and the fine cover over coarse tailings profile shows water balance similar to that of profile FF, therefore, are not discussed any further. In addition to above mentioned water balance results for FC-1 and FC-2, two additional representative climate ensembles were also analyzed and their water balance results are shown in Appendix-D.

3.7.4 Annual variations in water storage and oxygen flux

The box and whisker plots for change is annual storage, ΔS (difference in NI and DP) and oxygen flux are presented in Figure 3.12 for the both fine and coarse tailing covers for all the climates. The change in storage of the cover layer is determined by estimating the quantity of water entering or leaving the top (ground surface) and bottom boundary (cover tailings interface) of the cover. As mentioned earlier, the meteoric water that enters or leaves the cover surface at the top boundary is called $NI.$

A portion of this water can makes its way into the tailings and is known as DP. In some instances, for shallow groundwater table depth and tailings with high *AEV*, water from the tailings can also enter the cover via capillary action. The difference between the NI and DP predicts the changes in the cover storage (saturation). The positive value of ΔS represents the gain in storage while the negative predicts the loss of in cover storage. The value of ΔS is related to the ingress of the oxygen in the sense that it effects the cover saturation which is the controlling parameter for oxygen transport. It should be noted that the cumulative value of ΔS indicates the net water loss or gain during the active period.

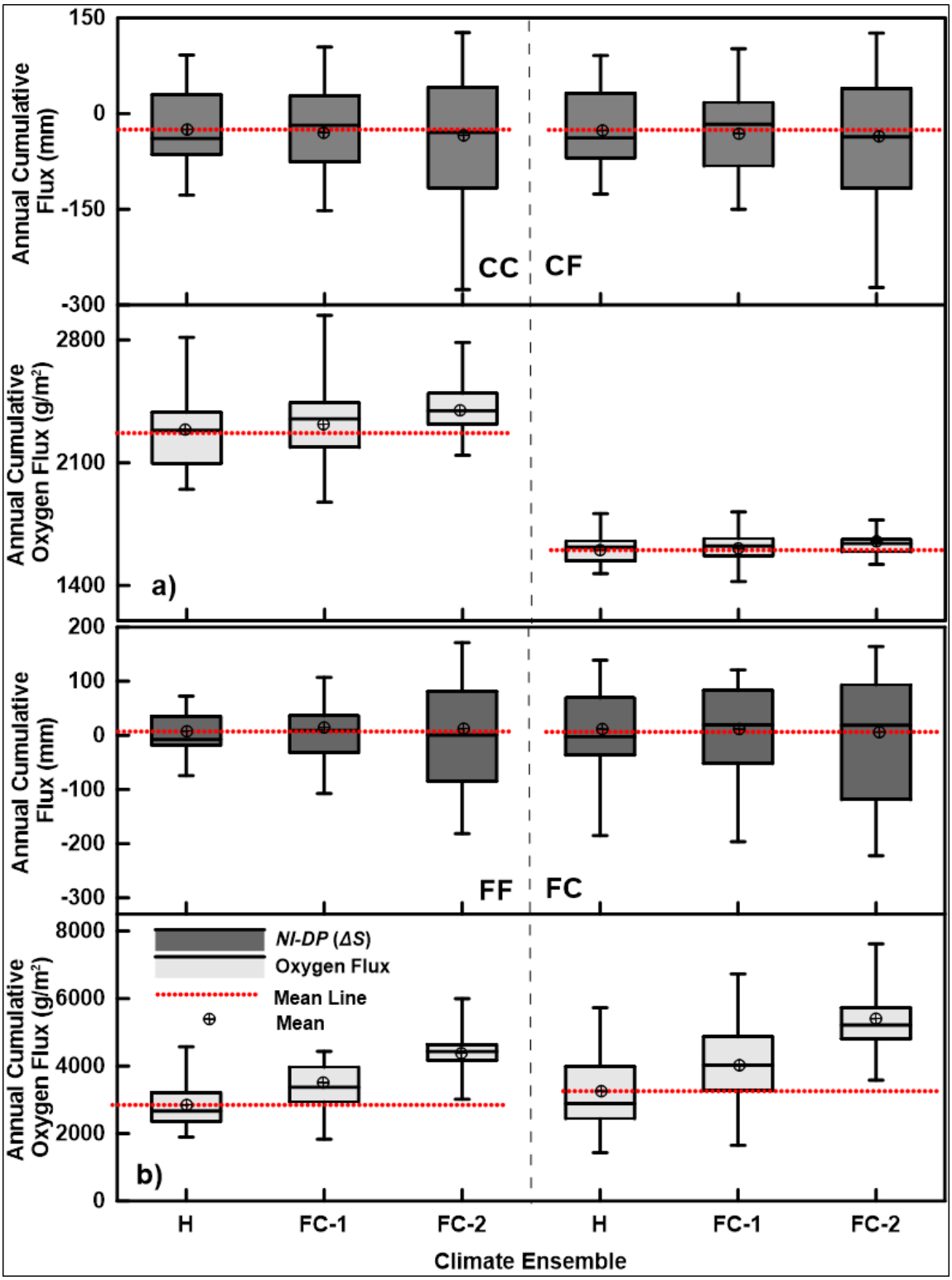

Figure 3.12. Box and whisker plots for the annual change in storage and surface oxygen flux for a) the CC and CF profiles and b) the FF and FC profiles.

Figure 3.12a shows the box and whisker plots of the annual ΔS and oxygen flux for all the cover profiles. The results indicate that for the CC profile the mean annual ΔS (30 years) are -24, -22 and -42 mm for the base, *FC-1* and *FC-2* future climates, respectively. Therefore, it can be concluded that the difference in mean values for base and future climates is minimal. However, the year to year variation in ΔS for the future climates is much larger than the base climate. For example, the difference in maximum and minimum annual ΔS for the CC profile is 219, 256 and 403 mm for base, *FC-1* and *FC-2* climates respectively. This increasing trend (in the range) reflective of more year to year variation and existence of extreme weather years in the future climate ensembles. More variation can be seen for future climate ensemble *FC-2*. Similar observations regarding the changes in ΔS can also be made for CF profile and ΔS values for CC and CF profiles are very similar.

Figure 3.12a also shows the box and whisker plots for the annual oxygen flux for the coarse tailing covers. For cover profile CC, it can be observed that changes in cover saturation result in variations in yearly flux values. Larger year to year variation can be observed for *FC-1*, while larger mean and median increases can be observed for future climate *FC-2*. For cover profile CF, it can be observed that oxygen flux values are much smaller than the values for CC profile. This result seems surprising, as ΔS values for the both profiles are quite similar. Figure 3.13 shows the time history of saturation for the CC and CF profiles for the base climate. This figure shows that the saturation profiles for CC and CF have quite difference. For example, for the CF cover profile the reactive tailings remain at saturations higher than 90%. This is in contrast to the CC profile where most of the reactive tailings remain at saturations levels between 40 and 50%. Additionally, it can

also be observed that the cover of the CF profile has much higher saturations than for the CC profiles. The higher tailings and cover saturation in the CF profile is due to higher *AEV* of the fine reactive tailings and which is responsible for lower oxygen flux in the CF profile. Therefore, it can be concluded that the performance of coarse cover lying over fine reactive tailings is less dependent on the climate and will be less prone to future climate changes.

Figure 3.12b shows the change in saturation and oxygen flux values for the FF and FC profiles. The change in saturation for these profiles are similar to those predicted for the coarse cover profiles. It can be observed that with the changing climate larger variation in year to year in saturation can be observed. It can also be observed that this variation is more pronounced for fine cover lying over fine tailings. The oxygen flux values for the FF and FC profiles shown in Figure. 3.12b indicate that oxygen flux increase considerably for the future climates *FC-1* and *FC-2* in comparison to the base climate. This increase is greater for *FC-2* as compared to *FC-1*. It can also be observed that FC profiles shows more sensitivity to future climates than the FF profile. This is consistent with our observation from coarse cover profiles, where cover overlying fine tailings showed less dependence on climate. Based on the observations made for all cover profiles, it can be concluded that larger quantities of oxygen will enter the fine covers with changing climate.

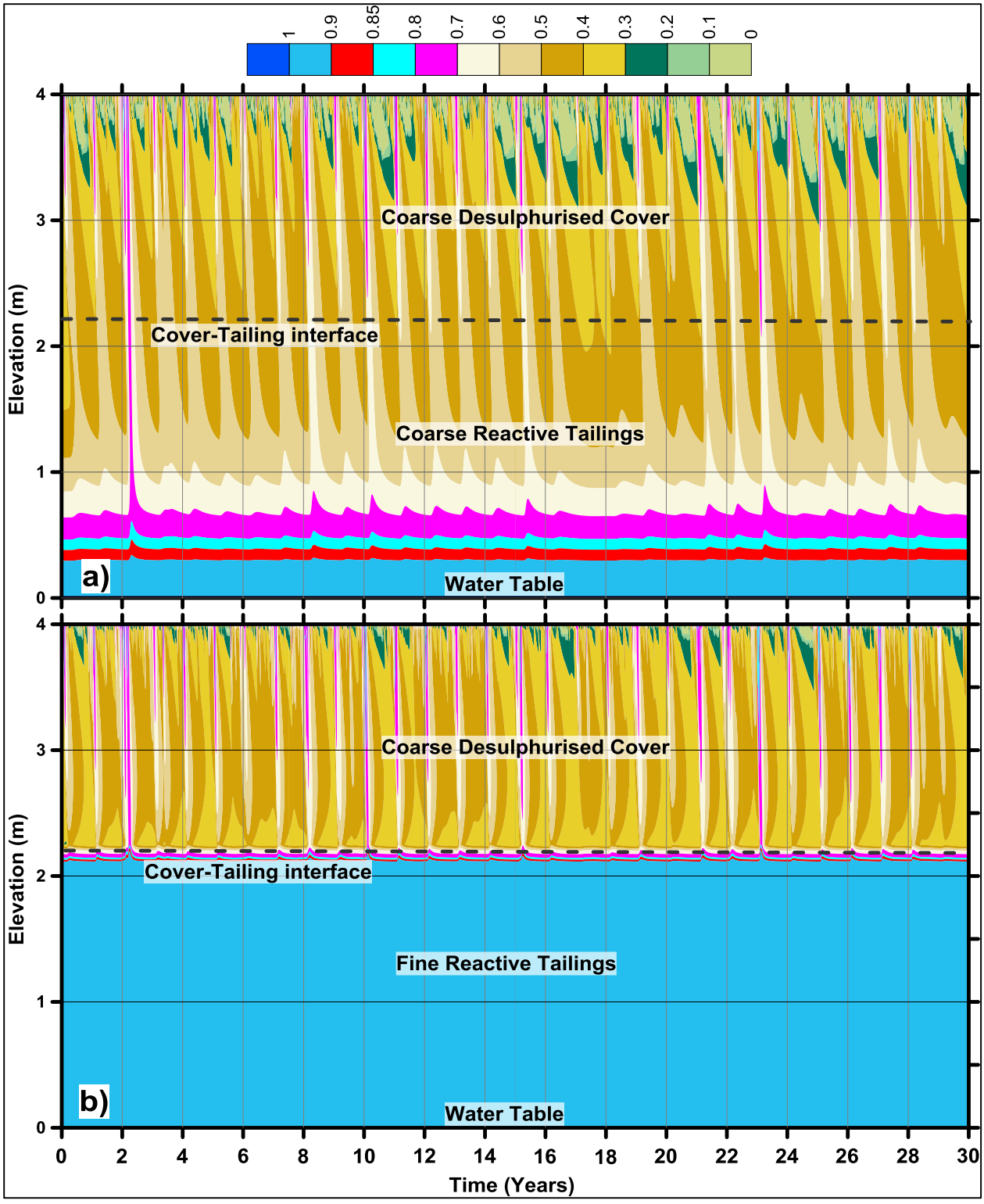

Figure 3.13. Time saturation plot with depth for a) CC profile, b) CF profile.

3.7.5 Cumulative oxygen fluxes

Figure 3.14 shows a comparison of the 30-year cumulative oxygen flux values for all profiles predicted at the cover surface and the cover tailings interface. The coarse tailing covers (CC and CF profiles) reveal a smaller variation in cumulative oxygen flux for all climates. The variations in the surface oxygen flux for future climates are shown as a percentage change relative to the base climate in Figure 3.15. The results indicate that these changes are minimal. These further reinforce earlier observations that performance of coarse covers will not be impacted by the changing climate. It should be noted that based on the results presented in the previous section for CC cover profile some variation in yearly oxygen flux values is expected for changing climate. However, in the cumulative sense these only account for 2 and 5% change in relation to the base climate.

The 30-year cumulative oxygen flux values for the fine cover profiles in Figure 3.14 indicate considerable differences compared to the coarse cover profiles. For fine cover profiles, the oxygen flux at the tailings cover interface is negligible. This is not a surprising result, as the presence of fine tailings in tailings and/or cover are expected to maintain higher levels of saturation resulting in minimal oxygen ingress. Figure 3.16 shows the saturation time history of the FF and CF profiles for 30 years of base climate. The saturation time history of the FF profile shows that saturation of the fine acid generating tailings never falls below 85%. This is due to the location of the groundwater table depth and high *AEV* of the tailings. It can also be observed that the cover comprising of the desulfurized fine tailings is also very effective in maintaining higher saturations and the bottom 30 cm of the cover always remains at saturation in excess of 85%. The time history of saturation for the FC profile is also shown in the same figure. It can be observed that

for most of the coarse acid generating tailings the saturation varies from 20 to 60%. However, the cover saturation near the cover tailings interface remains above 85 %. There are only a few instances during the 30-year period when saturation at the interface is 70% or slightly lower.

Figures 3.14 and 3.15 also show the oxygen flux values at the cover surface for fine covers. It can be seen that the flux values increase with changing climate. Larger changes in the 30-year cumulative flux values for FF and FC profiles can be observed for the *FC-2* climate ensemble. In relation to the base climate the flux values for FF cover profile increase by 18 and 53% for the *FC-1* and *FC-2* climates respectively. Similarly, for the FC cover profile the oxygen flux at the cover surface increases by 24 and 65% for the *FC-1* and *FC-2* climates respectively. The increase in surface oxygen flux for fine cover profiles is related to the higher effective reactive coefficient (K_r) of the fine tailings as compared to the coarse. The K_r value of fine tailings is an order of the magnitude larger than for the coarse tailings material (K_r for fine 44 year^{-1} and K_r for coarse is 3.44 year^{-1}). The other reason could be due to the increased evaporative demand because of the changing climate. The fine cover will retain more water in the near surface resulting in decrease in cover saturations with increased oxygen ingress at the surface.

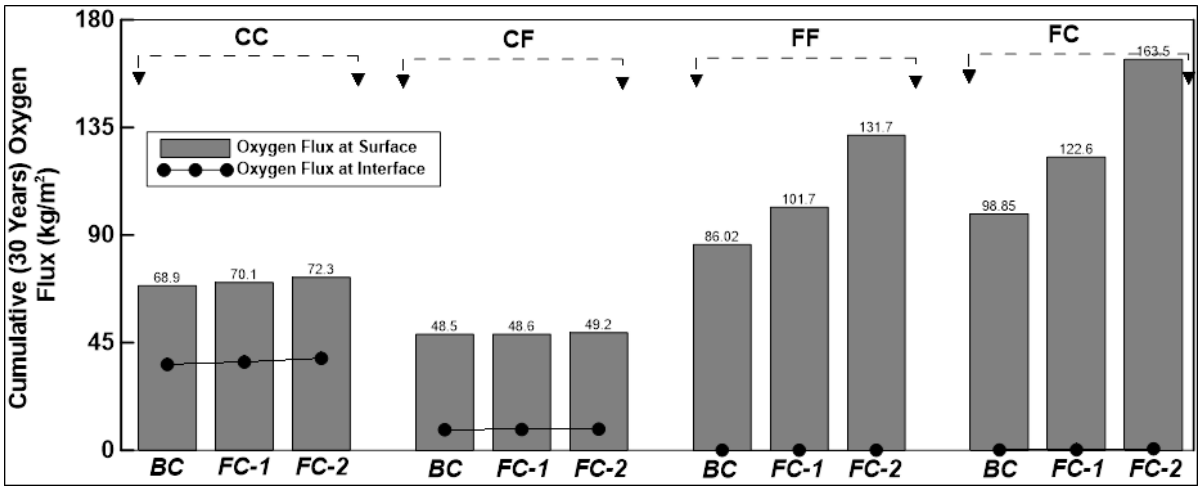

Figure 3.14. Cumulative (30 years) oxygen flux at the coarse and fine tailings covers for the base and the future climates.

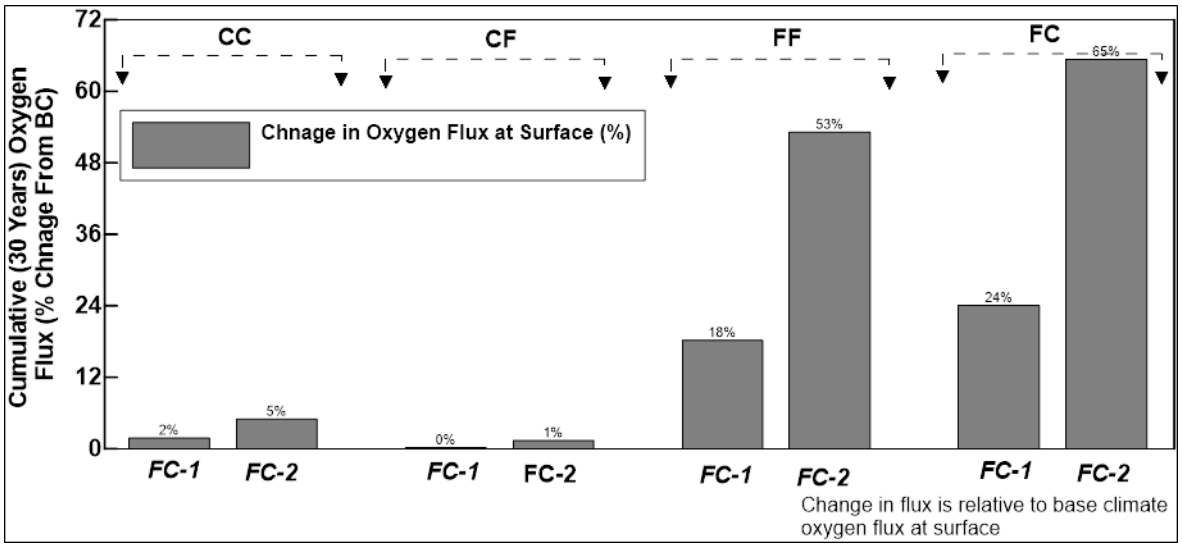

Figure 3.15. Change in the cumulative (30 years) oxygen flux (%) at the coarse and fine tailings covers for the base and the future climates.

The results reveal that the FC profile has the largest variation in the cumulative water and the oxygen flux and is observed as one of the most sensitive to the climate variations (Figure 3.12b and 3.14). The profile CF represents the most accurately as-built configuration of tailings cover over reactive tailings at Detour Lake Mine. Therefore, the

FC and CF profiles are selected further to assess the temporal effects of climate changes on these profiles.

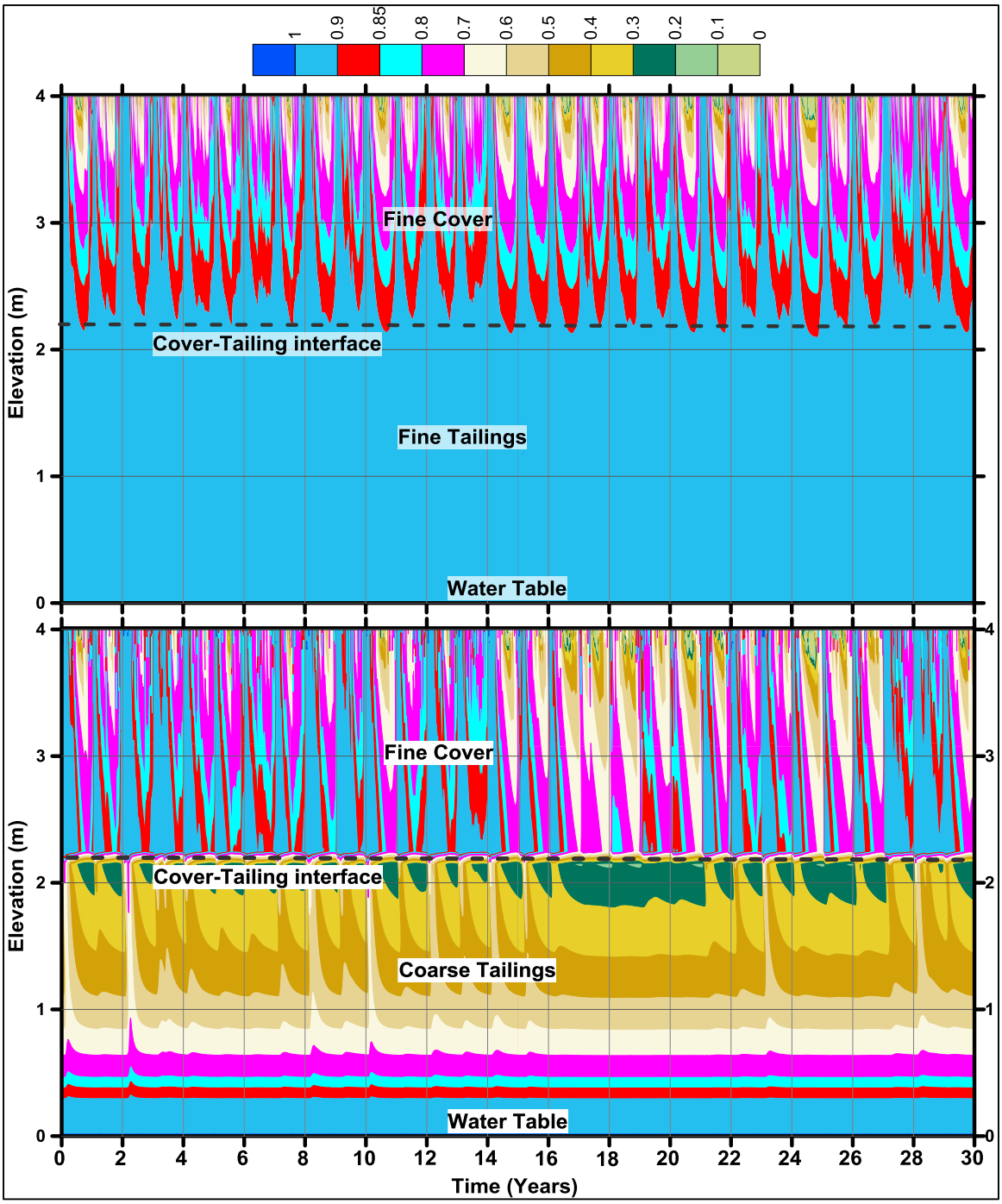

Figure 3.16. Time saturation plot with depth for a) FF profile, b) FC profile.

Time histories of saturation and oxygen concentration versus depth for the *CF* profile for all design climates are shown in Figure 3.17. The Figures 3.17a-c show the saturation depth plots whereas the figures 3.17d-f show concentration depth plots for the three climates. Figures 3.17 a-c clearly show that the tailings are nearly 100 % saturation except the region close to the interface for all climates. The saturations at the interface are consistently between 60 and 70 % for CF profile for all climates. There are also some instances when the saturation becomes more than 85 % at the interface. The time history of saturation with depth in the cover is generally in the range between 30 and 50 % during *BC, FC-1* and *FC-2* with some dry spells when the saturation in the covers drops in the range between 10 and 20 %. These low saturations in the cover are more obvious near the cover surface. These low saturation conditions are more frequent in *FC-1* and *FC-2* (every year) and the depth of these low saturation contours can reach up to a depth of 1.75 m below the cover surface especially during *FC-2*. It can be concluded that the cover saturation with depth is decreasing with change in climate and the saturation starts decreasing from the surface and as the climate get drier the low saturation contour progresses further down.

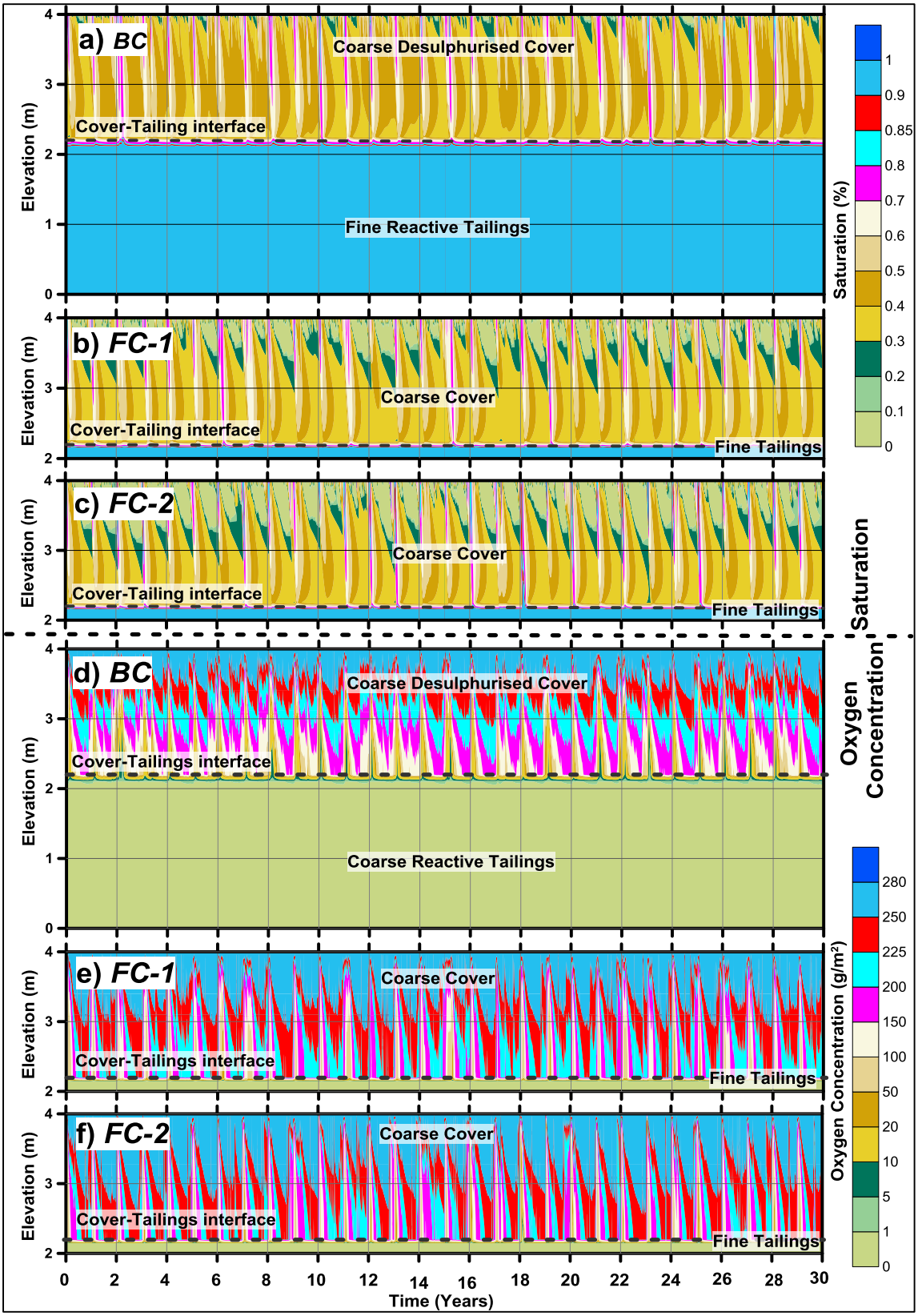

Figure 3.17. 30-year time histories for the CF profile. Saturation for climates a) *BC*, b) *FC-1*, and c) *FC-2*; and oxygen concentration for climates d) *BC*, e) *FC-1* and f) *FC-2*.

Oxygen concentration inversely follows the saturation plots (Figure 3.17d-f). As the tailings remain nearly saturated, the oxygen ingress in the tailings is almost zero during all climates. Almost one-fourth of the upper portion of the cover receives high oxygen concentration (~280 g/m^2) during *BC*. The high oxygen concentration contours almost reach the upper half of the cover for *FC-1* climate and go beyond this depth that for the climate *FC-2*. However, there are instances when the oxygen concentration drops in the range between 150 and 250 g/m^2 near the cover surface. The oxygen concentration in the cover near the interface are generally in the range between 100 and 200 g/m^2 for base climate and between 200 to 250 g/m^2 for future climates respectively. The reason for the high oxygen concentration in the cover near the interface during the future climate is due to lower saturation contours near the interface. It can be concluded that the no sufficient oxygen will pass through the cover in to the tailings but the with climate change conditions the more presence of oxygen near the interface is expected.

The 30-year time histories for saturation and oxygen concentration versus depth for the FC profile of all the design climates are shown in Figure 3.18. The Figures 3.18a -c show the saturation depth plots whereas Figures 3.18d-f show concentration depth plots for *BC*, *FC-1* and *FC-2* respectively. In this figure it can be observed that the saturation in the tailings increases with depth and tailings becomes saturated at a depth of 4.0 m (which is groundwater table). The time saturation plot also shows that the saturation in the tailings near the interface is between 20 and 30 % for all climates (Figure 3.18a-c). However, there are instances when the saturation increases in the range between 30 to 50 % and these cases are more obvious in *BC*. The fine cover of the profile FC is expected to have high saturation in the cover layer. The upper portion of the cover up to about 0.6

m experiences a wide range of saturation conditions (between 20 and 95 %). Beyond this depth the cover saturation is normally in the range between 60 and 95 %. The saturation in the cover near the interface is generally higher than 85 %, However, there are instances when the saturation over the interface is below 85 % and these instances are more common during *FC-2*.

As the saturation over the interface remains 85 % in most of the instances, therefore, the oxygen concentration in to the tailings is extremely low (Figure 3.18d-f). However, the instances when the saturation at the interface is below 85 %, the oxygen concentration between 0 and 1 g/m^2 can be observed in to the tailings for all climates. For *FC-1* and *FC-2*, there are instances when the concentration in the tailings increases to a range between 5 and 10 g/m^2. Also there are few years during *FC-2 (year 3, 7, and 23)* when the concentration goes pass this range up to 20 g/m^2. This is due to lower saturation near the interface during this time of the year. Similar to the saturation plots, the oxygen concentration in the upper portion (0 to 0.6 m approximately) is highly variable which falls in the range between 100 and 280 g/m^2. Beyond this depth the oxygen concentration is generally in the range between 5 and 100 g/m^2. Overall, the fine cover maintains high saturation during 30-year time near the interface which results in the low ingress of oxygen in to the tailings during all climates.

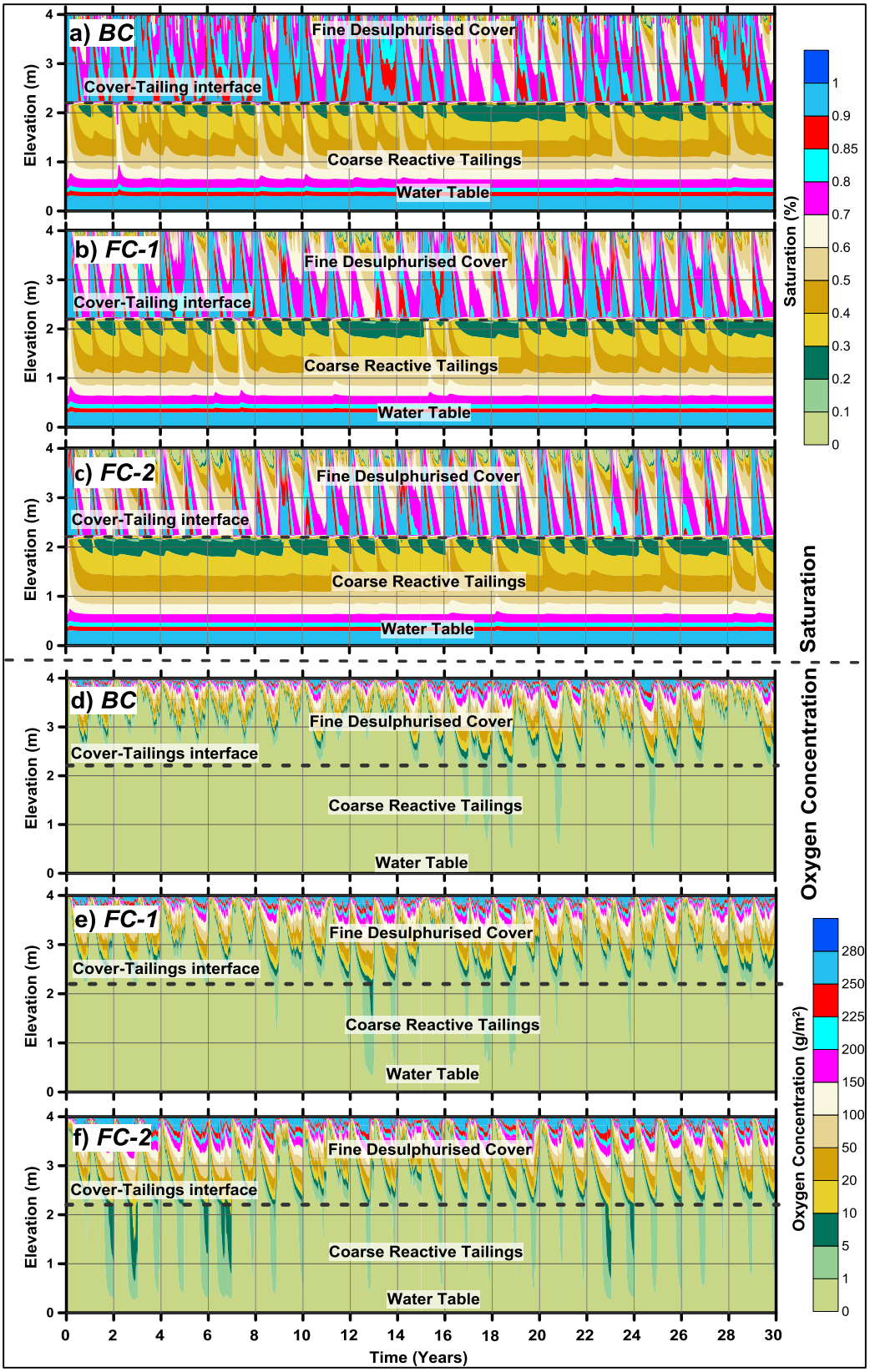

Figure 3.18. 30-year time histories for the FC profile. Saturation for climates a) *BC*, b) *FC-1*, and c) *FC-2*; and oxygen concentration for climates d) *BC*, e) *FC-1* and f) *FC-2*.

3.8 Discussion

For coarse tailings covers a considerable amount of oxygen flux at the tailings cover interface was predicted (Figure 3.13), however the results indicate that their performance will not deteriorate with changing climate (Fig. 3.14). Although the year to year variation in the oxygen ingress is expected in the future, the cumulative 30-year oxygen ingress is not much different in the coarse covers for all climates. The effectiveness of the coarse cover generally depends on the underlying tailings. The covers placed over the fine tailings have shown higher saturation along the cover-tailings interface due to high *AEV* value of the tailings materials.

Fine tailing covers (*FF* and *FC* profiles) have shown a greater sensitivity to climate change (Figure 3.14 and 3.15). High saturation levels in the fine tailing covers (due to their high *AEV*) result in the higher actual evaporation rate due to the continuous availability of water at or near the surfaces (Figure 3.11). The increasing evaporative demands for future climates (Figure 3.11), ends up in increased loss of moisture. In case of fine tailings cover over fine tailings (*FF*), the cover saturation can increase with capillary rise from groundwater table. Therefore, the increasing loss of moisture in the cover due to climate change will be compensated through the capillary rise action. However, a disconnect exits in the FC case between the groundwater table and the fine tailings cover due to existence of the groundwater table within the coarse tailings (*AEV*=6kPa or 0.6 m). Therefore, for the FC profile the moisture loss due to increasing evaporative demand is likely to create considerable reduction in the saturation which potentially cannot be compensated from the groundwater table through capillary rise.

Although oxygen flux transmitting to the underlying tailings through fine tailing covers is minimal (~0 kg/m^2), they experience relatively high oxygen fluxes at the cover surface. In other words, the fine tailing covers have higher oxygen concentration than the coarse covers. This increases the possibility of oxygen reaction with residual sulphide contents in desulphurized tailings materials which can add up to the expected production of AMD (Demers et al. 2008). It is therefore, of prime importance to select the desulphurized tailings cover materials with low sulphide concentrations to avoid additional production of AMD.

Groundwater table is one of the key considerations for preliminary design of the tailings covers. The fluctuations in the depth of water level are expected due to climate change (Stratos lnc. 2011). Reduction in annual precipitation and increase in annual evaporation can result in lowering of the water table. For the climate *FC-2*, the predicted cumulative PE is roughly 24 % higher than precipitation. If these changes will result in lowered groundwater table depth, the performance of the covers can be compromised.

3.9 Concluding Remarks

Performance of tailing covers under changing climates was assessed at a site in Northern Ontario. Covers constructed with coarse and fine desulphurized tailings were analyzed for historical and future climatic conditions. Predictions of future climate were made with general circulation models (GCM) using different representative concentration pathways (RCP). The performance assessment of tailing covers was carried out using the software VADOSE/W. The water balance assessment for covers constructed with coarse materials are expected to have water gain conditions at the cover surface for dry and wet years of

future climates. The fine tailings covers are expected to show different behavior during dry and wet years for future climates. It is expected that net water loss conditions will occur during the dry year and water gain conditions during wet year for future climatic conditions. The fine tailings cover maintain high saturation as compared to the coarse cover which results in the low oxygen ingress for all climates. Coarse tailing covers are more effective in controlling oxygen ingress when placed over fine tailings as opposed to the coarse tailings. The results of this study suggest that the effect of climate change on coarse tailing covers will be marginal resulting in a maximum increase of 7 % in oxygen flux values in comparison to the base climate. Again, the performance of fine tailing cover was observed to be more effective for the case when they are placed over fine tailings as opposed to the coarse tailings. Unlike the coarse covers, fine tailing covers showed a significant variation in their performance with changing climate. For the fine covers, the 30-year cumulative oxygen flux entering the reactive tailings was almost negligible (~0 kg/m^2), however the oxygen flux entering the cover could potentially be significantly higher for changing climate.

The results in this study are based on the modelling of a single layer tailings cover assuming that the flow is primarily vertical. This assumption can have implications to the water balances results, because generally the covers are placed at a certain angle to regulate the surface water. In this regard, 2D simulations could be helpful to understand lateral flow effects and its implications on cover saturation and oxygen ingress. It is also expected that the hydraulic properties of the cover materials will change with time. These changes should also be considered in the future studies. The behavior of single layer coarse and fine tailings cover is assessed against climate change. The current study only

focuses on carrying out the analysis for the selected single layer cover profiles. However, considering the heterogeneity at the site, more combinations of cover profiles need to be analyzed. Based on the outcome of this research, a fine cover layer overlain by a thin evaporative barrier layer (coarse) could be an excellent option to avoid ingress of oxygen by maintaining high saturation in the cover layer. However, this cover combination needs to be further evaluated under future climate conditions.

Chapter Four: Post-construction Performance Evaluation of Monolithic Desulphurised Tailings Cover

4.1 Abstract

Soil covers are used for final closure of landfill waste and mine tailings containments. They act as a thin interface to create a disconnect between the atmosphere and underlying waste. Soil covers are placed over reactive mine tailings to limit water percolation and oxygen ingress into the tailings and thereby reduce the amount of acid mine drainage. Climate is a fundamental design parameter for the design of soil covers as it controls the water balance at the ground surface. Climate can also bring physical changes in the soil cover materials due to freeze/thaw, dry/wet cycles. These changes result in alteration of hydraulic properties which in turn control the performance of these covers. In this research, expected post-construction changes in hydraulic properties of the fine tailing covers due to post-constructional variations in the climate and other physical and chemical processes are studied at a site in Northern Ontario. Soil atmosphere modelling using historical and future climates and as-built and post-constructed hydraulic properties were used to estimate the impact of post-construction changes on the long term performance of the covers. Historical climate was considered as a baseline against which the changes due to the future climate (climate change) to be quantified. Based on the review of the literature it was predicted that the expected changes in soil cover hydraulic properties will increase in saturated hydraulic conductivity and saturated volumetric water content and decrease in air entry pressure. Based on the modelling results it was found that for covers that are constructed with fine materials, the

cover performance may improve over a shorter term after its construction. However, the performance may deteriorate with time after that, especially if the climate is predicted to be drier in the future.

4.2 Introduction

Soil covers, a thin interface between the atmosphere and underlying waste is used for final closure of landfill waste and mine tailing containments (INAP 2003; Fredlund et al., 2012). Soil covers are generally aimed to control infiltration and to provide an oxygen barrier layer to the underlying waste. Apart from this, these covers also provide structural stability and promote vegetation layer over these containments (INAP 2003).

Soil covers are typically designed using numerical modelling techniques. The viability of these techniques must be demonstrated before they can be used for construction with confidence. Modelling techniques which have the capability to model long-term behavior of the soil cover are generally used for the design. In addition to the model selection, the choice and selection of appropriate input parameters is of equal importance. Soil hydraulic properties are one of the key input parameters for numerical modelling of soil covers and are typically obtained from measurements on laboratory specimens during the design phase to predict the performance of soil covers (Benson et al., 1995, 2007).

However, soil hydraulic properties are expected to vary with time after construction due to site specific physical, biological and chemical processes (Meiers et al., 2011). Freeze/thaw and dry/wet cycles produce physical changes in fine cover material. These processes bring volume changes due to development of secondary structures or fractures

in the soil which lead to the creation of voids or macro pores (Boynton and Daniel 1985; Pincus et al., 1995; Eigenbrod 1996; Cao et al., 2017). During biological process (root growth and death cycle), the roots intrude into the soil cover and create voids (Scanlan 2009). Later on, decay of these roots in the cover layer create channel like structures which significantly affect its hydrologic behavior. Similarly, burrowing animals affect the hydraulic behavior by creating direct channels for movement of water, vapors and other animals in the soil covers layers (Benson et al., 2007; Scanlan 2009; Meiers et al., 2011). Creation of channels (or macro pores) within the soil structure allows more water infiltration in the cover material down to waste material.

Several studies have been conducted to see the effects of freeze/thaw, wet/dry cycles on hydraulic properties of fine materials (e.g. Kim and Daniel 1992; Benson et al., 1995; Omidi et al., 1996; Lin and Benson 2000; Qi et al., 2006; Rayhani et al., 2007; Tang and Yan 2015; De Camillis et al., 2016). An increase in hydraulic conductivity of the fine cover materials for dry/wet cycle is reported in all of these studies. It has also been reported that the increase is substantial, generally in first few dry/wet and freeze/thaw cycles. For the following cycles, the increase in hydraulic conductivity is relatively insignificant.

Climate is an important factor which plays a key role in the performance and integrity of the soil cover systems. It not only impacts the performance of soil covers through precipitation, but also controls the aforementioned influencing processes (freeze/thaw and dry/wet). Increases in precipitation generally saturates dry surface of the soil cover resulting in increased hydraulic conductivity due to reduction in matric suction of the surface cover material. Similarly, frequent cycles of extreme temperatures can generate desiccation cracks on dry surfaces of fine cover materials due to their shrinkage

properties (Omidi et al., 1996; Rayhani et al., 2007). These cracks significantly influence the hydraulic conductivity and water storage capacity by providing easy access for water to infiltrate.

Benson et al., (2007) carried out field and laboratory testing across various States in the United States, to find out the effects of different processes on the soil cover hydraulic properties. By comparing the as-built and post-construction test results, they concluded that hydraulic parameters of soil covers had significantly evolved during their observation period (2001-2004). They observed that saturated hydraulic conductivity of soil covers increased up to a factor of 10,000. Similarly, saturated volumetric water content observed a maximum increase by a factor of two. Meiers et al. (2011) also carried out field testing to measure the post-construction changes in the cover materials at a site in Northern Alberta, Canada and concluded that saturated hydraulic conductivity increased by one to two orders of magnitude for multilayered soil covers between the years 2000 and 2004.

Although studies by Benson et al. (2007) and Meiers et al. (2011) measured the changes in soil cover material with time, they did not attempt to predict the performance of soil covers under these post-construction changes.

The objective of this study is to estimate the post-construction changes in the soil hydraulic parameters for the cover material and to predict its impacts on the cover performance. In addition, this study will examine the impacts of climate change on soil covers which have undergone post-construction changes to examine how climate change will affect the cover performance.

To accomplish these objectives, a soil cover at Detour Lake Mine in Ontario Canada was selected for evaluation. This soil cover is monolithic and there is abundance of information available in literature for this cover (e.g. Dobchuk 2002; Dobchuk et al., 2013, 2003; Micheal 2010; McNeill 2016).

4.3 Soil Cover Design Profiles

The soil covers at Detour Lake Mine are represented in this study to be composed of 1.8 m of fine material placed on top of a 2.2 m thick tailings. Figure 4.1 shows a schematic of the cover profiles used in this study. In this study, two types of tailings materials are considered; one comprising of coarse material and the other of fine material. This results in two cover tailings design profiles. The first profile represents the geometrical configuration of fine over fine (FF) where desulphurized tailing cover (onward called as fine tailings cover) material is underlain by the fine reactive tailings (onward called as fine tailings). The second profile represents the geometry where fine tailings cover is underlain by the coarse reactive tailings, FC (onwards called as coarse tailings). These are the same representative profiles which were earlier used by Dobchuk (2002) and Dobchuk et al. (2013). The ground water depth is considered to be 4.0 m below the top of the cover layer. The profiles when the post-construction properties of the fine material are considered, are denoted as F'F and F'C.

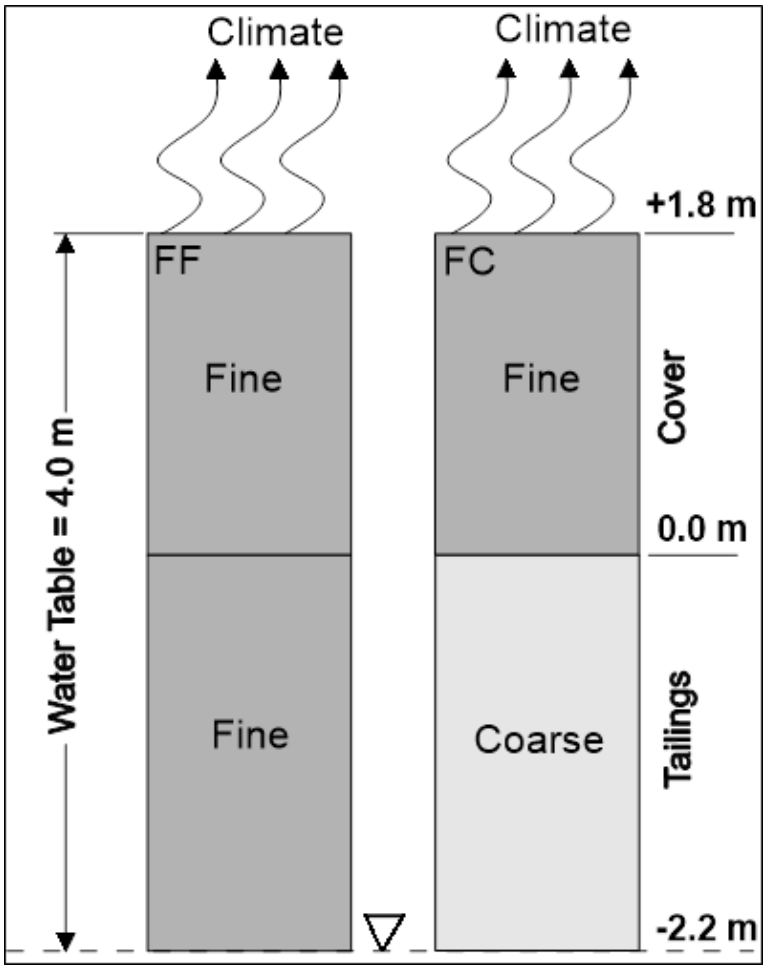

Figure 4.1. Schematic of the cover model.

4.4 Numerical Modelling

In order to evaluate the performance of these soil cover profiles, a soil-atmospheric numerical modelling exercise was carried out. The commercially available numerical model, Vadose/W (GEO-SLOPE 2016) was selected for this study. This software solves water flow problem in 1D and 2D model using modified form of Richards' equation in saturated and unsaturated flow conditions. Additionally, this software also solves the governing differential equation for the oxygen transport through reactive variably saturated soils. The governing equation is a modified form of Fick's second law and

details of the various parameters can be found elsewhere (GEO-SLOPE 2014). This numerical model was selected in this study due to its previous uses in similar research studies (e.g. Demers et al., 2009; Micheal 2010; Shurnik et al., 2012; Pabst et al., 2017).

The climate boundary conditions were applied at the top while the bottom boundary conditions were considered as zero pressure head at groundwater table. The climate boundary consists temperature, relative humidity, wind speed, precipitation and calculated potential evaporation. In addition to climate, oxygen flux boundary conditions are also applied on the both ends of the model. The concentration of oxygen in the atmosphere which 280 g/m^2 is applied at the top end (ground surface) of the model. The zero oxygen concentration is considered under saturated condition, therefore, the bottom boundary condition represented by water table assumes zero oxygen concentration.

4.4.1 Material properties

4.4.1.1 As-built material properties

The as-built hydraulic parameters of the cover and tailing materials are given in Table 4-1. These parameters were measured by Dobchuk (2002) and later on used by Dobchuk et al. (2013) and Ahmad et al. (2018) in their numerical models to predict the cover performance.

Table 4-1. As-built hydraulic parameters for cover and tailing material (Dobchuk et al., 2013)

Hydraulic parameter	*Fine (F)*	*Coarse (C)*
θ_s *(m³/m³)*	0.4276	0.4617
θ_r *(m³/m³)*	0.0009	0.0004
k_s *(m/s)*	$1x10^{-7}$	$1x10^{-6}$
Ψ_a *(kPa)*	50	6
n	2.6	1.94

4.4.1.2 Prediction of post-construction hydraulic properties

To date, there are no known measured post-construction soil properties for the tailings covers at Detour Lake Mine. However, there is a body of literature that has measured and/or predicts post-construction changes in cover material properties after several years at other locations (INAP 2003; Benson et al., 2007; Rayhani et al., 2007; Meiers et al., 2011).

A statistical relationship has been developed between the as-built and the post-construction hydraulic parameters by Benson et al. (2007), which can be used to predict post-construction hydraulic changes in cover materials. Benson et al. (2007) observed that changes in the hydraulic parameters with time had little relevance to the location of the cover site as similar changes in hydraulic parameters were observed in the locations with humid or semiarid and warm climates. Therefore, their methodology will be used in this study to predict the post construction changes in the tailing covers at Detour Lake site.

Benson et al. (2007) measured the post construction hydraulic changes of water balance covers one to four years after construction at ten different test sites in the USA. The climate at these sites range from “arid” to “humid” according to the climate classification described in UNESCO (1979). Covers at majority of these sites consisted of fine materials. Initially, undisturbed samples during construction were collected to carry out laboratory tests for determining saturated hydraulic conductivity (k_s) and soil water characteristic curve (SWCC). Additional sampling was done at the same test sites, one to four years after the cover construction for determining k_s and SWCC again.

The relationship of the as-built hydraulic properties versus the ratio of post-construction hydraulic parameters to respective as-built hydraulic properties are reproduced in Figure 4.2 thru 4.5. Figure 4.2 shows a plot between the ratio of post-construction and as-built saturated volumetric water content (θ_{sp}/θ_s) versus as-built saturated volumetric water content (θ_s). The majority of measured data shown in Figure 4.2 indicates that larger changes were measured with time after construction. It can also be observed that in general larger changes are associated with cover materials which had lower as-built θ_s values. This figure shows saturated volumetric water content data for the time period of one to four years. The plotted data falling above the horizontal dashed line (light gray at Y=1) shows that the cover materials have undergone the hydraulic changes with increase in θ_s with time. The plotted data which falls below the horizontal line shows decrease in θ_s with time while the points on the line shows no change in θ_s with time after construction. The majority of the data points fall between two continuous black line which give the extreme limit of the plotted data. A dashed line in the middle of two continuous line called as design line was drawn by the Benson et al. (2007) to be used for the prediction of post-

construction saturated volumetric water content. The dotted vertical lines show the θ_s value for distinctive materials as defined in Carsel and Parrish (1988) Considering as-built θ_s of 0.427 for the fine tailing cover, the ratio θ_{sp}/θ_s can be evaluated, which is 1.09 as shown in Figure 4.2. By multiplying this ratio with as-built value, the predicted θ_{sp} can be determined which is in this case calculated as 0.469.

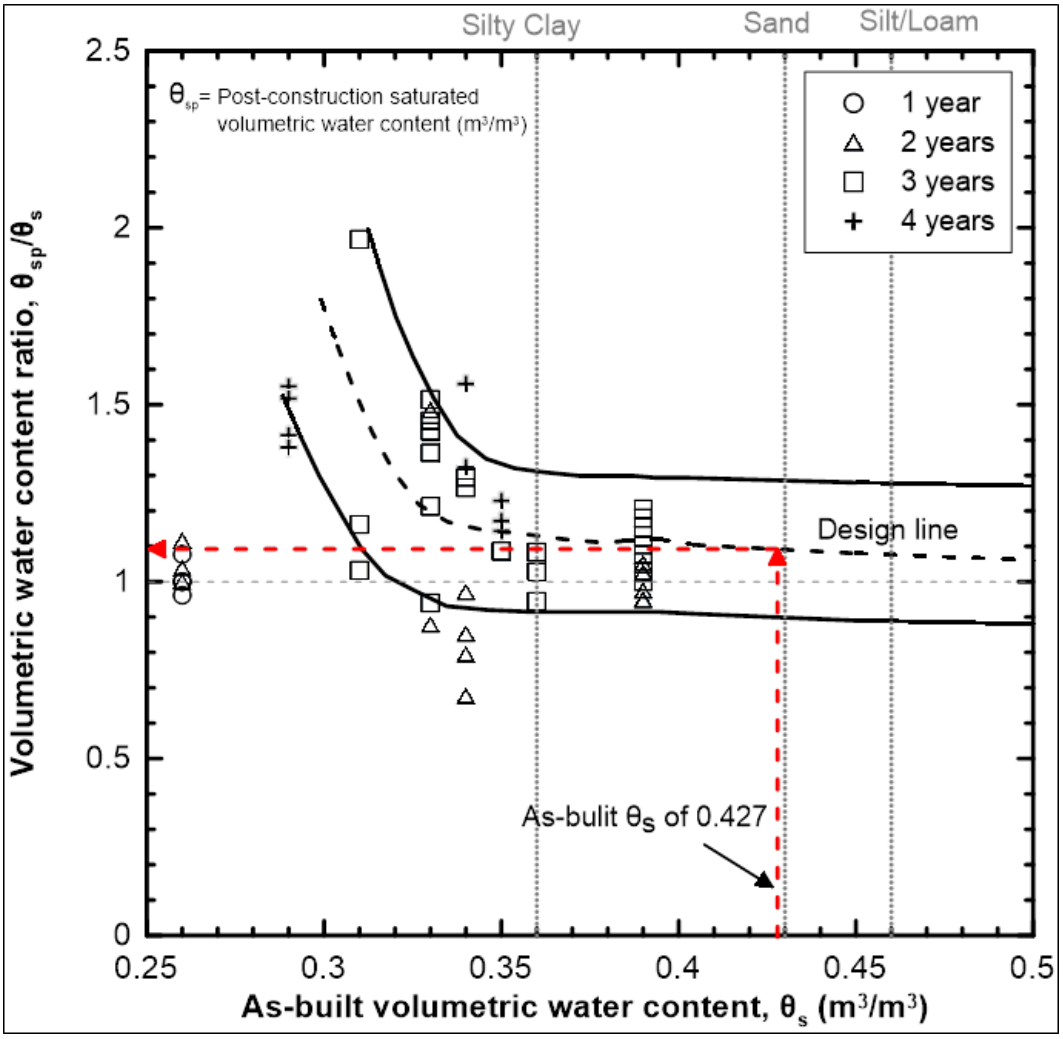

Figure 4.2. Ratio of post-construction saturated volumetric water content to as built saturated volumetric water content (θ_{sp}/θ_s) versus as-built saturated volumetric water content (θ_s) (Benson et al., 2007).

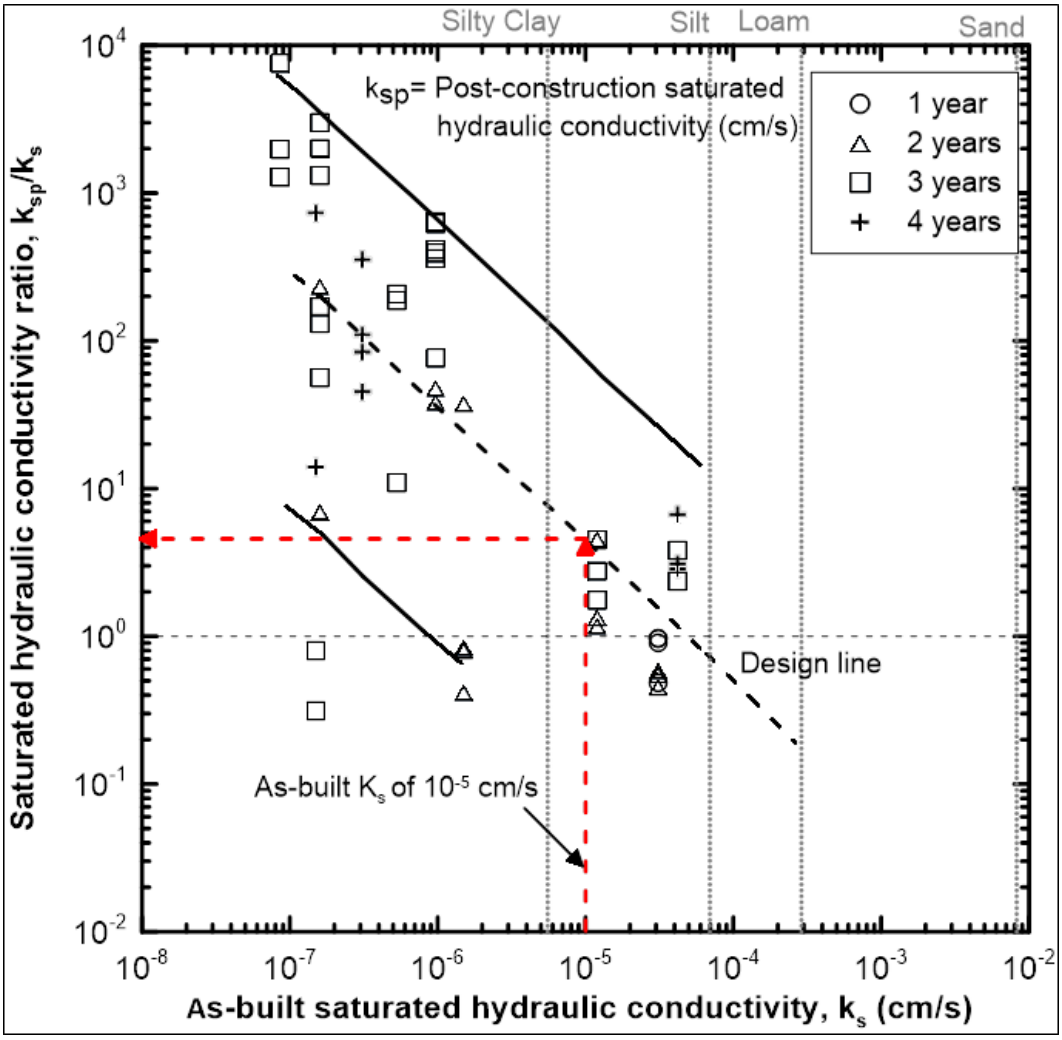

Figure 4.3. Ratio of post-construction saturated hydraulic conductivity to as built saturated hydraulic conductivity (k_{sp}/k_s) versus as-built saturated hydraulic conductivity (k_s) (Benson et al., 2007).

Figure 4.3 shows ratio of post-construction and as-built saturated hydraulic conductivity values (k_{sp}/k_s) versus as-built saturated hydraulic conductivity (k_s). Review of this figure indicates that the changes in hydraulic conductivity with time appear to be dependent on the as-built k_s.values. It can be observed that coarse materials which had relatively high k_s values showed relatively smaller (or negligible) changes with time as compared to the materials (fine) which had lower as-built k_s values. Post-construction changes in

saturated hydraulic conductivity can be observed to increase in the range of 10 to 10000 times for different cover materials. Using the as-built k_s of 1x10^{-7} m/s (1x10^{-5} cm/s) for fine tailings cover, the k_{sp} can be calculated as 6x10^{-7} m/s (6x10^{-5} cm/s) as shown in Figure 4.3. However, for analysis purpose the post-construction k_{sp} is considered as 1x10^{-6} m/s (1x10^{-4} cm/s) which is an order of magnitude larger than as-built k_s.

The ratio of post-construction and as-built condition α (α_p/α) versus α in as-built condition (α) is shown in Figure 4.4. The parameter α is an empirical parameter in the van Genuchten (1980) equation to describe the SWCC, and its reciprocal is related to the air entry pressure (Ψ_a) of the material. Figure 4.4 shows that the covers consisting of fine materials showed more sensitivity to the time dependent changes in α as compared to the coarser cover materials. In other words, the Ψ_a of fine cover material is expected to lower appreciably with time. For current study the post-construction α_p of 1.07 kPa^{-1} ($\Psi_a = 30\ kPa$) can be calculated using as-built α of 0.02 kPa^{-1} ($\Psi_a = 50\ kPa$) with help of Figure 4.4 for fine tailing cover material.

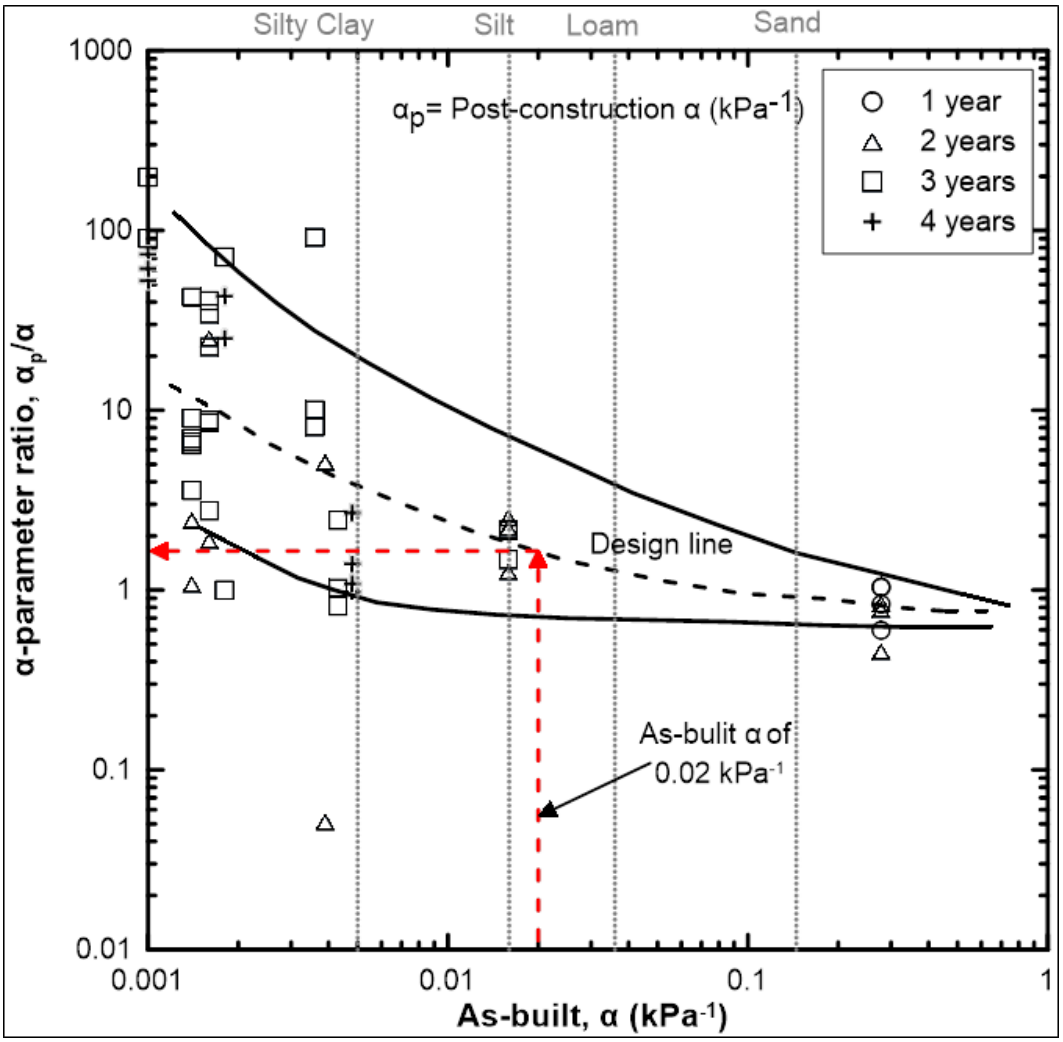

Figure 4.4. Ratio of post-construction α relative to its as-built condition (α_p/α) versus α in as-built condition (α) (Benson et al., 2007).

Similarly, Figure 4.5 shows the ratio of post-construction and as-built n value (n_p/n) versus as-built n value (n). Review of this figure indicates that the changes in n value with time appear to be dependent on the as-built n values. Using the as-built n of 2.6 for fine tailings cover, the n_p can be calculated as 1.2 as shown in Figure 4.5. The term n is an empirical parameter which generally controls the slope of the SWCC (van Genuchten 1980) The term n is also related to pore size distribution index value of the soil. The larger value of n corresponds to the more uniform pore size in the soil and steeper slope curve.

The values of as-built and respective post-construction hydraulic parameters are tabulated in Table 4-2.

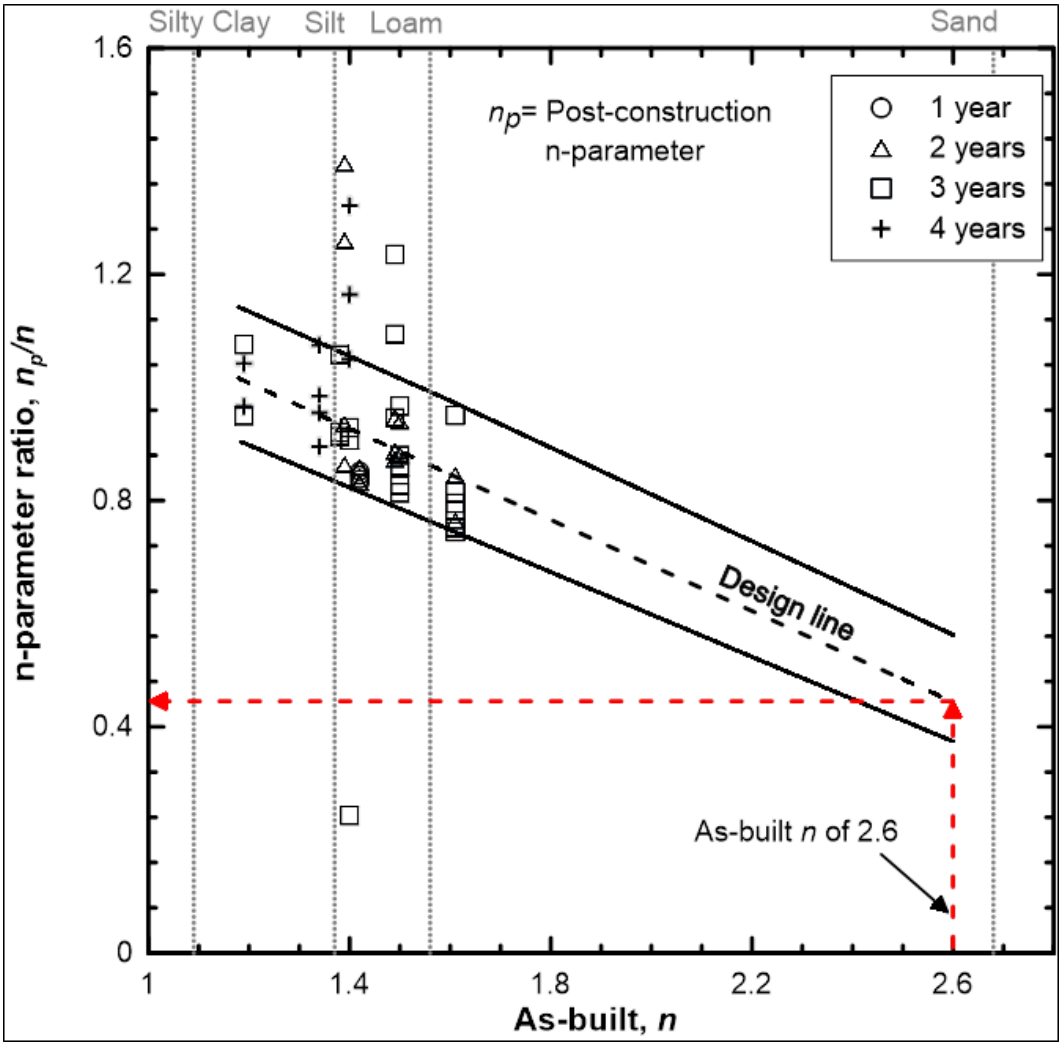

Figure 4.5. Ratio of post-construction n relative to as built condition (n_p/n) versus n in as-built condition (n) (Benson et al., 2007).

Table 4-2. Summary of as-built and post-construction hydraulic parameters for Detour Lake cover material (Dobchuk et al., 2013).

Cover hydraulic parameter	*As-built (design)*	*Post-construction*
θ_s *(m³/m³)*	0.427	0.467
k_s *(m/s)*	1x10^{-7}	1x10^{-6}
Ψ_a *(kPa)*	50	30
n	2.6	1.2

4.4.1.3 SWCC and hydraulic conductivity function

Considering the predicted post-construction changes in the tailing cover material, the soil water characteristics curve can be plotted using van Genuchten (1980) mathematical model, shown in Eq. (4.1);

$$\Theta = \frac{\theta - \theta_r}{\theta_s - \theta_r} = \left[\frac{1}{1+(\alpha\Psi)^n}\right]^m \quad (4.1)$$

Where;

$n, m \; and \; \alpha$ = van genuchten empirical parameters, and ($m = 1 - 1/n$)

Θ = normalized water content or dimensionless water content form or also called effective saturation

The hydraulic conductivity function can be predicted with SWCC using a closed form equation proposed by van Genuchten (1980) which can be written as follows:

$$k = k_s \Theta^l \left[1 - \left(1 - \Theta^{\frac{1}{m}}\right)^m\right]^2 \quad (4.2)$$

where l is constant and generally taken as 0.5.

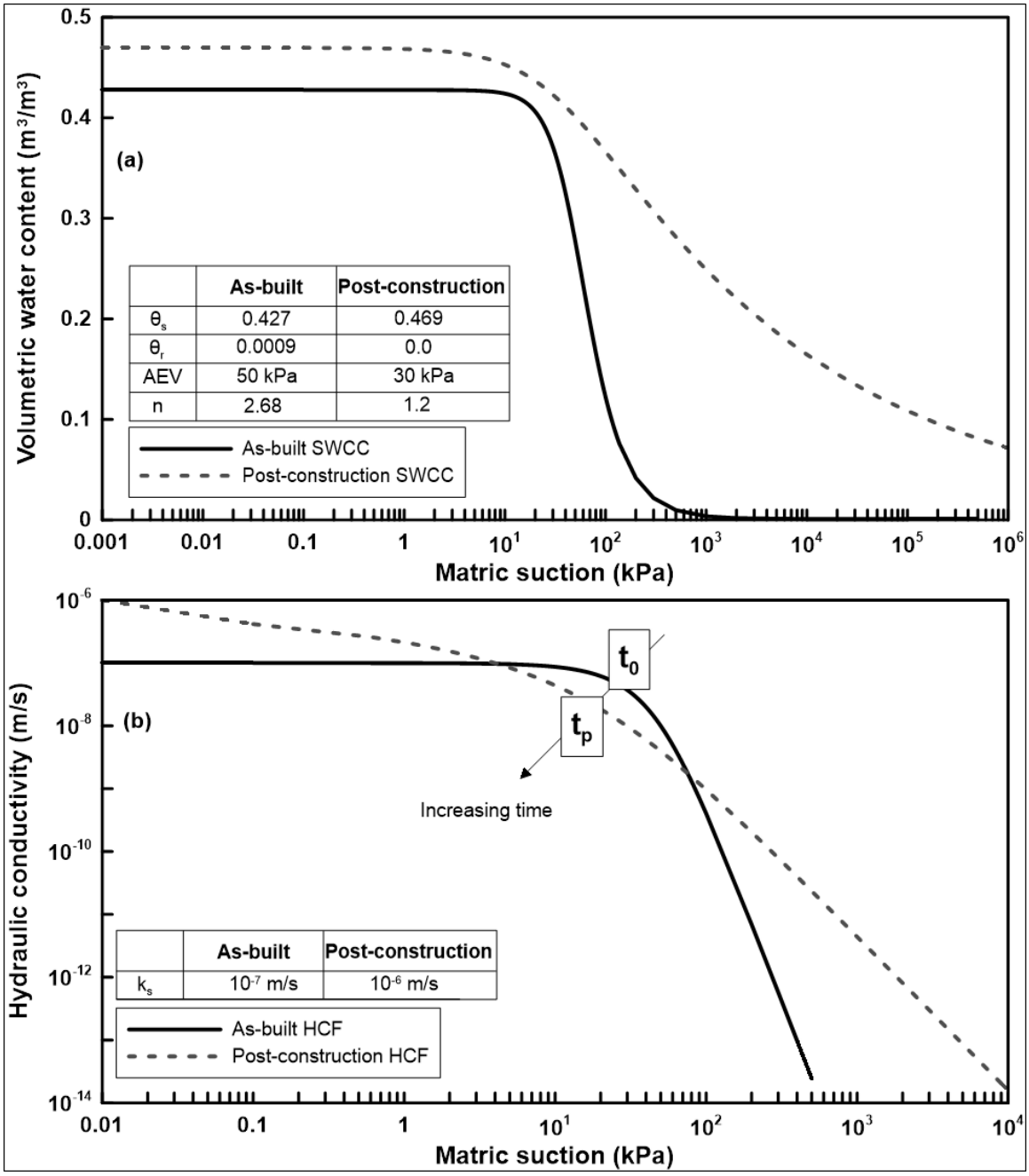

Figure 4.6. Soil hydraulic parameters for as-built and predicted post-construction cover materials; a) soil water characteristics curves, SWCCs; b) hydraulic conductivity functions, HCFs.

Figure 4.6a shows the SWCCs for as-built and predicted post-construction fine tailings cover material. It shows that θ_{sp} is more than θ_s. Similarly, hydraulic conductivity functions (HCFs) for as-built and post-construction cover materials are shown in Figure 4.6b. The volume changes due to dry/wet and freeze thaw cycles can reduce the density of the post-construction materials and can result in formation of larger pores and broader pore size distribution (Albrecht and Benson, 2001). In Figure 4.6a, the post-construction SWCC curve shows a relatively flatter curve with lower air entry value which agrees with the observation by Albrecht and Benson (2001). The post-construction processes (dry/wet, freeze/thaw) can also cause desiccation cracking. The cracking in the soil due to these processes brings changes in the soil structure which results in increased saturated hydraulic conductivity.

4.4.2 Climate

Daily metrological data recorded from 1981 to 2010 in Timmins, ON was used in the numerical model (closest Environment Canada weather stations to the Detour Lake site). A single year climate dataset measured at site is also available. The comparison of this data with climate normals for Timmins indicated that the climate at both locations is comparable (Ahmad, 2018). The compiled data set at Timmins comprised of daily records of temperature, relative humidity, wind speed, precipitation and calculated net radiations. All measured climate parameters (excluding precipitation) along with calculated net solar radiations were used to estimate the daily potential evaporation using methodology described by Penman (1948). Average annual precipitation and potential evaporation are 826 mm and 680 mm, respectively for the design climate (30 years). The climate

classification using the annual moisture index indicated that the climate of the site can be classified as humid (Ahmad, 2018).

The prediction of future climate can be carried out using general circulation models (GCMs). General circulation models are mathematical equations based on the laws of thermodynamics. These equations are generally used in computer models to simulate the earth's atmosphere using different levels of concentration of greenhouse gases (GHG). Intergovernmental panel on climate change (IPCC, 2013) have suggested a range of representative concentration pathways (RCPs) to exhibit different level of GHG emission by the end of year 2100. Four different RCPs; RCP 2.6, RCP 4.5, RCP 6.0, and RCP 8.5 are suggested by IPCC. RCP 2.6 assumes that GHG emission peaks during 2010-2020 whereas RCP 4.5 takes up maximum emission around 2040. The concentration of GHG will peak around 2080 for RCP 6.0. The RCP 8.5 suggests that the emission of GHG will continue to increase till end of this century (IPCC, 2013).

In this study, a base climate (*BC*) and a predicted future climate (*PFC*) consisting of 30-year period are considered. The predicted future climate data set was acquired from Ontario Climate Data Portal (OCDP). The acquired data was predicted using HadGEM2-ES, a Hadley Centre Met. Office UK standard climate prediction model (Jones et al., 2011). The RCP selected was RCP 8.5, allowing for the study to examine the worst case climate scenario. Further details about the prediction of future climate for range of RCPs using HadGEM2-ES models can be found in Ahmad et al. (2018). Average annual precipitation and potential evaporation were found to be 968 mm and 950 mm respectively for this future climate scenario, with a climate classification of 'moist humid' (Ahmad, 2018).

In this study, the as-built profiles are considered for the base case (*BC*) climate only. Whereas the post-construction profiles are modelled for both the base case and the predicated future climate (*PFC*) scenarios. Modelling the as-built and post-construction profiles for the *BC* will allow to examine the effect on cover performance due to changes in hydraulic properties. While modelling the post-construction profiles with *PFC* will not only examine the effects due to post constructional changes but also due to climate change scenario.

4.5 Results and Discussion

The tailings management facilities for reactive tailings are designed in a manner to limit acid mine drainage (AMD). Acid mine drainage is an acidic fluid which is produced form the sulphide-bearing material of the mining wastes when they come in contact with oxygen and water (Akcil and Koldas, 2006). The tailing covers are generally designed to limit the interaction of sulphide-bearing material with atmospheric oxygen. These covers generally work on the principle of maintaining a high saturation in cover material to control oxygen ingress.

Therefore, it is important to examine the moisture changes in the as-built and post-construction tailings cover materials due to the changing climate. The moisture variation in the cover layers due to climate change can be predicted by estimating water balance at the ground surface. Therefore, the performance of FF, FC, F'F, and F'C profiles was examined from several perspectives, including water balance and oxygen concentration.

4.5.1 Water balance

Water balance quantifies the amount of water which actually enters and leaves the cover surface, which is important information for determining the change in the degree of saturation in a cover layer. The water balance results are compared for different times during the 30-year period. Dry and wet years were identified based on the ratio of average yearly precipitation (P) and potential evaporation (PE). For example, wet year refers to a year in the thirty year data set where P/PE ratio is highest. Similarly, the dry year refers to a year in the thirty year data set where P/PE ratio is lowest. The results of the dry and wet year are compared with the 30-year average results in Figure 4.7.

Figure 4.7a and b show the dry, wet, and average water balance for profiles F'F and F'C for *PFC* respectively. In these figures the quantities which appear as negative value show water leaving the cover surface considered water loss, while the positive value shows water gain conditions or water entering into the cover at the surface. The deep percolation (DP) which is measured at cover-tailings interface, appears as negative when water moves upward at the interface from the tailings to the cover layer, while the negative value shows that the water moves downward at the interface and enters in to the tailings from the cover layer. The cumulative precipitation (P) is highest (922 mm) during wet year followed by average year (735 mm) and then dry year (492 mm). The increase in precipitation relative to dry year is 49 % and 87 % for average and wet year respectively.

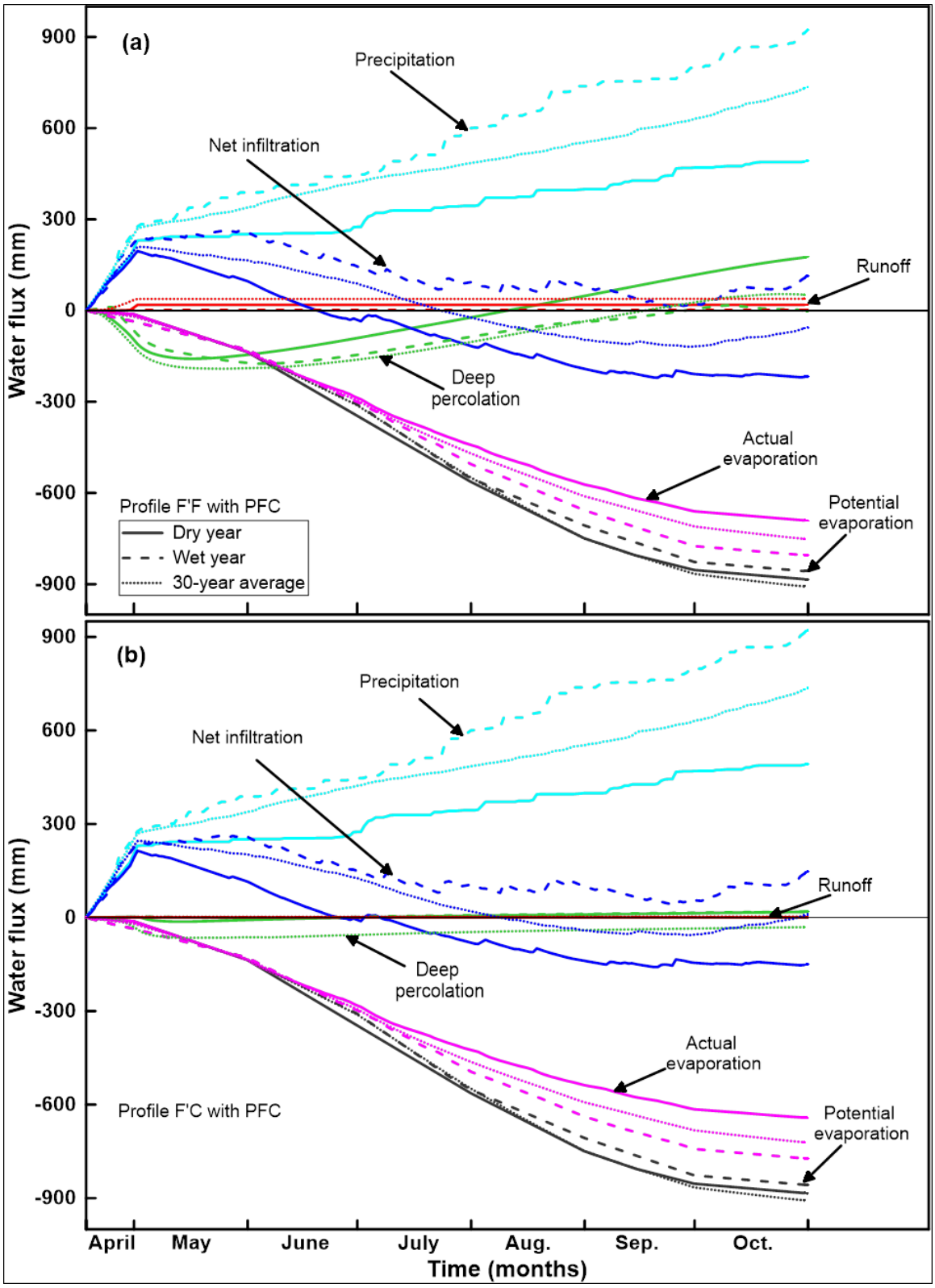

Figure 4.7. Water balance at ground surface under predicted future climate for post-construction profiles; a) profile F'F, and b) profile F'C.

Cumulative runoff (RO) depends on precipitation intensity and water retention/conduction capacity of the cover layer surface. If precipitation intensity is more than k_s, then the portion of precipitation in excess of k_s may contribute towards generation of RO. In profile F'F (Figure 4.7a), RO was observed to reach up to 5 % of the cumulative precipitation. The RO is generally generated if the precipitation intensity exceeds the k_s and/or near surface layers reach their storage capacity. The fine tailings cover in case of F'F profile holds a relatively high storage due to high capillary fringe developed over the water table (due to higher air entry pressure (Ψ_a) of the fine tailings layer). Although, in case of F'F profile the maximum precipitation intensity event is less than the k_s of the cover layer (47 mm/day < 86.4 mm/day), the higher Ψ_a of both cover and tailings layer keeps the saturation level relatively high and creates storage induced runoff especially during initial days of the active years (starts of snow melting). Conversely, the for profile F'C (Figure 4.7b), the RO is almost negligibly small due to presence coarse tailings layer which has relatively very low Ψ_a and limited capillary rise over the water table.

In contrast to precipitation values, the potential evaporation (PE) values for dry, wet and average years are quite similar. However it should be noted that, a higher PE does not necessarily translates to high actual evaporation (AE) values. This is due to the fact that AE not only depends on the evaporative energy but also on the availability of water near ground surface. For example, cumulative AE is the highest in the wet year even though PE during this year is the lowest (both Figure 4.7a and b). For both cover profiles, cumulative AE generally follows precipitation trends.

Cumulative net infiltration (NI) is the amount of water entering the cover. The NI can be estimated by subtracting the AE and RO from the P. The cumulative NI for profile F'F is maximum during wet year followed by 30 year average and then dry year which is similar to the trends in P (Figure 4.7a). During the dry and average years, cumulative NI is negative due to higher AE and lower P (AE>P). This creates a water deficit (negative NI) by losing (evaporating) a certain portion of soil storage. However, for the wet year, cumulative AE is less than cumulative P, resulting in a positive NI where the cover is therefore gaining water from atmosphere (Figure 4.7a). For the F'C profile, the tailing cover gains net water flux during the wet years (due to $AE < P$) and water deficit conditions exists during the dry year (due to AE>P). However, 30-year average of the F'C profile showed neutral water balance with no gain and no loss of water at end of the year.

The difference in the water balances of the corresponding years between F'F and F'C profiles can be understood well if we look at the processes occurring in the both profiles. There two competing processes; one is upward movement of water due to capillary rise and the other is the downward movement due to gravity. The capillary rise is high in case of profile F'F as compared to F'C due to difference in the Ψ_a of the tailings. The downward movement is generally accelerated due to amount of precipitation other than its material characteristics. For example, in a wet year there is more precipitation resulting in more downward movement of water in the profiles (Figure 4.7a and b), thus countering the capillary rise. In dry year the capillary rise is greater than the downward flux of infiltrating water.

The deep percolation (DP) is the portion of downward infiltrating water which makes its way into the underlying tailings. The DP is also controlled by the capillary rise and downward flow due to gravity. If the contribution of capillary rise is more than the downward flow due to gravity the DP is recorded as positive. For both profiles, there is a net gain in the tailing at the start of spring infiltration. With passage of time there is a capillary rise and water starts moving upward to the covers which is more obvious in profile F'F due to high Ψ_a of the tailings (Figure 4.7a). In case of profile F'F, at the end of the year the water gain conditions exist in the cover during wet year and 30-year average. While the water balance for profile F'C shows a smaller variation in DP during the dry, wet, and 30 year average years as compared to profile F'F (Figure 4.7b) due to lower air entry pressure of the tailings layer.

The water balance for as-built and post construction profiles are shown in Table 4-3 for the dry, wet, and 30 average years carried out for the base and predicted future climates. From the table it is evident that cumulative NI for 30 year average and wet year generally increases when the as-built properties change to post-construction properties for base and future climates. In contrast, NI decreases during the dry year. The changes in NI are most significant for the FF profile as compared to the FC profile.

On average, the fine tailing covers at Detour Lake site are expected to experience water deficit conditions during approximately 50 % of their total time period (which is active year from April to October). This is due to the drier climate predictions for the area. The effects of drier climate are more obvious in F'F as compared to F'C. The post-construction cover

profiles are more conductive as compared to the as-built which results in higher net infiltration during wet climate and lower NI during drier climate (Table 4-3).

Table 4-3. Water balance components at the end of the year during base and future climates for profiles FF, F'F, FC and F'C

Para-meters (mm)	***Base Climate (BC)***											
	FF			*F'F*			*FC*			*F'C*		
	Dry	Avg.	Wet	Dry	Avg.	Wet	Dry	Avg.	Wet	Dry	Avg.	Wet
P	469	658	840	469	658	840	469	658	840	469	658	840
PE	-744	-640	-612	-744	-640	-612	-744	-640	-612	-744	-640	-612
AE	-611	-620	-611	-621	-616	-610	-593	-616	-612	-594	-607	-610
NI	-146	11	200	-152	35	221	-125	27	203	-126	48	223
DP	124	-10	-128	116	-38	-201	12	-29	-64	8	-57	-109
RO	4	27	28	1	6	7	1	15	27	1	1	8

Para-meters (mm)	***Predicted Future Climate (PFC)***											
	FF			*F'F*			*FF*			*F'F*		
	Dry	Avg.	Dry	Avg.	Dry	Avg.	Dry	Avg.	Dry	Avg.	Dry	Avg.
P	492	735	922	492	735	922	492	735	922	492	735	922
PE	-884	-908	-858	-884	-908	-858	-884	-908	-858	-884	-908	-858
AE	-671	-738	-818	-691	-751	-805	-633	-716	-773	-642	-721	-773
NI	-211	-73	88	-217	-56	114	-141	1	147	-150	11	148
DP	169	78	79	176	51	-2.6	16	-3	16	18	-31	19
RO	92	70	16	19	40	2	1	19	1	0	3	0

4.5.2 Oxygen flux

The oxygen transport through the tailings covers primarily occurs through molecular diffusion. The rate of oxygen diffusion in air is four orders of magnitude higher than that in water (Akcil and Koldas 2006; Bussie`re and Aubertin 1999; Mbonimpa et al., 2003). Generally, a continuous air phase exists if the cover saturation is less than 85 % (Yanful 1993). Therefore, oxygen transport through such covers is significantly high. However, if

saturation exceeds 85 % then oxygen transport through diffusion becomes extremely slow in the cover layer because of disassociated air phase (Yanful 1993).

One of the criteria to assess the performance of tailing covers is to measure its ability to limit oxygen diffusion. The degree of saturation controls the oxygen diffusion rate in tailing covers. Changes in cover saturation occur due to changes in NI and DP. The net amount of water which enters in to the cover from atmosphere (NI), increases the degree of saturation. However only a portion of NI will contribute towards the long term storage of the cover. In many instances, a portion of NI can move downwards to the underlying tailings under the action of gravitational forces. Assuming that the lateral movement of infiltrating water is insignificant, the difference in NI and DP can be taken as net change in the soil-water storage in the cover layer. In other words, more NI and less DP will result in higher degree of saturation in covers. It is important to note here, that due to the sign convention used (for NI and DP) in the current study, the sum of NI and DP will actually estimate the changes in the soil saturation in the cover layer.

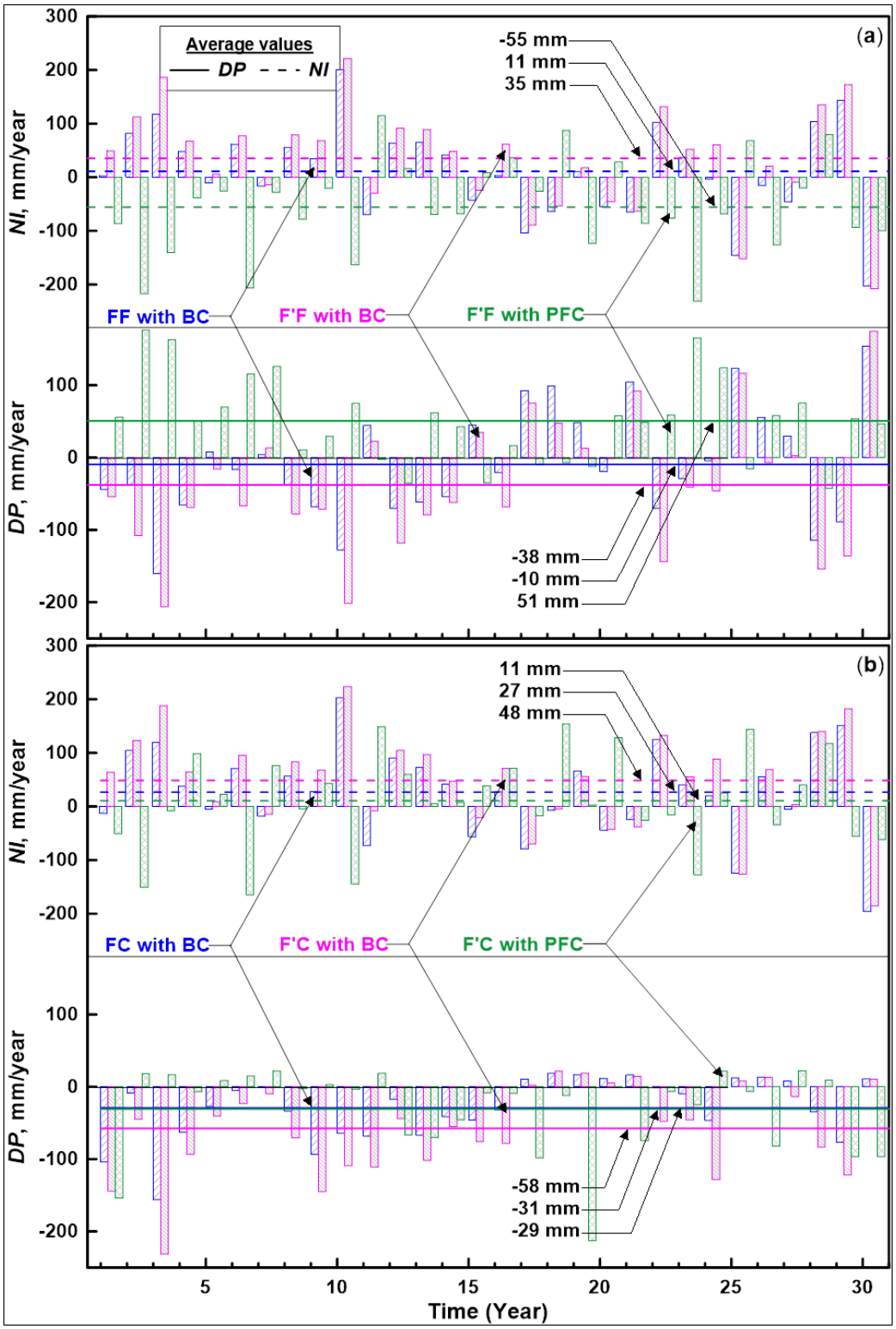

Figure 4.8. Annual net infiltration and deep percolation for as-built and post-construction covers with base and future climate for a) fine cover over fine tailings profiles; b) fine cover over coarse tailings profiles.

Figure 4.8a and b represent 30 years of annual cumulative net infiltration and deep percolation for as-built and post-construction cover profiles for the base and future climatic conditions. Figure 4.8a shows the results for fine tailing cover material over fine tailings profiles (FF and F'F) and Figure 4.8b for fine tailings cover over coarse tailings profiles (FC, F'C). When the hydraulic properties change from as-built to post-construction for the *BC* case, a distinct increase in the average NI is seen (Figure 4.8a and b). The 30 year average NI of the *BC* for the FF profile increased from 11 mm to 35 mm. Similarly, it increases from 27 to 48 mm for FC. In contrast the NI for the post-construction profiles (F'F and F'C) of *PFC* decreases relative to their as-built cases.

Similarly, annual DP with their 30-year averages are shown in Figure 4.8. Generally, the years with high NI also have high DP (for all cover scenarios under both the BC and *PFC*). The 30 year average DP of the *BC* for the FF profile contributed to the cover storage a flux of 28 mm (from -10 to -38 mm). In contrast, a flux of 27 mm flows out of the cover layer (from -31 to -58 mm) for FC profile. However, the DP for the post-construction profiles (F'F and F'C) of *PFC* shows a net contribution of water relative to their as-built cases.

Figure 4.9 shows the annual oxygen flux for as-built and post construction covers with base and future climates. If we compare this figure with Figure 4.8, it can be observed that the oxygen flux follows the reverse trend of NI. Generally, the years with higher NI and DP can be observed to have lower oxygen flux. Average cumulative oxygen flux decreases for all the profiles with base climate when the cover hydraulic properties change from as-built to post-construction (Figure 4.9a &b). However, it increases when

the post-construction profile is modelled for future climatic conditions. For example, the average cumulative oxygen flux for the as-built, *BC* profile FF is 2.9 kg/m^2/year and it reduces to 1.6 kg/m^2/year for F'F. The average cumulative *OF* becomes 3.1 kg/m^2/year when F'F is carried out for the *PFC*.

As the post-construction changes in the cover materials result in an increase in θ_s and k_s values and decrease in air entry pressure (Benson et al., 2007),one can conclude that the oxygen flux could potentially reduce due to post-constructional changes. This reduction will be the result of expected increase in NI as was shown in Figure 4.9 for both cover profiles under base climatic conditions . However, if drier climatic conditions at the site are expected in future (Ahmad 2018). the post-construction fine cover material (which holds low retention and high conduction) will facilitate the evaporation process. This would result in water deficit conditions in the covers. The expected water deficit conditions in the cover layer for future climate would result in higher oxygen flux entry in to the cover layer (Figure 4.9a and b)

Post-construction hydraulic changes in the cover material and predicted climate changes have shown greater effects on fine tailings cover placed over coarse tailings than those placed over the fine tailings. For examples, average annual oxygen flux increase by 27 % (3.3 kg/m^2 to 4.2 kg/m^2) for profile with fine tailings cover over coarse tailings as compared to 6 % (2.9 kg/m^2 to 3.1 kg/m^2) for fine tailings cover over fine tailings (Figure 4.9a and b). This is due to lower capillary rise from coarse tailings layer (Figure 4.7b).

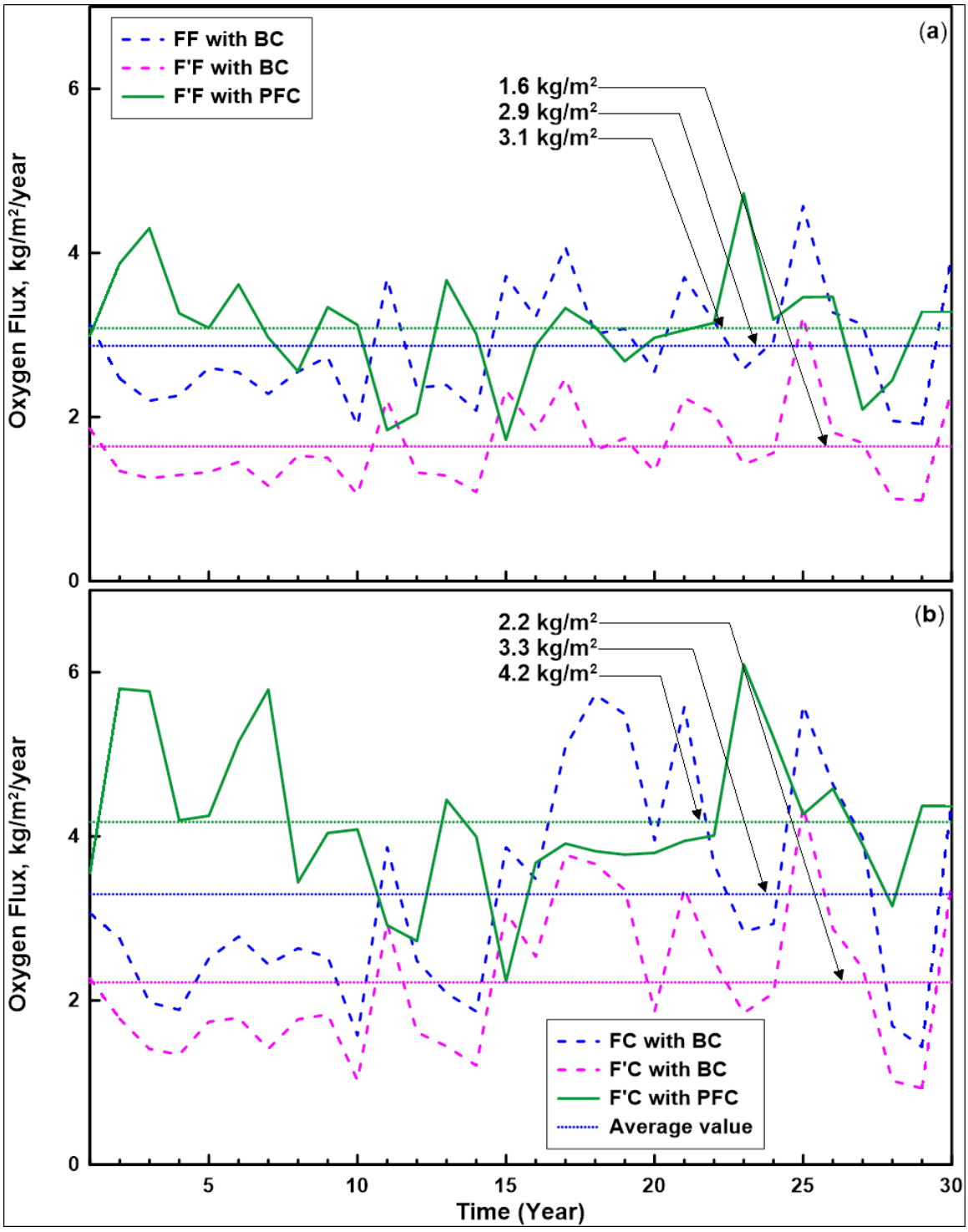

Figure 4.9. Annual oxygen flux for as-built and post-construction covers with base and future climate for a) fine cover over fine tailings profiles; b) fine cover over coarse tailings profiles.

4.5.3 Sensitivity analysis

The as-built soil hydraulic properties generally change to post-construction properties through an evolutionary process (Benson et al., 2007; Meiers et al., 2011). In other words, the soil hydraulic parameters of a fine tailings will progressively change to post-construction state over time. Therefore, it is important to evaluate how sensitive the tailings cover is to individual parameter change.

To accomplish this, multi-parameter sensitivity analyses was carried out using the predicted future climate for both cover profiles. The sensitivity analysis examined air entry pressure, depth to the ground water table, and saturated hydraulic conductivity to see how they individually impact, NI, DP and oxygen flux. According to Benson et el., (2007), the saturated hydraulic conductivity and air entry pressure are subject to change significantly after construction due to various physical and biological processes. These two parameters, therefore, are selected for sensitivity analysis. Moreover, the fluctuations in groundwater depth are also expected due to climate change (Stratos Inc., 2011). Therefore, the post-construction model was also examined under shallow and deep groundwater table conditions. The air entry pressure was varied from 15 kPa (half of as-built value) to 60 kPa (doubled to the as-built value). The depth to the groundwater table was varied from 2 m to 8 m, and k_s was varied from 10^{-7} m/s to 10^{-5} m/s. All the sensitivity simulations results are compared with the results of the post-construction profiles for future climatic conditions.

4.5.3.1 Net Infiltration

Figure 4.10a shows tornado plots of 30 year cumulative NI for profile F'F. The horizontal lines represent variation in NI with change in air entry value pressure (Ψ_a), depth to groundwater table and saturated hydraulic conductivity. The solid vertical line represents the base NI value with which other values can be compared. This line shows the NI for the F'F profile with *PFC*. Two vertical dashed lines show value of NI for fine tailings covered by as-built fine cover and post-construction fine cover respectively with base climatic conditions.

It can be observed that when the Ψ_a drops to 15 kPa (from the as-built 30 kPa) the net infiltration increases from -1675 to 1215 mm. In contrast, when the Ψ_a increases to 60 kPa, the NI drops from -1675 to -6188 mm. This is because the higher Ψ_a of the fine tailing cover maintains high saturations in near surface which results in higher amount of AE and as a result of higher AE, the NI value reduces considerably. It can also be observed that lowering the groundwater table depth from 4 to 8 m shows a behavior shift from negative to positive NI with change of more than 2500 mm over the 30 year period. Similar observation can also be made for decreasing the k_s value, which shows a change of approximately 2000 mm. A significant decrease in NI is observed by increase in Ψ_a and k_s. The shallower groundwater table shows a significant decrease in NI.

Increasing the Ψ_a of the cover layer in profile F'C shows a limited effects on NI as shown in Figure 4.10b while lowering the Ψ_a does show some increase in the NI but not of the range as it did increase in profile F'F. However, the profile has experienced significant

drop in NI for shallow groundwater table. Increase in k_s and deeper depth of water table have shown no considerable effects on NI.

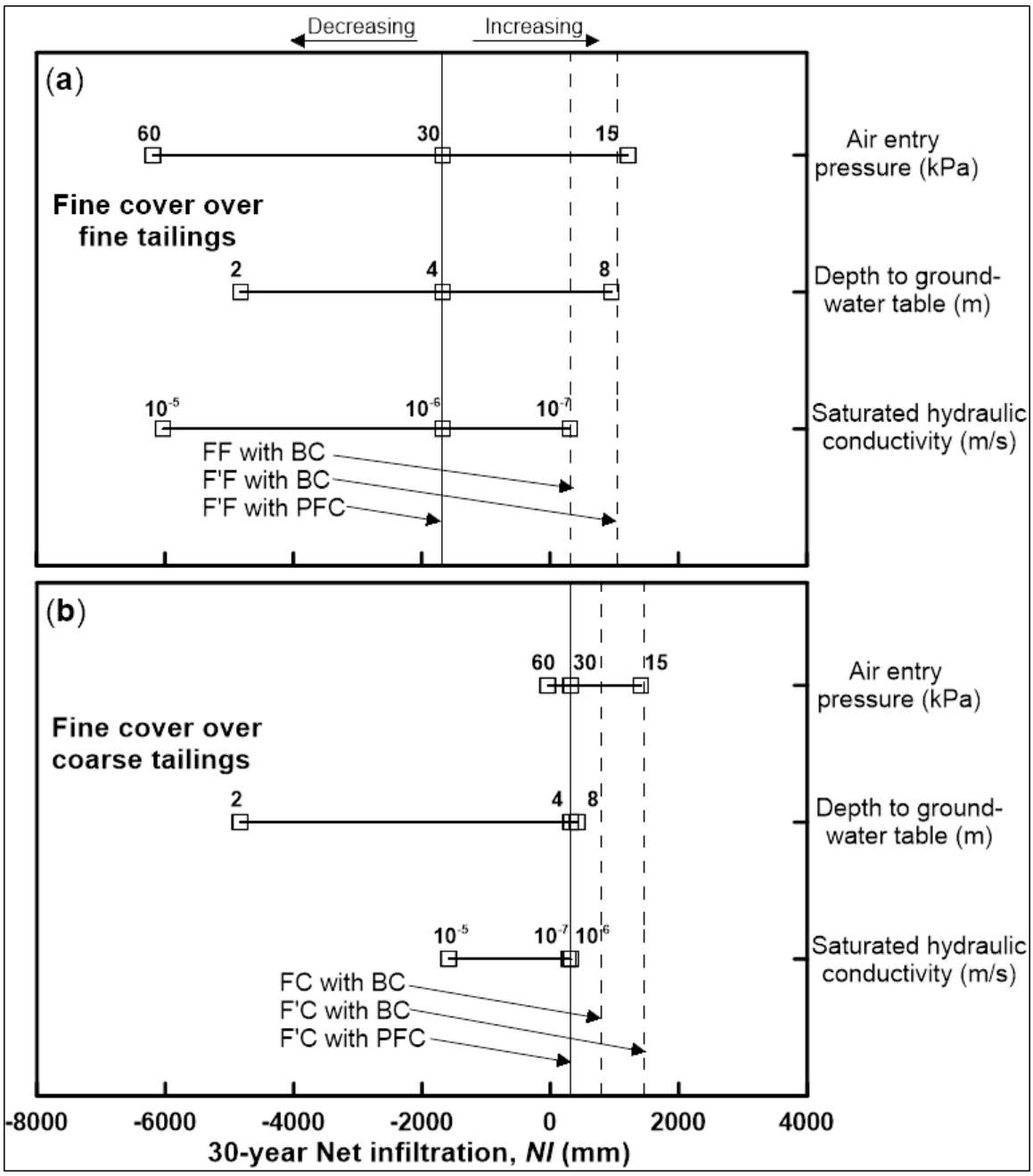

Figure 4.10. Tornado plot of 30-year cumulative *NI* for a) fine cover over fine tailings materials, and b) fine cover over coarse tailings materials.

4.5.3.2 Deep percolation

Tornado plots for 30 year cumulative DP for profile F'F and F'C are shown in Figure 4.11. Figure 4.11a shows results for profile F'F. According to this figure the DP for profile F'F shows greater sensitivity to all the parameters considered as part of the sensitivity analyses, namely, Ψ_a, depth to the groundwater table and k_s. The reduction in Ψ_a and k_s and increase in groundwater table depth from their respective baseline values indicate reversal in water balance for the cover, where net water gain conditions change to water loss conditions. This is indicated by similar decrease of more than 3000 mm in the DP when Ψ_a and k_s were increased from 30 to 60 kPa and 10^{-6} to 10^{-5} m/s respectively.

In contrast to F'F, the profile F'C indicated limited sensitivity to Ψ_a and k_s values for DP quantities (Figure 4.11b). The profile F'C did show behavioral change (downward flow to upward flow) with a decrease of more than 5000 mm in DP when depth to the groundwater table was reduced from 4 to 2 m. An increase of k_s from 10^{-6} to 10^{-5} m/s also indicated behavior shift with limited decrease of more than 1000 mm in DP over 30 year period.

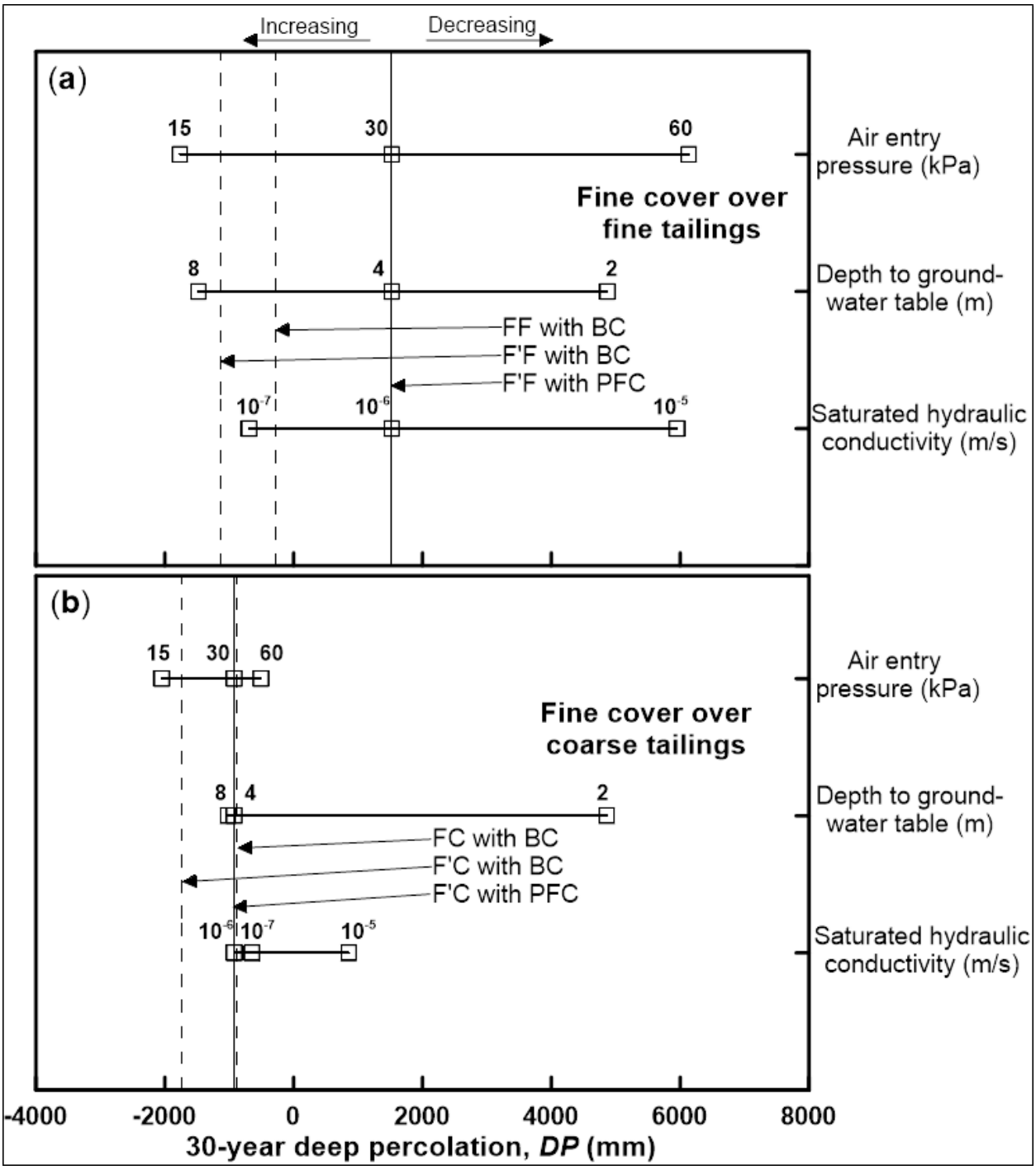

Figure 4.11. Tornado plot of 30 year cumulative *DP* for a) fine cover over fine tailings materials, and b) fine cover over coarse tailings materials.

4.5.3.3 Oxygen flux

Figure 4.12 shows the variations in the 30-year cumulative oxygen flux at the cover surface for profiles F'F and F'C for a range of parameters selected for the sensitivity analysis. Figure 4.12a shows a tornado plot of oxygen flux for profile F'F. The oxygen flux increased from 92.5 kg/m^2 to the more than 130 kg/m^2 when the Ψ_a has reduced to half of its original value for the cover layer. Lowering the groundwater table to twice of its original depth also resulted in similar increase in the oxygen flux. Interestingly, a decrease in the oxygen flux of about 60 kg/m^2 can be observed when Ψ_a, groundwater table and k_s are increased from 30 to 60 kPa, 4 to 2 m (increase in water table with reference to cover surface) and 10^{-6} to 10^{-5} m/s respectively.

The tornado plot of oxygen flux at the cover surface for profile F'C is shown in Figure 4.12b. By raising the water table to 2 m, the ingress of oxygen flux at the cover surface in profile F'C reduces by more than two-third of its value when water table depth was at 4 m. Conversely, the ingress of oxygen flux is insensitive to the water table depth increase from the baseline value of 4m. An equivalent change of approximately 17 kg/m^2 over a period of 30 year is observed in oxygen flux when Ψ_a is either increased (60 kPa) or decreased (15 kPa) form it original value of 30 kPa. It can also be observed that by changing the k_s value from 10^{-6} to 10^{-5} m/s shows a significant increase in oxygen flux of more than 60 kg/m^2 at the cover surface.

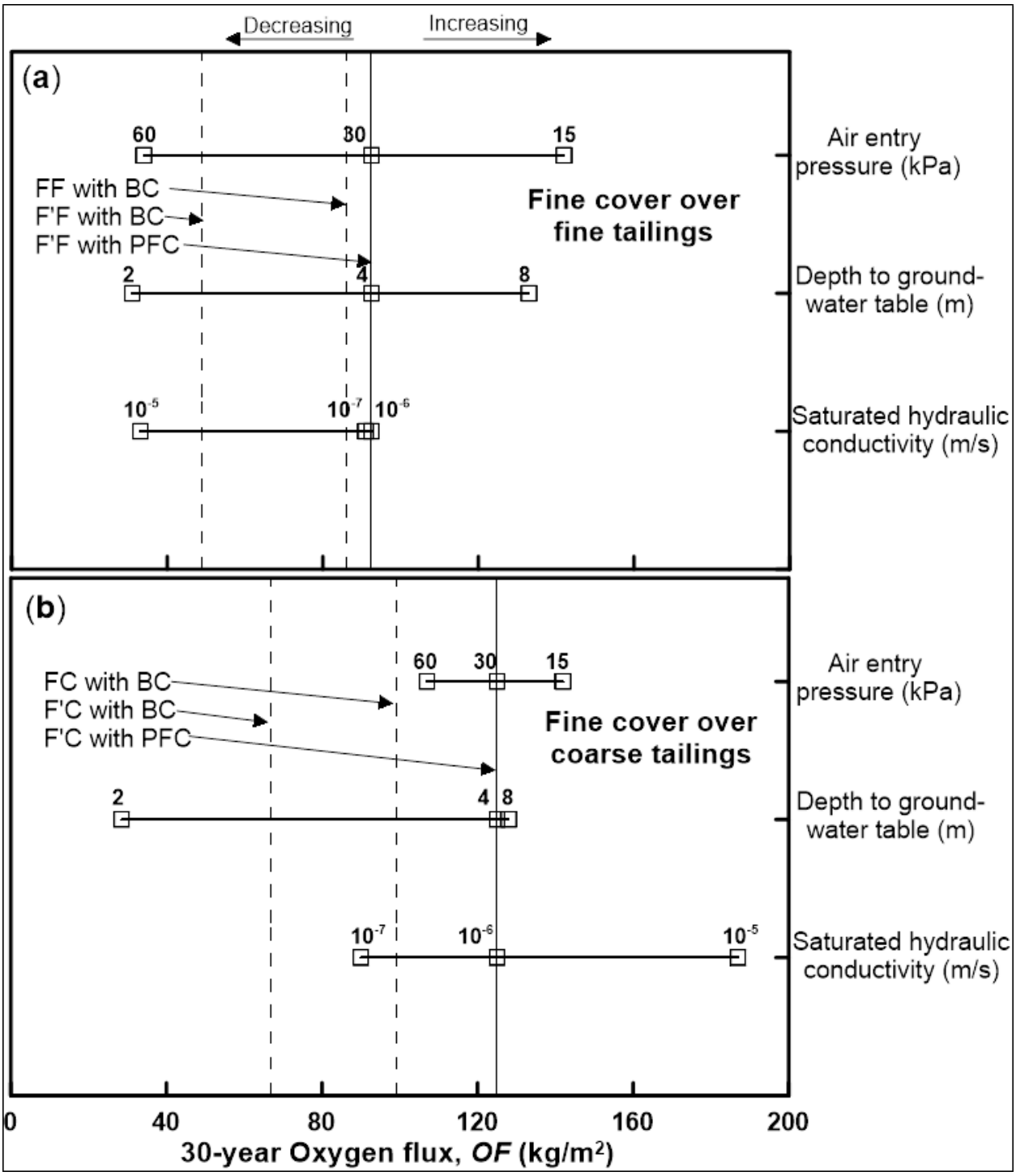

Figure 4.12. Tornado plot of 30-year cumulative oxygen flux for a) fine cover over fine tailings materials, and b) fine cover over coarse tailings materials.

Based on this sensitivity study, it can be concluded that oxygen flux is the most sensitive to the depth of the groundwater table and Ψ_a of the cover material. When the groundwater depth is considered at 2 m, the GWT starts interacting with the atmosphere because of the shallower depth. This results in increased saturation of the cover although the net water loss conditions will be observed at the ground surface. Although this will result in less oxygen flux in the cover, however the movement of water from the tailings into the cover will potentially bring the contaminants from the tailings in to the cover and probably at the ground surface (Figure 4.10 thru 4.12). In contrast, the interaction of GWT is limited with the atmosphere when the groundwater depth is considered at 4 m. In this case net water deficit conditions will be observed in the cover layer due to higher downward flow of infiltrated water into the tailings from the cover. This would increase the potential ingress of the oxygen in the cover layer (Figure 4.9a, 4.10a and 4.11a).

Oxygen flux is relatively insensitive to the deeper groundwater depths for profile F'C due to the capillary barrier which exists between the fine tailings cover and the coarse tailings layer (Figure 4.12b). The capillary barrier is created when a fine material layer is placed over coarse layer with considerable difference in their Ψ_a and HCFs (Stormont and Anderson, 1999). The cover and tailing layers have considerably different Ψ_a and HCFs for profile F'C which establishes a capillary barrier between both layers. However, this is true for the case when tailings layers have considerably dry conditions (water table at 4 m below the cover surface). But when the groundwater depth is considered to be 2.0 m which is only 20 cm below the cover-tailings interface, the tailings layer is almost saturated (95 %). Due to higher saturation, HCF of coarse tailings material near the interface becomes comparable to HCF of overlying fine tailings cover material. Therefore,

breakthrough occurs between two layers which results in high flux movement around interface (Figure 4.11a).

Oxygen flux has also shown greater sensitivity to air entry pressure. Oxygen flux changes are almost evenly distributed from the base case (fine cover *PFC* which is 92 and 125 kg/m^2 respectively for F'F and F'C)) if we reduced the value to one half (15 kPa) or doubled (60 kPa) the air entry pressure for profile F'C (Figure 4.12b). However, change in oxygen flux from the base case is about 11 % more when Ψ_a= 15 kPa as compared to Ψ_a= 60 kPa for profile F'F (Figure 4.12a).

The role of k_s is also important in controlling the oxygen flux. The change in k_s value impacts the conduction ability of the cover material. It facilitates the two competing processes; one is the downward flow of infiltrating water due to gravity and the other is the upwards flow due to capillarity. Oxygen flux increases with increase in cover k_s for the profile F'C (Figure 4.12b), it was observed, that that capillary rise is dominated the cover and upwards movement of water resulted in higher actual evaporation. The capillarity of the coarse tailing layer in this case is limited therefore, the upward movement of groundwater flow from the tailings to the cover is considerably low. In this instance the cover experiences water deficient conditions due to relatively higher actual evaporation and not enough contribution of the groundwater table to the cover layer to maintain higher saturation resulting in increased ingress of oxygen at the cover surface.

For the case of F'F with high k_s, the process of capillarity will dominate due to fine cover and tailings material which will result in higher water flux movement from cover to the tailings. The higher k_s value of the cover material can increase the storage the capacity

of the cover layer. The actual evaporation can also be increase due to increase in saturation in the near surface layer due to capillarity. The net effects in this case results in less ingress of oxygen into the cover surface (Figure 4.10a and 4.11a).

4.6 Summary and Concluding Remarks

The performance of covers for as-built and post-construction hydraulic properties of the cover material at Detour Lake Mine site was investigated. Two different cover profiles were considered. The first profile was fine desulphurized cover overlying coarse sulphidic tailings. The second profile was fine desulphurized cover overlying fine sulphidic tailings. The impact of climate change on the post-construction cover material hydraulic properties was examined for both the profiles.

As the soil hydraulic properties of the fine cover layers will evolve with post-construction process improvement in the cover performance in terms of controlling the oxygen ingress to the cover surfaces is expected. However, these performance gains will only be possible as long as the baseline climatic conditions prevail. In instances the future climate becomes drier the gain in the cover performance will be offset by the change in climatic parameters and performance could potentially become worse. As mentioned above that the cover performance is expected to become better as longs as climate conditions in the future remains similar to the base climatic condition. In such instance, the post-construction changes are expected to increase the performance of a fine tailings cover over fine tailings by 45 % (cumulative annual oxygen flux reduced from 2.9 kg/m^2 to 1.6 kg/m^2). The enhancement for fine tailing cover over coarse tailings is expected to be 33 % for (oxygen flux reduced from 3.3 kg/m^2 to 2.2 kg/m^2), which is less than the fine cover

over fine tailings. Overall, it is expected that in the tailings management facility, cover performance at locations where fine tailings rest over fine tailings would perform better for future hydrological and climatic change conditions. The results of the study also suggest that the cover performance is not only dependent on the hydraulic properties of the cover materials but also on the properties of the tailings.

Multi-parameter sensitivity analyses indicated that depth to groundwater table and changes in the air entry pressure have greater effect on cover performance for both cover profiles. Lowering of the groundwater depth and decrease in the air entry pressure generally produced larger oxygen flux as compared to the baseline conditions. Conversely, the shallower groundwater depth and increased air entry pressure reduced the oxygen entry to the cover. Changes in saturated hydraulic conductivity also affected the cover performance. It was noted that a decrease in oxygen flux for F'F and an increase in oxygen flux for F'C was observed, when k_s was increased. Reduction in k_s showed no significant effects on oxygen flux for F'F but it did show a decrease in oxygen flux for F'C.

The results in this study are based on the assumption that post-construction hydraulic changes in cover material have achieved a state where no further changes are expected to occur in the future. Also, prediction of post-construction hydraulic parameters at Detour Lake site is made on the assumption that the process responsible for the post-constructional changes in the cover material are similar to that as pointed out by Benson et al. (2007).

The tailings covers are modelled prior to their construction to examine whether they can withstand against the future adverse processes it may encounter. Therefore, the

prediction of the future climate and its associated effects on the soil cover material are fundamentally important. Based on this study, it can be concluded that fine tailings cover performance may improve over a shorter term after its construction. However, the performance may deteriorate with time after that, especially when the climate is predicted to be drier in the future. The verification of these modelling results through prototype field scale test would be an interesting contribution to the field of tailings cover performance.

Chapter Five: Conclusions and Recommendations

5.1 Summary

The current study was aimed to model the effects of climate change on the performance of desulphurized tailings covers constructed at Detour Lake mine in Northern Ontario, Canada. To predict the effect of future climate on the tailings covers, the base line conditions were established first using the measured historical climate.

The research is to be divided into three distinct sequential steps. In the first step, the climate classification of the Detour Lake mine was carried out based on annual moisture index (Thornthwaite and Hare, 1955) using historical measured climate for the period 1980-2010. The classification based on historical climate established a bench mark against which all future climate scenarios can be compared. In the second step, the future climate data was compiled and classified for the period between 2011-2100. Based on the detailed analysis and review of the future climate data, climate data sets representative of the worst case scenario (in which low availability of water at ground surface) were selected for numerical modelling. The third step involved the soil-atmosphere modelling of the cover profiles using the base and selected future climates. In this phase different combinations of cover profiles were modelled using a software which is capable of solving the equations for variably saturated flow and oxygen transport. The modelling of the cover profiles was carried out using the as-built hydraulic properties. In addition to as-built hydraulic properties, the fine cover layers were also modelled considering post-construction hydraulic parameters. The climate boundary condition

comprising of historical and future climate data was applied at the top the cover profile, while the bottom boundary condition was constant head.

5.2 Overall Conclusions

The effects of climate change on coarse and fine monolithic desulphurized tailings covers are studied in chapter 3 of this thesis. The key findings related to chapter 3 are concluded at the end of the chapter. At the end of chapter four, the conclusions of the study related to the effects of hydrological changes on the performance of monolithic desulphurized tailings covers under future climate are summarized. The overall conclusions from this research are summarized in the following sections.

5.2.1 Climate change

The increasing trend of temperature is expected to continue during this Century considering the current growth (industrial and economical). By the end of this Century, the mean annual temperature near Detour Lake mine can potentially increase up to 11 °C. The potential evaporation (PE) is also expected to follow the temperature trend and the mean annual PE could increase by as much as 39 % for the active period. For most of the climate change scenarios, the precipitation also shows an increasing trend with increase up to 20% expected during the period 2070-2100.

5.2.2 Effects of climate change on the soil cover at detour lake mine site

Coarse tailing covers occupy the majority of the existing cover at Detour Lake mine. However, previous field studies have indicated that at many locations the cover comprises

of the fine desuluphurized tailings. In general, the cover and underlying tailings are quite heterogeneous due to method employed for tailings deposition and cover placement. The modeling and associated analyses carried out as part of this research indicate that the climate change effects on the coarse tailings covers will be limited due to their higher conduction and low retention characteristics. The low retention and high conduction properties of coarse materials enhance infiltration and limit evaporation. In contrast, the covers constructed with finer materials have relatively high retention and low conduction, and therefore maintain high saturation near to the ground surface. This results in decreased infiltration and enhanced evaporation, making the cover more vulnerable to performance degradation especially during the dry spells of future climates.

Much emphasis of this study was to examine the effects of climate change on tailings covers which perform on a principle of maintaining the high saturation (>85 %) in the cover layer to limit oxygen ingress. Therefore, the driest expected climates in the future were selected for this study to examine the performance of covers under worst conditions. Based on the compiled future climate data sets, it is evident that the amount of annual precipitation will increase in majority of the instances in the future. In these instances, higher infiltration can result in generation of increased flux of leachate in the tailings for coarse tailings covers. The higher amount of precipitation can also result in increased surface runoff in the areas where fine tailings covers exist at the site.

The hydrological changes especially in the fine tailings cover materials are expected in the future due to dry/wet, and freeze/thaw cycles at the site. These changes on the time scale of climate change could potentially increase the conduction of the fine tailings cover. The increase in conduction of the fine material can impact two competing processes; one

downward flow of infiltrated water due to gravity and other upwards movement of water due to capillarity. The net direction of water in the cover is controlled by the climate conditions. Therefore, performance of cover will be compromised due to increasing evaporation rate in dry climates. Whereas, the performance of cover may improve due to higher infiltration during wet climates (spells of large amount of precipitation).

Based on the multi-parameter sensitivity analysis, it can be concluded that the depth to the groundwater table and air entry value of the cover materials are the two main performance controlling factors for fine tailings covers.

5.2.3 Prediction of relative humidity using temperature records

Measurements of relative humidity are needed to simulate the soil-atmosphere modelling. Different methods to estimate the relative humidity data were explored, because in most instances relative prediction of future climates are not available. According to the definition, relative humidity is the ratio of partial pressure of water vapors in the air to the saturated vapor pressure at given temperature. The saturated vapor pressure can be estimated using dew point temperature. In this regards the prediction of relative humidity estimates using the prediction of dew point temperature data proposed Kimball el al., (1996) was found one of the feasible methods. The estimates of relative humidity data were compared with the measure data and showed a close comparison. Moreover, the numerical simulation results using the measured and estimate relative humidity data also resulted in close comparison. The prediction of the dew point temperature using the Kimball et al., (1996) empirical relationship resulted in a close comparison of the measured and predicted relative humidity. This empirical relationship requires maximum

and minimum temperatures, daily potential evaporation and annual precipitation. The prediction of maximum and minimum temperatures and daily precipitation are generally available using general circulation models and predictions of daily potential evaporation can be calculated based on the available predictions of temperature records.

5.3 Contribution of This Research

The current study to quantify the effects of climate changes on soil cover is the first detailed study on this topic. The earlier studies by MEND (2011) and Shurnik et al., (2012) do not have specific details related to future climate classification and behavior of soil cover under probable worst case scenarios. In addition to climate change, the current study also discusses about the hydrological changes (after construction) in the fine cover profiles. The soil covers performance is evaluated using the post-construction changes and their behavior under climate change and such studies, to best of the author's knowledge, have never been done earlier.

5.4 Recommendations for Future Studies

The current study considered monolithic covers of a specified thickness, which were modelled in one dimensional domain. Considering the heterogeneity at the site, multi-layered lithological conditions may occur which might require multi-layered profile. In this regards models with different possible layers and thickness can be adopted to examine the effects on the performance of the cover and how they behave under climate change scenarios.

The covers simulated using one dimensional domain may not represent the actual site conditions. The covers are generally placed sloping outward to avoid accumulation of surface runoff. However, on this specific site, the cover is placed close to the impoundment dam, therefore, surface runoff from the slope of the dam can potentially affect the water balance at the cover surface. The effects of runoff from the neighboring slope should be modeled using a 2D model.

The long-term historical climate data at Detour Lake mine is not available, therefore, soil atmosphere modelling was carried out using detailed climate data at one of the stations at Timmins. It is, therefore, recommended that long-term climate monitoring at Detour Lake mine should be considered in order to check the adequacy of the assumptions made in the study.

The current study considers an assumption that the active period does not change. However, as per the compiled climate data, it is clear that the active period at site changes every year. Considering the actual duration of active period in the modeling would be useful to verify the assumption.

References

(Chapter 1)

Aachib, M., Mbonimpa, M., and Aubertin, M. 2004. Measurement and prediction of the oxygen diffusion coefficient in unsaturated media, with applications to soil covers. Water, Air, and Soil pollution, 156(1): 163–193.

Akcil, A., and Koldas, S. 2006. Acid Mine Drainage (AMD): causes, treatment and case studies. Journal of Cleaner Production, 14(12–13): 1139–1145. doi: 10.1016/j.jclepro.2004.09.006.

Barrow, E., Maxwell, B., and Gachon, P. 2004. Climate variability and change in Canada: past, present and future, ACSD Science Assessment Series No. 2, Meteorological Service of Canada, Environment Canada, Toronto, Ontario.

Bashir, R., Vardon, P.J., and Sharma, J. 2015. Discussion: Climatic influence on geotechnical infrastructure: a review. Environmental Geotechnics, 2(4): 249–252. doi:10.1680/envgeo.14.00049.

Bussie`re, B., and Aubertin, M. 1999. Clean tailings as cover material for preventing acid mine drainage: an in situ experiment. In Proceedings of Sudbury ’99 Mining and the Environment II, Sudbury, Ontario, 1: 19–28.

Dagenais, A. M., Aubertin, M., and Bussière, B. 2006. Parametric study on the water content profiles and oxidation rates in nearly saturated tailings above the water table. In Proceedings of the 7th International Conference on Acid Rock Drainage (ICARD). p. 405420.

Dagenais, A. M., Aubertin, M., Bussière, B., and Martin, V. 2005. Large scale applications of covers with capillary barrier effects to control the production of acid mine drainage. Proceedings of post-mining, 16–17.

Demers, I., Bussière, B., Benzaazoua, M., Mbonimpa, M., and Blier, A. 2008. Column test investigation on the performance of monolayer covers made of desulphurized tailings to prevent acid mine drainage. Minerals Engineering, 21(4): 317–329. doi: 10.1016/j.mineng.2007.11.006.

Dobchuk, B., Nichol, C., Wilson, G.W., and Aubertin, M. 2013. Evaluation of a single-layer desulphurized tailings cover. Canadian Geotechnical Journal, 50(7): 777–792. doi:10.1139/cgj-2012-0119.

Ethier, M. P., Bussière, B., Broda, S., and Aubertin, M. 2018. Three-dimensional hydrogeological modeling to assess the elevated-water-table technique for controlling acid generation from an abandoned tailings site in Quebec, Canada. Hydrogeology Journal, doi:10.1007/s10040-017-1713-y.

Gosselin, M., Mbonimpa, M., Aubertin, M., and Martin, V. 2011. An Investigation of the effect of the degree of saturation on the oxygen reaction rate coefficient of sulphidic tailings.

Houghton, J.T., and IPCC (Editors). 2001. Climate change 2001: The scientific basis: contribution of Working Group I to the third assessment report of the Intergovernmental Panel on Climate Change. Cambridge University Press, Cambridge; New York.

IPCC. 2007. Climate Change 2007: Synthesis Report. Contribution of Working Groups I, II and III to the Fourth Assessment Report of the Intergovernmental Panel on Climate Change [Core Writing Team, Pachauri, R.K and Reisinger, A. (eds.)]. IPCC, Geneva, Switzerland. IPCC, Geneva.

IPCC. 2014. Climate Change 2014: Synthesis Report. Contribution of Working Groups I, II and III to the Fifth Assessment Report of the Intergovernmental Panel on Climate Change [Core Writing Team, R.K. Pachauri and L.A. Meyer (eds.)]. IPCC, Geneva, Switzerland.

Lindsay, M.B.J., Moncur, M.C., Bain, J.G., Jambor, J.L., Ptacek, C.J., and Blowes, D.W. 2015. Geochemical and mineralogical aspects of sulfide mine tailings. Applied Geochemistry, 57: 157–177. doi: 10.1016/j.apgeochem.2015.01.009.

Mekis, É., and Vincent, L.A. 2011. An overview of the second generation adjusted daily precipitation dataset for trend analysis in Canada. Atmosphere-Ocean, 49(2): 163–177. doi:10.1080/07055900.2011.583910.

MEND. 2011. Climate change and acid rock drainage - Risk for the Canadian mining sector.

Nicholson, R.V., Gillham, R.W., Cherry, J.A., and Reardon, E.J. 1989. Reduction of acid generation in mine tailings through the use of moisture-retaining cover layers as oxygen barriers. Canadian Geotechnical Journal, 26(1): 1–8.

Pabst, T., Aubertin, M., Bussière, B., and Molson, J. 2014. Column tests to characterize the hydro geochemical response of pre-oxidized acid-generating tailings with a

monolayer cover. Water, Air, & Soil Pollution, 225(2). doi:10.1007/s11270-013-1841-5.

Pabst, T., Aubertin, M., Bussière, B., and Molson, J. 2017. Experimental and numerical evaluation of single-layer covers placed on acid-generating tailings. Geotechnical and Geological Engineering, 35(4): 1421–1438. doi:10.1007/s10706-017-0185-0.

Pachauri, R.K., and IPCC (Editors). 2008. IPCC, 2007: Climate Change 2007: Synthesis Report. Contribution of Working Groups I, II and III to the Fourth Assessment Report of the Intergovernmental Panel on Climate Change [Core Writing Team, Pachauri, R.K and Reisinger, A. (eds.)]. IPCC, Geneva, Switzerland. IPCC, Geneva.

Ren, L., Arkin, P., Smith, T.M., and Shen, S.S.P. 2013. Global precipitation trends in 1900-2005 from a reconstruction and coupled model simulations: Global Precipitation Trends. Journal of Geophysical Research: Atmospheres, 118(4): 1679–1689. doi:10.1002/jgrd.50212.

Trenberth, K.E. 1999. Conceptual Framework for Changes of Extremes of the Hydrological Cycle with Climate Change. In Weather and Climate Extremes: Changes, Variations and a Perspective from the Insurance Industry. Edited by T.R. Karl, N. Nicholls, and A. Ghazi. Springer Netherlands, Dordrecht. pp. 327–339. doi:10.1007/978-94-015-9265-9_18.

Yanful, E.K. 1993. Oxygen diffusion through soil covers on sulphidic mine tailings. Journal of Geotechnical Engineering, 119(8): 1207–1228.

Yanful, E.K., Samad, M., and Mian, H. 2004. Shallow Water Cover Technology for Reactive Sulphide Tailings Management. Waste Geotechnics, (2004): 42–51.

(Chapter 2)

Aachib, M., Mbonimpa, M., Aubertin, M., 2004. Measurement and prediction of the oxygen diffusion coefficient in unsaturated media, with applications to soil covers. Water. Air. Soil Pollution. 156, 163–193.

Akcil, A., Koldas, S., 2006. Acid Mine Drainage (AMD): Causes, treatment and case studies. J. Clean. Prod. 14, 1139–1145. https://doi.org/10.1016/j.jclepro.2004.09.006

Aubertin, M., Aachib, M., Authier, K., 2000. Evaluation of diffusive gas flux through covers with a GCL. Geotextile. Geomembrane. 19.

Barbour, S.L., 1998. Nineteenth Canadian Geotechnical Colloquium: The soil-water characteristic curve: a historical perspective 35, 22.

Barbour, S.L., Wilson, G.W., St-Arnaud, L.C., 1993. Evaluation of the saturated–unsaturated groundwater conditions of a thickened tailings deposit. Canadian Geotechnical. Journal 30, 935–946. https://doi.org/10.1139/t93-091

Benson, C.H., Abichou, T.H., Olson, M.A., Bosscher, P.J., 1995. Winter effects on hydraulic conductivity of compacted clay. Journal of Geotechnical Engineering. 121, 69–79. https://doi.org/10.1061/(ASCE)0733-9410(1995)121:1(69)

Benson, C.H., Sawangsuriya, A., Trzebiatowski, B., Albright, W.H., 2007. Post-construction changes in the hydraulic properties of water balance cover Soils. Journal Geotech. Geoenvironmental Eng. 133, 349–359. https://doi.org/10.1061/(ASCE)1090-0241(2007)133:4(349)

Bitterlich, S., Durner, W., Iden, S.C., Knabner, P., 2004. Inverse estimation of the unsaturated soil hydraulic properties from column outflow experiments using free-form parameterizations. Vadose Zone J 3, 11.

Brooks, R.H., Corey, A.T., 1966. Properties of porous media affecting the fluid flow. Irrigation Drainage Division. 92, 61–88.

Brooks, R.H., Corey, A.T., 1964. Hydraulic properties of porous media 37.

Buckingham, E., 1907. Studies on the movement of soil moisture 64.

Bussie`re, B., Aubertin, M., 1999. Clean tailings as cover material for preventing acid mine drainage: an in situ experiment. Proc. Sudbury ’99 Min. Environ. II Sudbury Ont. 1, 19–28.

Camargo, A.P., Marin, F.R., Sentelhas, P.C., 1999. Adjust of the Thornthwaite’s method to estimate the potential evapotranspiration for arid and superhumid climates, based on daily temperature amplitude. Rev Bras Agrometeorol 7, 251–257.

Collin, M., 1998. The Brsbon pilot project: numerical simulation of water and oxygen transport in the soil covers at the mine waste deposits (No. 4763). Swedish Environmental Protection Agency.

Collin, M., 1987. Mathematical modelling of water and oxygen transport in layered soil covers for deposits of pyritic mine tailings. Royal Institute of Technology. Department of Chemical Engineering, S-100 44 Stockholm, Sweden.

Collin, M., Rasmuson, A., 1988. Gas diffusivity models for unsaturated porous media. Soil Science American Journal 52, 1559–1565.

Crank, J., 1975. The mathematics of diffusion, Second. edition. Oxford University Press 1975.

Demers, I., Bussière, B., Benzaazoua, M., Mbonimpa, M., Blier, A., 2008. Column test investigation on the performance of monolayer covers made of desulphurized tailings to prevent acid mine drainage. Miner. Eng. 21, 317–329. https://doi.org/10.1016/j.mineng.2007.11.006

Demers, I., Bussière, B., Mbonimpa, M., Benzaazoua, M., 2009. Oxygen diffusion and consumption in low-sulphide tailings covers. Can. Geotech. J. 46, 454–469. https://doi.org/10.1139/T08-132

Dobchuk, B., 2002. Evaluations of the effectiveness of desulphurized tailings cover at Detour Lake Mine.

Dobchuk, B., Nichol, C., Wilson, G.W., Aubertin, M., 2013. Evaluation of a single-layer desulphurized tailings cover. Can. Geotech. J. 50, 777–792. https://doi.org/10.1139/cgj-2012-0119

Dunne, T., Black, R.D., 1970. An experimental investigation of runoff production in permeable soils. Water Resource. Res. 6, 478–490. https://doi.org/10.1029/WR006i002p00478

Dwyer, S.F., 2003. Water balance measurements and computer simulations of landfill covers. The University of New Mexico Albuquerque, New Mexico.

Elberling, B., 2005. Temperature and oxygen control on pyrite oxidation in frozen mine tailings. Cold Reg. Sci. Technol. 13.

Estabragh, A.R., Moghadas, M., Moradi, M., Javadi, A.A., 2017. Consolidation behavior of an unsaturated silty soil during drying and wetting. Soils Found. 57, 277–287. https://doi.org/10.1016/j.sandf.2017.03.005

Fredlund, D.G., Rahardjo, H., Fredlund, M.D., 2012. Unsaturated soil mechanics in engineering practice. John Wiley & Sons, Inc., Hoboken, New Jersey.

Freeze, R.A., Cherry, J.A., 1979. Groundwater. Prentice-Hall, Englewood Cliffs, N.J.

Government of Canada, E. and C.C.C., 2017. Environment and climate change Canada - Climate Change - Climate Modelling and Analysis. Available from https://www.ec.gc.ca/ccmac-cccma/ [accessed 09 May 2017].

Penman, H. L., 1948. Natural Evaporation from Open Water, Bare Soil and Grass.

Horton, R.E., 1933. The Role of infiltration in the hydrologic cycle. Trans. Am. Geophys. Union 14, 446. https://doi.org/10.1029/TR014i001p00446

Houghton, J.T., Intergovernmental Panel on Climate Change (Eds.), 2001. Climate change 2001: the scientific basis: contribution of Working Group I to the third assessment report of the Intergovernmental Panel on Climate Change. Cambridge University Press.

IPCC, 2013. Climate Change 2013: The Physical Science Basis. Contribution of Working Group I to the Fifth Assessment Report of the Intergovernmental Panel on Climate Change. Cambridge University Press.

Karmakar, R., Das, I., Dutta, D., Rakshit, A., 2016. Potential effects of climate change on soil properties: A review. Sci. Int. 4, 51–73.

MacKay, P.L., 1997. Evaluation of oxygen diffusion in unsaturated soils 200.

Mbonimpa, M., Aubertin, M., Bussière, B., 2011. Oxygen consumption test to evaluate the diffusive flux into reactive tailings: interpretation and numerical assessment. Can. Geotech. J. 48, 878–890. https://doi.org/10.1139/t11-015

Meiers, G.P., Barbour, S.L., Qualizza, C.V., Dobchuk, B.S., 2011. Evolution of the hydraulic conductivity of reclamation covers over sodic/saline mining overburden. J. Geotech. Geoenvironmental Eng. 137, 968–976. https://doi.org/10.1061/(ASCE)GT.1943-5606.0000523

Mein, R.G., Larson, C.L., 1973. Modeling infiltration during a steady rain. Water Resource. Res. 9, 384–394. https://doi.org/10.1029/WR009i002p00384

Mekis, É., Vincent, L.A., 2011. An overview of the second generation adjusted daily precipitation dataset for trend analysis in Canada. Atmosphere-Ocean 49, 163–177. https://doi.org/10.1080/07055900.2011.583910

Micheal, M., 2010. Modeling of predicted performance of the desulphurized tailings cover at Detour Lake Mine. University of British Columbia.

Mualem, Y., 1976. A new model for predicting the hydraulic conductivity of unsaturated porous media. Water Resource Res. 12, 513–522. https://doi.org/10.1029/WR012i003p00513

Musso, G. (Ed.), 2013. Coupled phenomena in environmental geotechnics. CRC Press. https://doi.org/10.1201/b15004

Nahlawi, H., Kodikara, J.K., 2006. Laboratory experiments on desiccation cracking of thin soil layers. Geotech. Geol. Eng. 24, 1641–1664. https://doi.org/10.1007/s10706-005-4894-4

Nicholson, R.V., Gillham, R.W., Cherry, J.A., Reardon, E.J., 1989. Reduction of acid generation in mine tailings through the use of moisture-retaining cover layers as oxygen barriers. Can. Geotech. J. 26, 1–8.

Nicholson, R.V., Gillham, R.W., Reardon, E.J., 1988. Pyrite oxidation in carbonate-buffered solution: 1. Experimental kinetics. Geochim. Cosmochim. Acta 52, 1077–1085. https://doi.org/10.1016/0016-7037(88)90262-1

Ogden, F.L., Lai, W., Steinke, R.C., Zhu, J., Talbot, C.A., Wilson, J.L., 2015. A new general 1-D vadose zone flow solution method: 84 Years After Richards: A New Vadose Zone Solution Method. Water Resour. Res. 51, 4282–4300. https://doi.org/10.1002/2015WR017126

Ouangrawa, M., Molson, J., Aubertin, M., Bussière, B., Zagury, G.J., 2009. Reactive transport modelling of mine tailings columns with capillarity-induced high water saturation for preventing sulfide oxidation. Appl. Geochem. 24, 1312–1323. https://doi.org/10.1016/j.apgeochem.2009.04.005

Pabst, T., Aubertin, M., Bussière, B., Molson, J., 2014. Column tests to characterize the hydro-geochemical response of pre-oxidized acid-generating tailings with a monolayer cover. Water. Air. Soil Pollution, 225. https://doi.org/10.1007/s11270-013-1841-5

Pereira, A.R., Pruitt, W.O., 2004. Adaptation of the Thornthwaite scheme for estimating daily reference evapotranspiration. Agric. Water Manag. 66, 251–257. https://doi.org/10.1016/j.agwat.2003.11.003

Philip, J.R., 1957. The theory of infiltration: 1. The infiltration equation and its solution. Soil Sci. 83, 345–358.

Ren, L., Arkin, P., Smith, T.M., Shen, S.S.P., 2013. Global precipitation trends in 1900-2005 from a reconstruction and coupled model simulations: Global Precipitation Trends. J. Geophys. Res. Atmospheres 118, 1679–1689. https://doi.org/10.1002/jgrd.50212

Richards, L.A., 1931. Capillary conduction of liquids through porous mediums. Physics 1, 318–333. https://doi.org/10.1063/1.1745010

Romano, C.G., Mayer, K.U., Jones, D.R., Ellerbroek, D.A., Blowes, D.W., 2003. Effectiveness of various cover scenarios on the rate of sulfide oxidation of mine tailings. J. Hydrol. 271, 171–187.

Rowe, R.K., Booker, J.R., 1985. 1-D Pollutant Migration in Soils of Finite Depth. J. Geotech. Eng. 111, 479–499. https://doi.org/10.1061/(ASCE)0733-9410(1985)111:4(479)

Runkles, J.R., 1956. Diffusion, sorption and depth distribution of oxygen in soils 163.

Scanlan, C.A., 2009. Evaluation of the Long-Term Performance of Dry Cover Systems. University of Western Australia.

Shurnik, R.E., O'Kane, M.A., Green, R., 2012. Simulation of seven years of field performance monitoring at Rio Tinto Iron Ore, Mount Tom Price mine using soil-plantatmosphere numerical modelling. Aust. Cent. Geomech.

Stormont, J.C., Anderson, C.E., 1999. Capillary barrier effect from underlying coarser soil layer. J. Geotech. Geoenvironmental Eng. 125, 641–648. https://doi.org/10.1061/(ASCE)1090-0241(1999)125:8(641)

Troeh, F.R., Jabro, J.D., Kirkham, D., 1982. Gaseous diffusion equations for porous materials. Geoderma 27, 239–253. https://doi.org/10.1016/0016-7061(82)90033-7

Vadose Zone Modeling with VADOSE/W, 2014. GEO-SLOPE Int. Ltd 1400 633 – 6th Ave SW Calg. Alta. Can. T2P 2Y5 242.

van Genuchten, M.T., 1980. A Closed-form Equation for Predicting the Hydraulic Conductivity of Unsaturated Soils1. Soil Sci. Soc. Am. J. 44, 892–898. https://doi.org/10.2136/sssaj1980.03615995004400050002x

Williams, L.O., Hoyt, D.L., Dwyer, S.F., Hargreaves, G.A., Zornberg, J.G., 2011. Design criteria and construction of a capillary barrier cover system: the rocky mountain arsenal experience. American Society of Civil Engineers, pp. 996–1005. https://doi.org/10.1061/41165(397)102

Wilson, G.W., 1990. Soil evaporative fluxes for geotechnical engineering problems (PhD Thesis). Department of Civil and Geological Engineering, University of Saskatchewan, Saskatoon, SK.

Wilson, G.W., Fredlund, D.G., Barbour, S.L., Pufahl, D.E., 1997. The use of ground surface moisture flux boundary conditions in geotechnical engineering 4.

Yanful, E.K., 1993. Oxygen diffusion through soil covers on sulphidic mine tailings. J. Geotech. Eng. 119, 1207–1228.

Yanful, E.K., Samad, M., Mian, H., 2004. Shallow Water Cover Technology for Reactive Sulphide Tailings Management. Waste Geotech. 42–51.

Yesiller, N., Miller, C.., Inci, G., Yaldo, K., 2000. Desiccation and cracking behavior of three compacted landfill liner soils. Eng. Geol. 57, 105–121. https://doi.org/10.1016/S0013-7952(00)00022-3

(Chapter 3)

Aachib, M., Aubertin, M., and Mbonimpa, M. 2002. Laboratory measurements and predictive equations for gas diffusion coefficient of unsaturated soils (Access from CGS_IAH Conf. Niagara Falls, to be published)

Aachib, M., Mbonimpa, M., and Aubertin, M. 2004. Measurement and prediction of the oxygen diffusion coefficient in unsaturated media, with applications to soil covers. Water, Air, and Soil Pollution, 156(1): 163–193.

Aubertin, M., Industrial NSERC Ecole Polytechnique – UQAT Chair, 2005. Unpublished presentation.

Aubertin, M., Aachib, M., and Authier, K. 2000. Evaluation of diffusive gas flux through covers with a GCL. Geotextiles and Geomembranes, 18: 215-233.

Barbour, S.L., Wilson, G.W., and St-Arnaud, L.C. 1993. Evaluation of the saturated–unsaturated groundwater conditions of a thickened tailings deposit. Canadian Geotechnical Journal, 30(6): 935–946. doi:10.1139/t93-091.

Bashir, R., Vardon, P.J., and Sharma, J. 2015. Discussion: Climatic influence on geotechnical infrastructure: a review. Environmental Geotechnics, 2(4): 249–252. doi:10.1680/envgeo.14.00049.

Camargo, A.P., Marin, F.R., and Sentelhas, P.C. 1999. Adjust of the Thornthwaite's method to estimate the potential evapotranspiration for arid and superhumid climates, based on daily temperature amplitude. Rev. Bras. Agrometeorol., 7(2): 251–257.

Collin, M., and Rasmuson, A. 1988. Gas diffusivity models for unsaturated porous media. Soil Science Amer. J., **52**: 1559–1565.

Crank, J. 1975. The Mathematics of Diffusion. In Second. Oxford University Press 1975.

Dagenais, A-M., Aubertin, M. and Bussière, B. 2006. "Parametric study on the water content profiles and oxidation rates in nearly saturated tailings above the water table." In Proceedings of the 7th International Conference on Acid Rock Drainage (ICARD), 2630:405420.

Dagenais, AM., Aubertin, M., Bussière, B. and Martin, V. 2005. Large scale applications of covers with capillary barrier effects to control the production of acid mine drainage. Proceedings of Post-Mining, 16–17.

Demers, I., Bussière, B., Benzaazoua, M., Mbonimpa, M., and Blier, A. 2008. Column test investigation on the performance of monolayer covers made of desulphurized tailings to prevent acid mine drainage. Minerals Engineering, 21(4): 317–329. doi: 10.1016/j.mineng.2007.11.006.

Deng, Z., Liu, J., Qui, X., Zhou, X., and Zhu, H. 2017. Downscaling RCP8.5 daily temperatures and precipitation in Ontario using localized ensemble optimal

interpolation (EnOI) and bias correction. Climate Dynamics, 1–21. doi:10.1007/s00382-017-3931-3.

Dobchuk, B. 2002. Evaluations of the effectiveness of desulphurized tailings cover at Detour Lake Mine. M.Sc. thesis, University of Saskatchewan, Saskatoon, SK.

Dobchuk, B., Nichol, C., Wilson, G.W., and Aubertin, M. 2013. Evaluation of a single-layer desulphurized tailings cover. Canadian Geotechnical Journal, 50(7): 777–792. doi:10.1139/cgj-2012-0119.

Dobchuk, B.S., Wilson, G.W., and Aubertin, M. 2003. Evaluation of a Single-Layer Desulfurized Tailings Cover.

Ethier, Marie-Pier, Bussière, B., Broda, S., and Aubertin, M. 2018. Three-dimensional hydrogeological modeling to assess the elevated-water-table technique for controlling acid generation from an abandoned tailings site in Quebec, Canada." Hydrogeology Journal, January. https://doi.org/10.1007/s10040-017-1713-y.

Geo-Slope International Ltd. 2016. GEO-SLOPE > Products > GeoStudio. Available from https://www.geo-slope.com/products/geostudio [accessed 16 March 2017].

Geo-Slope International Ltd. 2014. 2014. Vadose Zone Modeling with VADOSE/W. Available from https://www.geo-slope.com/ [accessed 14 April 2017].

Gosselin, M., Mbonimpa, M., Aubertin, M., and Martin, V. 2011. An investigation of the effect of the degree of saturation on the oxygen reaction rate coefficient of sulphidic tailings.

Mbonimpa, M., Aubertin, M., Aachib, M., and Bussière, B. 2003. Diffusion and consumption of oxygen in unsaturated cover materials. Canadian Geotechnical Journal, 40(5): 916–932. doi:10.1139/t03-040.

MEND. 1996. Review of use of an elevated water table as a method to control and reduce acidic drainage from tailings, MEND Report 2.17.1.

MEND. 1997. Review of Water Covers Sites and Research Projects, MEND Project 2.18.1.

MEND. 2011. Climate change and acid rock drainage - Risk for the Canadian mining sector.

Mylona, E., Xenidis, A., Csövári, M., and Németh, G. 2007. Application of dry covers for the closure of tailings facilities. Land Contamination & Reclamation, 15(2): 163–182. doi:10.2462/09670513.849.

Nicholson, R.V. 1984. Pyrite oxidation in carbonate-buffered systems: experimental kinetics and control by oxygen diffusion in porous media. Ph.D. thesis, University of Waterloo, Waterloo, Ontario.

Nicholson, R.V., Gillham, R.W., Cherry, J.A., and Reardon, E.J. 1989. Reduction of acid generation in mine tailings through the use of moisture-retaining cover layers as oxygen barriers. Canadian Geotechnical Journal, 26(1): 1–8.

OCDP. 2018. Ontario Climate Change Projections. Available from http://lamps.math.yorku.ca/OntarioClimate/index.htm [accessed August 1, 2018].

Pabst, Thomas, Aubertin, M., Bussière, B., and Molson, J. 2014. Column tests to characterize the hydro-geochemical response of pre-oxidized acid-generating tailings with a monolayer cover. Water, Air, & Soil Pollution 225 (2).

Penman, H.L. 1948. Natural evaporation from open water, bare soil and grass. Available from http://www.jstor.org/stable/98151.

Pereira, A.R., and Pruitt, W.O. 2004. Adaptation of the Thornthwaite scheme for estimating daily reference evapotranspiration. Agricultural Water Management, 66(3): 251–257. doi:10.1016/j.agwat.2003.11.003.

Pk, Shubra. 2017. Effects of climate change on soil embankments. M.Sc. thesis, York University Toronto ON.

Romano, C.G., Mayer, K.U., Jones, D.R., Ellerbroek, D.A., and Blowes, D.W. 2003. Effectiveness of various cover scenarios on the rate of sulfide oxidation of mine tailings. Journal of Hydrology, 271(1–4): 171–187.

Runkles, J.R. 1956. Diffusion, sorption and depth distribution of oxygen in soils. 163.

Shurnik, R.E., O'Kane, M.A., and Green, R. 2012. Simulation of seven years of field performance monitoring at Rio Tinto Iron Ore, Mount Tom Price mine using soil-plant atmosphere numerical modelling. Australian Centre for Geomechanics,

Stratos Inc. 2011. Climate Change and Acid Rock Drainage – Risks for the Canadian Mining Sector.

Tegos, A., Efstratiadis, A., Malamos, N., Mamassis, N., and Koutsoyiannis, D. 2015. Evaluation of a Parametric Approach for Estimating Potential Evapotranspiration Across Different Climates. Agriculture and Agricultural Science Procedia, 4: 2–9. doi: 10.1016/j.aaspro.2015.03.002.

Thornthwaite, C.W. 1931. The Climates of North America: According to a New Classification. Geographical Review, 21(4): 633. doi:10.2307/209372.

Thornthwaite, C.W. 1948. An approach toward a rational classification of climate. Geographical Review, 38(1): 55. doi:10.2307/210739.

Thornthwaite, C. W., and Hare, F. K. 1955. Climatic classification in forestry, Unasylva, Vol. 9, pp. 50–59.

Thornthwaite, C. W., and Mather, J. R. 1955. The water balance; publications in climatology, Vol. 8, No. 1, Laboratory of Climatology, Centerton, NJ.

Tran, D-T-Q., 2013. Re-visitation of actual evaporation theories (PhD Thesis). Department of Civil and Environmental Engineering, University of Alberta, Edmonton, Alberta.

Troeh, F.R., Jabro, J.D., and Kirkham, D. 1982. Gaseous diffusion equations for porous materials. Geoderma, 27(3): 239–253. doi:10.1016/0016-7061(82)90033-7.

Walter, Gary R, and Philippe, D. 2007. “Evaluation of approaches to simulate engineered cover performance and degradation.” NRC-02-07-006. Centre for Nuclear Waste Regulatory Analyses San Antonio, Texas.

Wilson, G.W., 1990. Soil evaporative fluxes for geotechnical engineering problems (PhD Thesis). Department of Civil and Geological Engineering, University of Saskatchewan, Saskatoon, SK.

Wilson, G.W., Fredlund, D.G., and Barbour, S.L. 1994. Coupled soil-atmosphere modeling for soil evaporation. Canadian Geotechnical Journal, Vol. 31, No. 2, pp. 151–161.

Yanful, E.K. 1993. Oxygen diffusion through soil covers on sulphidic mine tailings. Journal of Geotechnical Engineering, 119(8): 1207–1228.

Yanful, E.K., Samad, M., and Mian, H. 2004. Shallow Water Cover Technology for Reactive Sulphide Tailings Management. Waste Geotechnics, (2004): 42–51.

(Chapter 4)

Akcil, A., and Koldas, S. (2006). Acid Mine Drainage (AMD): Causes, treatment and case studies. J. Clean. Prod. *14*, 1139–1145.

Benson, C.H., Abichou, T.H., Olson, M.A., and Bosscher, P.J. (1995). Winter effects on hydraulic conductivity of compacted clay. J. Geotech. Eng. 121, 69–79.

Benson, C.H., Sawangsuriya, A., Trzebiatowski, B., and Albright, W.H. (2007). Post-construction changes in the hydraulic properties of water balance cover Soils. J. Geotech. Geoenvironmental Eng. 133, 349–359.

Boynton, S.S., and Daniel, D.E. (1985). Hydraulic conductivity tests on compacted clay. J. Geotech. Eng. 111, 465–478.

Bussie`re, B., and Aubertin, M. (1999). Clean tailings as cover material for preventing acid mine drainage: an in situ experiment. Proc. Sudbury ’99 Min. Environ. II Sudbury Ont. 1, 19–28.

Cao, L., Zhang, H., and Chen, Y. (2017). Hydraulic properties analysis of the unsaturated cracked soil. J. Shanghai Jiaotong Univ. Sci. 22, 35–44.

Carsel, R.F., and Parrish, R. S., Developing joint probability distributions of soil water retention characteristics, Water Resource. Res, 24, 755-769, 1988.

De Camillis, M., Di Emidio, G., Bezuijen, A., and Verástegui-Flores, R.D. (2016). Hydraulic conductivity and swelling ability of a polymer modified bentonite subjected to wet–dry cycles in seawater. Geotext. Geomembr. 44, 739–747.

Demers, I., Bussière, B., Mbonimpa, M., and Benzaazoua, M. (2009). Oxygen diffusion and consumption in low-sulphide tailings covers. Can. Geotech. J. 46, 454–469.

Dobchuk, B. (2002). Evaluations of the effectiveness of desulphurized tailings cover at Detour Lake Mine.

Dobchuk, B., Nichol, C., Wilson, G.W., and Aubertin, M. (2013). Evaluation of a single-layer desulphurized tailings cover. Can. Geotech. J. 50, 777–792.

Dobchuk, B., Wilson, G.W., and Aubertin, M. (2003). Evaluation of a Single-Layer Desulfurized Tailings Cover. 9.

Eigenbrod, K.D. (1996). Effects of cyclic freezing and thawing on volume changes and permeabilities of soft fine-gained soils. Can. Geotech. J. 33, 529–537.

Fredlund, D.G., Rahardjo, H., and Fredlund, M.D. (2012). Unsaturated soil mechanics in engineering practice (John Wiley & Sons, Inc., Hoboken, New Jersey).

van Genuchten, M.T. (1980). A closed-form equation for predicting the hydraulic conductivity of unsaturated soils. Soil Sci. Soc. Am. J. 44, 892–898.

GEO-SLOPE (2014). Vadose Zone Modeling with VADOSE/W.

Penman, H. L., (1948). Natural evaporation from open water, bare soil and grass.

INAP (2003). Evaluation of the long-term performance of dry cover systems (INAP).

IPCC (2013). Climate Change 2013: The Physical Science Basis. Contribution of Working Group I to the Fifth Assessment Report of the Intergovernmental Panel on Climate Change. Cambridge University Press.

Jones, C.D., Hughes, J.K., Bellouin, N., Hardiman, S.C., Jones, G.S., Knight, J., Liddicoat, S., O& amp;apos;Connor, F.M., Andres, R.J., Bell, C., et al. (2011). The HadGEM2-ES implementation of CMIP5 centennial simulations. Geosci. Model Dev. 4, 543–570.

Kim, W., and Daniel, D.E. (1992). Effects of Freezing on Hydraulic Conductivity of Compacted Clay. 15.

Lin, L.-C., and Benson, C.H. (2000). Effect of Wet-Dry Cycling on Swelling and Hydraulic Conductivity of GCLs. J. Geotech. Geoenvironmental Eng. 126, 40–49.

Mbonimpa, M., Aubertin, M., Aachib, M., and Bussière, B. (2003). Diffusion and consumption of oxygen in unsaturated cover materials. Can. Geotech. J. 40, 916–932.

McNeill, B. (2016). Geochemical and microbiological characterization of the historic waste rock piles at the Detour Lake Gold Mine. Master's Thesis. University of Waterloo.

Meiers, G.P., Barbour, S.L., Qualizza, C.V., and Dobchuk, B.S. (2011). Evolution of the hydraulic conductivity of reclamation covers over sodic/saline mining overburden. J. Geotech. Geoenvironmental Eng. 137, 968–976.

Micheal, M. (2010). Modeling of predicted performance of the desulphurized tailings cover at Detour Lake Mine. University of British Columbia.

Omidi, G.H., Thomas, J.C., and Brown, K.W. (1996). Effect of desiccation cracking on the hydraulic conductivity of a compacted clay liner. Water. Air. Soil Pollut. 89, 91–103.

Pabst, T., Aubertin, M., Bussière, B., and Molson, J. (2017). Experimental and numerical evaluation of single-layer covers placed on acid-generating tailings. Geotech. Geol. Eng. 35, 1421–1438.

Pincus, H., Benson, C., Chamberlain, E., Erickson, A., and Wang, X. (1995). Assessing Frost Damage in Compacted Clay Liners. Geotech. Test. J. 18, 324.

Stratos Inc. 2011. "Climate change and acid rock drainage – Risks for the Canadian Mining Sector." MEND Report 1.61.7.

Qi, J., Vermeer, P.A., and Cheng, G. (2006). A review of the influence of freeze-thaw cycles on soil geotechnical properties. Permafr. Periglac. Process. 17, 245–252.

Rayhani, M.H., Yanful, E.K., and Fakher, A. (2007). Desiccation-induced cracking and its effect on the hydraulic conductivity of clayey soils from Iran. Can. Geotech. J. 44, 276–283.

Scanlan, C.A. (2009). Evaluation of the long-term performance of dry cover systems. University of Western Australia.

Shurnik, R.E., O'Kane, M.A., and Green, R. (2012). Simulation of seven years of field performance monitoring at Rio Tinto Iron Ore, Mount Tom Price mine using soil-plantatmosphere numerical modelling. Aust. Cent. Geomech.

Stormont, J.C., and Anderson, C.E. (1999). Capillary barrier effect from underlying coarser soil layer. J. Geotech. Geoenvironmental Eng. 125, 641–648.

Tang, Y., and Yan, J. (2015). Effect of freeze–thaw on hydraulic conductivity and microstructure of soft soil in Shanghai area. Environ. Earth Sci. 73, 7679–7690.

Yanful, E.K. (1993). Oxygen diffusion through soil covers on sulphidic mine tailings. J. Geotech. Eng. 119, 1207–1228.

Appendix A. *Base climate data compilation and classification*

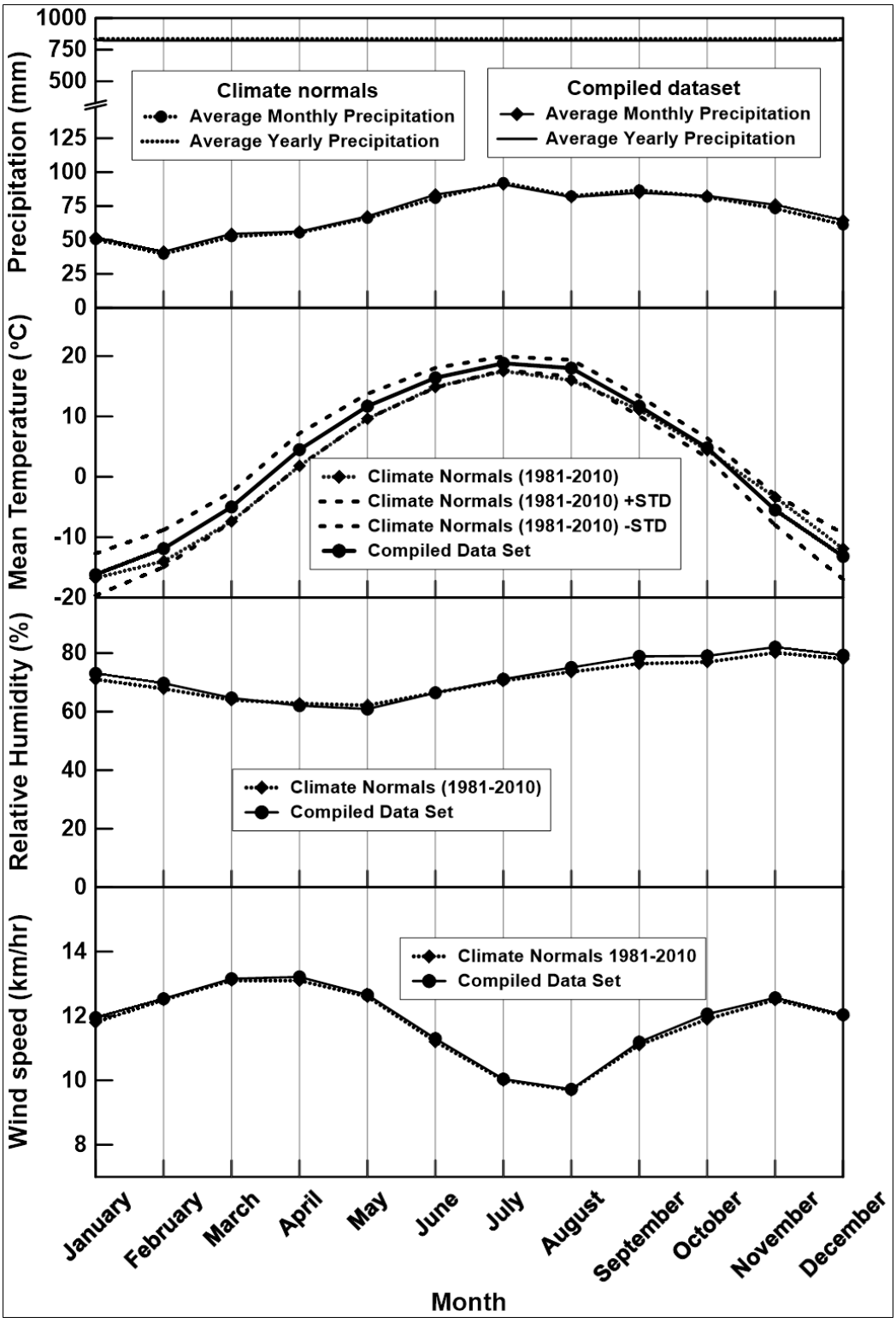

Appendix A 1. Timmins Victor Power Airport weather station climate data comparison with climate normals (1980-2010).

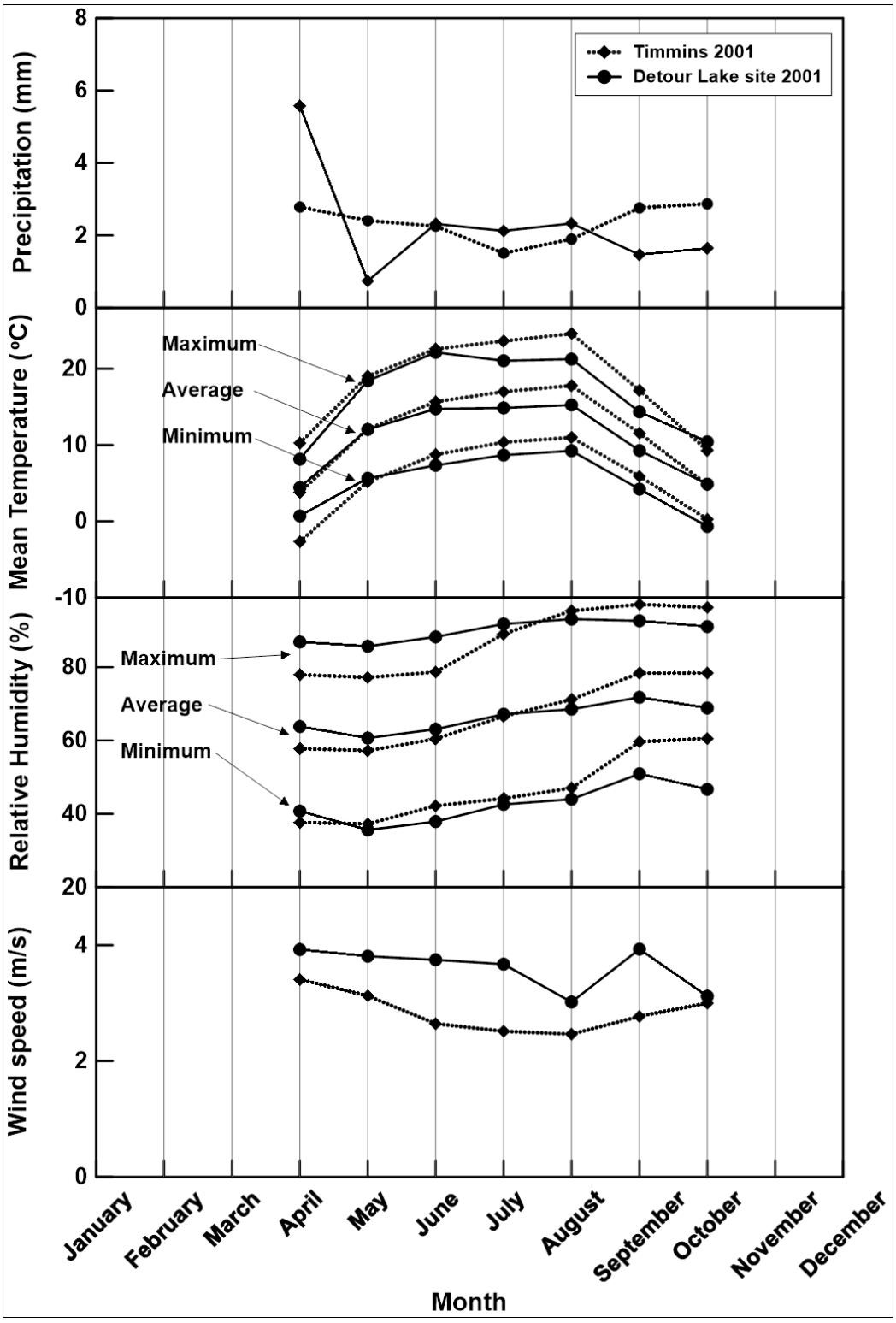

Appendix A 2. Timmins Victor Power Airport weather station climate data comparison with Detour Lake site weather station during active period of year 2001.

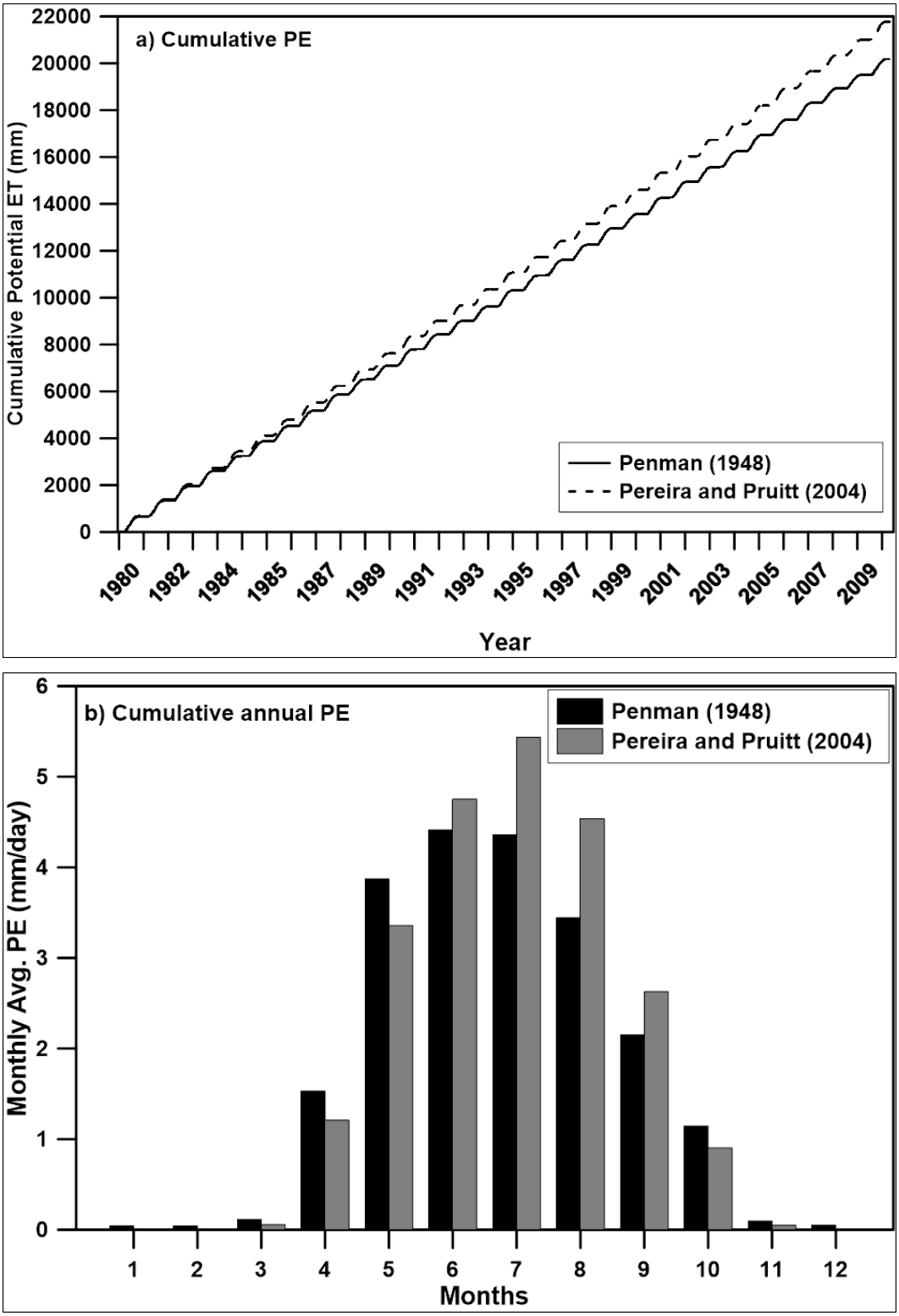

Appendix A 3. Comparison of a) cumulative potential evaporation (PE) & b) cumulative annual PE using Penman (1948) and Thornthwaite (1948) modified by Pereira and Pruitt (2004).

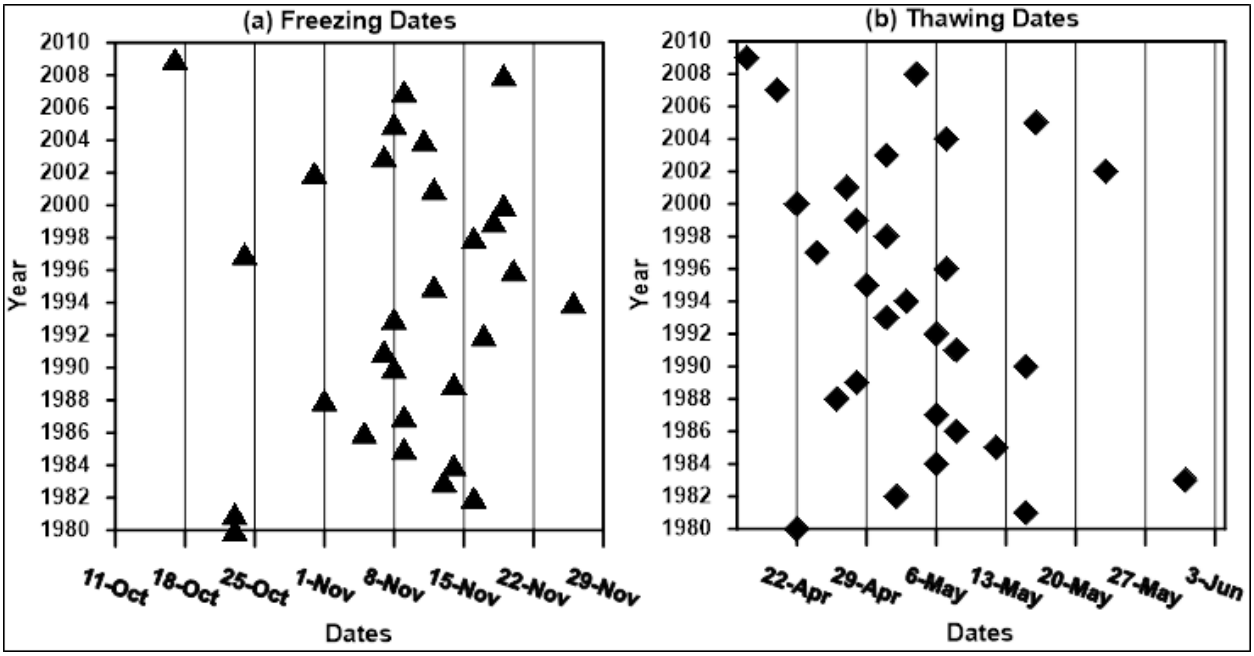

Appendix A 4. Freezing and Thawing dates of 30 year (1980-2010) for Timmins.

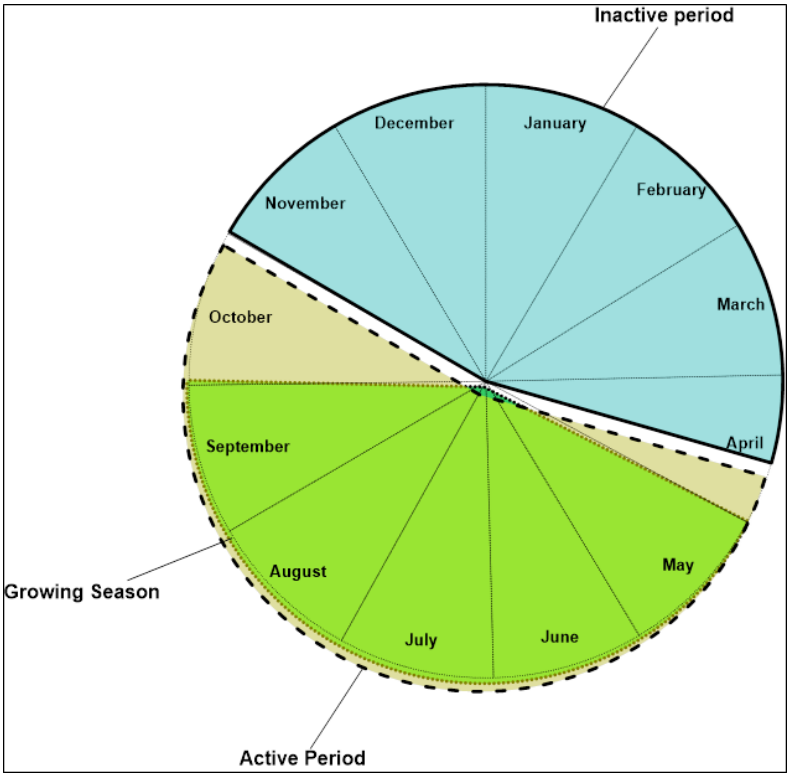

Appendix A 5. Active and Inactive portion of a year with respect to modelling near ground surface moisture movement.

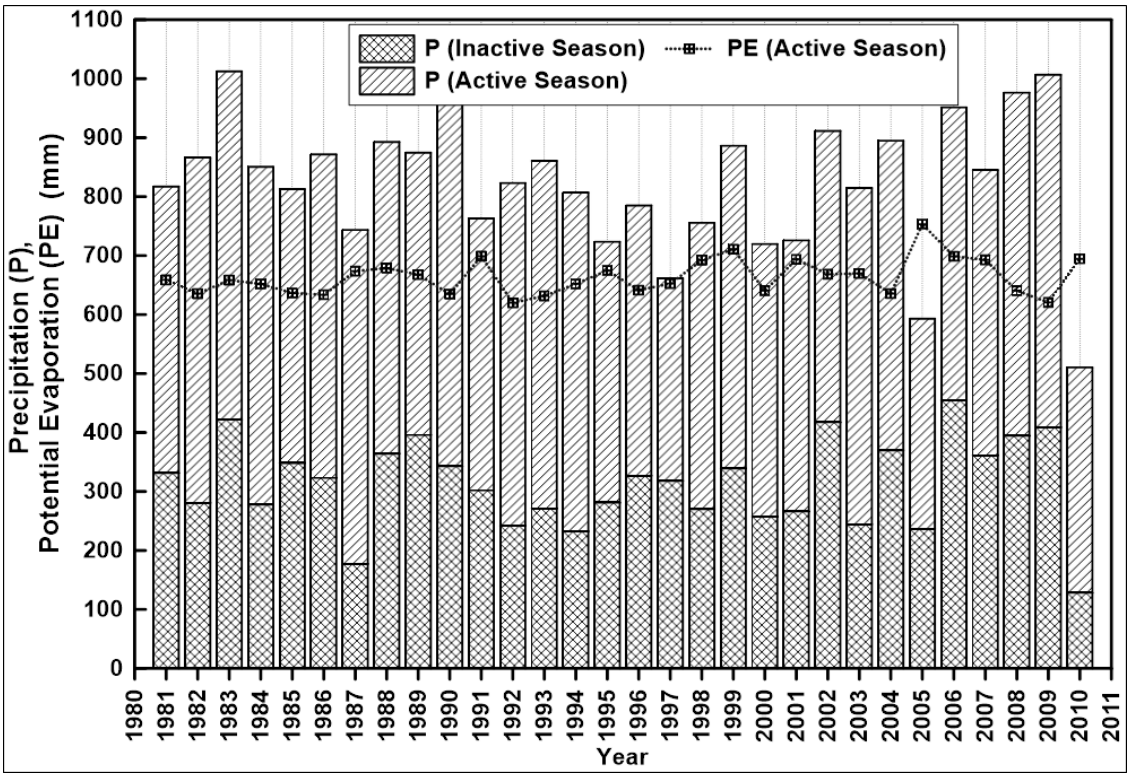

Appendix A 6. Active and Inactive portion of annual cumulative precipitation and potential evaporation for a period between 1980-2010.

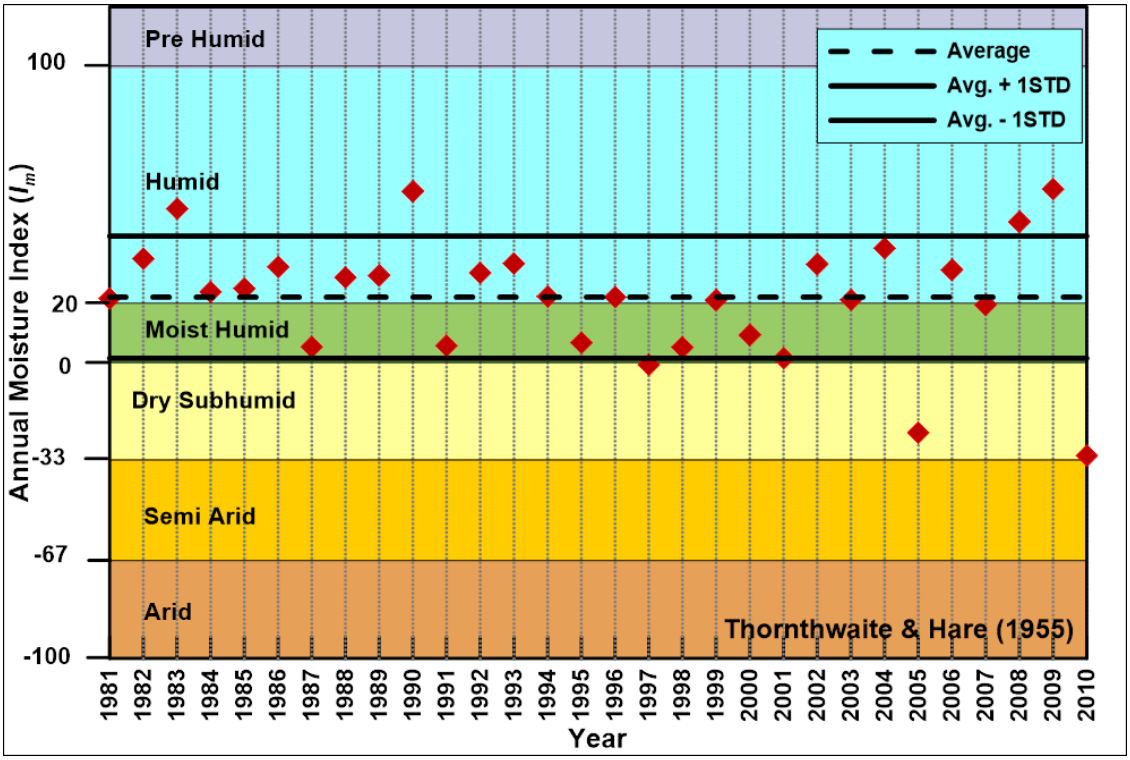

Appendix A 7. Thornthwaite annual moisture index (Im) for a period between 1980-2010.

Appendix B. *Climate change data.*

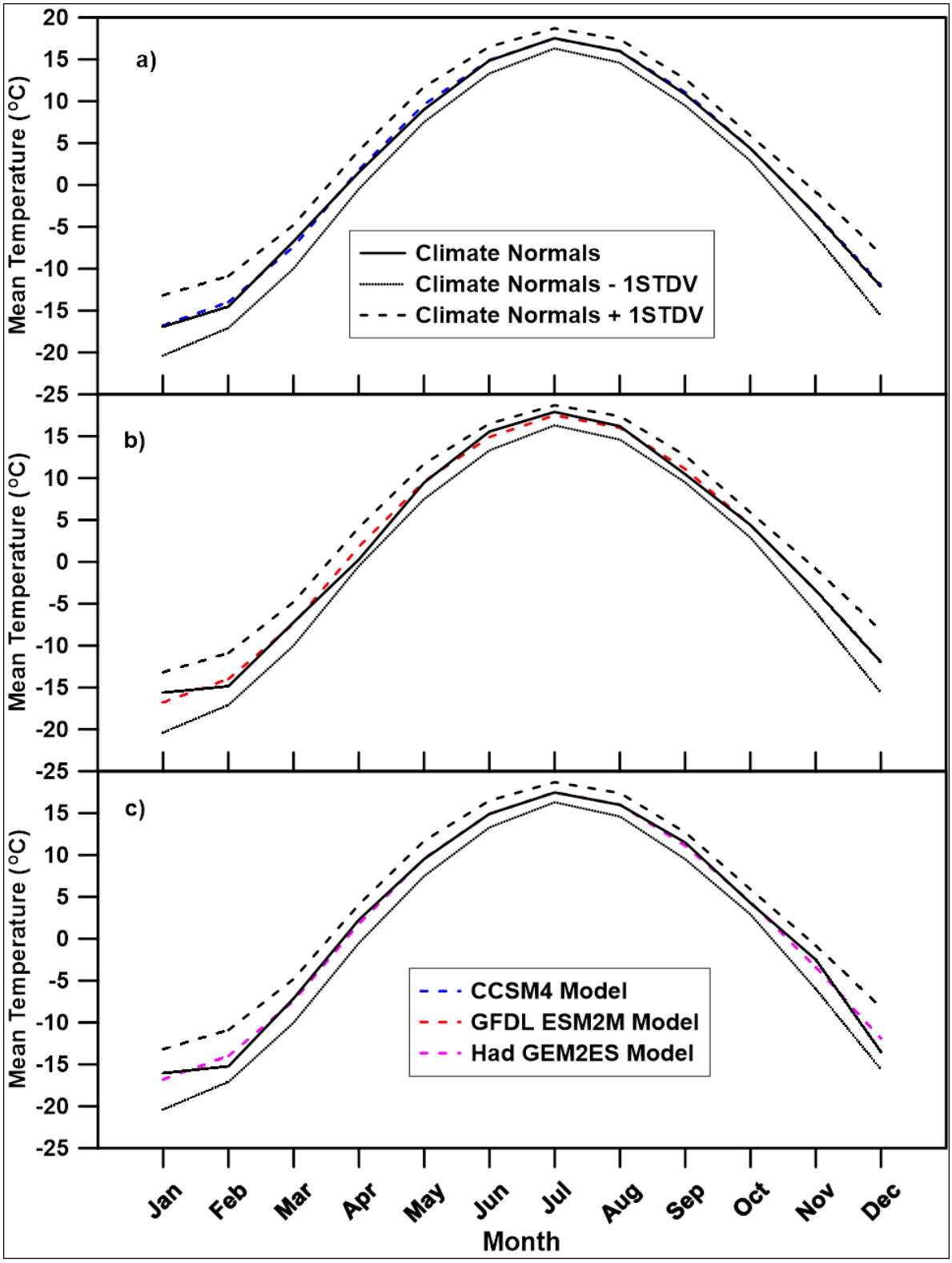

Appendix B 1. Comparison of climate normals (1981-2010) with predictions of mean monthly temperature using a) CCSM4, b) GFDL ESM2M, and c) Had GEM2ES models.

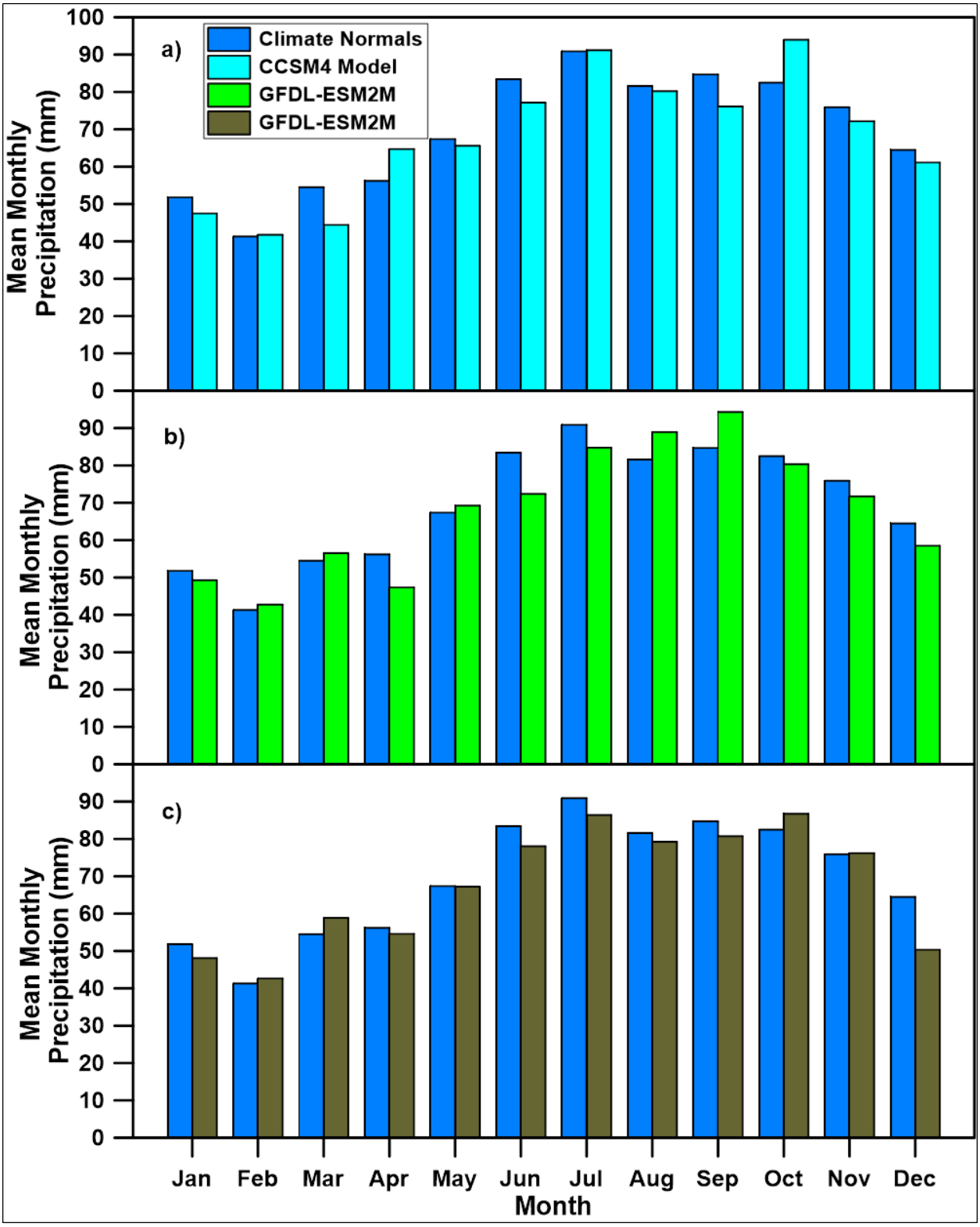

Appendix B 2. Comparison of climate normals (1981-2010) with predictions of mean monthly precipitation using a) CCSM4, b) GFDL ESM2M, and c) Had GEM2ES models.

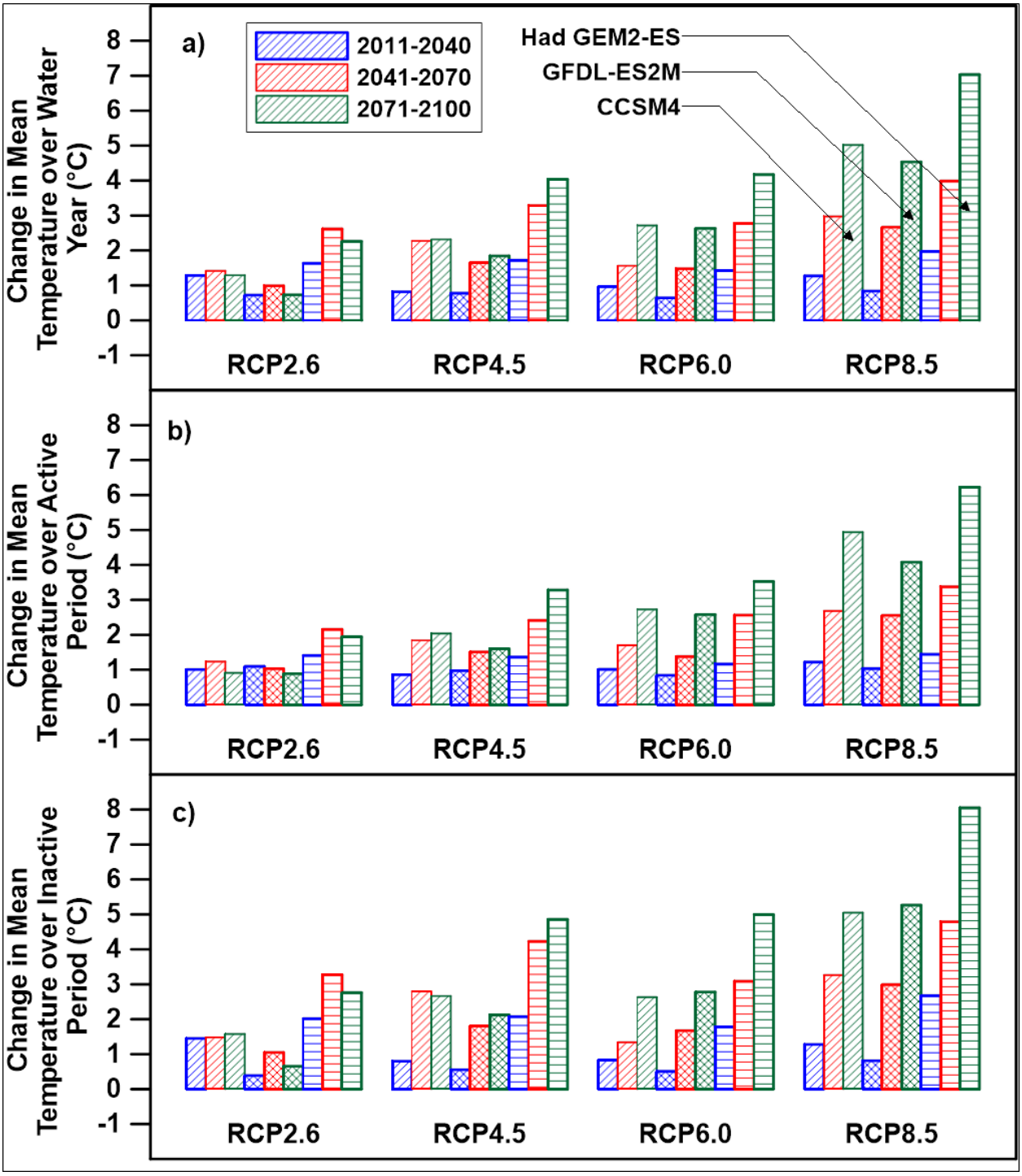

Appendix B 3. Projected percentage changes in annual mean temperature over (a) water year, (b) active period, and (c) inactive period.

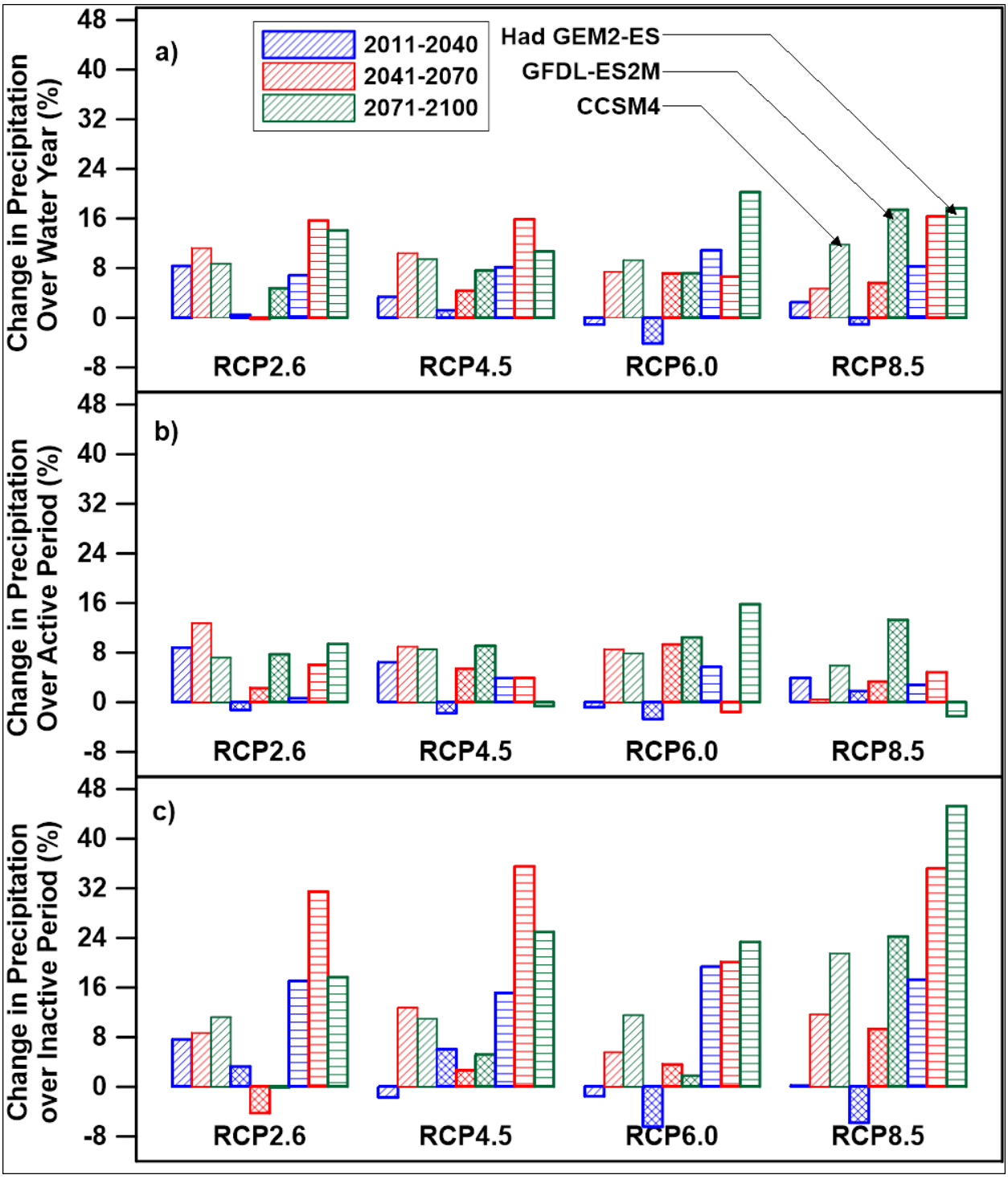

Appendix B 4. Projected percentage changes in annual precipitation over (a) water year, (b) active period, and (c) inactive period.

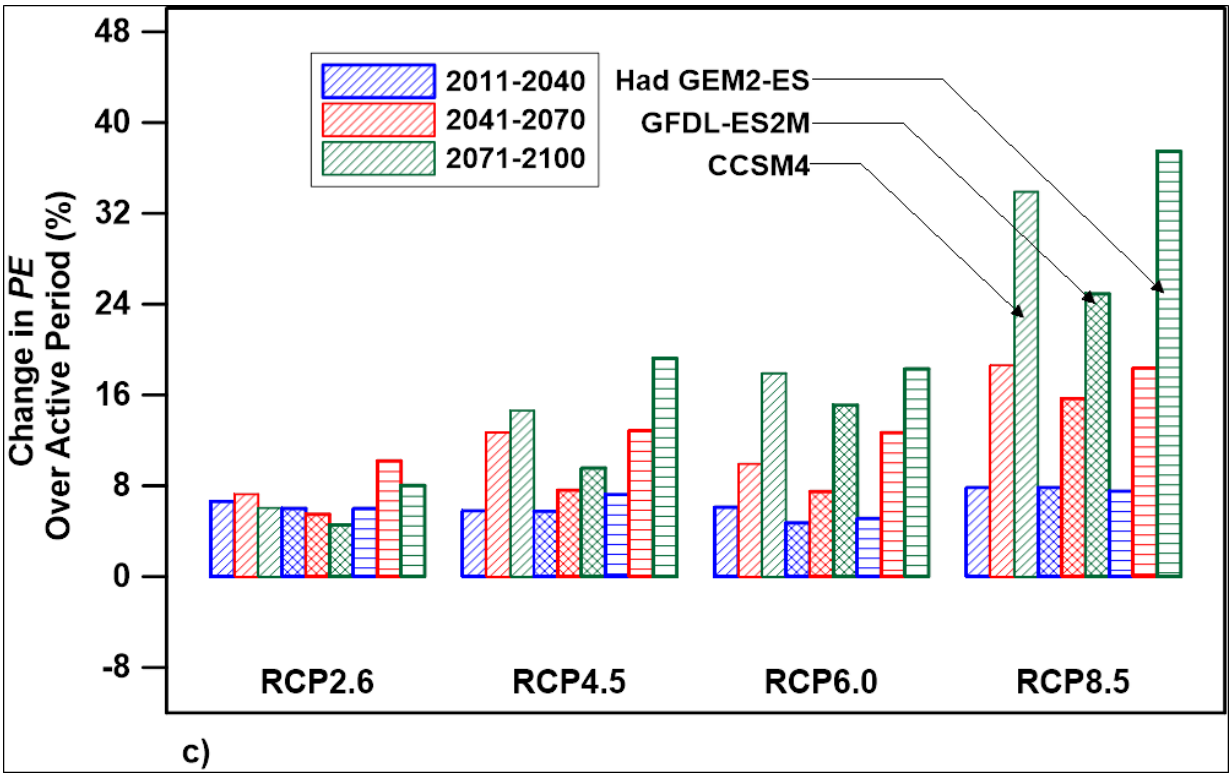

Appendix B 5. Projected percentage changes in annual potential evaporation over active period.

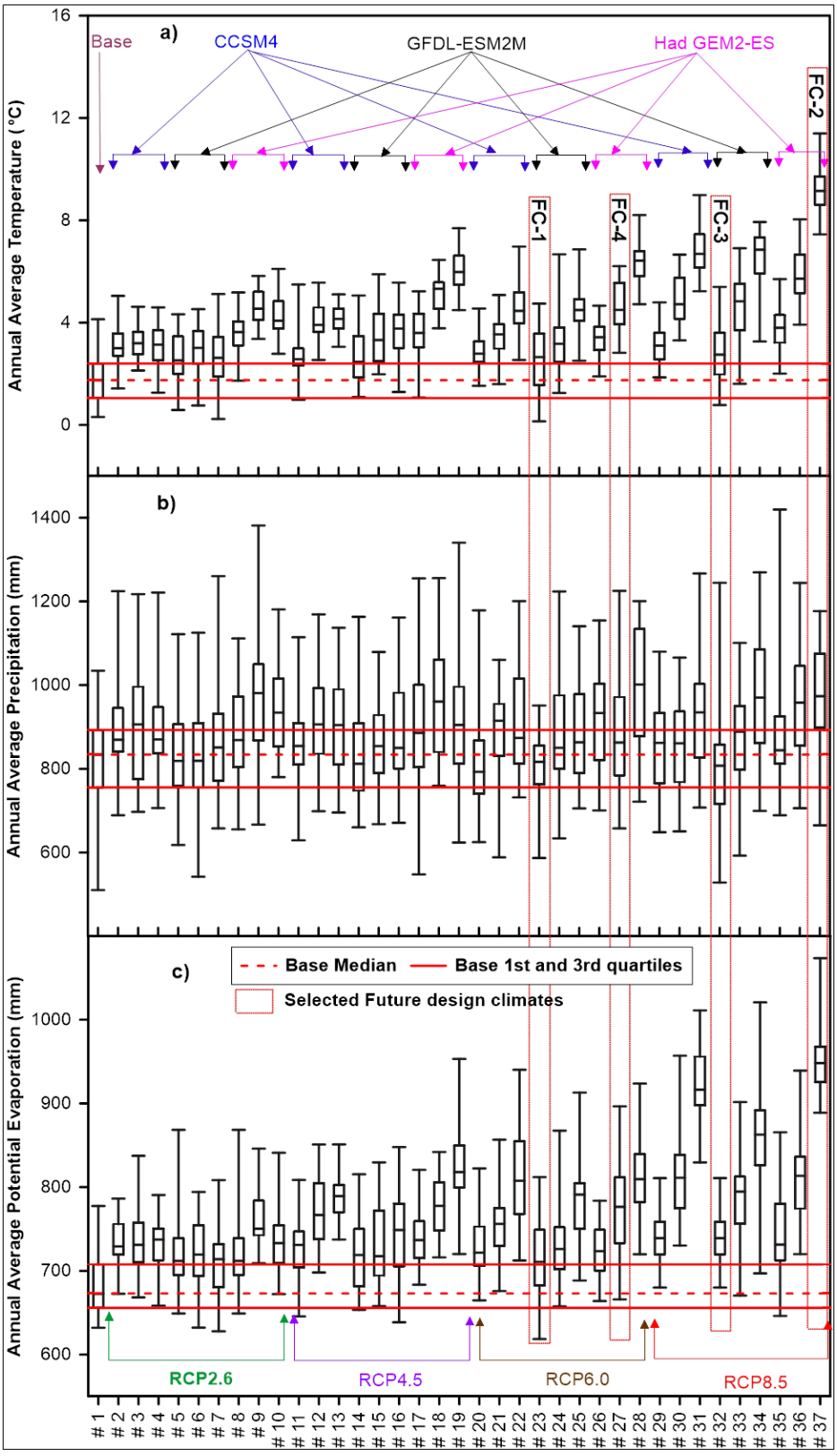

Appendix B 6. Box and whisker plots for a) annual average temperature, b) annual cumulative precipitation, and c) annual cumulative potential evaporation.

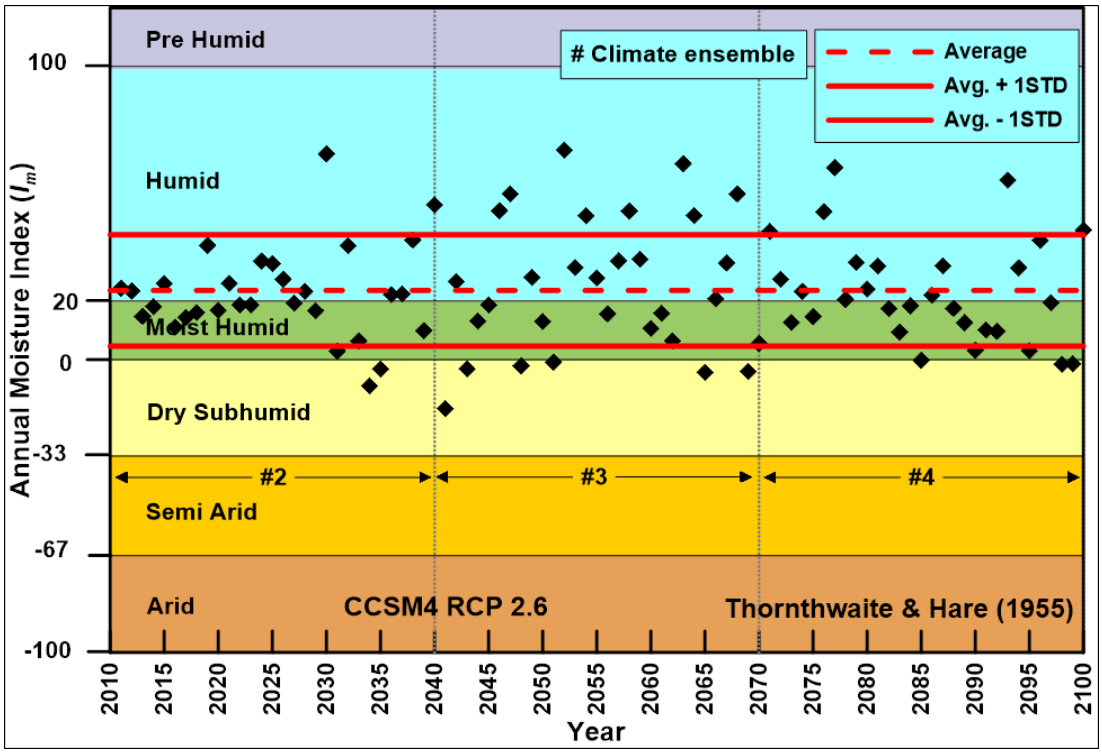

Appendix B 7. Projected annual moisture index for 90 year (2011-2100) using CCSM4 model with RCP 2.6.

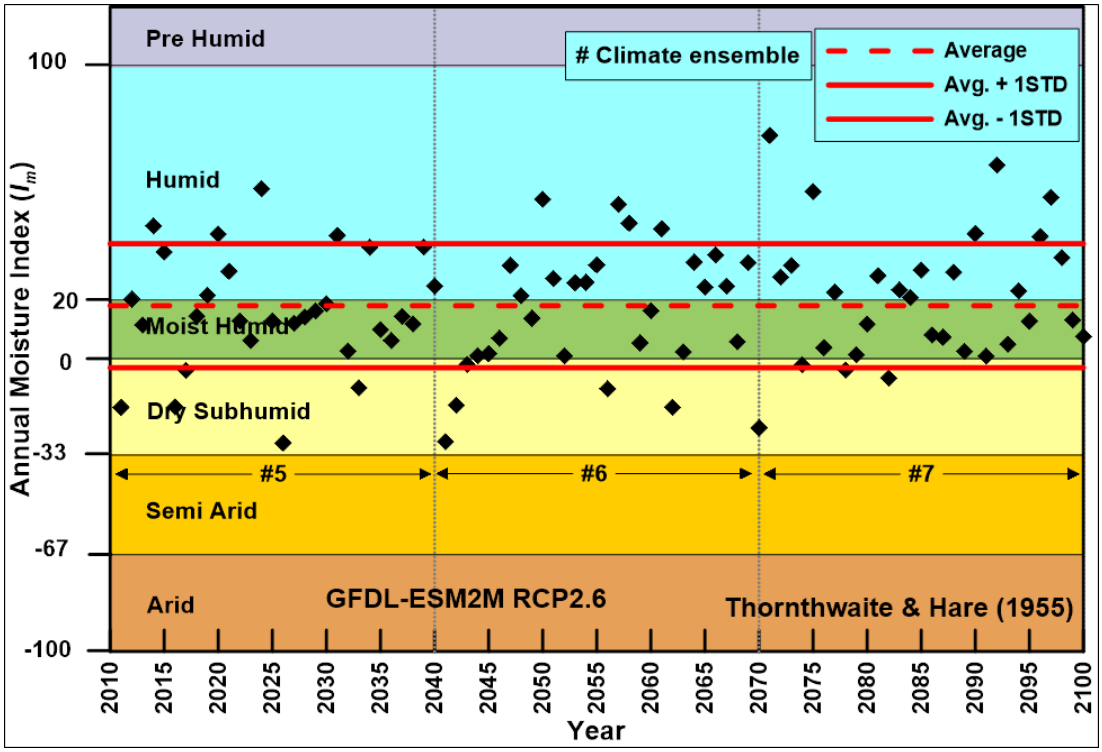

Appendix B 8. Projected annual moisture index for 90 year (2011-2100) using GFDL-ESM2M model with RCP 2.6.

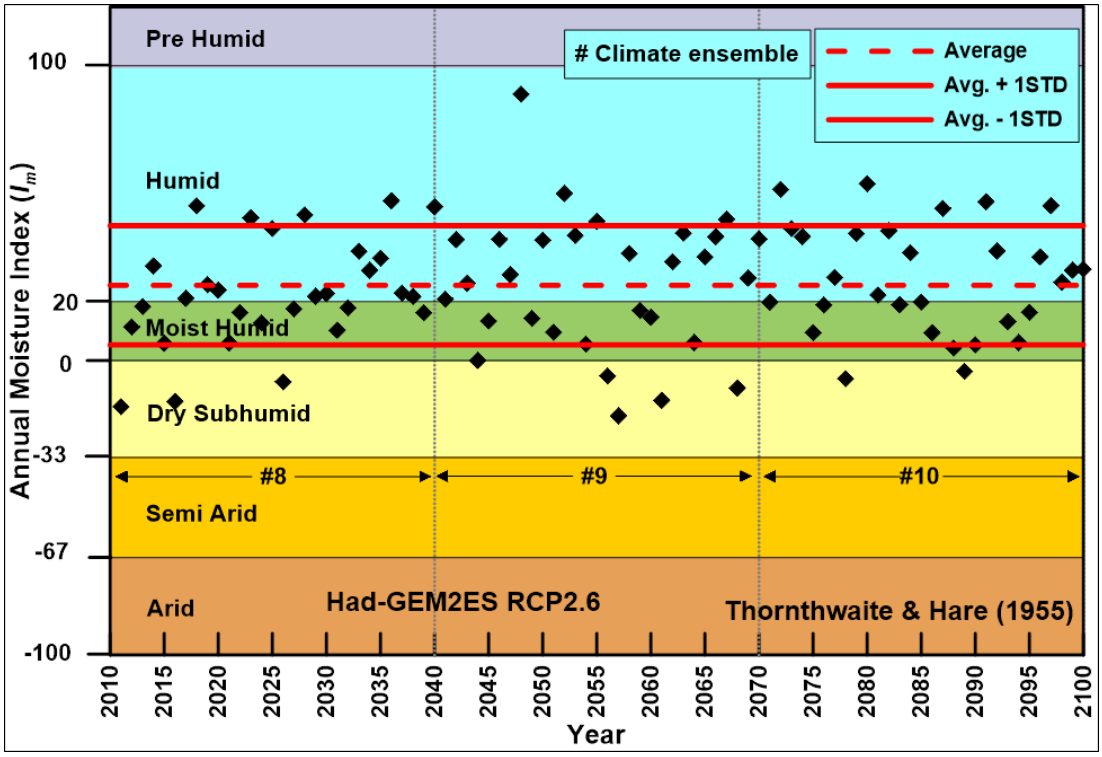

Appendix B 9. Projected annual moisture index for 90 year (2011-2100) using Had-GEM2ES model with RCP 2.6.

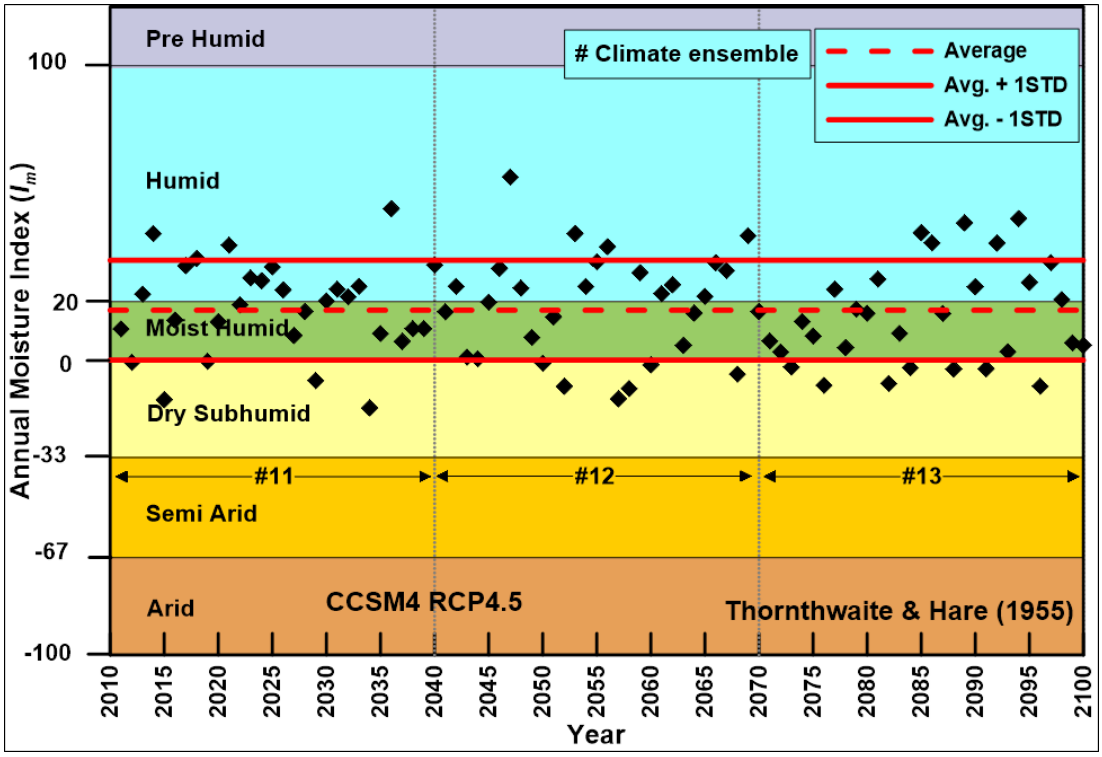

Appendix B 10. Projected annual moisture index for 90 year (2011-2100) using CCSM4 model with RCP 4.5.

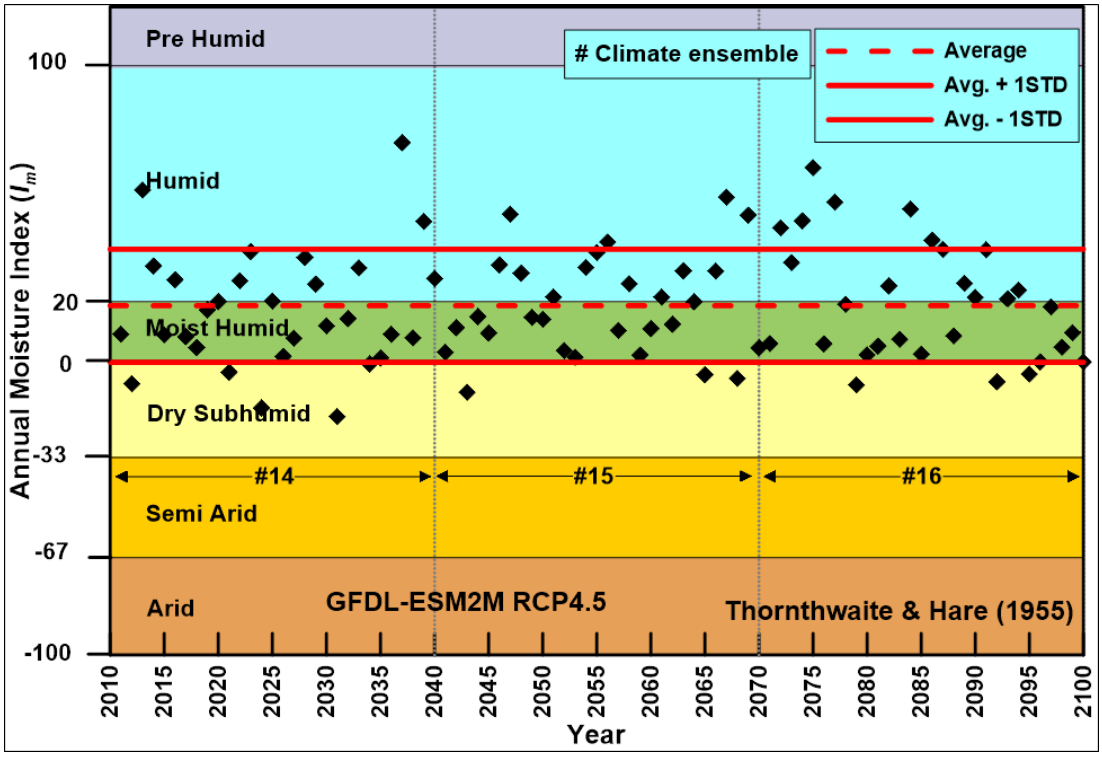

Appendix B 11. Projected annual moisture index for 90 year (2011-2100) using GFDL-ESM2M model with RCP 4.5.

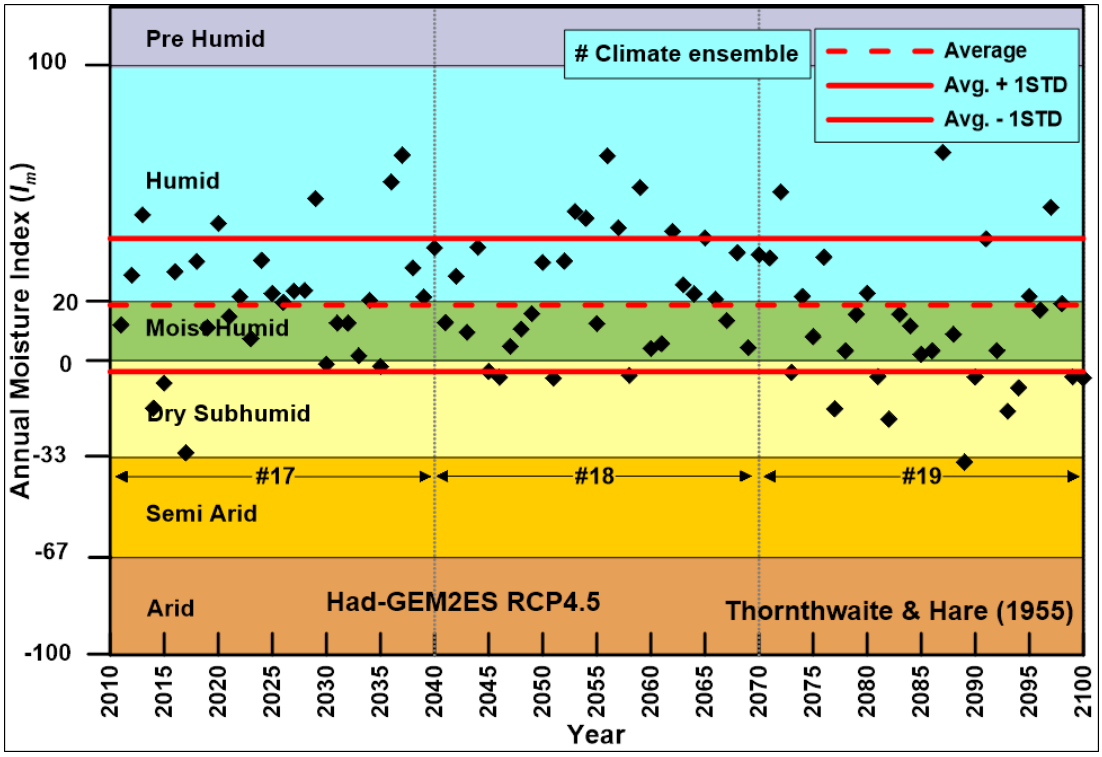

Appendix B 12. Projected annual moisture index for 90 year (2011-2100) using Had-GEM2ES model with RCP 4.5.

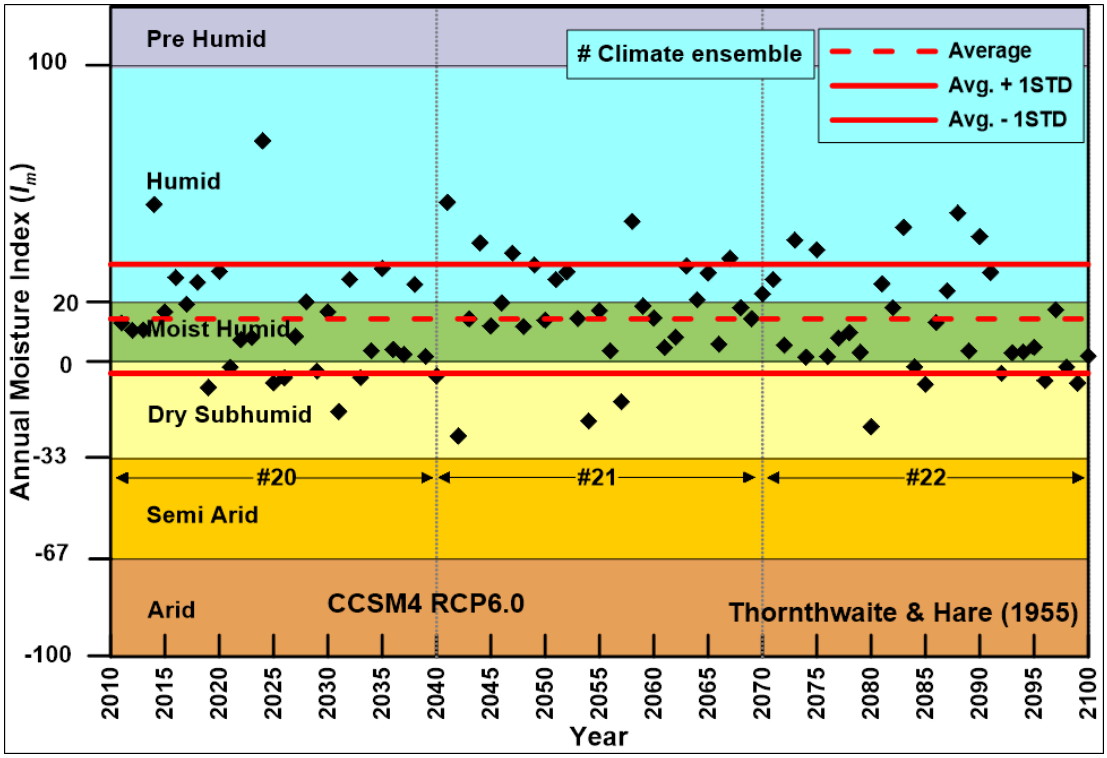

Appendix B 13. Projected annual moisture index for 90 year (2011-2100) using CCSM4 model with RCP 6.0.

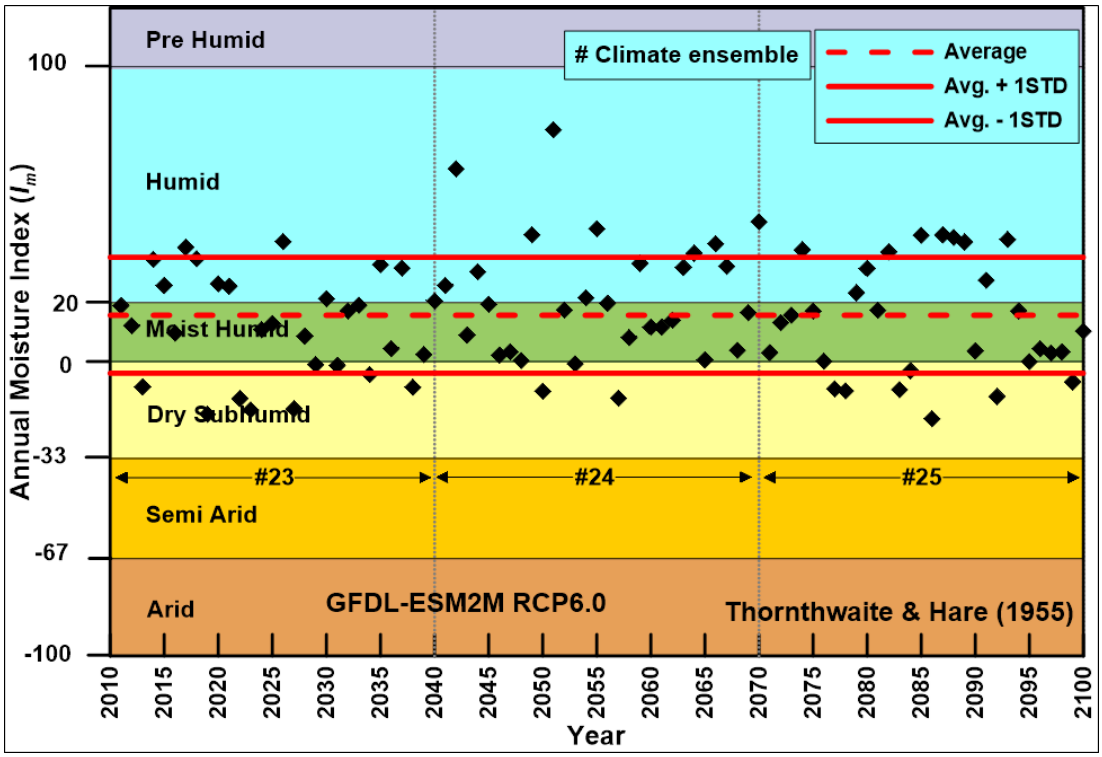

Appendix B 14. Projected annual moisture index for 90 year (2011-2100) using GFDL-ESM2M model with RCP 6.0.

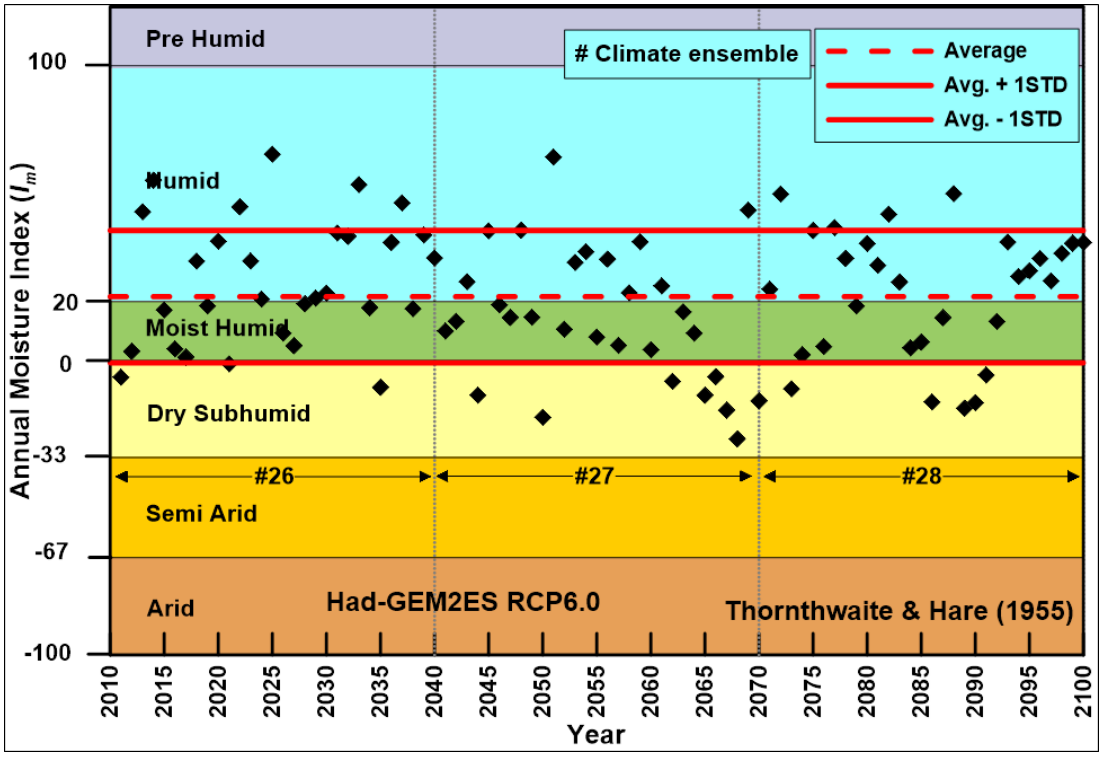

Appendix B 15. Projected annual moisture index for 90 year (2011-2100) using Had-GEM2ES model with RCP 6.0.

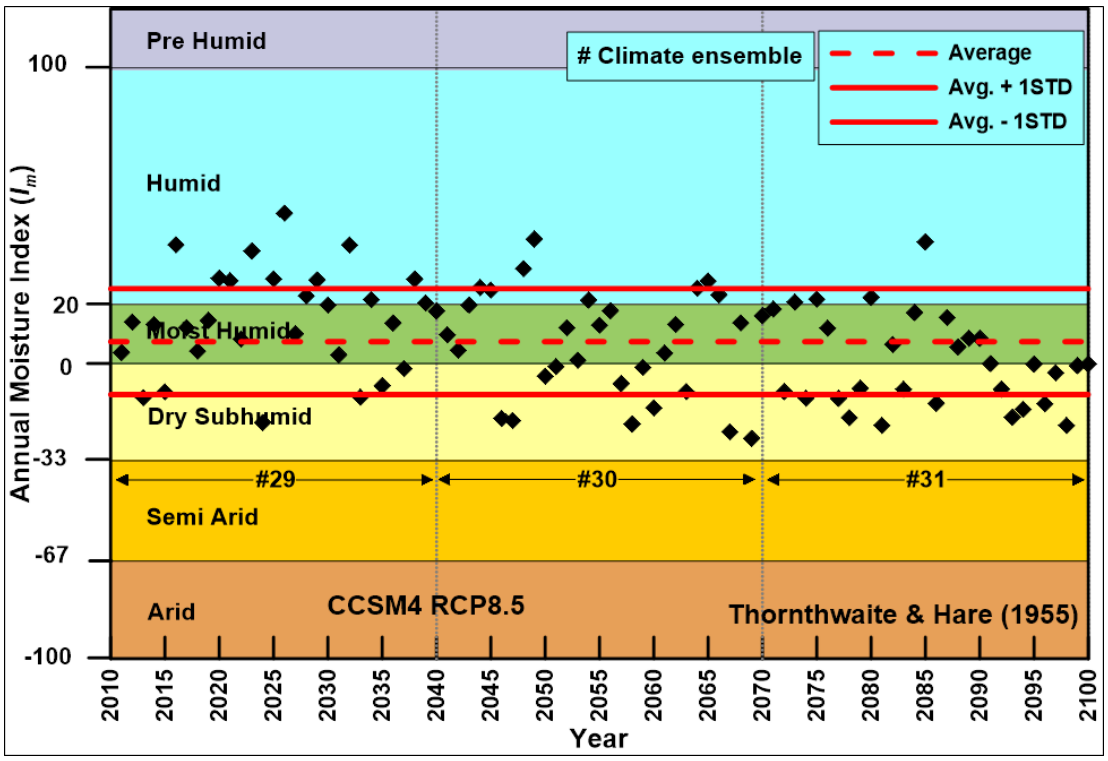

Appendix B 16. Projected annual moisture index for 90 year (2011-2100) using CCSM4 model with RCP 8.5.

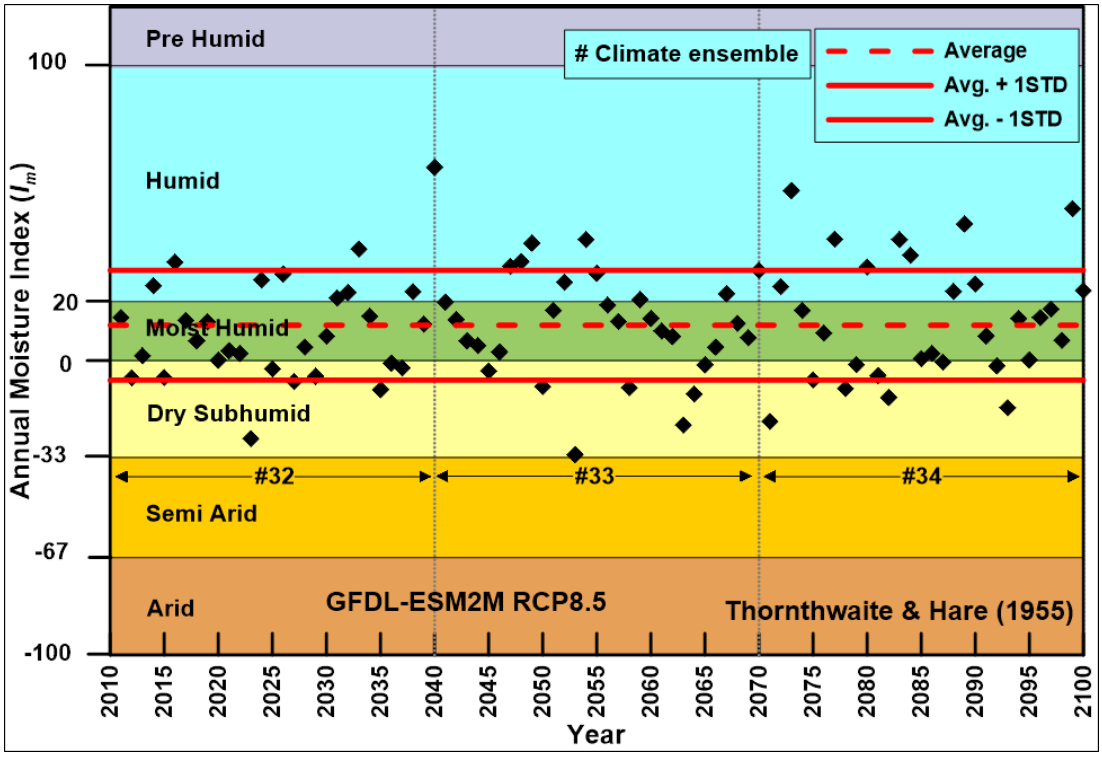

Appendix B 17. Projected annual moisture index for 90 year (2011-2100) using GFDL-ESM2M model with RCP 8.5.

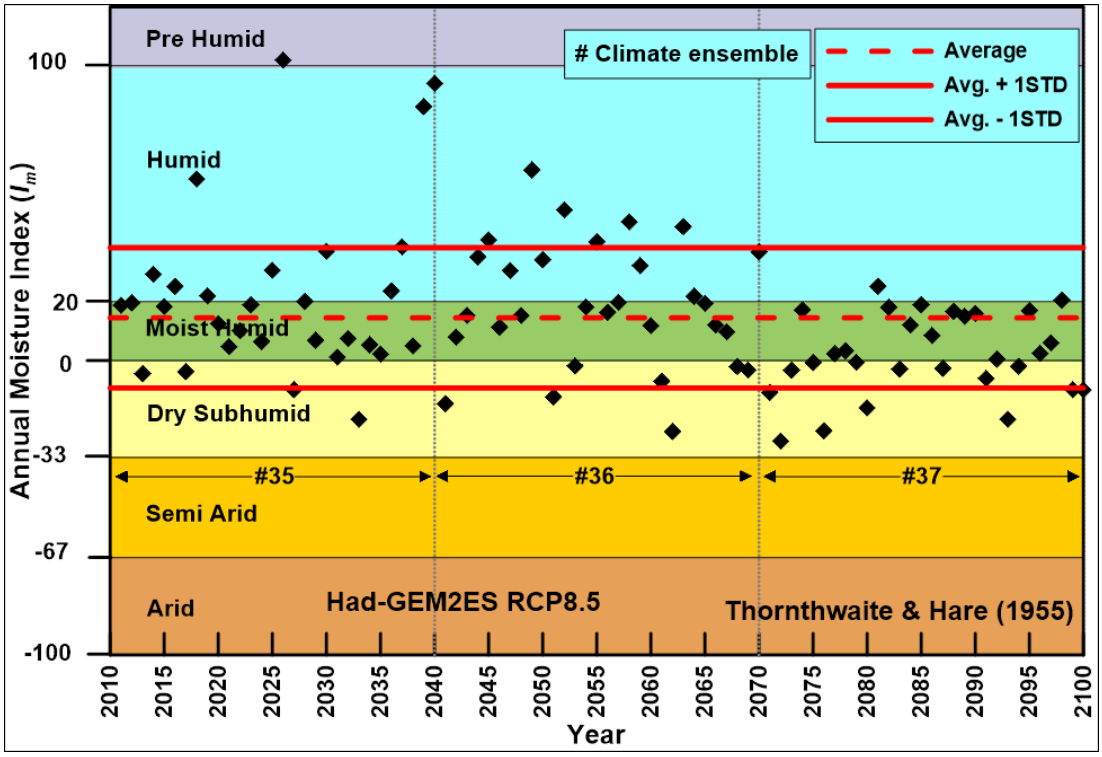

Appendix B 18. Projected annual moisture index for 90 year (2011-2100) using Had-GEM2ES model with RCP 8.5.

Appendix C. *Prediction of relative humidity for future climate data.*

Table. Statistical performance of selected models for prediction of relative humidity: ME, mean error; RMSE, root mean square error; NSE, Nash-Sutchliffe efficiency; RHmax and RHmin, daily maximum and minimum relative humidity; Single year (1990) and 25 years

Data Year	Model (dew-point Temp	Mean	ME	RMSE	NSE
RH_{max} –single year	Kimball (1996)	96	0.92	7.28	-0.47
(1990)	Lawrence (2005)	97	1.87	7.02	-0.37
RH_{max} –25 years (1970	Kimball (1996)	97	4.35	**9.94**	-0.46
- 1994)	Lawrence (2005)	97	5.143	10.07	-0.51
RH_{min} –single year	Kimball (1996)	45	-7.68	**16.98**	0.22
(1990)	Lawrence (2005)	36	-15.79	24.79	-0.66
RH_{min} –25 years (1970	Kimball (1996)	45	-3.92	**15.22**	0.28
- 1994)	Lawrence (2005)	35	-13.81	25.72	-1.06

Appendix C 1. Statistical performance of selected models for prediction of relative humidity at Timmins for climate data between (1970-1994).

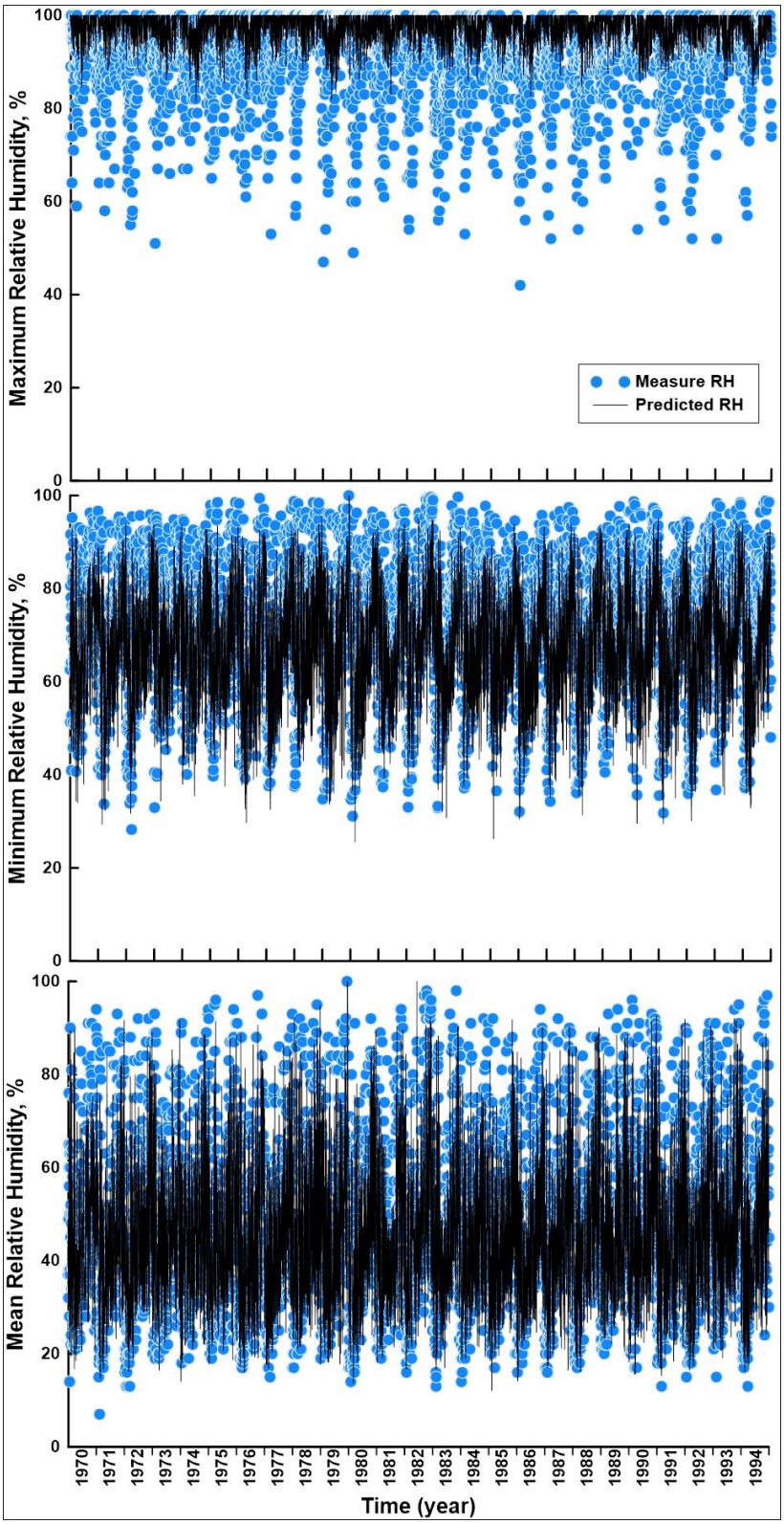

Appendix C 2. Comparison of measured and predicted relative humidity at Timmins for the duration 1970-1994.

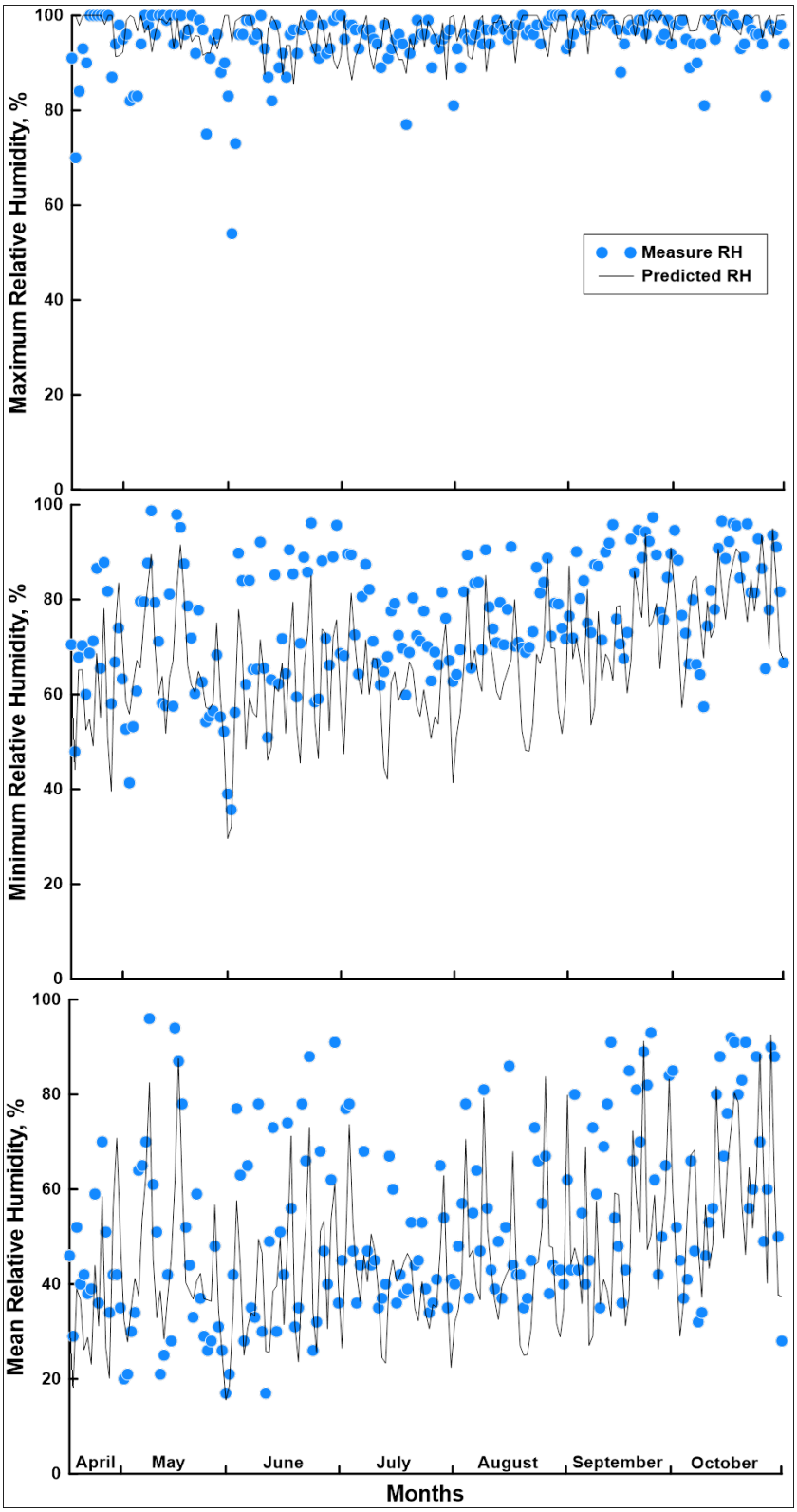

Appendix C 3. Comparison of measured and predicted relative humidity at Timmins for the active year 1990.

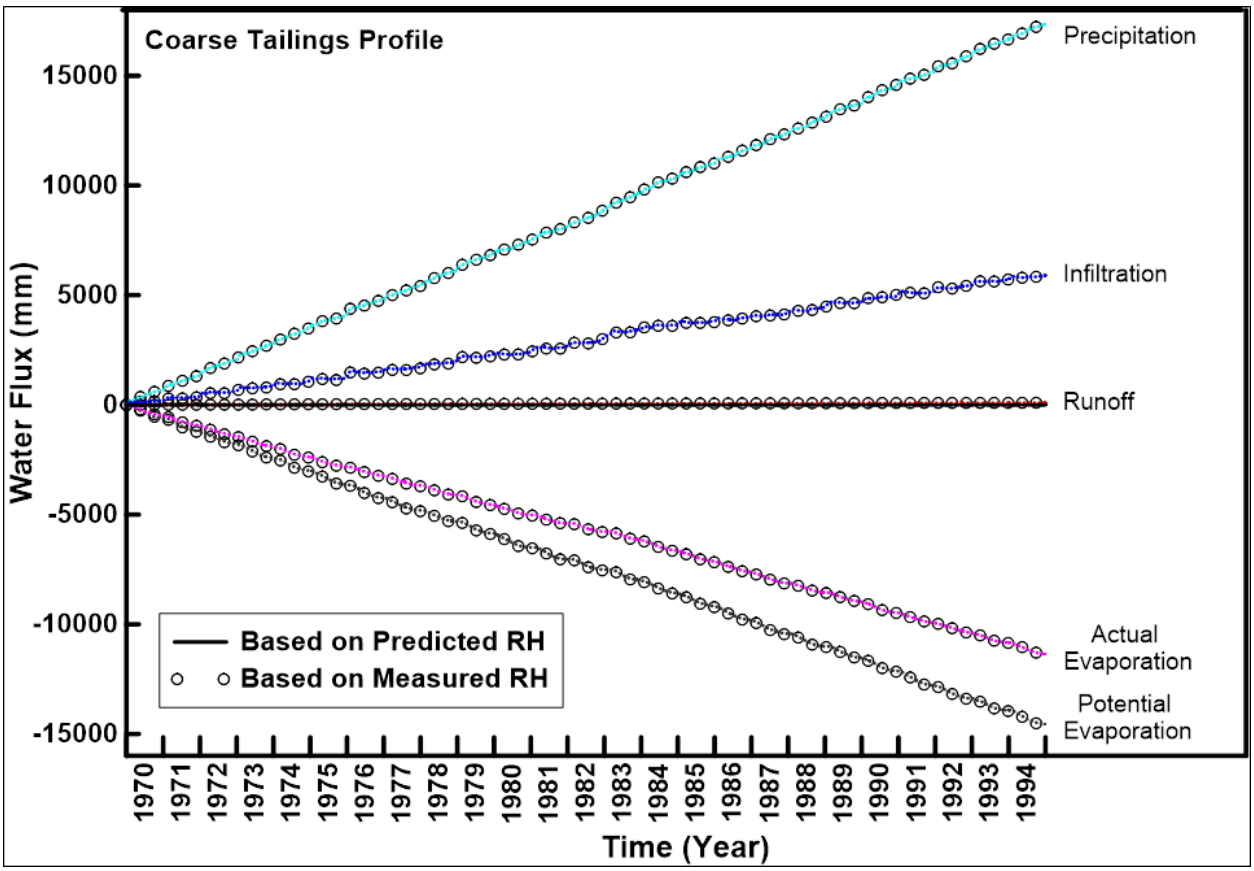

Appendix C 4. Comparison of water balance based on measured and predicted relative humidity at Timmins for the duration 1970-1994.

Appendix D. *Water balance for several cover profiles under representative future climates.*

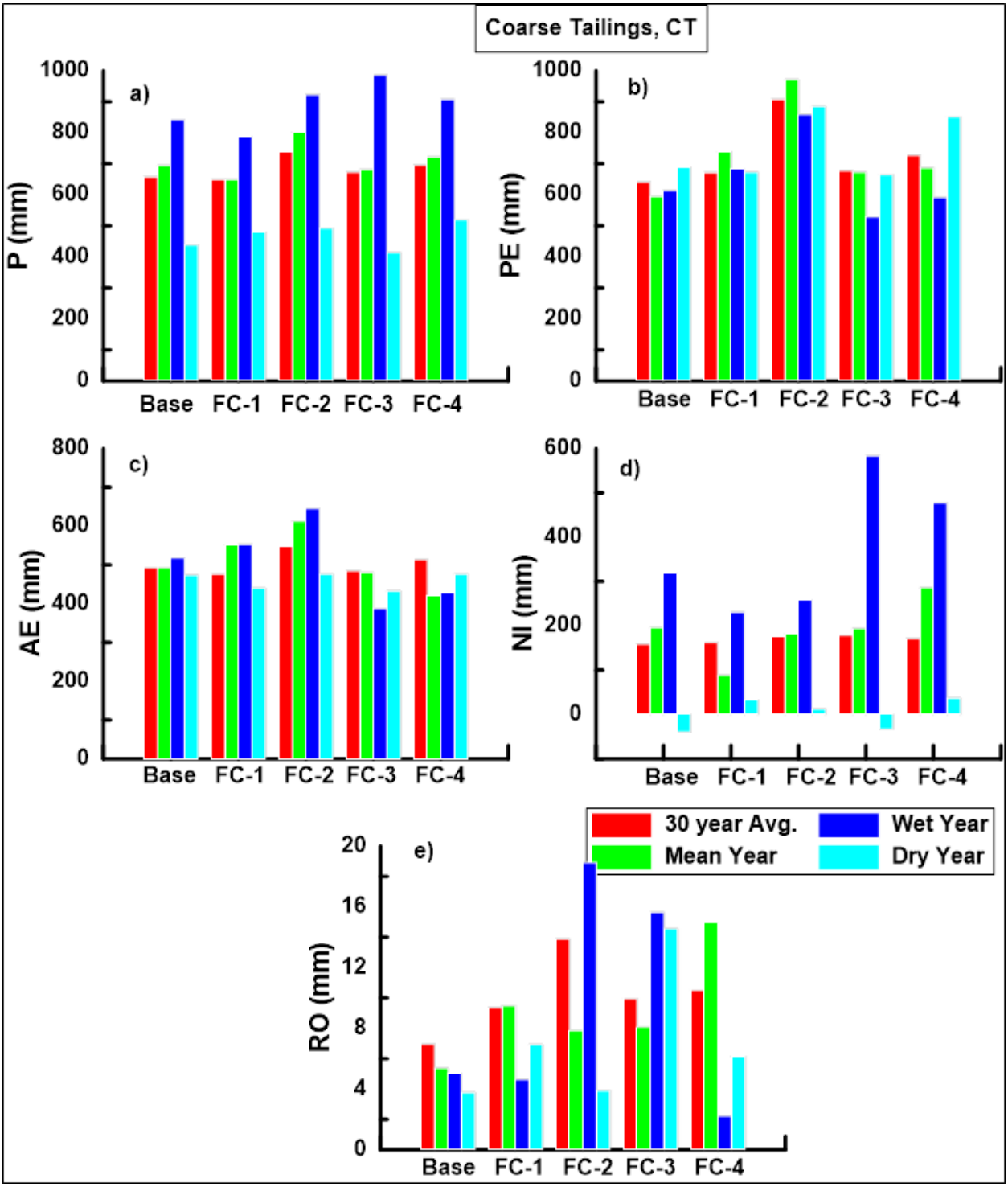

Appendix D 1. Water balance for coarse tailings (CT) for various representative future climates.

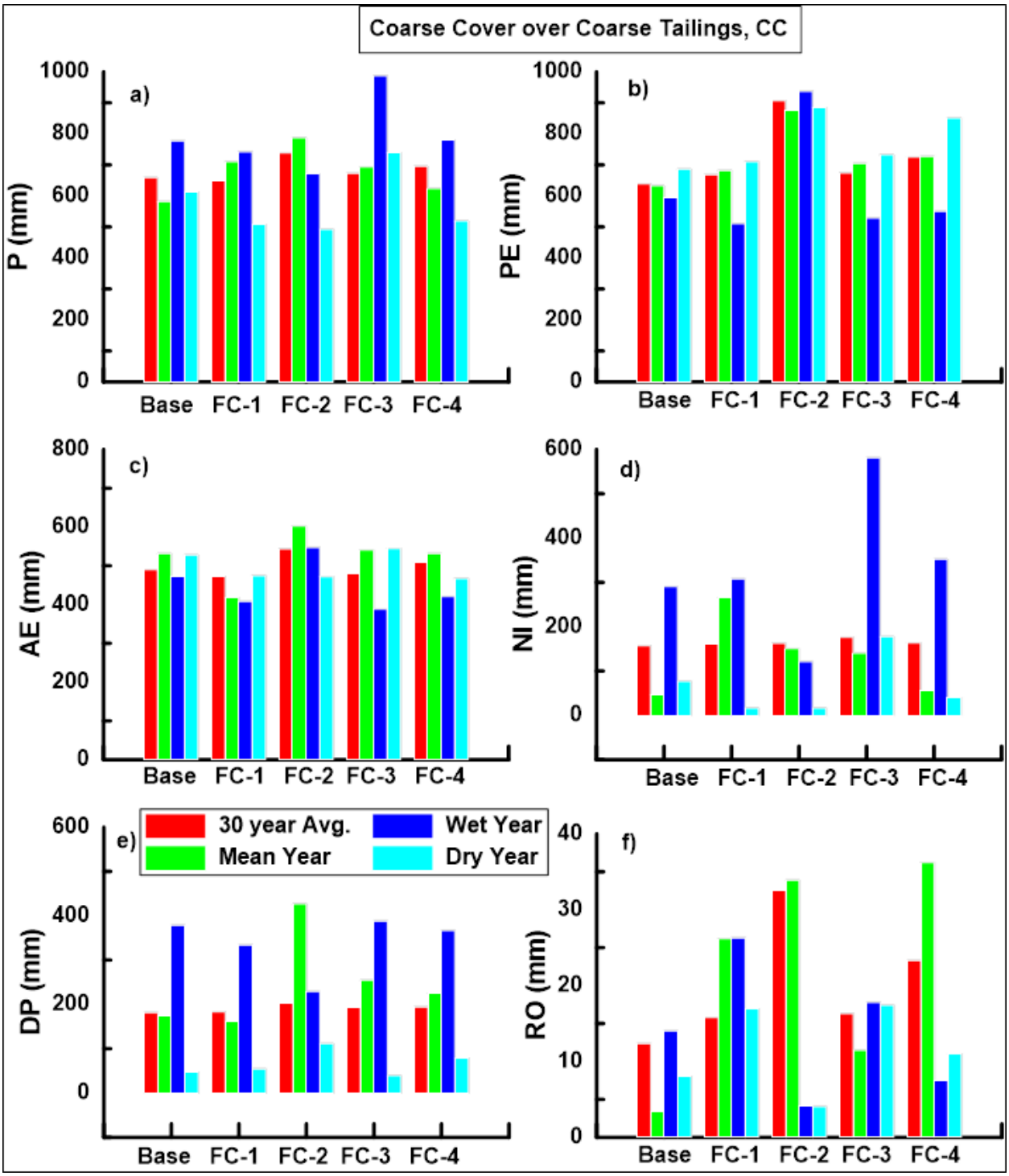

Appendix D 2. Water balance for coarse cover over coarse tailings (CC) for various representative future climates.

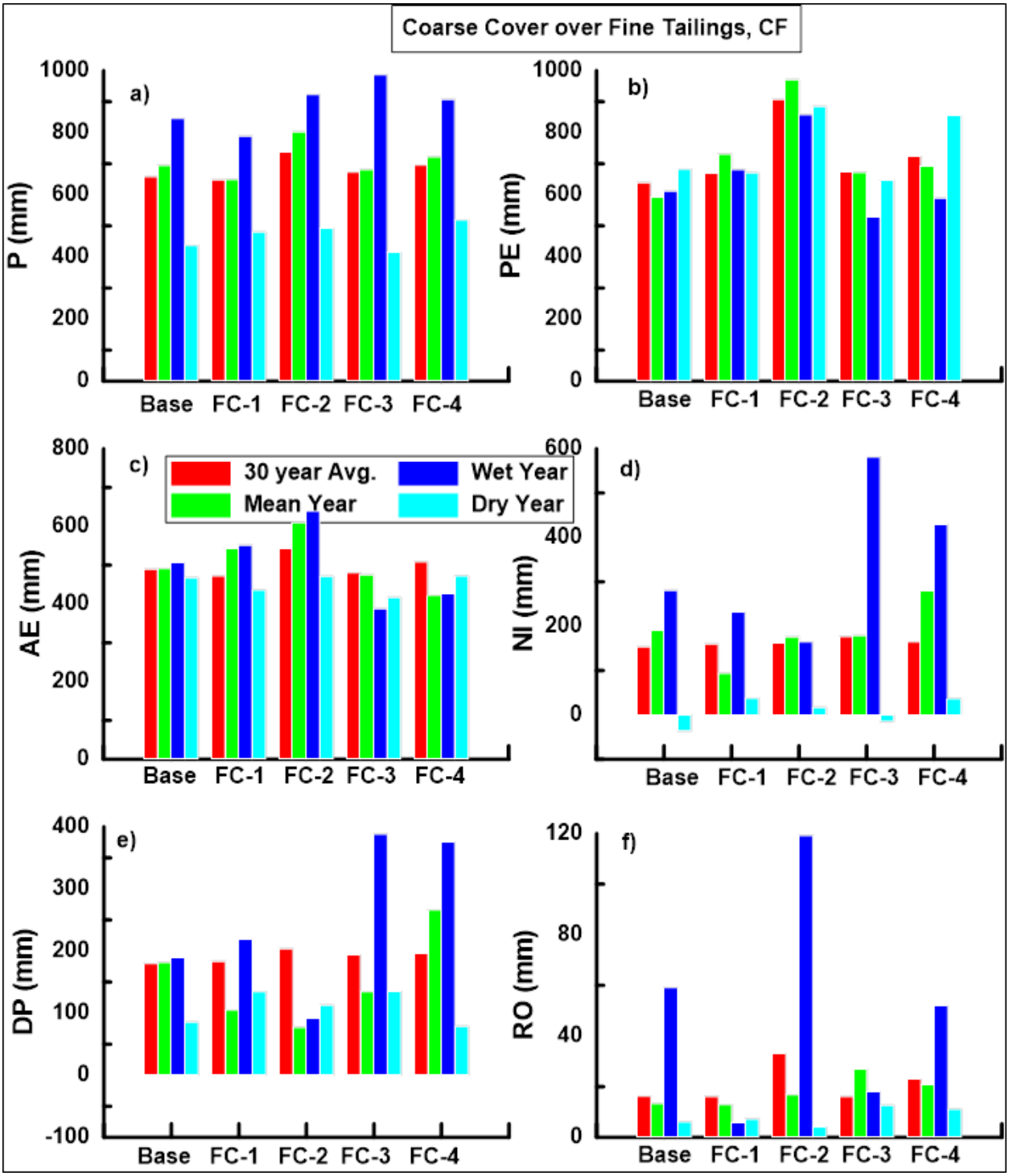

Appendix D 3. Water balance for coarse cover over fine tailings (CF) for various representative future climates.

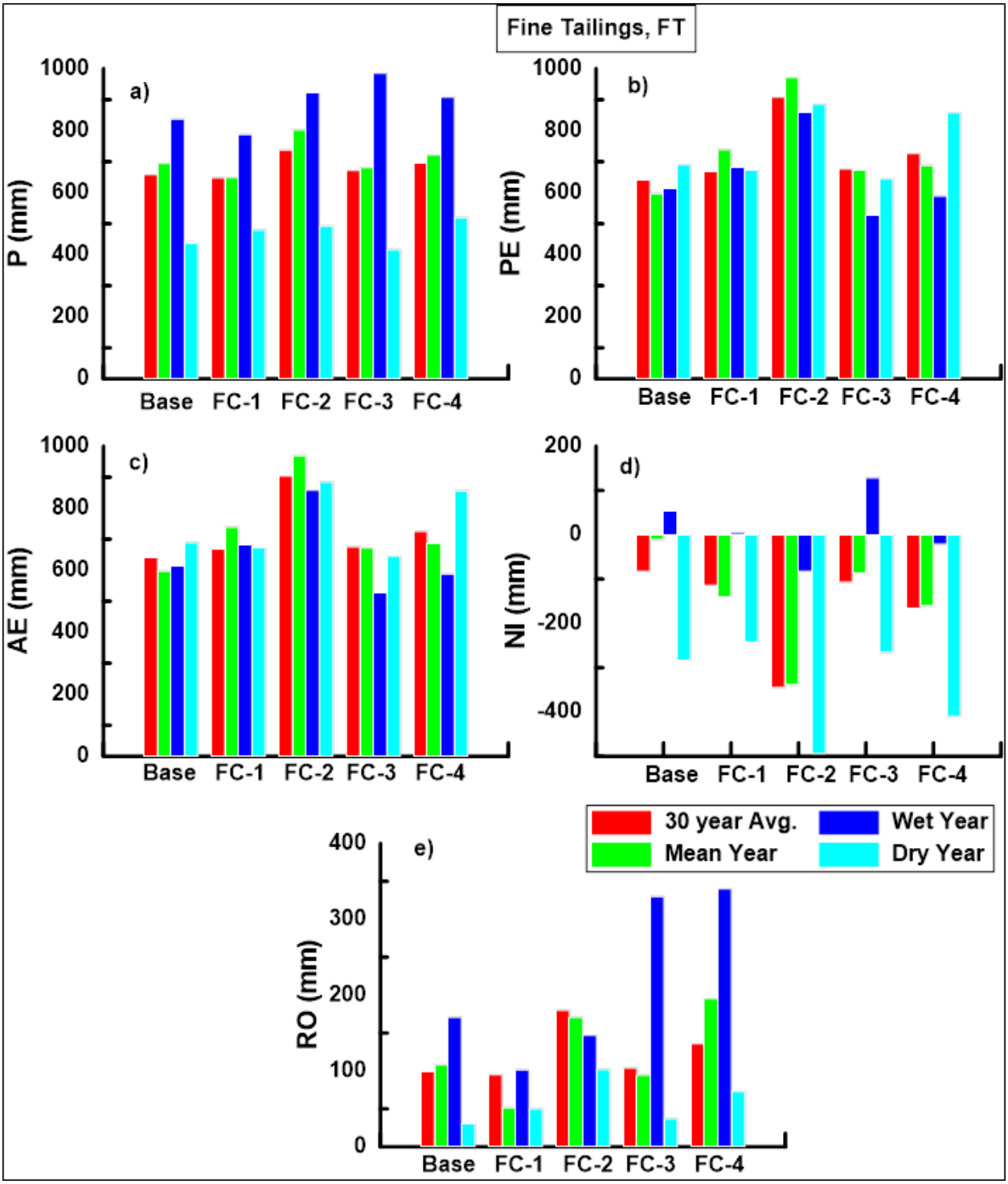

Appendix D 4. Water balance for fine tailings (FT) for various representative future climates.

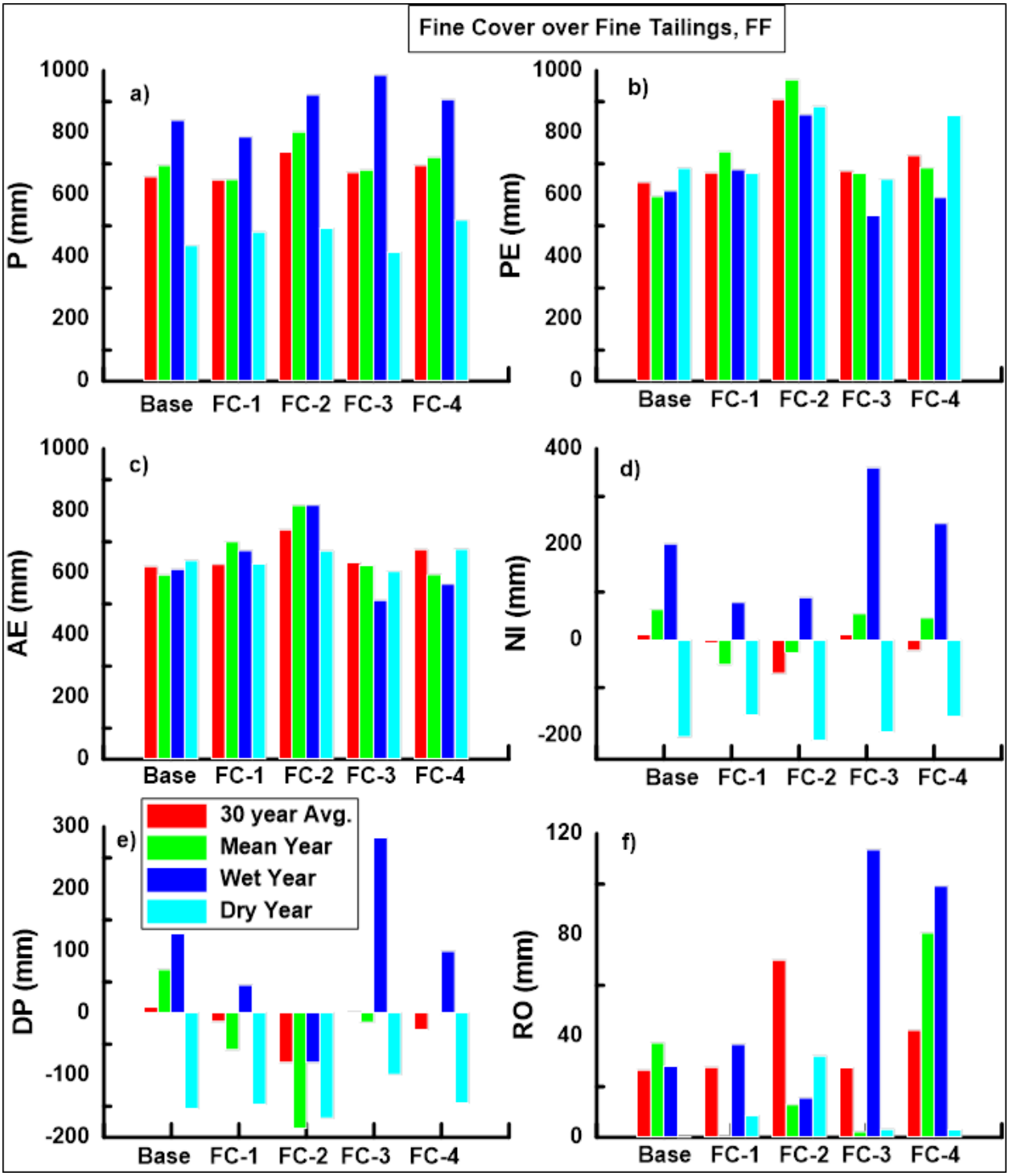

Appendix D 5. Water balance for fine cover over fine tailings (FF) for various representative future climates.

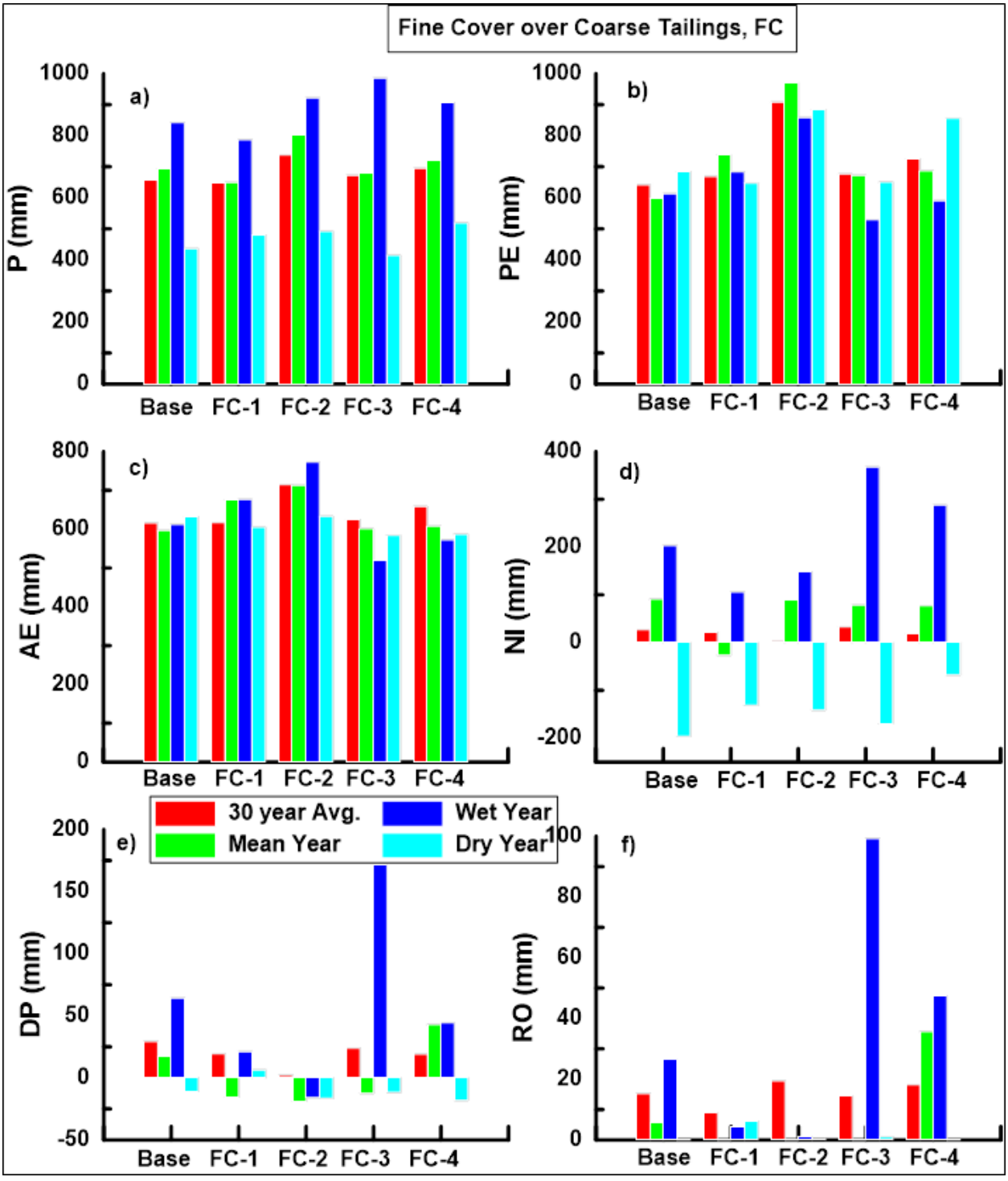

Appendix D 6. Water balance for fine cover over coarse tailings (FF) for various representative future climates.